Jour. Sci. Hiroshima Univ., Ser. C, Vol. 9, No. 3, 495–595 (1992)

Tectonic Evolution of the Sambagawa Schists and its Implications in Convergent Margin Processes

By

Ikuo HARA, Tsugio SHIOTA, Kei HIDE, Kenji KANAI, Masumi GOTO, Sachiyo SEKI, Kenji KAIKIRI, Kenji TAKEDA, Yasutaka HAYASAKA, Takami MIYAMOTO, Yasuhiro SAKURAI and Yukiko OHTOMO

with 3 Table and 118 Text-figures

(Received, May 29, 1992)

Abstract: The Sambagawa schists as high P/T metamorphic rocks are a member of Mesozoic accretionary complexes developed in the southern front of the Kurosegawa-Koryoke continent of Southwest Japan. The Mesozoic accretionary complexes are divided into four megaunits developed as nappes, Chichibu megaunit II, Sambagawa megaunit, Chichibu megaunit I and Shimanto megaunit in descending order of structural level. The Chichibu megaunit II consists of three accretionary units developed as nappes, late early Jurassic unit, late middle Jurassic unit and latest Jurassic unit (Mikabu unit) in descending order of structural level. The Chichibu megaunit I consists of five accretionary units developed as nappes, late middle Jurassic unit (Niyodo unit), late Jurassic unit, Valanginian unit, Barremian unit and Albian unit in descending order of structural level. The Shimanto megaunit, which just underlies the Chichibu megaunit I, is Cenomanian-Turonian accretionary unit and Coniacian-Campanian accretionary unit. The schists, which underlie the Chichibu megaunit II, all have been so far called the Sambagawa schists. These are divided into six units, Saruta unit, Fuyunose unit, Sogauchi unit, Sakamoto unit, Oboke unit and Tatsuyama unit in descending order of structural level, which show different tectono-metamorphic history and different radiometric ages from each other. The Sakamoto unit, Oboke unit and Tatsuyama unit have been assumed with reference to their radiometric ages and structural relations to belong to the late middle Jurassic accretionary unit of the Chichibu megaunit I (high pressure equivalent of the Niyodo unit), the Cenomanian-Turonian accretionary unit of the Shimanto megaunit and the Coniacian-Campanian accretionary unit of the Shimanto megaunit respectively in this paper. The upper member of the Sambagawa schists, Saruta unit, Fuyunose unit and Sogauchi unit, is therefore called the Sambagawa megaunit in this paper.

The northern half and the southern half of the Sambagawa megaunit are intercalated as nappes between the Chichibu megaunit II and the Oboke unit and between the Chichibu megaunit II and the Sakamoto unit respectively. The constituent units of the Chichibu megaunit II, Sambagawa megaunit and Shimanto megaunit clearly show a downward younging age polarity, as compared with each other with reference to the oldest one of radiometric ages (= metamorphic ages) of each unit. The Chichibu megaunit II and the Chichibu megaunit I show the same radiometric ages as compared between them with the same fossil age. The Saruta unit, Fuyunose unit and Sogauchi unit have therefore been assumed to be high pressure equivalent of Valanginian unit, that of Barremian unit and that of Albian unit of the Chichibu megaunit I respectively. These high pressure units were exhumed, separating the Chichibu supermegaunit into the Chichibu megaunit II and the Chichibu megaunit I and thrusting up onto the Chichibu megaunit I.

On the basis of the growth history of amphibole in hematite-bearing basic schists of the Sambagawa megaunit, it has been assumed that the highest temperature metamorphism of the Fuyunose unit occurred, when it had been coupled with the Saruta unit which was exhuming, and that of the Sogauchi unit did through its coupling with the Fuyunose and Saruta units which were exhuming. In the subduction zone which was responsible for the formation of the Sambagawa megaunit, namely, the peak metamorphism of a newly subducted unit appears to have occurred when it had been coupled with previously subcreted units which were exhuming. It has been also clarified that the subduction of a new unit occurred mixing the lower pressure part of the pre-existing subcretion unit as tectonic blocks. There is a distinct difference in the oldest one of radiometric ages between constituent units of the Sambagawa schists, showing a downward younging age polarity. The oldest one of radiometric ages of each unit appears to approximate to the age of the ending of peak metamorphism and to the age (Eh age) of the beginning of its exhumation. Such the tectonics of the Sambagawa megaunit would be explained in term of two-way street model. Because the age (Sub age) of the beginning of the subduction of each unit can be assumed from its fossil age, the average velocity of the subduction and that of the exhumation of the Sambagawa megaunit in Shikoku have roughly been estimated to be ca. 0.9 mm/year and ca. 2.0 mm/year respectively. Deformation of quartz, whose style depends strongly upon strain rate, resulted in type I crossed girdle without conentration in Y even in the depth part of more than 10kb of the subduction zone, which was placed under temperature condition of much higher than 500°C, unlike the cases of magma-arcs where quartz c-axis fabrics with maximum concentration in Y are found in gneisses produced under temperature condition of lower than 500°C. Quartz deformation in the depth part of 15-17kb of the subduction zone appears to have occurred as dominant prism slip.

The hanging wall of the Kurosegawa-Koryoke continent, which was placed at the depth of ca. 15-17 kb, thrust onto the Saruta unit at the depth of ca. 10-11 kb, accompanying intermingling of constituent rocks of the former and the latter and also mixing of various depth parts of the latter. The highest temperature metamorphism of the Saruta unit, which appears to have occurred under metamorphic condition of lower P/T than under that relat-

ed to the formation of the general type of high P/T type metamorphic rocks, is ascribed to a contact metamorphism related to the overthrusting of the Kurosegawa-Koryoke continent. The thrusting of the Kurosegawa-Koryoke continent is ascribed to its collision with the Hida continent.

The coupling of the previously subcreted Saruta unit with the newly subcreted Fuyunose unit occurred accompanying nearly isobaric cooling of the former. The great exhumation of the Saruta nappe (I + II) and Fuyunose nappe schists with great volume began together with the subcretion of the Sogauchi unit. The beginning age of the exhumation of the Sambagawa schists with great volume appears to coincide with that of the subduction of the Kula-Pacific ridge in Kyushu-Shikoku, which has been assumed by Kiminami *et al.* (1990). Namely, their great exhumation occurred with the progress of the subduction of the Kula-Pacific ridge with an eastward younging age polarity. The exhumation units, which were developed after the Mikabu unit, clearly show an eastward younging age polarity. Namely, these comparable with the Saruta unit, Fuyunose unit and Sogauchi unit are not found in central Japan and the Kanto Mountains. Rock deformation in the deformation related to the exhumation of the Sambagawa schists and their underlying schists appears to have commonly been of flattened type in mean strain.

During the Ozu phase when the Kula-Pacific ridge subducted to the greater depth, the collapse of the Kurosegawa-Koryoke continent took again place, accompanying that of the pile nappe structures of the Sambagawa megaunit, Chichibu megaunit I and Oboke unit, and the thermal gradient along the plate boundary greatly changed, giving rise to medium P/T type metamorphism in the subduction zone (formation of the Tatsuyama nappe schists).

The geological structures of the Sambagawa megaunit consist thus of two types of pile nappe structures, pre-Ozu phase pile nappe structures and Ozu phase pile nappe structures. The former is structures related to the coupling of the exhuming units (= previously subcreted units) with the newly subcreted unit. The latter is structures showing the collapse of the former. The Ozu phase pile nappe structures are further divided into the pile nappe structures formed during the earlier stage (Tsuji stage) of the Ozu phase and these formed during the later stage (Futami stage). The former is disharmonic with reference to movement picture with the latter: The deformation related to the formation of the former, accompanying exhumation of the Oboke nappes, appears to contain a component of northward displacement, while that for the latter does a component of southward displacement. After the Ozu phase deformation the Sambagawa megaunit suffered the Hijikawa-Oboke phase folding, forming a series of sinistral en echelon upright folds.

The relationship between the above-mentioned tectonic events of the Sambagawa megaunit and its surroundings and their radiometric ages is summarized as follows:

Deformation	Events	Ages
Sic deformation	deformation related to the formation of Si schistosity in cores of garnet of the Saruta unit	
Bic deformation	deformation related to the formation of snow-ball structures of cores of garnet of the Saruta unit	
Sim deformation	deformation related to the formation of Si schistosity in inner mantles of garnet of the Saruta unit	
Bim deformation	folding of Sim schistosity	
Nd phase	crystallization of garnet inner mantles and plagioclase porphyroblasts cores of the Saruta unit under non-deformational condition	
Som deformation	deformation related to the formation of Si schistosity in garnet outer mantles and plagioclase porphyroblast inner mantles of the Saruta unit	
Wd phase	crystallization of garnet outer mantles and plagioclase porphyroblast inner mantles under non-deformational condition	
Spm phase	peak metamorphism of the Saruta unit	
Sb1 deformation	deformation related to the coupling of the Saruta nappes and the Fuyunose unit; beginning of retrograde metamorphism of the Saruta nappes and peak metamorphism of the Fuyunose unit	94-88Ma
Sb2-1 deformation	beginning of exhumation of the Saruta and Fuyunose nappes and their coupling with the Sogauchi unit beginning of subduction of the Kula-Pacific ridge	88-85Ma
Sb2-2 deformation	exhumation of the Saruta, Fuyunose and Sogauchi nappes and their coupling with the Chichibu megaunit I	85-82Ma
Sb3 deformation	exhumation of the Saruta, Fuyunose, Sogauchi and Chichibu megaunit I nappes and their coupling with the Oboke unit (Shimanto megaunit)	82-74Ma
Ozu deformation	collapse of initial pile nappe structures of the Saruta, Fuyunose, Sogauchi, Chichibu megaunit I and Oboke nappe	
Tsuji stage	formation of the Tsuji nappe, Inouchi melange zone and Ojoin melange zone, accompanying exhumation of the Oboke nappes.	74-63Ma
Futami stage	thrusting of the Chichibu megaunit II and Kurosegawa-Koryoke continent onto the Sambagawa megaunit and Chichibu megaunit I. exhumation of medium P/T type metamorphics (Tatsuyama unit) produced in the subduction zone owing to the subduction of the Kula- Pacific ridge.	62-?Ma
Hijikawa-Oboke deformation	formation of a series of sinistral en echelon upright folds	> 50Ma

Contents

I. Introduction

The Sambagawa schists, which are exposed in the Outer Zone of southwest Japan just on the south of the Median Tectonic Line (MTL) (Fig. 1), are considered to be a typical one of high P/T type metamorphic rocks and to have been produced at a late Mesozoic convergent margin (*e.g.* Miyashiro, 1973). The highest pressure condition, where the Sambagawa schists were produced, appears to be of more than 10kb (Enami, 1983; Hara *et al.*, 1984a; Takasu, 1989). It can be therefore said that the study on the tectono-metamorphic processes of the Sambagawa schists is available to understand behaviour of geological bodies subducted to and underplated in the depth zone of ca. 35 km of convergent plate margins. Tectonic evolution of the Sambagawa schists will be outlined in this paper, attempting to draw some aspects of tectonics of sediment subduction, underplating and exhumation at the convergent plate margin concerned. The recent investigation of tectonics of convergent plate margins has proposed various models for mechanism of exhumation of high P/T type metamorphic rocks as represented by Cloos and Sherve (1988), Platt and Wallis (1991) and some others. The data for tectonic evolution of the Sambagawa schists presented in this paper appear to suggest the availability of a two-way street model for mechanism of exhumation of high P/T type metamorphic rocks at convergent plate margins. The deformation of the continental margin (Kurosegawa-Koryoke continent), which occurred during the formation processes of the Sambagawa schists, as well as the nature of subducting plate, appears to have greatly influenced their tectono-metamorphic processes. Such convergent margin processes will be comprehensively described in this paper.

Acknowledgements

The authors gratefully thank the Emeritus Professor G. Kojima of the Hiroshima University for his continued encouragement and critical discussion over many years during the course of their work on the Sambagawa schists. Their thanks are also due to Mr. A. Minami of the same University, who has kindly done a vast number of chemical analysis of metamorphic minerals, and to Dr. K. Nagao of the Institute for Study of the Earth's Interior, Okayama University, for his assistance in measurement of K-Ar ages of metamorphic minerals. The authors's works have been partly supported by the Grant in Aid for Scientific Researches of the Ministry of Education of Japan.

II. Division of Geological Units

The pre-Cretaceous terranes of Southwest Japan consist of the Hida Terrane, Inner accretionary supermegaunit (IA supermegaunit), Kurosegawa-Koryoke Terrane and Outer accretionary supermegaunit (OA supermegaunit) as shown in Fig. 1. The Hida Terrane is a nappe, which consists of granitic rocks and gneisses and is emplaced on the IA supermegaunit (Komatsu *et al.*, 1985a,b; Hara *et al.*, 1985, 1986a). The IA supermegaunit consists of accretionary complexes of Silurian - earliest Cretaceous ages, which were developed in southern front of the Hida continent as the root zone of the Hida Terrane and have so far been called Sangun-Renge belt, Akiyoshi unit, Maizuru unit, Suo unit, Chizu unit, Kuga-Tamba-Mino-Ashio unit (Fig. 1) (cf. Ichikawa, 1990).

The Kurosegawa-Koryoke Terrane is a continent [Kurosegawa-Koryoke continent (K-continent)] and its associated accretionary complexes with high P/T type metamorphic rocks, which came into juxtaposition with the IA supermegaunit during early Cretaceous age. Relict fragments of this terrane are now found on the north and the south of the MTL. Those on the north of the MTL are Higo andalusite - sillimanite type metamorphic rocks of 235 Ma with granitic rocks of 229 Ma (cf. Yamaguchi and Minamishin, 1987; Osanai, 1991 personal communication), Kiyama high P/T type metamorphic rocks of 303-444 Ma (Miller *et al.*, 1965; Hayase and Ishizaka, 1967; Ueda and Onuki, 1969), Asaji metamorphic rocks (Karakida *et al.*, 1969; Hayasaka *et al.*, 1989) with granitic rock of 160 Ma (Osanai *et al.*, 1992) and Mizukoshi Formation of late Permian age (Yanagida, 1958) in Kyushu, arc-type metagabbros of ca. 250 Ma (Kagami *et al.*, 1987; Tainosyo *et al.*, 1989) in Seto Inland Sea - Kii Peninsula, and Asakawazawa granite mylonites in the Oshima district, Central Japan, which show radiometric age of 152Ma (Ohtomo & Kagami, 1990; Ohtomo *et al.*, in preparation), showing that relict fragments of the Kurosegawa-Koryoke Terrane rocks are widely exposed only in Kyushu (Fig. 1). The OA supermegaunit is Jurassic - Cretaceous ones of accretionary complexes developed in the southern front of the K-continent.

Namely, the name of the Kurosegawa-Koryoke Terrane is for the K-continent and associated pre-Jurassic accretionary complexes, for convenience' sake. The constituents of the Kurosegawa-Koryoke Terrane on the south of the MTL are developed as nappes on the OA supermegaunit (*e.g.* Fig. 2). These consist of rocks, which have so far been described in terms of the Kurosegawa rocks and associated late Paleozoic - late Mesozoic well-bedded clastic sequence in Kyushu to the Kanto Mountains (cf. Yoshikura *et al.*, 1990; Takeda *et al.*, 1992), Karasaki nappe and its equivalents in western Shikoku (cf. Takeda *et al.*, 1987, 1992; Hara *et al.*, 1990a) and Koryoke rocks in the Kanto Mountains

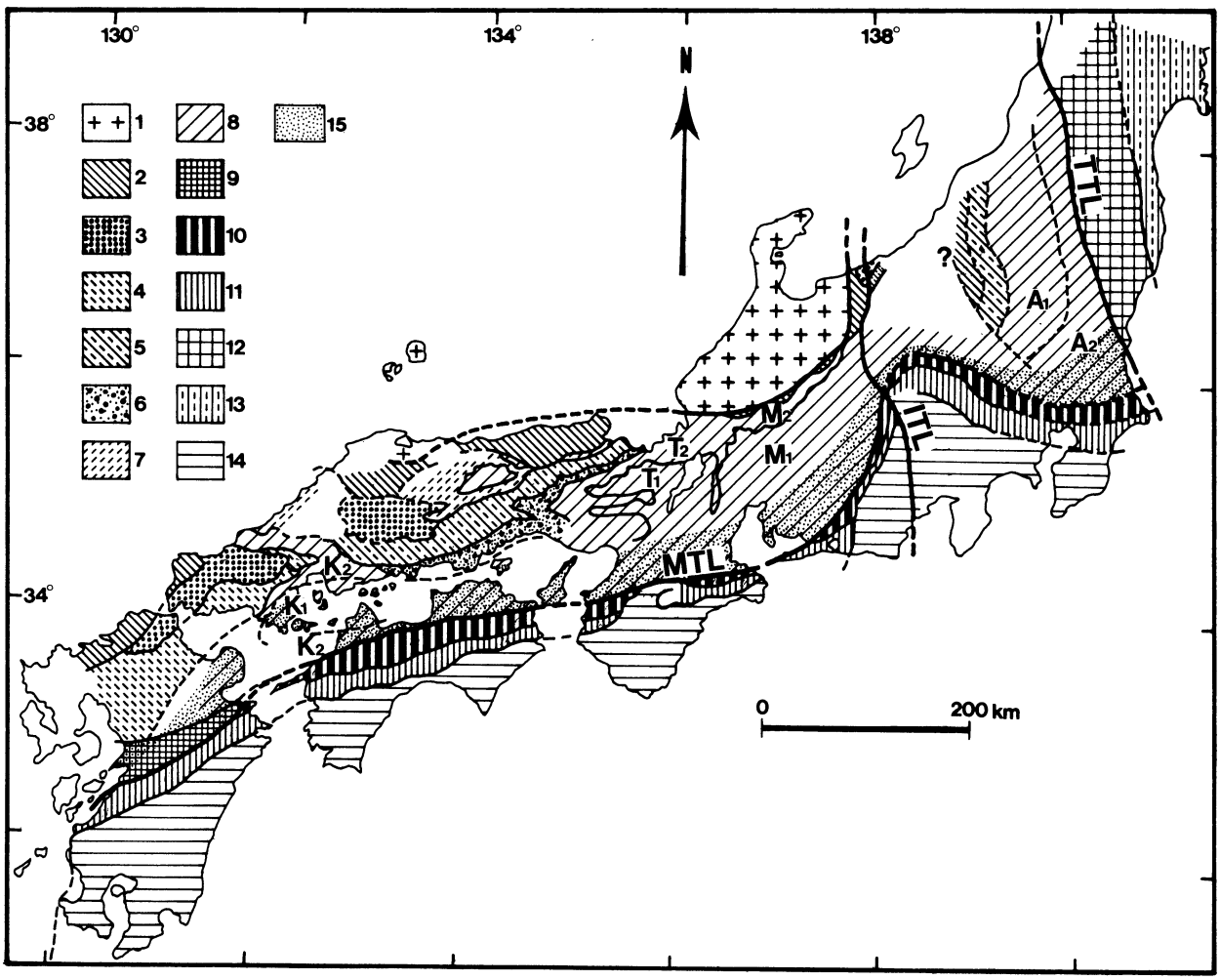

Fig. 1 Diagram showing the division of geological units of Southwest Japan and the location of the Sambagawa megaunit. 1: Hida Terrane, 2: Sangun-Renge megaunit, 3: Akiyoshi unit, 4: Suo unit, 5: Maizuru unit, 6: Ultra-Tamba unit, 7: Chizu unit, 8: Kuga (K2 unit, K1 unit)-Tamba (T2 unit, T1 unit)-Mino (M2 unit, M1 unit)-Ashio (A2 unit, A1 unit) megaunit, 9: Kurosegawa-Koryoke Terrane, 10: area containing Sambagawa megaunit, 11: area containing Chichibu megaunit I and Chichibu megaunit II, 12: Abukuma metamorphic belt, 13: Southern Kitakami Terrane, 14: Shimanto megaunit, 15: Ryoke metamorphic belt, MTL: Median Tectonic Line, ITL: Itoigawa-Shizuoka Tectonic Line, TTL: Tanakura Tectonic Line.

Fig. 2 Diagram showing the division of geological units (a) and geological structure (b and c) of the southern part of central Shikoku [compiled from Kochi Prefecture's (1991) and the present authors' data].
(a) 1: Alluvium, 2: Tertiary igneous dykes, 3, 4, 5, 7, and 8: Chichibu megaunit I [3: Susaki Formation (Albian-Cenomanian), 4: Hayama Formation (Aptian-Albian), 5: Shindoi Formation (age unknown), 7: Sakamoto-Niyodo nappe (late Middle Jurassic) 8: Sambosan Formation (Lower Cretaceous)], 6: Sambagawa megaunit, 9: Mikabu nappe (a: Mikabu greenstones, b: pelitic-psammitic schists), 10: Nakatsuyama nappe (late Middle Jurassic), 11, 12, 13 and 14: Kurosegawa-Koryoke Terrane [11: Ino Formation (metamorphics), 12: Permian accretionary complexes, 13: terrigeneous stratified sediments (Permian-Cretaceous), 14: Silurian-Devonian rocks], 15: antiform, 16: synform, 17: nappe boundary, X-X' and Y-Y': profile lines. (b) and (c) A: Silurian-Devonian rocks, B: limestone, C: Mikabu greenstones.

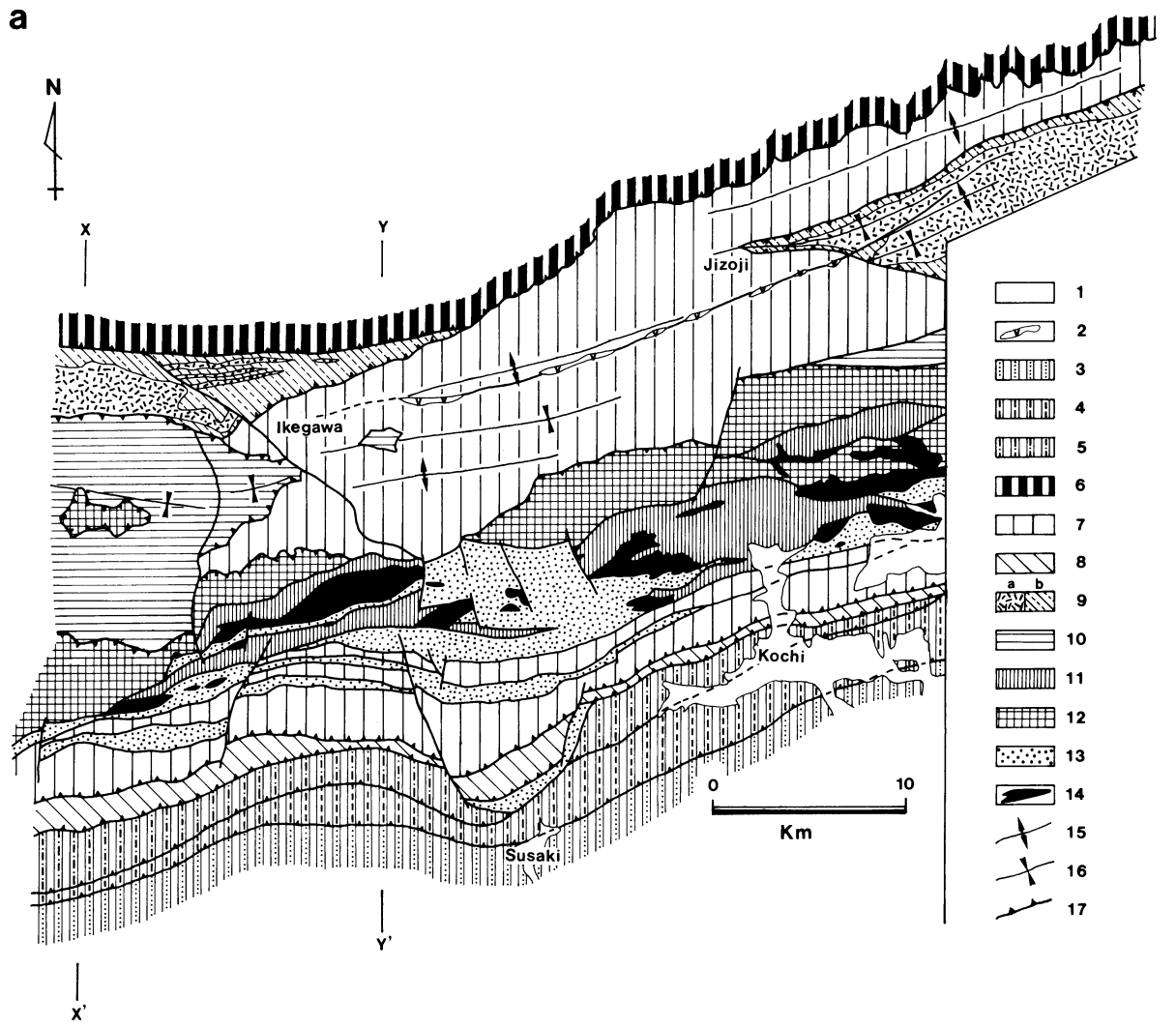
a
N
X
Y
Jizoji
Ikegawa
Kochi
Susaki
0
10
Km
Y'
X'
1
2
3
4
5
6
7
8
a b
9
10
11
12
13
14
15
16
17

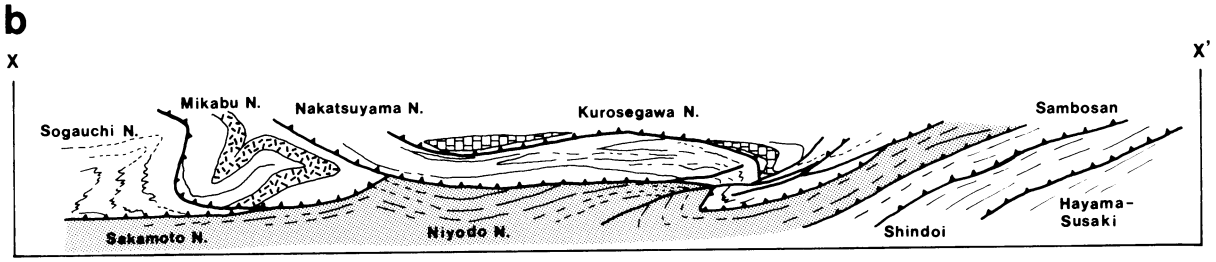
b
X
X'
Mikabu N.
Nakatsuyama N.
Kurosegawa N.
Sambosan
Sogauchi N.
Hayama-
Susaki
Sakamoto N.
Niyodo N.
Shindoi

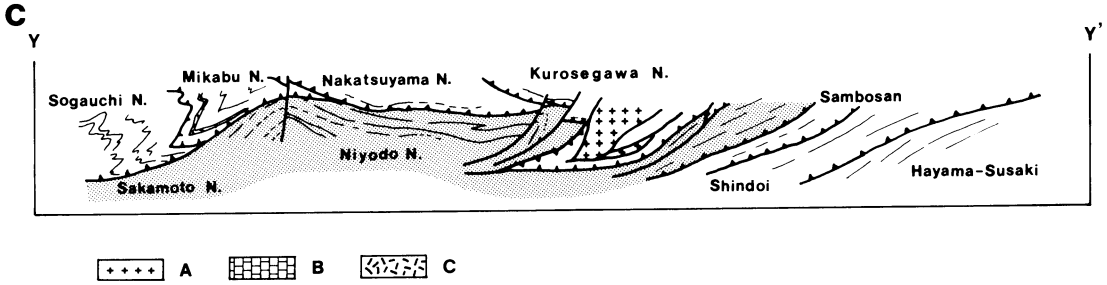
c
Y
Y'
Mikabu N.
Nakatsuyama N.
Kurosegawa N.
Sogauchi N.
Sambosan
Niyodo N.
Sakamoto N.
Shindoi
Hayama-Susaki

A
B
C

(cf. Hayama, 1991). The Kurosegawa rocks consist of granitic rocks of 150-600 Ma, high temperature type metamorphic rocks with granulite facies rocks of 97-450 Ma, accretionary complexes of Silurian - Permian ages, Siluro-Devonian volcaniclastic rocks and shelf deposits of Silurian - Jurassic ages (cf. Yoshikura *et al.*, 1990; Takeda *et al.*, 1992). The constituents of the Karasaki nappe are mylonites (Fig. 3) derived from granitic rocks and medium P/T type metamorphic rocks, which show radiometric age of 160 Ma (Takeda *et al.*, 1987). Their equivalents, which are exposed on the south of Yawatahama, western Shikoku, and have been described by Takeda *et al.* (1992), are epidote-amphibolite facies rocks of medium-pressure type with radiometric ages of 109-123 Ma. The Koryoke rocks contain granitic rocks and medium P/T type metamorphic rocks etc., which show radiometric ages of 250-270 Ma and of 50-112 Ma (Ono, 1983; Tokuda and Seo, 1985, Takagi

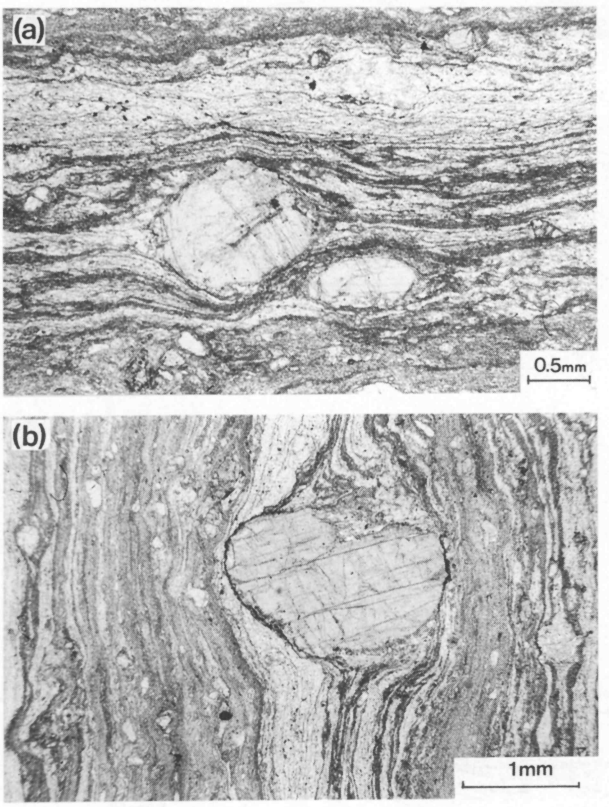

Fig. 3 Microphotographs of Karasaki mylonites of the Futami district.
a and b: ultramylonites with feldspar porphyroclasts derived from granitic rocks.

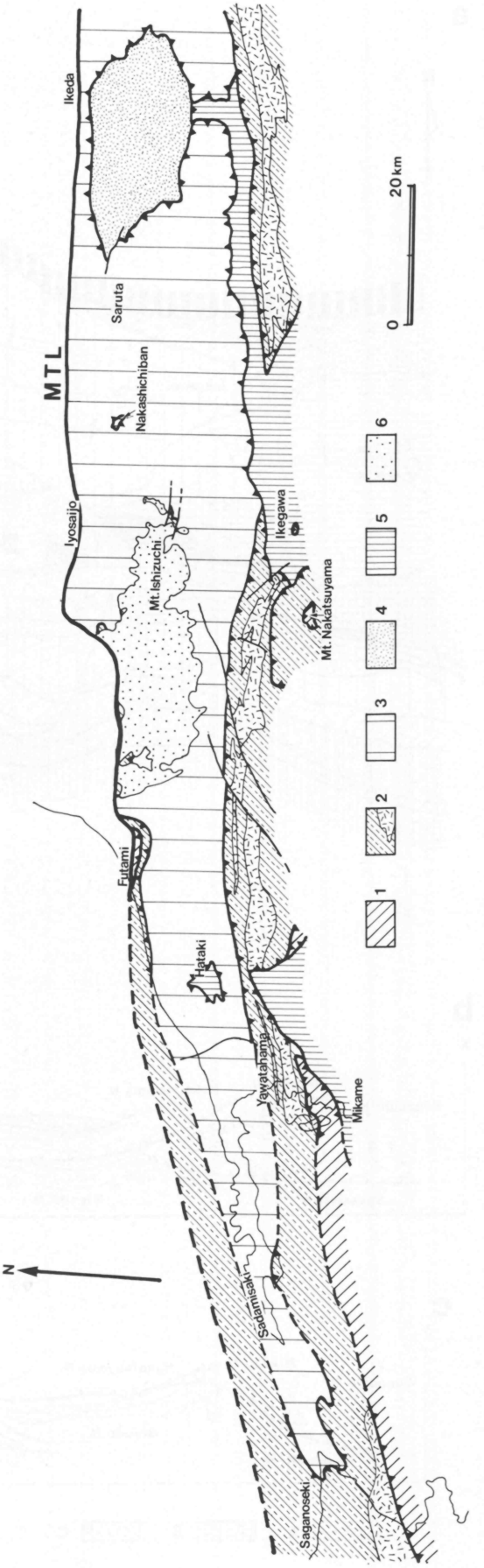

Fig. 4 Diagram showing the division of geological unit of eastern Kyushu-central Shikoku.
1: Kurosegawa-Koryoke Terrane, 2: Chichibu megaunit II, 3: Sambagawa megaunit, 4: Oboke unit (Shimanto megaunit), 5: Chichibu megaunit I, 6: Ishizuchiyama Tertiary System, MTL: Median Tectonic Line.

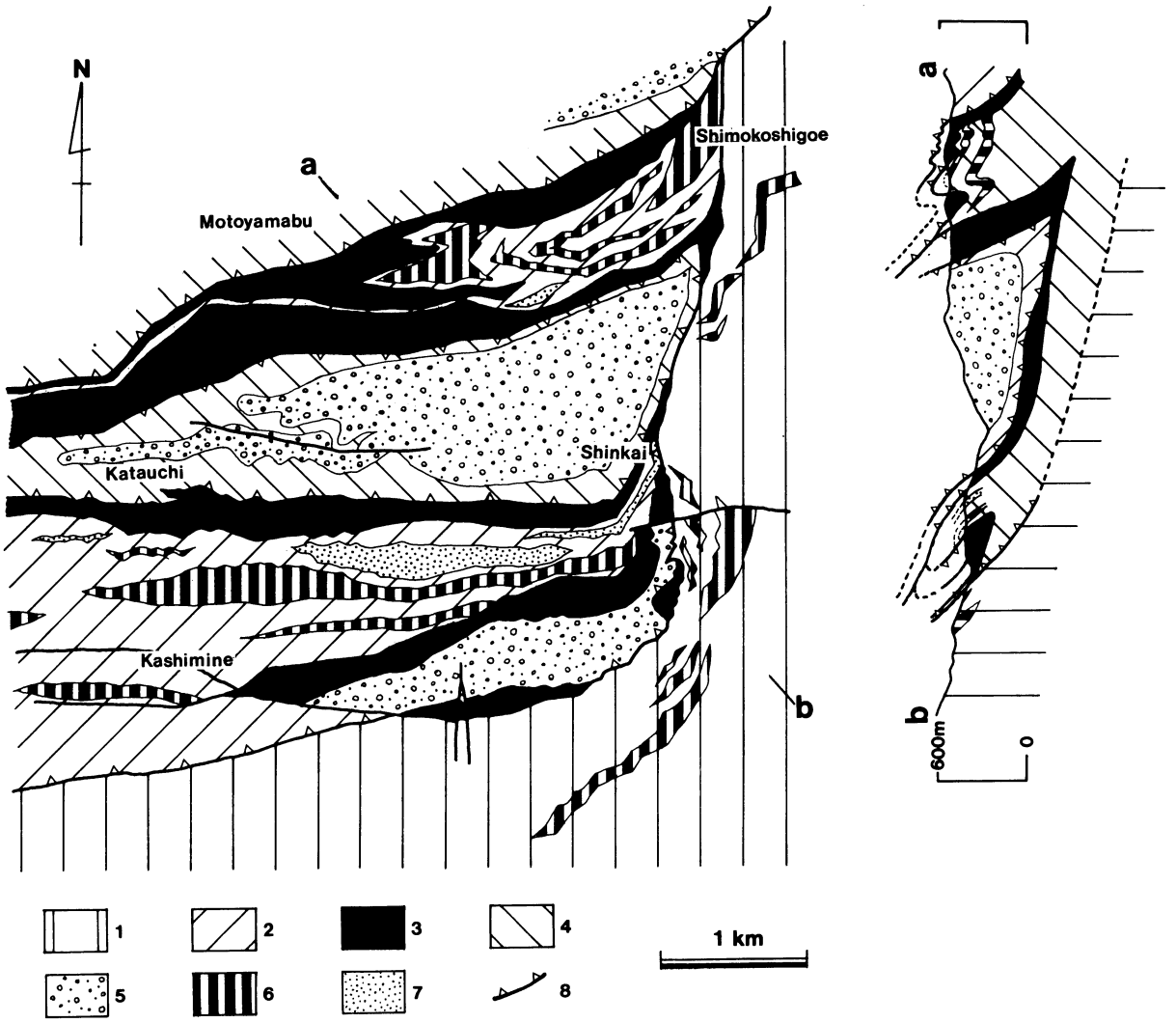

Fig. 5 Geological map and profile of the Shinkai district, Oita Prefecture (Sonoda and Hara, 1984).
1: pelitic-psammitic rocks of A formation (nappe), 2: pelitic-psammitic rocks of B formation (nappe), 3: nappe of Kurosegawa-Koryoke rocks, 4: pelitic-psammitic rocks of C formation (nappe), 5: Early Cretaceous sediments (Shinkai Formation, Yamabu Formation and Haidateyama Group) unconformablly deposited on nappes of 1, 2 and 3, 6: chert, 7: basic rocks, 8: nappe boundary. For fuller explanation see the text.

et al., 1989; Hayama *et al.*, 1990). Thus, it would be said that the Kurosegawa-Koryoke Terrane rocks developed on the south of the MTL contain products of high-temperature type metamorphism and acidic magmatism of Cretaceous age.

Just on the north of the MTL is developed the Ryoke metamorphic belt for high temperature type metamorphism and acidic magmatism (Fig. 1). The original rocks of the Ryoke metamorphic rocks consist of two components, Kuga-Tamba-Mino-Ashio unit of the IA supermegaunit, which are Jurassic - earliest Cretaceous accretionary complexes, and Kurosegawa-Koryoke Terrane. In the Ryoke belt are found the metamorphic and granitic rocks of Cretaceous age and also of Permian - Jurassic ages (Yamaguchi and Minamishin, 1987; Osanai, 1991 personal communication; Ohtomo and Kagami, 1990; Osanai *et al.*, 1992). It is clear that the high temperature type metamorphism and granite intrusion of Permian - Jurassic ages occurred only on the Kurosegawa-Koryoke Terrane, while these of Cretaceous age widely occurred on both IA supermegaunit and Kurosegawa-Koryoke Terrane. Cretaceous igneous and metamorphic rocks of the Kurosegawa-Koryoke Terrane as nappes on the south of the MTL must have also been derived from the Ryoke belt. The last age of the formation of the IA supermegaunit is comparable with age of its juxtaposition with the Kurosegawa-Koryoke belt. Jurassic - Cretaceous igneous activity in the Ryoke belt occurred before, during and after the juxtaposition event in question (Hara *et al.*, 1991a). The general trend of the Ryoke belt is oblique to that of the IA supermegaunit (Fig. 1). This would be related to the trend of the trench axis in the southern front of the K-continent (Hara *et al.*, 1991a).

The last one of accretionary complexes involved in the Kurosegawa-Koryoke Terrane is here defined to be of late Permian age, for convenience' shake. It is the Miyama Formation in Kyushu (Miyamoto *et al.*, 1985), Shingai Formation in Shikoku (Isozaki, 1986; Suzuki *et al.*, 1990a, b) and B formation in the Kanto Mountains (Tokuda,1986).

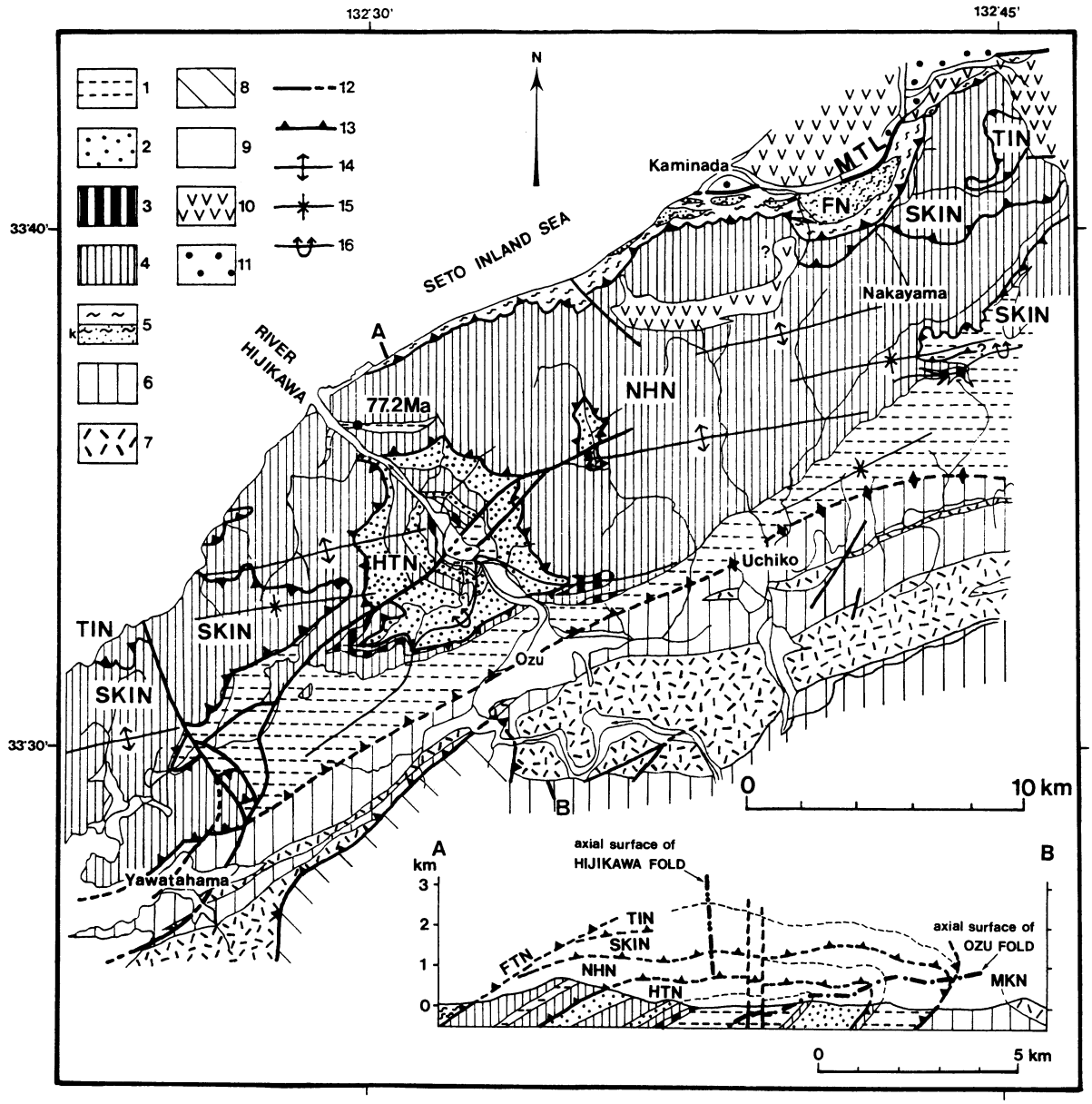

Fig. 6 Geological map and profile of western Shikoku [modified from Takeda and Hide (1991)].
1, 2, 3 and 4: Sambagawa megaunit (1: pelitic schist, 2: psammitic schist, 3: siliceous schist, 4: basic schist), 5: Futami nappe and Karasaki mylonites (k), 6 and 7: Chichibu megaunit II (6: pelitic-psammitic schist, 7: Mikabu greenstones), 8: Chichibu megaunit I, 9: Alluvium, 10: Tertiary System, 11: Izumi Group, 12: fault, 13: nappe boundary, 14: antiform, 15: synform, 16: overturned antiform.

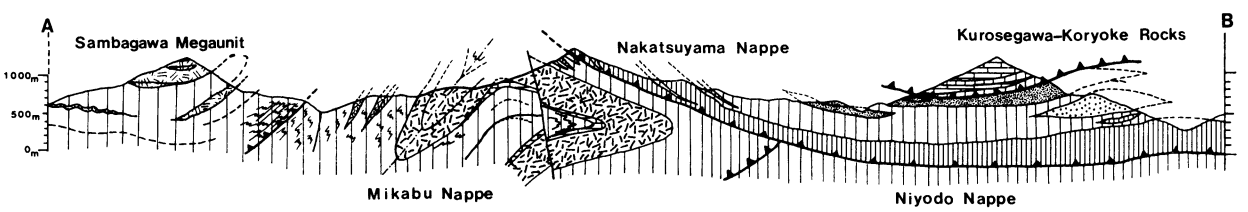

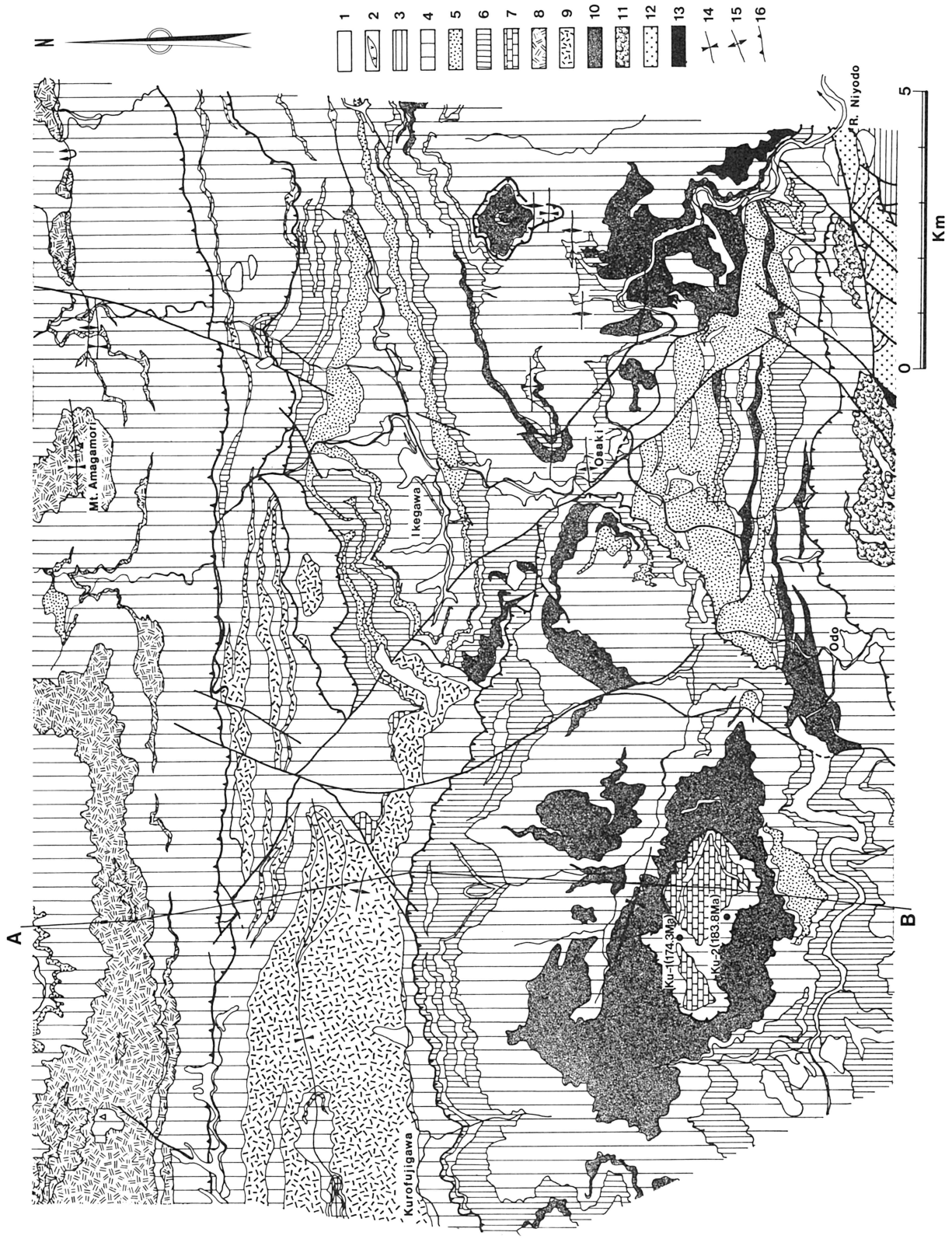

Fig. 7 Geological map and profile of the Ikegawa-Odo district [data of Tsukuda, Hara, Miyamoto, Tominaga and Tokuda (1992)]. 1: Alluvium, 2: Tertiary igneous dykes, 3: terrigeneous stratified sediments (Cretaceous), 4: pelitic rocks, 5: psammitic rocks, 6: chert, 7: limestone, 8: basic schist of the Sambagawa megaunit, 9: Mikabu greenstones, 10: basic rocks of the Nakatsuyama and Niyodo nappes, 11: basic rocks of the Kurosegawa-Koryoke Terrane, 12: Silurian-Devonian rocks of the Kurosegawa-Koryoke Terrane, 13: serpentinite, 14: synform, 15: antiform, 16: nappe boundary.

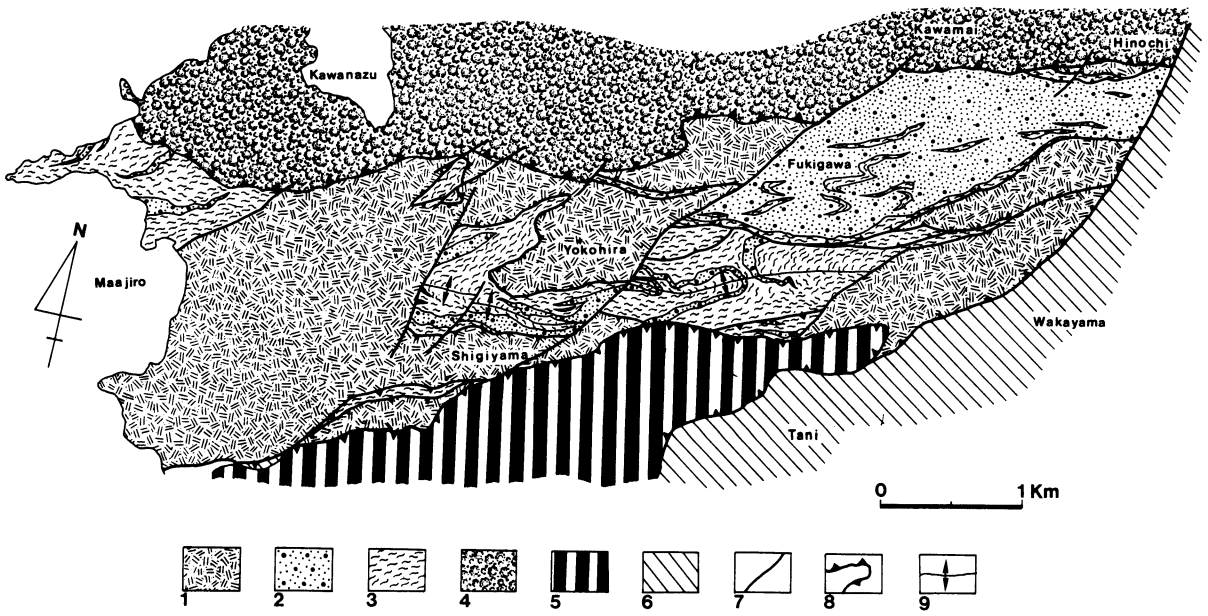

Fig. 8 Geological map of the Yawatahama district [partly modified from Makisaka *et al.* (1982)].
1: Mikabu greenstones, 2: basic schist, 3: pelitic-psammitic schist (chlorite zone but partly garnet zone), 4: Kawamai amphibolite, 5: Kurosegawa-Koryoke Terrane rocks, 6: Chichibu megaunit I, 7: fault, 8: nappe boundary, 9: antiform.

The OA supermegaunit is accretionary complexes, which had been newly developed in the southern front of the Kurosegawa-Koryoke Terrane since early Jurassic age. They are divided into four megaunits, Chichibu megaunit II, Sambagawa megaunit, Chichibu megaunit I and Shimanto megaunit in descending order of structural level as, for example, shown in Fig. 4.

The Kurosegawa rocks in Shikoku are mainly developed in the southern end of the Chichibu megaunit II (Fig. 2). Their distribution area has so far been called the middle zone of the Chichibu belt or Kurosegawa zone (Terrane) (cf. Yoshikura *et al.*, 1990). The Chichibu megaunit II on the north of the Kurosegawa Terrane has so far been called the northern zone of the Chichibu belt or Northern Chichibu Terrane (cf. Takeda *et al.*, 1977; Hada and Kurimoto, 1990). Many authors (*e.g.* Hada and Suzuki, 1983; Maruyama *et al.*, 1984; Faure, 1985; Isozaki, 1988; Yoshikura *et al.*, 1990) have assumed that the Kurosegawa Terrane is relict fragments of a continent subducted and underplated beneath the Sambagawa schists and the Northern Chichibu Terrane. While, on the basis of Sonoda and Hara's (1984) (Fig.5), Hirajima's (1984), Tokuda's (1986, Fig. 24) and Takeda *et al.*'s (1987) (Fig. 6) data for the struc-

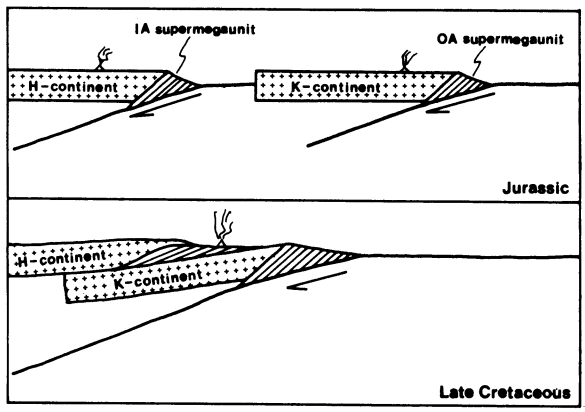

Fig. 9 Schematic diagram illustrating Jurassic-Cretaceous tectonics of Southwest Japan. For fuller explanation see the text.

Fig. 10 Geological map and profile of eastern Kyushu-Sadamisaki Peninsula of Shikoku [compiled from Yoshikawa *et al.* (1980), Sonoda (1985) and the present authors' data].
1 and 2: Saredani-Kabayama-Izushi nappe (1: basic schists, 2: pelitic-psammitic schists) of the Sambagawa megaunit, 3, 4 and 5: Chichibu megaunit II [3: Fukumizu Formation (melange zone mixing of various grades and lithofacies rocks), 4: Shiraki Formation consisting mainly of pelitic-psammitic schists and of garnet zone schists in lower part and chlorite zone schists in upper part, 5: Isshakuya Formation (a: pelitic-psammitic schists, b: Mikabu greenstones], 6: nappe boundary, 7: fault, 8: antiform, 9: synform.

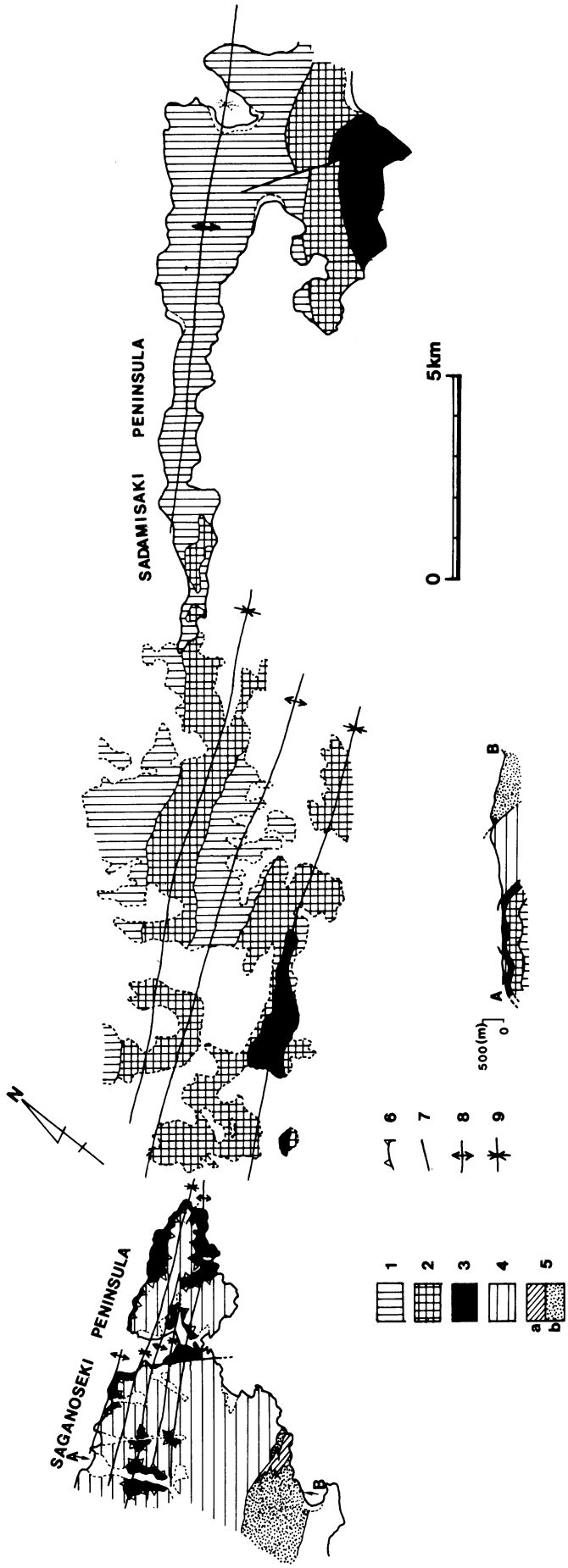
SADAMISAKI PENINSULA
SAGANOSEKI PENINSULA
5km
0
N
A
B
500(m)
0
1
2
3
4
5
a
b
6
7
8
9

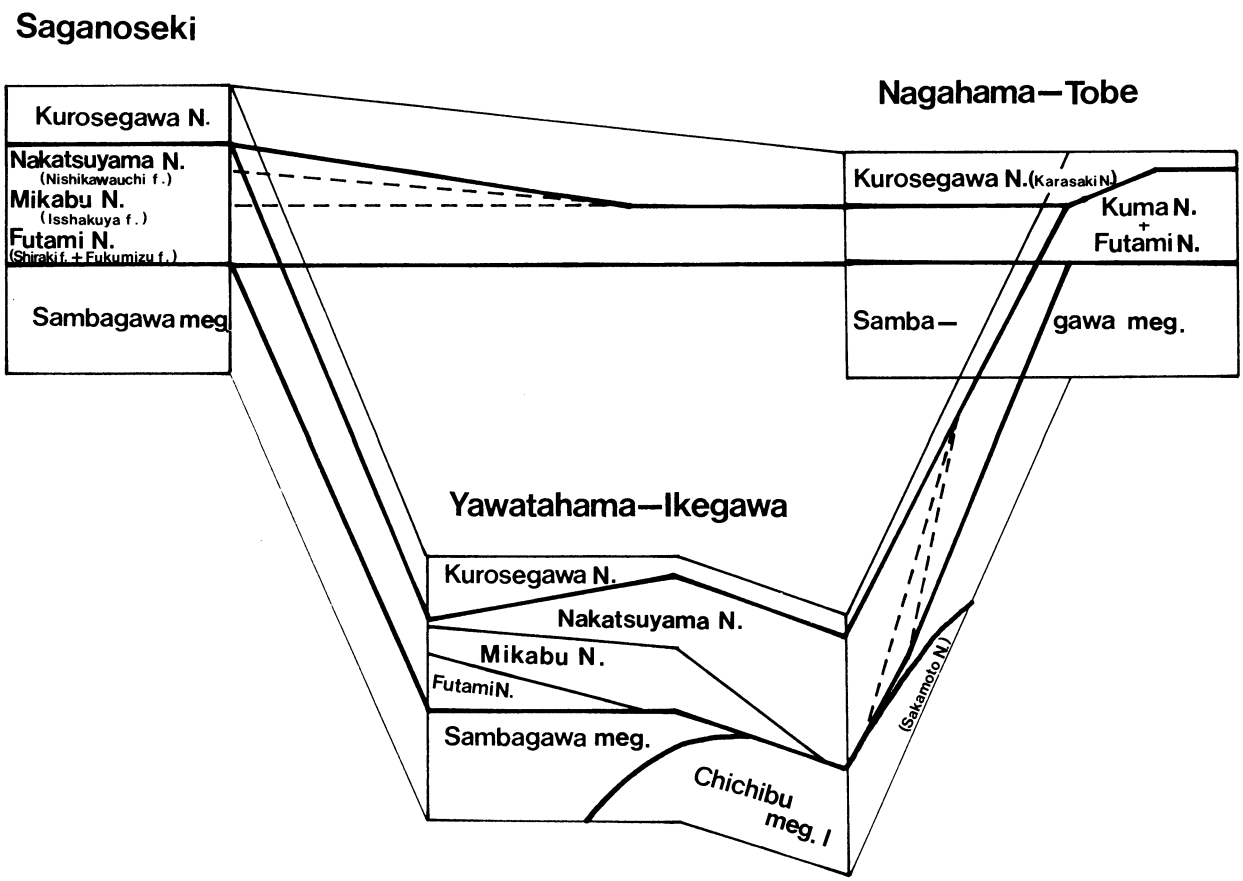

Fig. 11 Diagram showing structural relationship and correlation between constituents of eastern Kyushu, northern part of western Shikoku and southern part of western Shikoku.

Table 1. Radiometric age data for the Sambagawa megaunit and its surroundings

sample no.	material analyzed	K (wt%)	$^{40}Ar^*$ (Scc/g.10^{-5})	$^{40}Ar^*/^{40}K$	K-Ar age (Ma)
Ku-1	muscovite	3.94	2.799	1.062	174.3±5.3
Ku-2	muscovite	1.77	1.330	1.123	183.8±5.6
Na-1	muscovite	4.99	1.530	0.00458	77.2±3.9
Ob-1	muscovite	6.69	1.680	0.00376	63.4±3.2
Ki-1	muscovite	6.77	2.030	0.00448	75.6±3.8
Ki-2	muscovite	6.26	1.980	0.00473	79.7±2.5
Ki-3	whole rock	3.11	0.805	0.00387	65.5±3.3
Ki-4	muscovite	4.48	1.290	0.00430	72.9±2.3
Ki-4	whole rock	3.10	0.872	0.00426	71.1±2.2

$^{40}Ar^*$: radiogenic ^{40}Ar. Decay constants used to caluculate age are after Steiger and Jager (1977). $\lambda^{\beta} = 4.962 \times 10^{-10}$/yr, $\lambda^{\epsilon} = 0.581 \times 10^{-10}$/yr, $^{40}K/K = 1.167 \times 10^{-2}$ atm%, $^{40}Ar/^{36}Ar$ atmosphere = 295.5.
All analyzed samples are from pelitic schists. Ku: data from the Kurosegawa-Koryoke Terrane of Mt. Nakatsuyama (Fig.7), Na: data from the Sogauchi nappe of the River Hijikawa (Fig. 6), Ob: data from the Oboke nappe I of the Koboke district (Fig. 18), Ki: data from the Sambagawa megaunit and Shimanto megaunit of the Kuzuwa district, Kii Peninsula (Fig. 17).

tural relationship between the Kurosegawa rocks and other surrounding rocks, Hara *et al.* (1987) said that the former is placed as nappes on the latter and was derived as nappes from the Sambagawa-hokuenkoriku as a microcontinent [= Kurosegawa continent after Hara *et al.*(1990a) and Kurosegawa-Koryoke continent after Hara *et al.* (1991a) and in this paper], beneath which plate subduction responsible for the formation of the Sambagawa schists occurred.

Recently, Suzuki *et al.* (1990a, b) also said that late Permian accretionary complex as a member of the Kurosegawa-Koryoke Terrane in eastern Shikoku covers as a nappe the remaining member of the Northern Chichibu Terrane and that recrystallized muscovite in this accretionary complex shows radiometric ages of 190-210 Ma. Hara *et al.* (1991b), Isozaki *et al.* (1991) and the present authors (Table 1, Fig. 7) also reported that, in the Nakatsuyama district, central

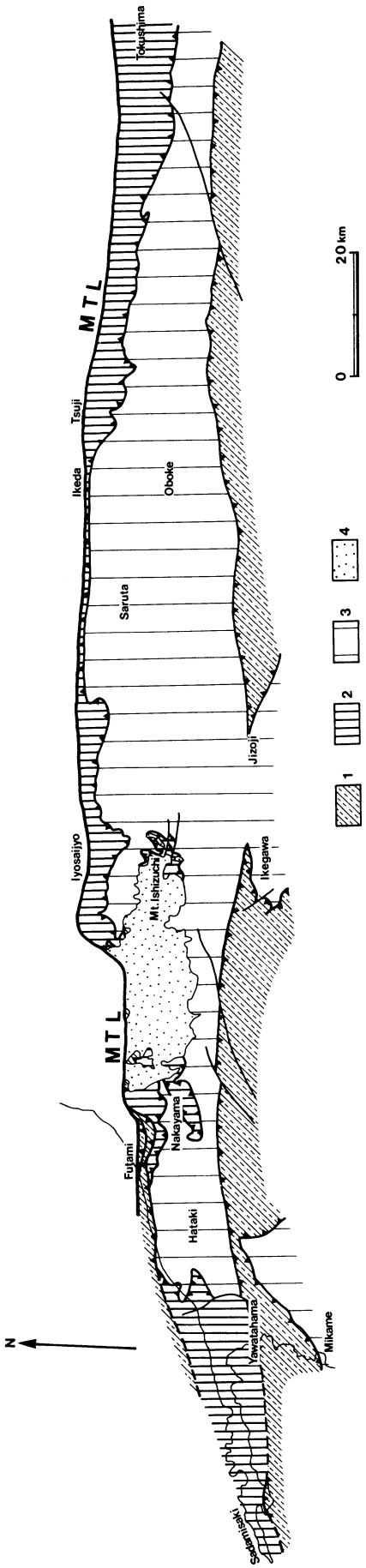

Fig. 12 Diagram showing the distribution of nappes in Shikoku which were produced by the Ozu phase deformation.
1: Chichibu megaunit II, 2: nappes of the Sambagawa megaunit produced by the Ozu phase deformation, 3: part of the Sambagawa megaunit, Chichibu megaunit I and Shimanto megaunit (Oboke unit), which was not modified by the Ozu phase deformation. 4: Ishizuchiyama Tertiary System.

Shikoku, a nappe of accretionary complex with recrystallized muscovite of analogous radiometric ages overlies the remaining member of the Northern Chichibu Terrane [Nakatsuyama nappe after Tsukuda *et al.* (1981) and Hada and Kurimoto (1990)] (Figs. 2 and 7). The nappe is comparable with that after Aiba (1982) which had been pointed out on other basis. Makisaka *et al.* (1982), Takeda and Makisaka (1991) and Takeda *et al.* (1992) also reported that, in the Mikame district, western Shikoku, the igneous and metamorphic rocks and well-bedded clastal sequence (Maana formation) of the Kurosegawa - Koryoke Terrane overlie as a nappe the Mikabu greenstones and associated schists (Fig. 8) and the nappe was transported from the north. The above-described data are consistent with Hara *et al.'s* (1987b) assumption on structural relationship between the Kurosegawa-Koryoke Terrane and other megaunits.

Thus, the development processes of the tectonic collage of Southwest Japan has been explained by Hara *et al.* (1991a) as schematically shown in Fig. 9. The ending of the formation of the IA supermegaunit is ascribed to the its juxtaposition with the Kurosegawa-Koryoke continent. The Jurassic acidic magmatisum of the Ryoke belt is that on the Kurosegawa-Koryoke continent, which occurred just before the juxtaposition of the IA supermegaunit with the continent. While the Cretaceous magmatism and high-temperature metamorphism of the Ryoke belt occurred during and after the juxtaposition tectonics. The collapse of the Ryoke belt and Kurosegawa-Koryoke continent, by which their nappes on the OA supermegaunit were produced, will be again in more details described in the later pages.

Fig. 4 illustrates the distribution of the Chichibu megaunit II, Sambagawa megaunit, Chichibu megaunit I and Shimanto megaunit. The Chichibu megaunit II covers as nappes both Sambagawa megaunit in the northern side and Chichibu megaunit I in the southern side. This megaunit in the southern side consists of three units, Sawadani-Higashiura unit, Nakatsuyama unit and Mikabu unit in descending order of stuructural level, which all are developed as nappes. The Sawadani-Higashiura unit, Nakatsuyama unit and Mikabu unit are, respectively, accretionary complexes of late early Jurassic age [Shimodake Formation (Miyamoto, 1990) and Unit B (Sonoda and Hara, 1984) (Fig. 5) in Kyushu; Sawadani nappe and Higashiura nappe in Shikoku (Tominaga, 1990)], of late middle Jurassic age [Hashirimizu Formation in Kyushu (Miyamoto *et al.*, 1989); Nakatsuyama nappe (Hada and Kurimoto, 1990) (Fig. 7) and Kenzan nappe (Tominaga, 1990)in Shikoku] and of latest Jurassic age [Mikabu unit in Shikoku (Iwasaki *et al.*,

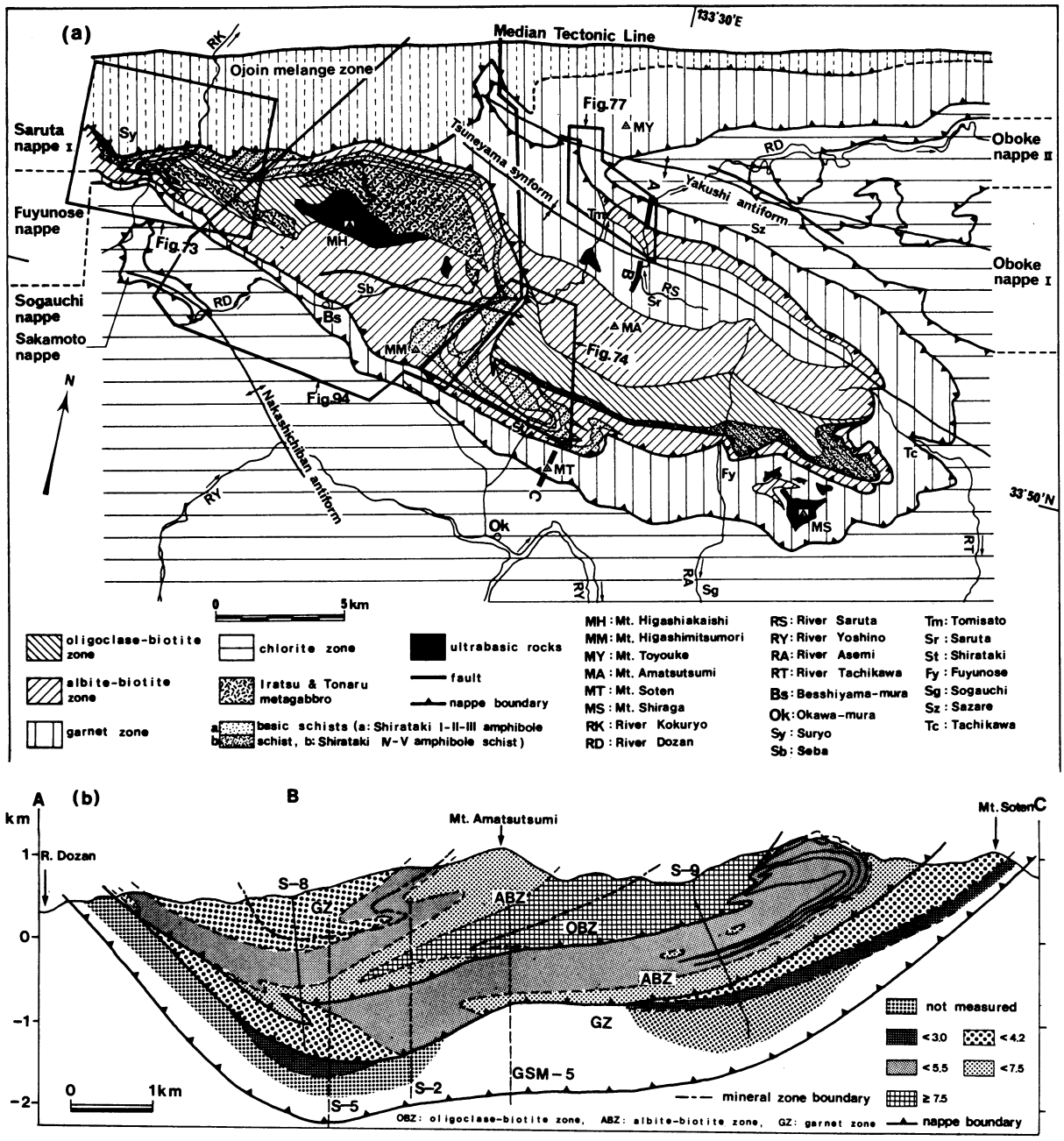

Fig. 13 Geological map (a) and profile (b) of the Sambagawa megaunit in central Shikoku [modified from Hara *et al.* (1990b)]. The diagram (b) also shows the spatial variation in Mg values of garnet in pelitic schists, which are minimum Mg content (%) measured at a fixed Mn content of 5% on the Mn-Fe-Mg diagram.

1984)]. It can be said that the constituent units of the Chichibu megaunit II are accretionary complexes, which were successively but episodically developed showing a downward younging age polarity from early Jurassic age to late Jurassic age. All constituent rocks of these three units are of lower metamorphic grade (chlorite zone).

While the Chichibu megaunit II in the northern side contains higher-grade metamorphic rocks. It is the Saganoseki nappe [Nishikawauchi formation (Teraoka, 1970; Hara *et al.*, 1990a) and Mikabu nappe {Mikabu greenstones (Isshakuya formation) and associated schists (Shiraki formation and Fukumizu formation)} (Sonoda, 1985) in descending order of structural level] in eastern Kyushu (Fig. 10), and Misaki formation (Hara *et al.*, 1977) (Fig. 10), Futami nappe (Takeda *et al.*, 1987; Hara *et al.*, 1990a) (Fig. 6) and Mikabu nappe [Mikabu greenstones and associated schists (Makisaka, 1982; Makisaka *et al.*, 1982; Hara *et al.*, 1990a; Takeda *et al.*, 1992)] (Fig. 8) in western Shikoku. The Saganoseki nappe schists (Shiraki formation and Fukumizu formation), the Futami nappe schists and the Mikabu nappe schists of the Mikame district contain garnet zone schists (Sonoda, 1985; Takeda *et al.*, 1987; Hara *et al.*, 1990a; Makisaka *et al.*, 1982; Takeda *et al.*, 1992), though the schists associated with the Mikabu greenstones

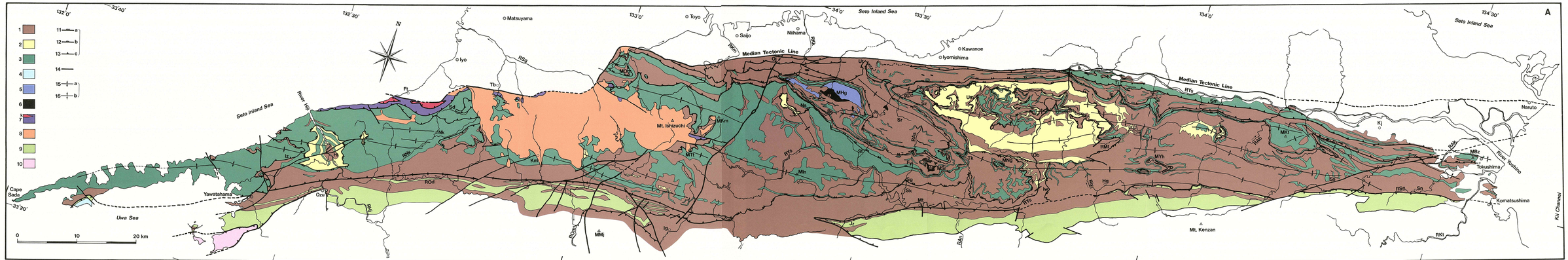

Fig. 14 Geological map (A) and structural map (B) of the Sambagawa metagneiss and its surrounding metagneiss (compiled from the data of most of papers described in References).
A) 1: pelitic schists, 2: psammitic schists, 3: basic and/or siliceous schists, 4: calcareous schists, 5 metagabbros such as Tonaru and Iratsu bodies , 6: ultrabasic rocks, 7: Futami nappe schists (Ir: Kurasaki mylonites), 8: Ishiuchiyama Tertiary System, 9: Mikabu greenstones, 10: Kurosegawa-Koryoku Terranes, 11: subzonian unit boundary, 12: nappe boundary in a subzonian unit, 13: nappe boundary of the Kotsu and Iwaki nappes, 14: boundary of the zone of uniform of the Hijikawa-Oboke phase, 16: axial trace of synform of the Hijikawa-Oboke phase.

B) 1: Kurosegawa-Koryoku Terrane, 2: Chichibu meganeiti II (Futami nappe, Mikabu nappe), 3: Saruta unit (a: Sarua nappe II, b: Sarata nappe I), 4: Fuyunose unit (a: Teiji nappe), 5 Omogisawa nappe, 6: Tenaro-Isoiu nappe, 7: Sendani-Kabuyama-Izushi nappe, 8: Sogusshi unit, 9: Oishi melange zone and Inoschi melange zone, 10: Chichibu meganeiti I (Shimanto meganeiti), 11: Shimanto meganeiti, 11: Shimanto meganeiti (Oboke nappe: a, Oboke nappe: b), 12: Ishiuchiyama Tertiary System, 13: nappe boundaries (a and b: boundaries of the pre-Oyu phase (a: boundary between subzonian units, b: nappe boundary in a subzonian unit), c: boundary of the Oyu phase), 14: fault of the post-Oyu phase, 15: axial traces of folds of the Hijikawa-Oboke phase (a: antiform, b: synform).
HiA: Hahayama antiform, HjA: Hijikawa antiform, HoA: Hosho antiform, IcA: Ichinomiya antiform, IkA: Ikasa antiform, IsA: Imado antiform, IoA: Mt. Ishido antiform, KgA: Kageno antiform, KmA: Kamiyama antiform, KsA: Kasugayama antiform, KwA: Kawaguchi antiform, MyA: Moriga antiform, MzA: Mizunokuchi pass antiform, NkA: Nakayama antiform, NoA: Nonowaki antiform, NsA: Nakashichihan antiform, ObA: Oboke antiform, OnA: Onogo antiform, SkA: Sakanomi antiform, SiA: Sakaidani antiform, YkA: Yakushi antiform, AiS: Aoife synform, BtS: Biasu synform, HtS: Hisamoue synform, IttS: Mt. Inamura synform, IzS: Izushi synform, KhS: Kohoke synform, KotS: Kuma synform, KtS: Kotsu synform, MtS: Mitsuchi synform, NgS: Nagasaka synform, SkS: Shiira synform, TtS: Taira synform, TmS: Mt. Tomochi synform, TnS: Tsunoyama synform.
Bs: Besshiyamamura, Fr: Futami, Fy: Fuyunose, Hg: Higashiiya, Hr: Haraki, Ig: Ikegawa, Ik: Ikada, Ir: Irazushi, Is: Iwahara, Ir: Izuki, Jr: Jizuki, Kj: Kamojima, Km: Kuma, Mr: Motoyama, Nk: Nakayama, Nu: Nakashichihan, Ob: Oboke, Oj: Ojuin, Sd: Sendani, Sg: Sogusshi, Sk: Sakanomi, Sm: Sadamitsu, Sr: Samegoshi, Sr: Sarua, Sr: Syounegi, Sr: Shiraiwa, Sr: Suzuo, Tb: Tobe, Tj: Tsuji, Tk: Tajikawa, Um: Umegahata, Ur: Urayama, Ys: Yasui, Yt: Yatsuo, Hgashidaisaki, MKr: Mt. Inamura, MKu: Mt. Kamegamori, MKt: Mt. Kotsu, MMj: Mt. Myojin, MNg: Mt. Nagasuke, MOm: Mt. Omogi, MSr: Mt. Shiraga, MTt: Mt. Tsutsujo, MYh: Mt. Yahata, RAb: River Arabuki, RAk: River Akui, RAr: River Asanai, RAs: River Asemi, RHj: River Hiji, RJy: River Iya, RKk: River Kokuryo, RKn: River Kamo, RKt: River Kanoura, RMt: River Matuo, RNk: River Nakayama, ROd: River Oda, ROm: River Omogo, RSg: River Sigeshi, RSn: River Sonoe, RSr: River Sarata, RYs: River Yoshino, RYn: River Dozan.

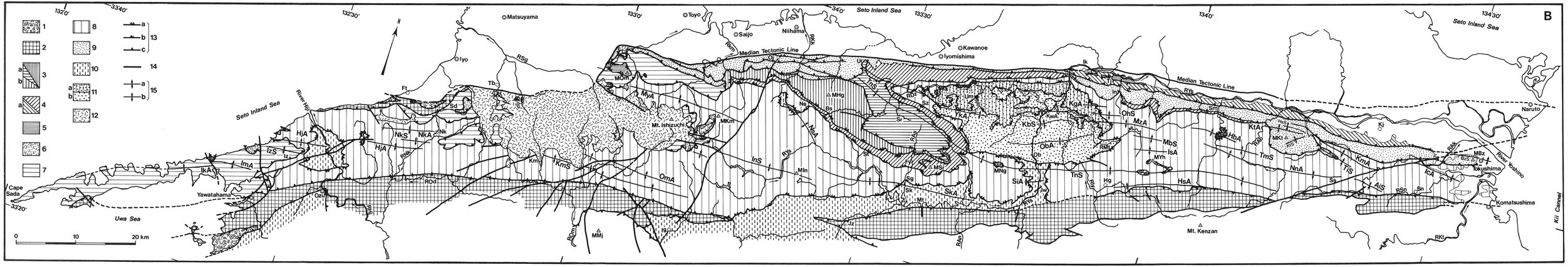
B
1
2
3
4
5
6
7
8
9
10
11
12
13
14
15
0
10
20 km
Matsuyama
Toyo
Saijo
Niihama
Kawanoe
Iyomishima
Iyo
Naruto
Komatsushima
Tokushima
Cape Sada
Yawatahama
Ozu
Uwa Sea
Seto Inland Sea
Kii Channel
River Hiji
River Yoshino
Median Tectonic Line
Mt. Ishizuchi
Mt. Kenzan
MOm
MKm
MHg
MMj
Ft
Tb
Sd
Ns
Be
Sr
Ry
Ik
Ig
Km
Mn
Ng
Sg
Sk
Ob
Hg
Sn
Ki
HjA
NkS
NkA
IzS
ImA
IkA
MyA
OmA
InS
MlnA
KmS
RSg
RSk
RIm
RIk
RIs
RSr
RMk
RMt
RKt
RYs
RYe
RNs
RBs
RKm
RKs
RBz
RSn
SiA
SkA
KbS
KgA
OhS
MzA
MbS
IsA
MYh
HsA
HbA
KtA
TmS
NnA
TtS
KmA
AlS
IcA
MBz
TkA

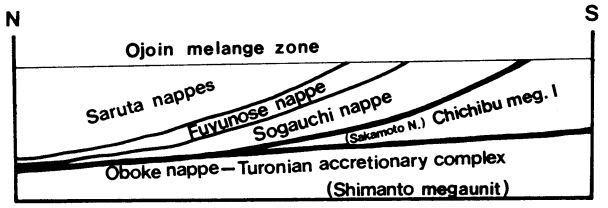

Fig. 15 Schematic diagram showing the pile nappe structures of the Sambagawa megaunit in central Shikoku.

on the east of the Mikame district and in central - eastern Shikoku do not contain any garnet zone, showing such a tendency that their metamorphic grade increases toward the west and the north. The structural correlation between the above-described nappes in Kyushu and western Shikoku is illustrated in Fig. 11.

In the Kuma Group of Middle Eocene age, which unconformablly covers the Karasaki nappe rocks, Futami nappe schists and Sambagawa megaunit schists (Figs. 4 and 6), are found pebbles such as pelitic schists and amphibolites, which show radiometric ages of 84-156 Ma, (Yokoyama and Itaya, 1990; Takasu, 1991). Because these pebble rocks are clearly older in radiometric age than the Sambagawa megaunit schists, Takasu (1990a) has assumed that the geological body as the root of the former is a nappe (Kuma nappe) being different from and overlying the latter. As mentioned in the later pages, radiometric ages of the Sambagawa megaunit schists are younger than 95Ma. While Takeda *et al.*'s (1992) data indicate that radiometric ages of schists of the Mikame district are 106-118 Ma. Thus, the Kuma nappe rocks may be roughly assumed to be equivalent to these schists, Futami nappe schists and Karasaki nappe rocks in harmonic relation with the structurally assumed correlation of Fig. 11.

The Sambagawa megaunit in Shikoku and Kyushu is divided into two parts, part with pre-Ozu phase pile nappe structures and part with pile nappe structures highly modified by the Ozu phase deformation, (Fig. 12). The Ozu phase deformation is one of the later phases deformations of the tectonic history of the Sambagawa megaunit, which will be in details explained in the later pages. The Sambagawa megaunit with the pre-Ozu phase pile nappe structures is divided into three units, Saruta unit, Fuyunose unit and Sogauchi unit in descending order of structural level, with reference to difference in tectono-metamorphic processes and radiometric ages, which will be in details explained in the later pages. The Saruta unit is developed as Saruta nappe II and Saruta nappe I, the Fuyunose unit as Fuyunose nappe and the Sogauchi unit as Sogauchi nappe (Figs. 6, 13 and 14a and b) (Hara *et al.*, 1988, 1990a, 1991a).

The Saruta nappe I, Fuyunose nappe and Sogauchi nappe clearly increase from the north to the south in thickness,

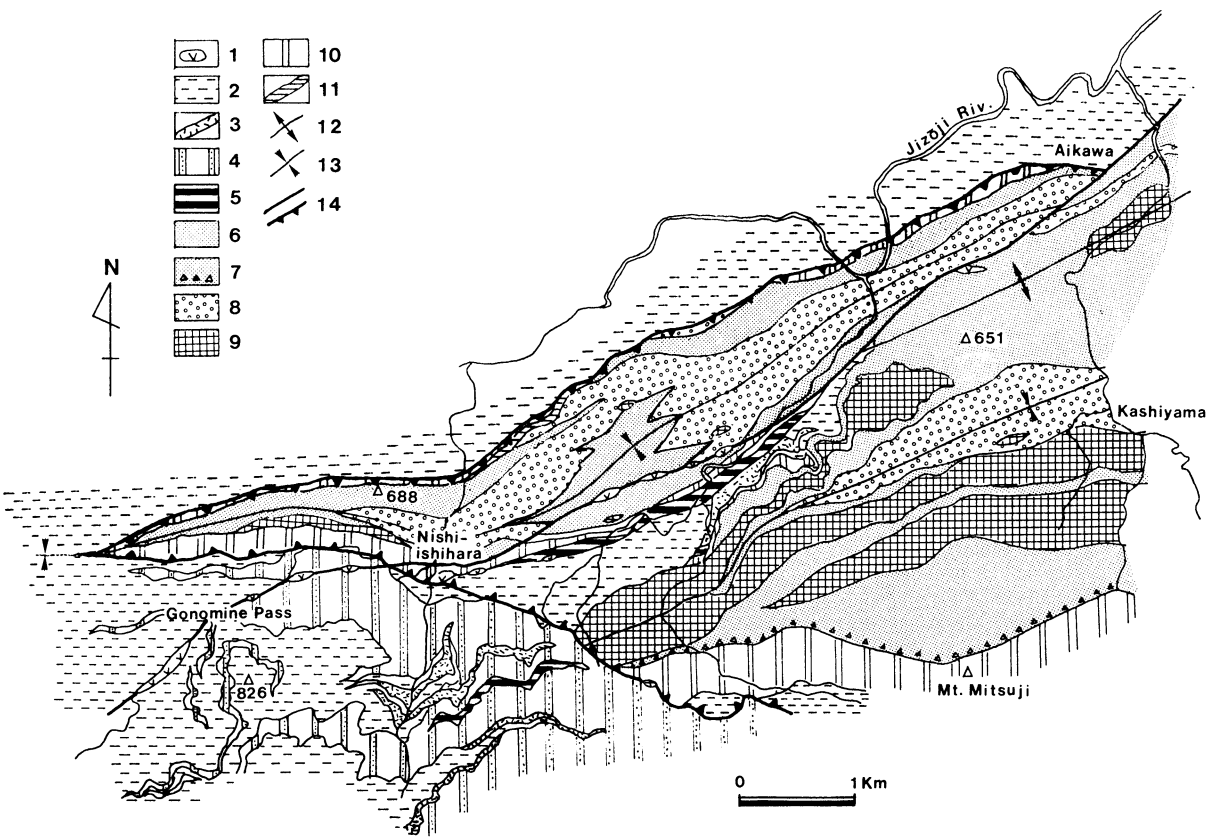

Fig. 16 Geological map of the Jizoji district [partly modified from Takeda (1984)].
1: Tertiary igneous dykes, 2: pelitic schists, 3, 4 and 5: Chichibu megaunit I (3: basic rocks, 4: chert, 5: limestone), 6 - 11: Mikabu nappe [6: basaltic (massive) lava and tuff, 7: "volcanic conglomerate", 8: pillow lava, pillow breccia and other breccia-bearing pyroclastic rocks, 9: gabbro, 10: siliceous schists, 11: calcareous schists], 12: antiform, 13: synform, 14: fault and nappe boundary.

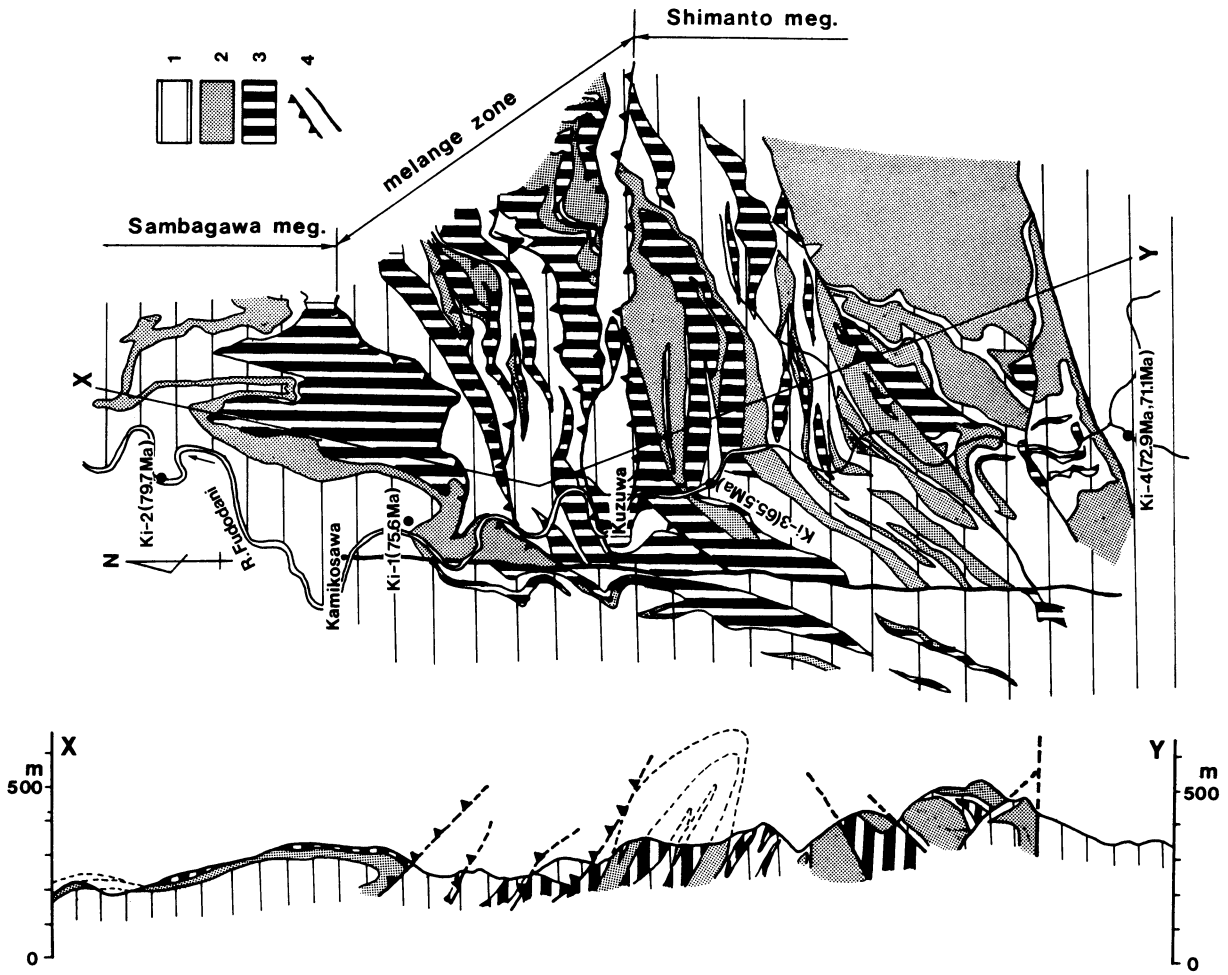

Fig. 17 Geological map and profile of the Kuzuwa district, Kii Peninsula [data of Tanino, Hara, Kanai and Hayasaka (1992)]. 1: pelitic rocks, 2: basic rocks, 3: siliceous rocks, 4: fault and nappe boundary. In melange zone is found the intermingling of the Sambagawa megaunit rocks and Shimanto megaunit rocks.

and the lower member of the Sogauchi unit disappears toward the east being cut across by the underlying units. Such a characteristics of the pile nappe structures of the Sambagawa megaunit, whose top is cut across by the nappes of the overlying Ozu phase pile nappe structures and Chichibu megaunit II, is illustrated by Fig. 14 and schematically by Fig. 15.

The Chichibu megaunit I in central Shikoku is developed as a nappe, which is covered by the Chichibu megaunit II in southern part, by the Mikabu unit in middle part (Takeda *et al.*, 1977; Tsukuda *et al.*, 1981; Takeda, 1984; Hada and Kurimoto, 1990) and by the Sogauchi nappe in northern part (Hara *et al.*, 1991a, b), as shown in Figs. 2, 7, 14 and 16. The nappe of the Chichibu megaunit I is comparable with the Niyodo nappe by Hada and Kurimoto (1990), showing that it is a late middle Jurassic accretionary complex. The northern part of the nappe, which is covered by the Sogauchi unit, has so far been called Sakamoto nappe (Hara *et al.*, 1990a).

The geological structure of eastern Kyushu - eastern Shikoku (Figs. 2 and 4) indicates that the Chichibu megaunit I is comparable with the geological unit, which has so far been described in terms of the Southern Chichibu Terrane and Sambosan Terrane by many authors (*e.g.* Sonoda and Hara, 1984; Ishida, 1985; Matsuoka and Yao, 1990; Tominaga, 1990). The uppermost member of the Chichibu megaunit I in eastern Kyushu, which is covered by the Chichibu megaunit II, is an accretionary complex of late middle Jurassic age [Unit A after Sonoda and Hara (1984)] (Fig. 5). According to the data of Ishida (1985) and Tominaga (1990), the Chichibu megaunit I (= Southern Chichibu Terrane) in eastern Shikoku, which is covered by the Chichibu megaunit II, appears to consist of accretionary complexes of late middle Jurassic age, latest Jurassic age, Valanginian age, Barremian age and Albian age in descending order, and is underlain by the Shimanto megaunit, showing that the formation of the accretionary complexes occurred successively but episodically with a downward younging age polarity.

The Shimanto megaunit in the region away to the south from the MTL is covered by the Albian accretionary complex of the Chichibu megaunit I (= Southern Chichibu Terrane) and its uppermost member is of Cenomanian-Turonian age, according to the data of Tominaga (1990) in eastern Shikoku. While, according to the data of Kanai *et al.* (1990) in the central part of Kii Peninsula, the

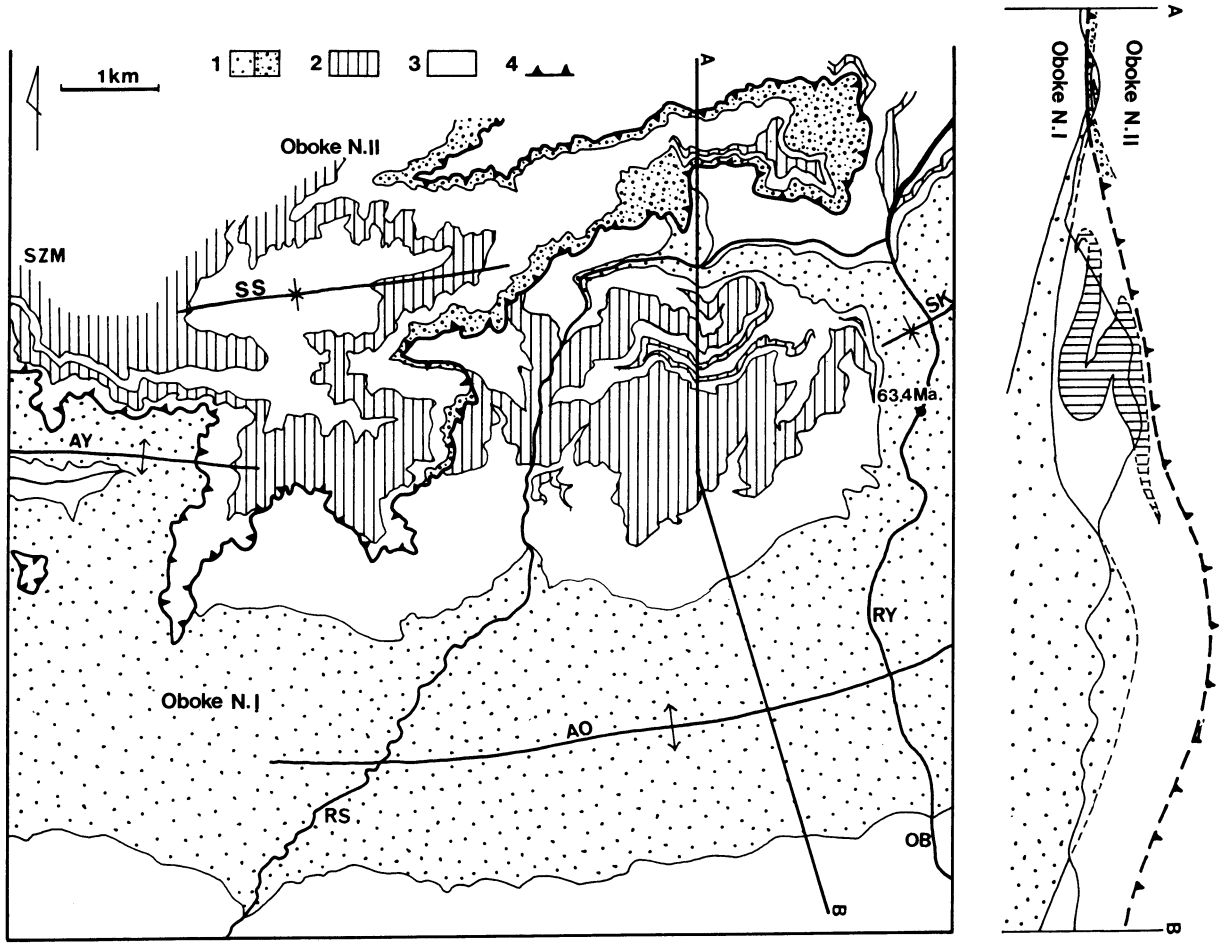

Fig. 18 Geological map of the Oboke district [data of Akiyama, Hara, Shiota and Hide (1989)].
1: psammitic schists, 2: basic schists, 3: pelitic schists, 4: nappe boundary, AO: Oboke antiform, AY: Yakushi antiform, SK: Koboke synform, SS: Shiozukamine synform, OB: Oboke, SZM: Shiozukamine, RY: River Yoshino, RS: River Shirakawa.

Shimanto megaunit in the region near the MTL, whose uppermost member is also an accretionary complex of Cenomanian-Turonian age, is covered by the lower member of the Sambagawa megaunit (Fig. 17), which is structurally regarded as an eastern extension of the Sogauchi nappe in Shikoku. In the region near the MTL of central Shikoku (Figs. 13 and 14), the Sogauchi unit is underlain by the Chichibu megaunit I (Sakamoto nappe) in its southern part and by the Oboke unit [Oboke nappe II and Oboke nappe I (Figs. 14 and 18)] in its northern part. As illustrated in Fig. 19 and mentioned in the later section, radiometric ages of muscovite flakes of the Oboke unit, which are regarded as the age of its metamorphism, are essentially the same as these of the uppermost member of the Shimanto megaunit in the central part of Kii Peninsula, which shows Cenomanian-Turonian fossil age (Kanai *et al.*, 1990). Regarding with such the data of structural position and radiometric ages, it has been assumed by Hara *et al.* (1990a, 1991a) that the Oboke unit is an accretionary unit of the same generation as the uppermost member of the Shimanto megaunit which is of Cenomanian - Turonian age.

On the basis of the above-mentioned evidence and consideration, the following points will be summarized about the relationship between the Sambagawa megaunit and its surrounding megaunits. In the region near the MTL the Sambagawa megaunit is intercalated between the Chichibu megaunit II as early Jurassic - late Jurassic accretionary complexes with downward younging age polarity and the uppermost member of the Shimanto megaunit as Cenomanian-Turonian accretionary unit, and in the region away to the south from the MTL the Chichibu megaunit I occurs as an wedge intercalated between the Sambagawa megaunit and the Shimanto megaunit (Fig. 15). The formation of the accretionary complexes from the Chichibu megaunit I to the uppermost member of the Shimanto megaunit occurred successively but episodically through the period from middle Jurassic age to Cenomanian-Turonian age, showing a downward younging age polarity. The lower units of the Chichibu megaunit II, which cover the Sambagawa megaunit, are of the same generation as the upper units of the Chichibu megaunit I, both being middle Jurassic and late Jurassic accretionary units. As mentioned in details in the later pages, radiometric ages of constituent units of the Chichibu megaunit II, Chichibu megaunit I and Shimanto megaunit, which are considered to be their metamorphic ages, show a clear downward younging age polarity

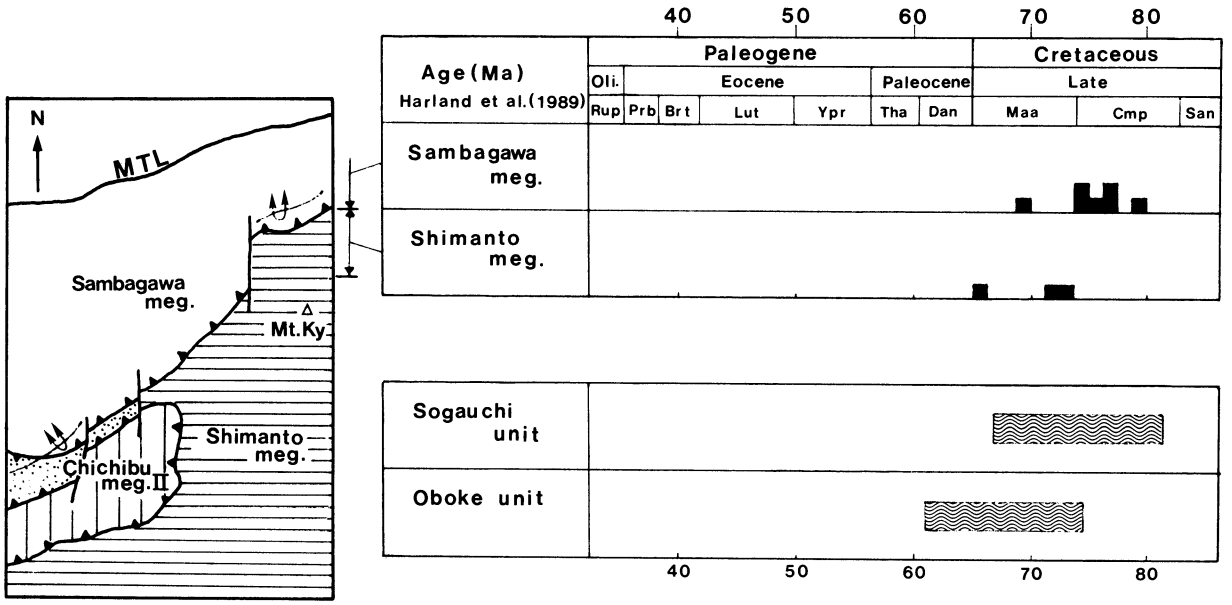

Fig. 19 K-Ar age data for muscovite in pelitic rocks of the Sambagawa megaunit and the Shimanto megaunit developed in the Kuzuwa district just on the north of Mt. Koyasan, Kii Peninsula [data from Kanai *et al.* (1990)]. Age data for the Sogauchi unit and Oboke unit in Shikoku are also shown in this diagram.

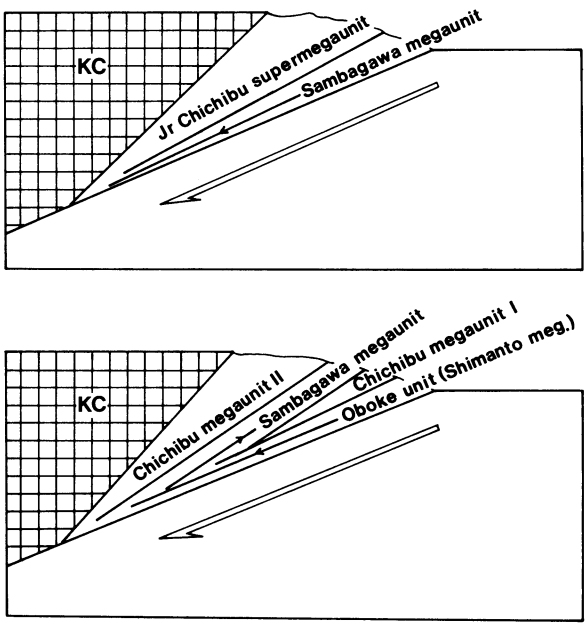

Fig. 20 Schematic diagram illustrating the style of exhumation of the Sambagawa megaunit giving rise to the separation of the Jurassic Chichibu supermegaunit into the Chichibu megaunit II and the Chichibu megaunit I. KC: Kurosegawa-Koryoke continent.

in harmonic fashion with their fossil ages. Analogous downward younging age polarity is also clearly found among the Chichibu megaunit II, the Sambagawa megaunit and the Shimanto megaunit. It has been therefore assumed by Hara *et al.* (1991a, b) that the Sambagawa megaunit is deeper equivalents of the lower units of the Chichibu megaunit I described by Ishida (1985), Valanginian, Barremian and Albian accretionary units, and that the exhumation of the former from the depth occurred along a route different from that of the latter, separating the Chichibu supermegaunit into the Chichibu megaunit II and the Chichibu megaunit I, as schematically shown in Fig. 20. The details of such the exhumation processes of the Sambagawa megaunit will be described in the next section.

III. Tectono-Metamorphic History of the Sambagawa Megaunit

The metamorphic facies analysis of the Sambagawa megaunit in central Shikoku has been performed by Kurata and Banno (1974), Higashino (1975), Enami (1983), Watanabe and Kobayashi (1984) and Banno and Sakai (1989), clarifying that the facies series of pelitic schists defined by minerals crystallized during the highest-temperature phase of metamorphism can be explained in terms of chlorite zone, garnet zone, albite-biotite zone and oligoclase-biotite zone and that, in the high grade part of the chlorite zone, crossite is found in hematite-bearing basic schists and, in its just underlying part of the chlorite zone, pelitic schists contain the quartz-lawsonite-albite assemblage. Banno and Sakai (1989) said that the boundary between the albite-biotite zone and the garnet zone occurs within the barroisite zone with reference to the highest-temperature phase mineral assemblage in hematite-bearing basic schists, while Hara *et al.* (1990a, b) showed that hornblende and glaucophane are in general found in these of the albite-biotite zone and these of the garnet zone respectively. According to Banno and Sakai (1989), the pressure and temperature conditions of the metamorphism for the above-mentioned

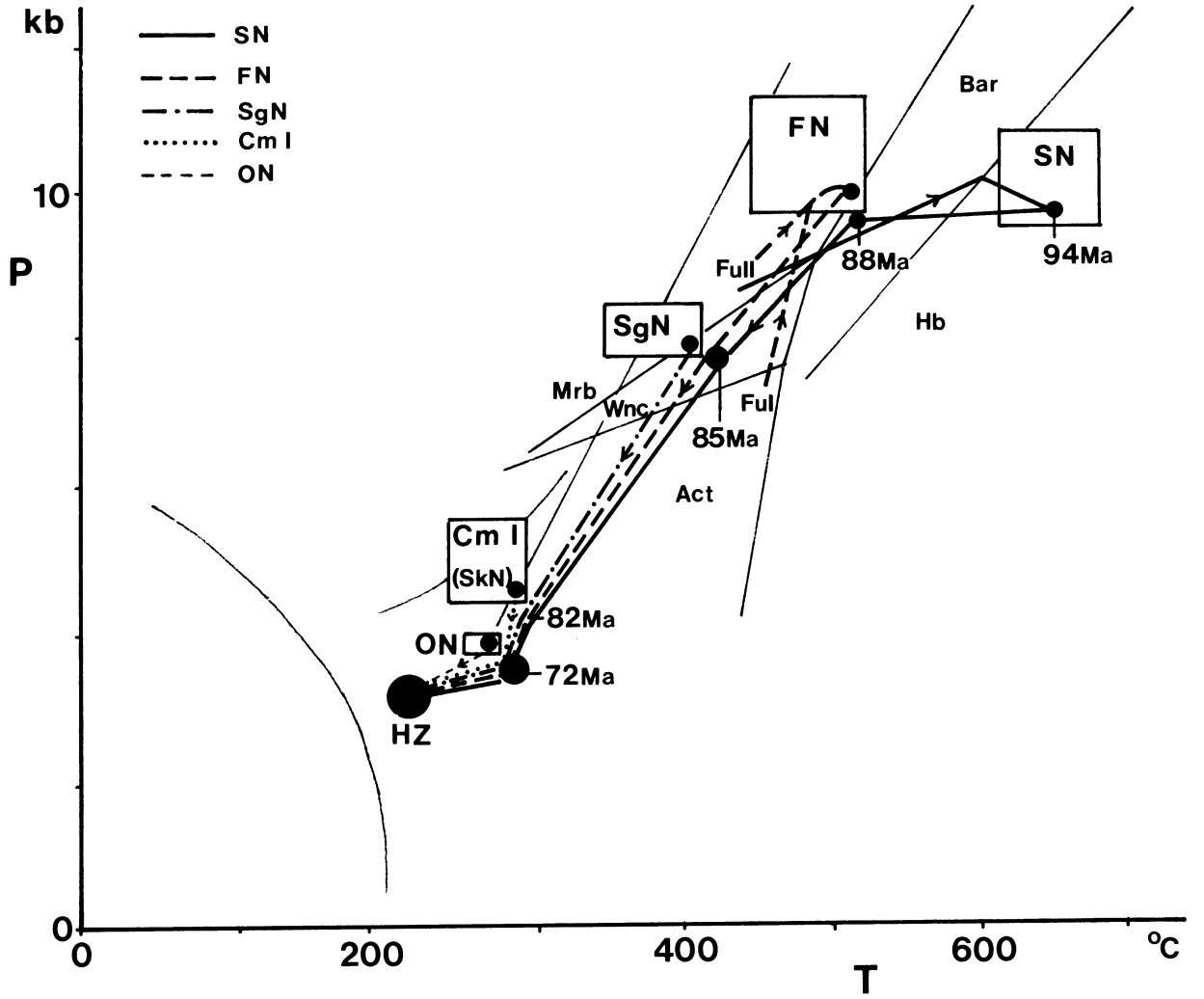

Fig. 21 P-T-t path of the Sambagawa megaunit in central Shikoku.
SN: Saruta nappes, FN: Fuyunose nappe (FuI: Fuyunose subunit I for the prograde phase, FuII: Fuyunose subunit II for the prograde phase), SgN: Sogauchi nappe, CmI: Chichibu megaunit I (SkN: Sakamoto nappe), ON: Oboke nappe, HZ: Hijikawa phase, Hb: hornblende, Bar: barroisite, Mrb: magnesio-riebeckite, Wnc: winchite, Act: actinolite, P: pressure, T: temperature.

zones appear to be illustrated in Fig. 21.

As shown in Fig. 13 for the part of the pre-Ozu phase pile nappe structures, the Saruta nappe II consists of a garnet zone in upper part, an albite-biotite zone in middle part and an oligoclase-biotite zone in lower part, the Saruta nappe I of an albite-biotite zone with blocks of oligoclase-biotite zone rocks, the Fuyunose nappe of a garnet zone, the Sogauchi nappe of a high grade part of the chlorite zone and the Chichibu megaunit I (Sakamoto nappe) of the chlorite zone with the quartz-lawsonite-albite assemblage. In western Shikoku is widely developed the western extension of the Sogauchi nappe, which overlies the Chichibu megaunit I [Hataki nappe (Figs. 6 and 14)]. In hematite-bearing basic schists are found crossite with high (Na + Al^{VI}) content for the eastern part of the Sogauchi nappe and crossite with low (Na + Al^{VI}) content - magnesio-riebeckite and/or winchite for the western part (Fig. 22). It may be thus roughly said, as schematically shown in Fig. 23, that the metamorphism occurred under the lower temperature and pressure condition in the latter than in the former.

The rock structure of the Sambagawa megaunit (Saruta unit, Fuyunose unit and Sogauchi unit), Chichibu megaunit I (Sakamoto nappe - Niyodo nappe) and Shimanto megaunit (Oboke unit) is generally characterized by schistosity of single set, which is commonly parallel to the lithologic layering and has been therefore so far called bedding schistosity by Japanese geologists, though many intrafolial (and rootles intrafolial) folds of various scales are frequently intercalated in the schistosity. The deformation of the Sambagawa megaunit and its surroundings appears to have been related to the formation of the bedding schistosity and intrafolial folds during the most phases of their subducting and exhumation processes. The generation processes of such the bedding schistosity and intrafolial folds of the Sambagawa megaunit have been examined by Hara *et al.* (1966, 1973) on the basis of analysis of pebble deformation and by Takagi and Hara (1979), Hara *et al.*

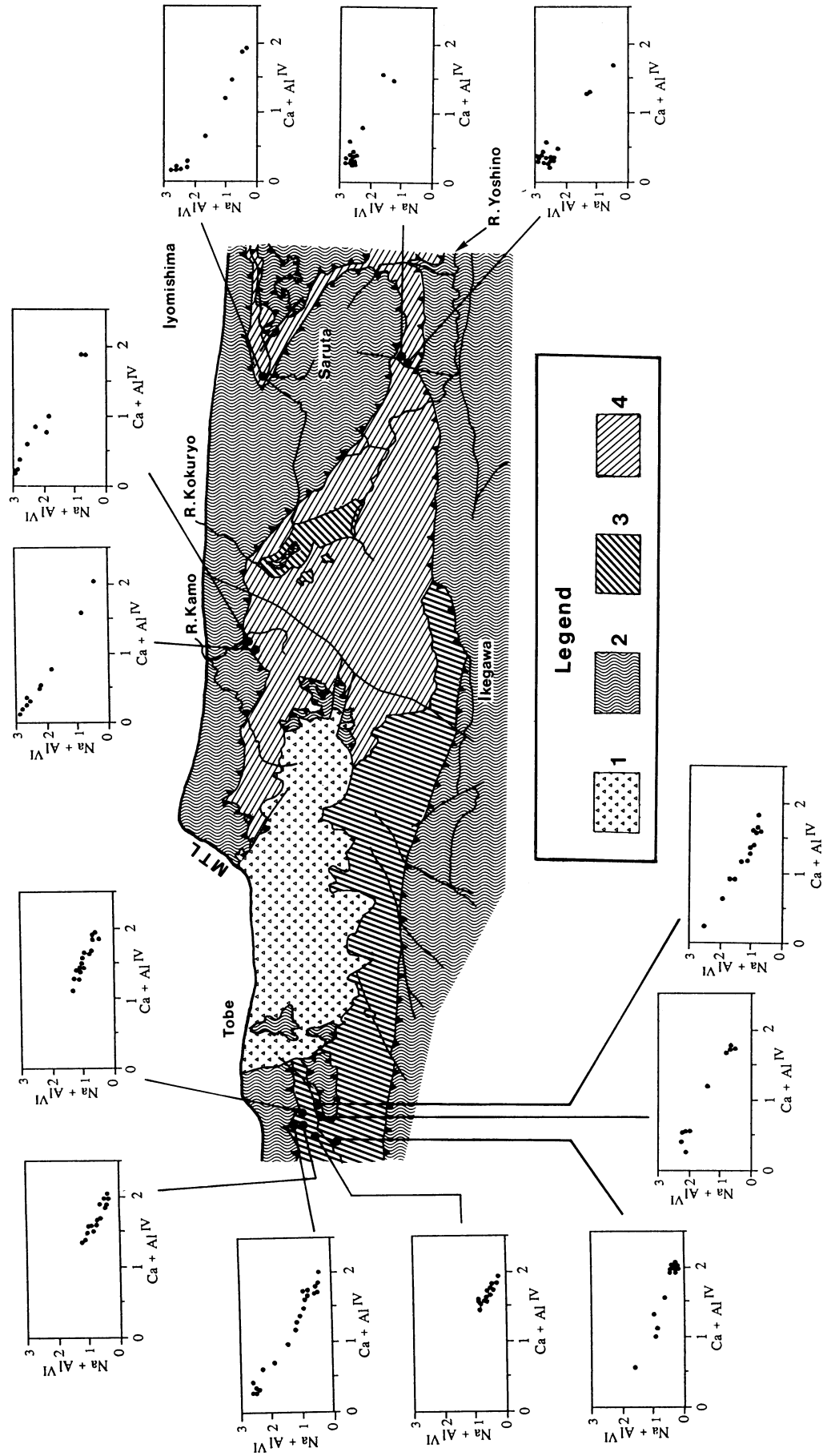
Iyomishima
Saruta
R.Kokuryo
R.Kamo
R.Yoshino
MTL
Tobe
Ikegawa
Legend
1
2
3
4
Na + Al^VI
Ca + Al^IV

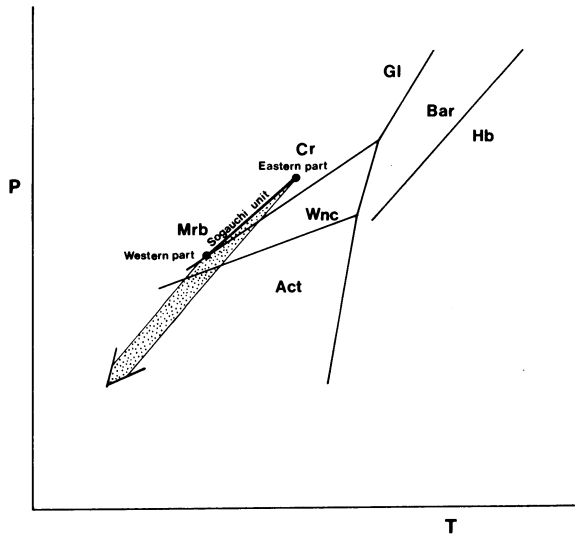

Fig. 23 Metamorphic condition of the Sogauchi unit assumed from the data of Fig. 22.

(1980a, 1983, 1984a, 1985, 1988, 1990a) and Maeda and Hara (1983, 1984) on the basis of analysis of relationships between the crystallization of its constituent minerals such as quartz, plagioclase, garnet, biotite, muscovite and amphibole and their deformation, clarifying its tectono-metamorphic history as shown in Fig. 24 (Hara *et al.*, 1990a, c). It has been also clarified by Hara *et al.* (1983, 1988) that such the deformation processes were commonly associated with the formation of quartz veins (faulting and fracturing) parallel and oblique to the bedding schistosity (Figs. 25 and 26). These works take over previous ones by some students of the Sambagawa schists such as Kojima (1958) and Hide (1961). The tectono-metamorphic processes of the Sambagawa schists, which produced such the nature of rock deformation and metamorphism, will be described in the following pages.

In Fig. 24 as a summary of the tectono-metamorphic processes of the Sambagawa schists, S as initial letter of each phase is S of schistosity. This is because the deformation of each phase is in general shown by the formation of single schistosity (or cleavage). c of ic is c of cores of garnet and i is i of internal schistosity (Si) in garnet cores. b of b1 (b2-1, b2-2 and b3) is b of initial letter of bed (lithologic layering). This is because the deformation of each phase is related to the formation of the bedding schistosity (Hara *et al.*, 1988, 1990a) and numbers 1, 2-1, 2-2 and 3 indicate order of its successive phases. B of Bic (and Bim) indicates snow ball Si in garnet cores (and Si fold in garnet inner mantles).

A. Tectono-Metamorphic History of Prograde Phase of the Saruta Unit

The tectono-metamorphic history of the Saruta unit will be first illustrated. According to Banno and Chii (1976) and Sakai *et al.* (1985), garnet in the Saruta unit and the Fuyunose unit show in general chemical zoning of normal type and grew under increasing temperature, except for its rims which show reverse zonation of chemical composition and grew under retrograde metamorphism. Such chemical zonation for the prograde phase is shown in the Mn-Fe-Mg diagrams of Fig. 27. In cores of garnet is quite rarely found detrital garnet, which show chemical zonation different from that produced under the Sambagawa metamorphism, as shown in Fig. 27-f. Analogous examples have been also described in the Saruta nappe (I + II) schists by Higashino and Takasu (1982).

Garnet in the Saruta unit, except for rims with reverse zonation, is frequently divided into two zones, cores and mantles (Fig. 28), with reference to discontinuity of Si fabrics, though mantles are frequently further divided into two subzones, inner mantles and outer mantles (Fig. 29) (Hara *et al.*, 1984a, 1986a; Maeda and Hara, 1984; Hara and Goto, 1986). The deformation of the Bic phase shown in Fig. 24 was responsible for the formation of snow ball textures of garnet cores (Fig. 28-a and b) and occurred during their growth. In Fig. 28-c and d and Fig. 30-b the Si schistosity Sic in garnet cores appears to be straight, suggesting that it grew under non-deformational condition during the Bic phase after the deformation [Sic deformation (Fig. 24)] related to the formation of Sic. It can be said that the Bic deformation was of non-penetrative type in the Saruta unit. The orientation pattern of Si schistosity Sim in garnet mantles of Fig. 28-c and d, which is discontinuous with Sic in garnet cores, indicates shear strain [Sim-Bim deformation in Fig. 24] around garnet cores, and garnet mantles grew under non-deformational condition during the Nd phase (Fig. 24) after the Sim-Bim deformation. While the Si fabric of garnet mantle of Fig. 30-b indicates flattening around garnet core.

Maeda and Hara (1984) described such Si fabrics of garnet mantles in a psammitic schist specimen as shown in Fig. 30-a and b: In Fig. 30-b Sic is oblique to and discontinuous with Sim, showing that Sim postdates Sic. In Fig. 30-a, also, Sim is deflected around garnet core, though it forms fold shape. They have therefore pointed out that Sim was produced around garnet cores under flattening [Sim deformation (Fig. 24)] and then folded [Bim deformation (Fig. 24)] before the growth of garnet mantles under non-deformational condition, distinguishing between the Sim deformation and the Bim deformation.

As garnet mantles are divided into two subzones (Fig. 29), Si fabrics of inner mantles and these of outer mantles are related to the deformation of the Sim-Bim phase and to that of the Som phase in Fig. 24 respectively. The orien-

Fig. 22 Diagram showing the spatial variation in chemical composition of amphibole in hematite-bearing basic schists of the Sogauchi nappe [compiled from data of Seki, Hara and Takeda (1992) and Nakamura (1991)].
1: Ishizuchiyama Tertiary System, 2: schists complexes overlying and underlying the Sogauchi nappe, 3 and 4: Sogauchi nappe (3: lower member, 4: upper member).

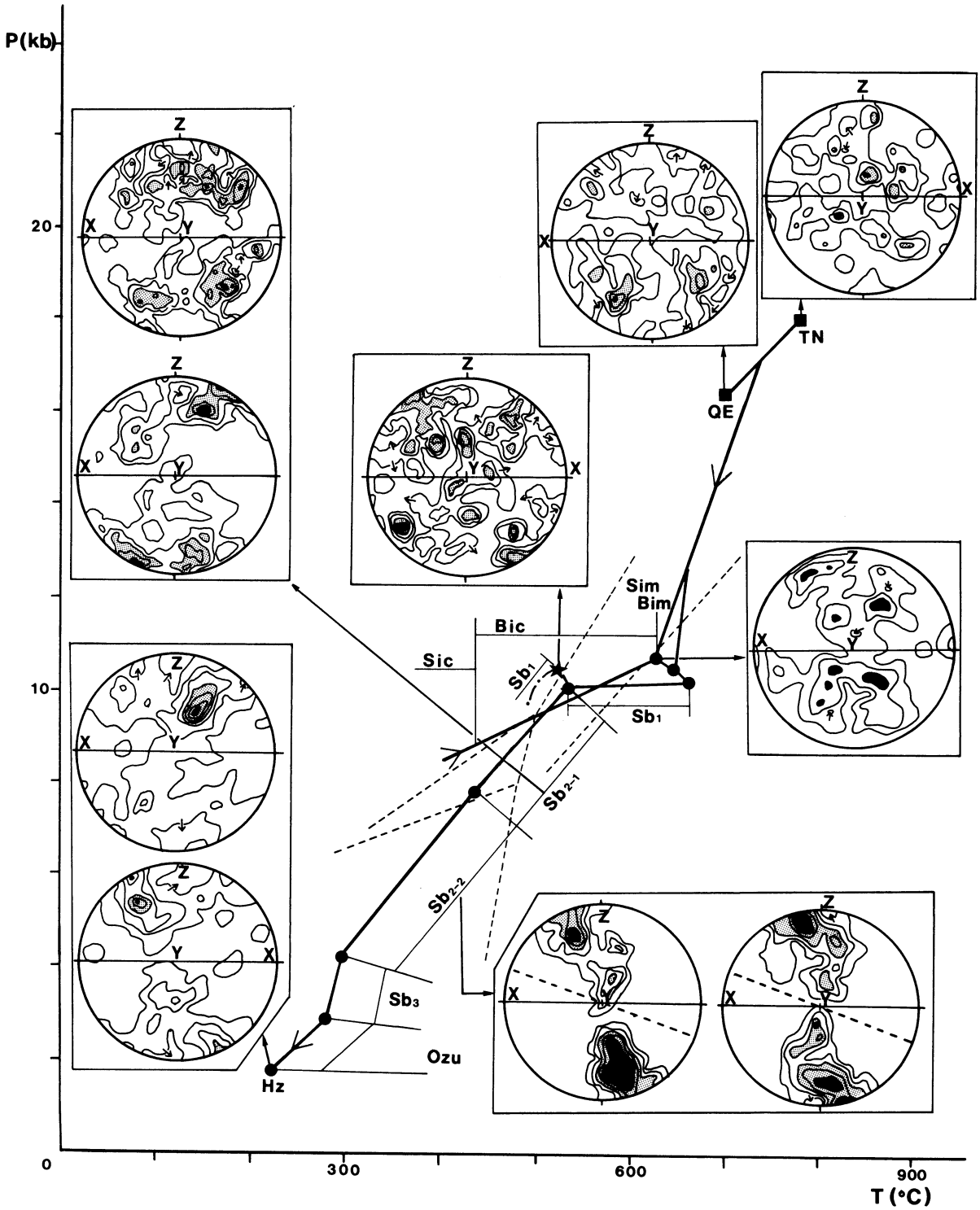

Fig. 24 Diagram showing the tectonic history of the Sambagawa megaunit and its surroundings and quartz c-axis fabrics produced during each tectonic event. The data of quartz fabrics are from Hara and Paulitsch (1971), Hara *et al.* (1989), Sakakibara *et al.* (1992) and the present authors. QE: quartz eclogite, TN: Tonaru metagabbro, solid star: Fuyunose nappe schists during the peak metamorphism, solid line and solid circles: deformation phases of the Saruta nappe (I + II) schists. Prism [a] slip appears to have been dominantly active only in quartz deformation under metamorphic conditions (eclogite facies) related to the formation of Tonaru metagabbro and quartz eclogite. For fuller explanation see the text.

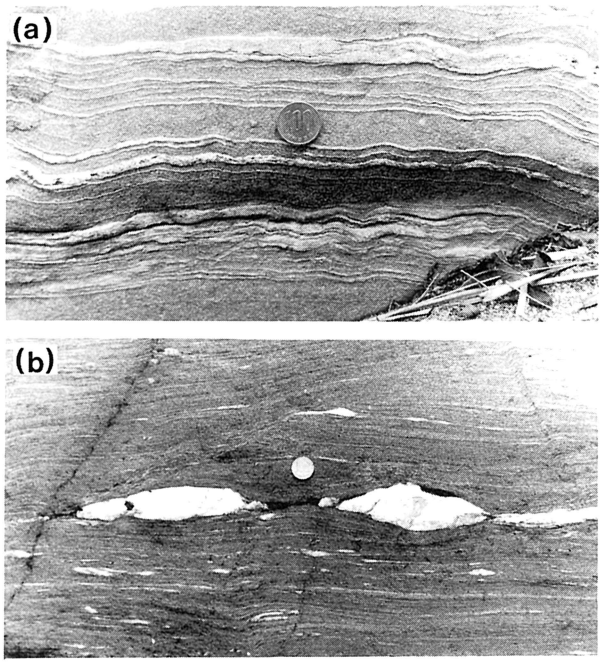

Fig. 25 Two examples of schistsosity-parallel quartz veins commonly developed in the various types schists of the Sambagawa megaunit and surroundings.
a) quartz veins in psammitic schists of the Oboke nappes of the Oboke district, which do not show vein-parallel shear but vein-normal extension.
b) quartz veins in pelitic schists of the Fuyunose nappe of the River Saruta district, which show vein-parallel shear.

Fig. 26 Diagram showing the frequency of development of schistsosity - parallel quartz veins in the River Saruta district as number of the veins found within each outcrop of 20 m as measured in a direction normal to the trend of the bedding schistsosity [data from Hara *et al.* (1988)]. The blank parts on the histogram correspond to these in which any outcrop is not found. n: number of quartz veins, 1: pelitic schists, 2: siliceous schists, 3: basic schists, GZ: garnet zone, BZ: biotite zone, TS: Tsuneyama synform.

tation pattern of Si schistosity around garnet cores and that around garnet inner mantles in Fig. 29-a and b both are ascribed to flattening. The boundaries between inner mantles and outer mantles are clearly, though partly, defined by dust rings. In Fig. 29-c and d they are almost completely shown by dust rings.

Fig. 31-a indicates that the growth stratigraphy of outer mantle is further divided into two subzones with reference to discontinuity of Si fabric, which correspond to the deformation of the Wd phase in Fig. 32. Such subzones of outer mantles are only rarely found, probably showing that the deformations during the Wd phase were not penetrative. Fig. 31-c indicates that the Si fabric in garnet is homogeneous in its whole part from central part to outer part, being characterized by development of a straight Si schistosity, though the chemical composition of its central part and that of its outer part are comparable with that of cores and that of outer parts of mantles of garnet grains in Figs. 28 and 29, as mentioned in the later pages. It would be now said that, as established with reference to Si fabrics of garnet, the deformation history of prograde phase of the Saruta unit is divided into Sic phase, Bic phase, Sim-Bim phase, Nd phase, Som phase and Wd phase in order of younging (Fig. 32) (Hara *et al.*, 1984a, 1990a) and that all the deformations during the Bic, Sim-Bim, Som and Wd phases were not completely penetrative throughout the Saruta unit schists. The Sim-Bim deformation and Som deformation appear to have commonly resulted in the formation of schistosity under mean strain of flattened type as based on observation of Si fabrics in many garnet grains. The schistosity must have been parallel to the lithologic layering.

The detailed observation of the chemical variation of garnet on Mn-Fe-Mg diagrams for the Saruta unit indicates that the boundaries between cores and inner mantles and between inner mantles and outer mantles are frequently defined also by a discontinuous increase in Mg content and by that in Mn content as shown in Fig. 33 (Hara and Goto, 1986; Hara *et al.*, 1990a, b), though the discontinuous changes occur in various styles and magnitudes as examined in the later pages. The last stage of the Wd phase, when outermost mantles of garnet with the lowest Mn content grew, i.e. the peak metamorphism occurred, will be here called Spm phase (Fig. 32). The bedding schistosity, which is deflected around garnet mantles (Figs. 28, 29 & 30), has been called Sbl schistosity. It appears to be of the same generation as garnet rims with higher Mn content, whose growth corresponds to the beginning of retrograde metamorphism during the Sbl phase in Figs. 24 and 32 (Hara *et al.*, 1990a). In pelitic schists of the oligoclase-biotite zone are rarely found fine garnet grains [Sb1 garnet (Hara *et al.*, 1990a)], whose whole parts from cores to rims have the same chemical composition as garnet rims with higher Mn content and Mg content, (Fig. 31-d). Garnet grains are

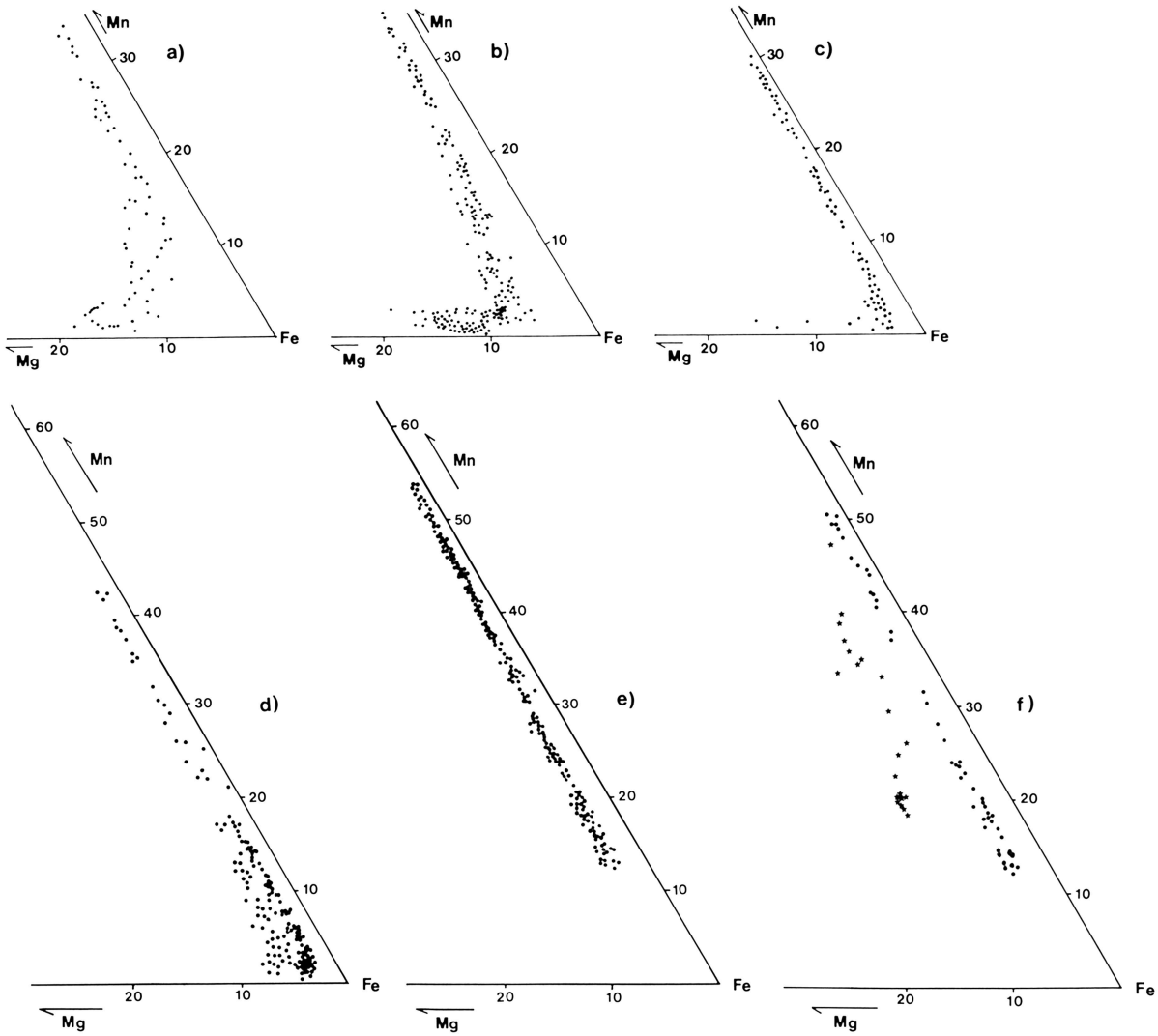

Fig. 27 a), b) and c): Mn-Fe-Mg diagrams for garnet in pelitic schists of the oligoclase-biotite zone of the Saruta nappes. a) data from some specimens of pelitic schists just adjacent with the Shirataki V amphibole schist of the Saruta nappe II, b) data from some specimens of pelitic schists of the northern part of the oligoclase-biotite zone of the Saruta nappe II in the Shirataki-Joshi district, c) data from some specimens of pelitic schists of the Saruta nappe I just in contact with the Tonaru metagabbro in the Hiuradani district. In these figures are clearly shown three variation types of chemical composition of garnet in pelitic schists found in the oligoclase-biotite zone. The pelitic schists just around the Tonaru metagabbro may have been derived from the greater depth than others. d) and e): Mn-Fe-Mg diagrams for garnet in pelitic schists of the Fuyunose nappe (garnet zone). d) data from the high-temperature part of the Fuyunose nappe of the River Asemi district, e) data from the low-temperature part of the Fuyunose nappe of the Shirataki district. f) data for garnet with cores of sedimentary garnet clasts (crosses) in pelitic schists of the Fuyunose nappe of the Shirataki district.

rarely replaced by the Sb1-foming amphibole in their pressure shadows (Fig. 31-e) in basic schists, in which amphibole shows the retrograde growth history of Type I (cf. Hara *et al.*, 1988, 1990b). While Fig.31-f suggests that mantles (lower Mn part) of garnet grains in pelitic-siliceous schists are replaced greatly by the Sb1-forming chlorite but in a little amount by the Sb1-forming biotite in their pressure shadows. But, Fig. 31-d shows biotite crystallized together with the Sb1 garnet with higher Mn and Mg content. The chemical composition of this biotite is essentially the same as that of the Sb1-forming biotite (Hara *et al.*, 1984a, 1990c). It can be therefore said that the growth of retrograde garnet occurred only during the high-temperature stage of the Sb1 phase and that the growth of Sb1 garnet as single grains in the high-temperature part of the Saruta nappe (I + II) schists is ascribed to their strong deformation during the Sb1 phase. As mentioned in the later page, garnet appears to have been deformed by pressure solution in the deformations of the later phases than the Sb1 phase (Hara *et al.*, 1984b).

Plagioclase in the Saruta unit is porphyroblasts containing other kinds of metamorphic minerals as inclusions (Figs. 34 and 35). On the basis of analysis of chemical composition of inclusion and matrix amphibole, Takagi and Hara (1978) clarified that plagioclase porphyroblasts in the Saruta unit crystallized during two phases of its tectono-

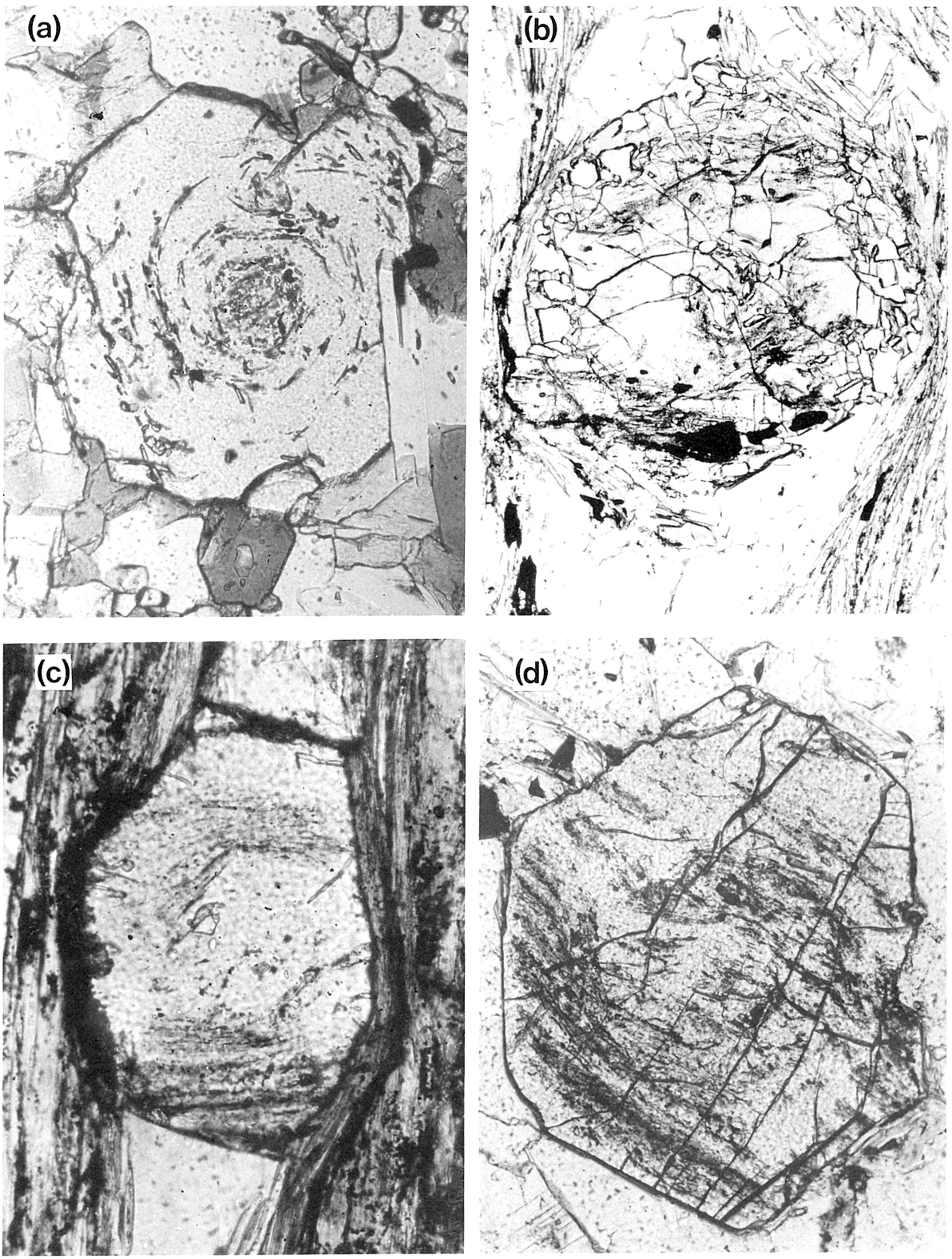

Fig. 28 Microphotographs of garnet in the Saruta nappe (I + II) schists, which is divided into two zones, cores and mantles, with reference to Si fabrics.
a) garnet with snow-ball core in basic schists of the Sebadani district, b) garnet with snow-ball core in pelitic schists of the oligoclase-biotite zone of the River Asemi district, c) garnet in pelitic schists of the Saruta nappe I of the Besshibashi district, consisting of core with straight Si schistsosity and mantle with shear strain type Si fabric, d) garnet in pelitic schists of the Saruta nappe I of the Shirataki district, consisting of core with straight Si schistsosity and mantle with shear strain type Si fabric.

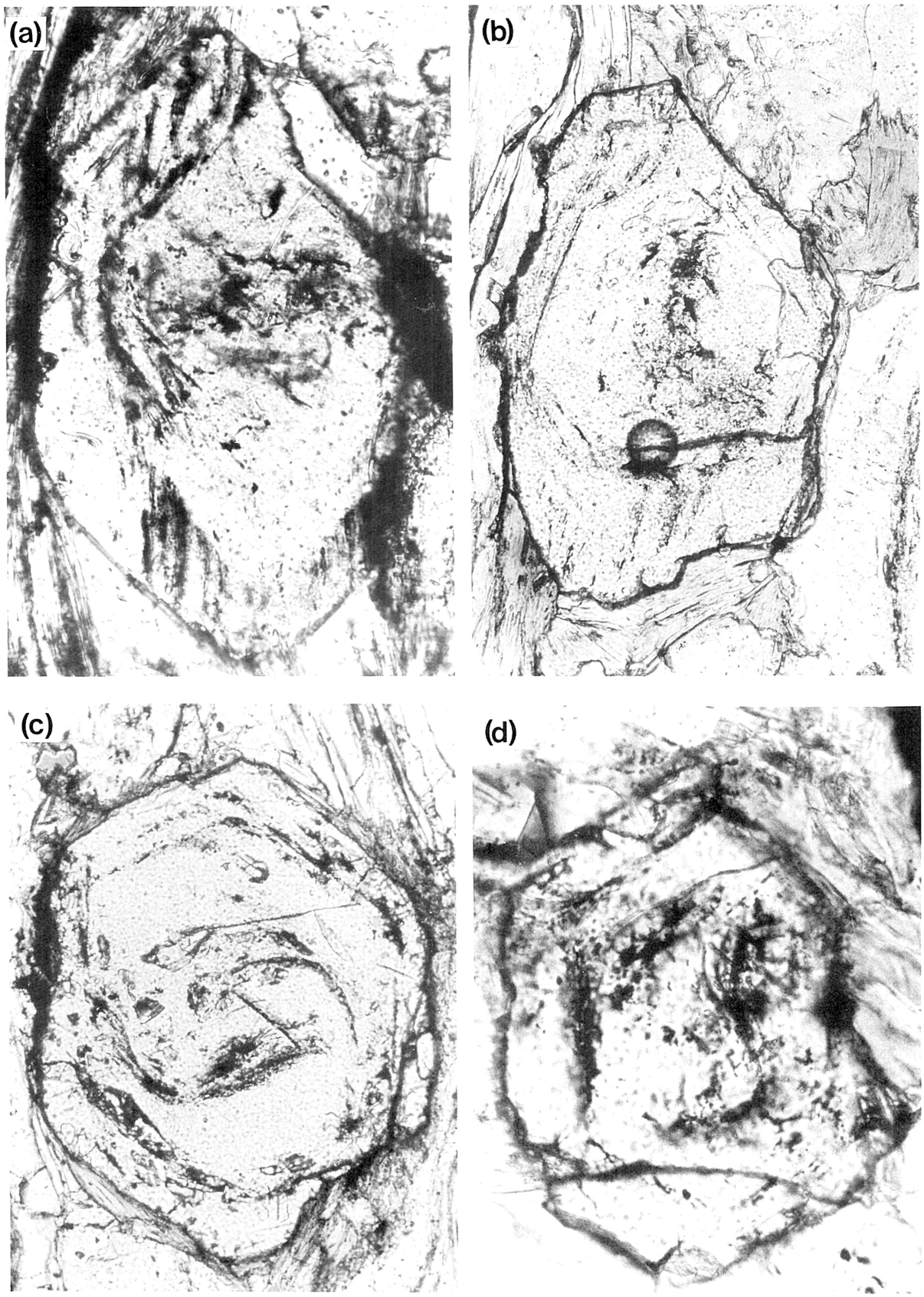

Fig. 29 Microphotographs of garnet in the Saruta nappe (I + II) schists, which is divided into three zones, cores, inner mantles and outer mantles, with reference to Si fabrics. a) and b) The boundary between core and inner mantle and that between inner mantle and outer mantle are partly defined by dust rings. Si fabrics of inner and outer mantles are of flattening type. The specimen (a) is from pelitic schists of the Saruta nappe I of the Togu district and the specimen (b) is from pelitic schists of the Saruta nappe II of the Joshi district. c) and d) The boundary between inner mantle and outer mantle is completely defined by a dust ring. The inner mantles are almost free from inclusion minerals and partly absent in a direction normal to the long axis of garnet as examined from the distribution of chemical composition.

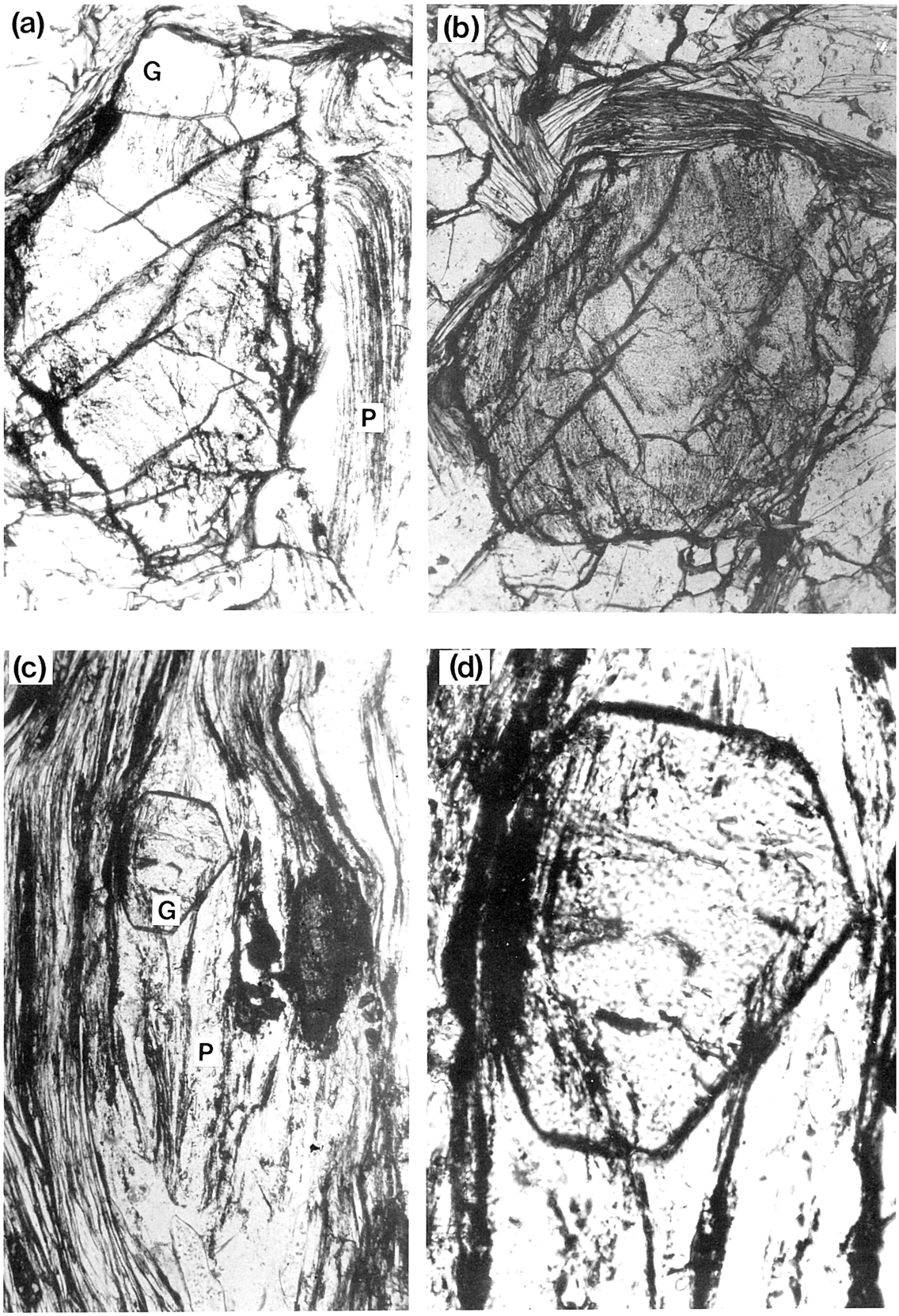

Fig. 30 Microphotographs showing the relationship between Si fabrics of garnet and plagioclase porphyroblast. a) and b) data from Maeda and Hara (1984).
Core of garnet (G) in (a) is free from inclusion minerals. Si fabric of garnet mantle and plagioclase porphyroblast (P) core in (a) shows a fold form. The Si fabric of garnet mantle in (b) is of flattening type. d) and c) Garnet (G) included in plagioclase porphyroblast core (P) in a specimen from pelitic schists of the Saruta nappe I in the Togu district, showing that the Si fabric of garnet mantle is continuous and harmonic with that of plagioclase porphyroblast core. This specimen is the same as that of Fig. 29-a. Garnet in plagioclase porphyroblast is free from the part corresponding to the outer mantle of garnet of Fig. 29-a.

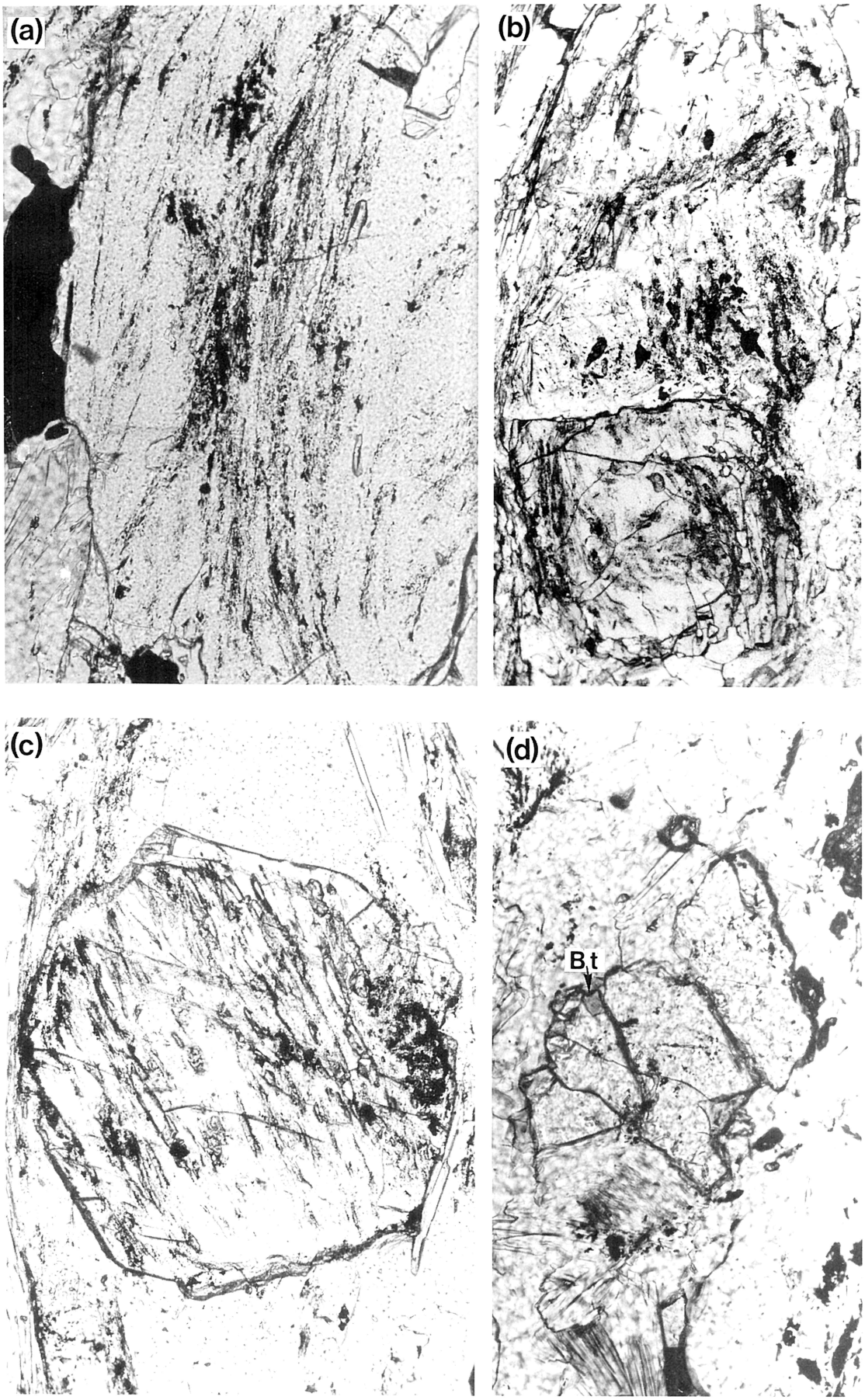
(a)
(b)
(c)
(d)
Bt

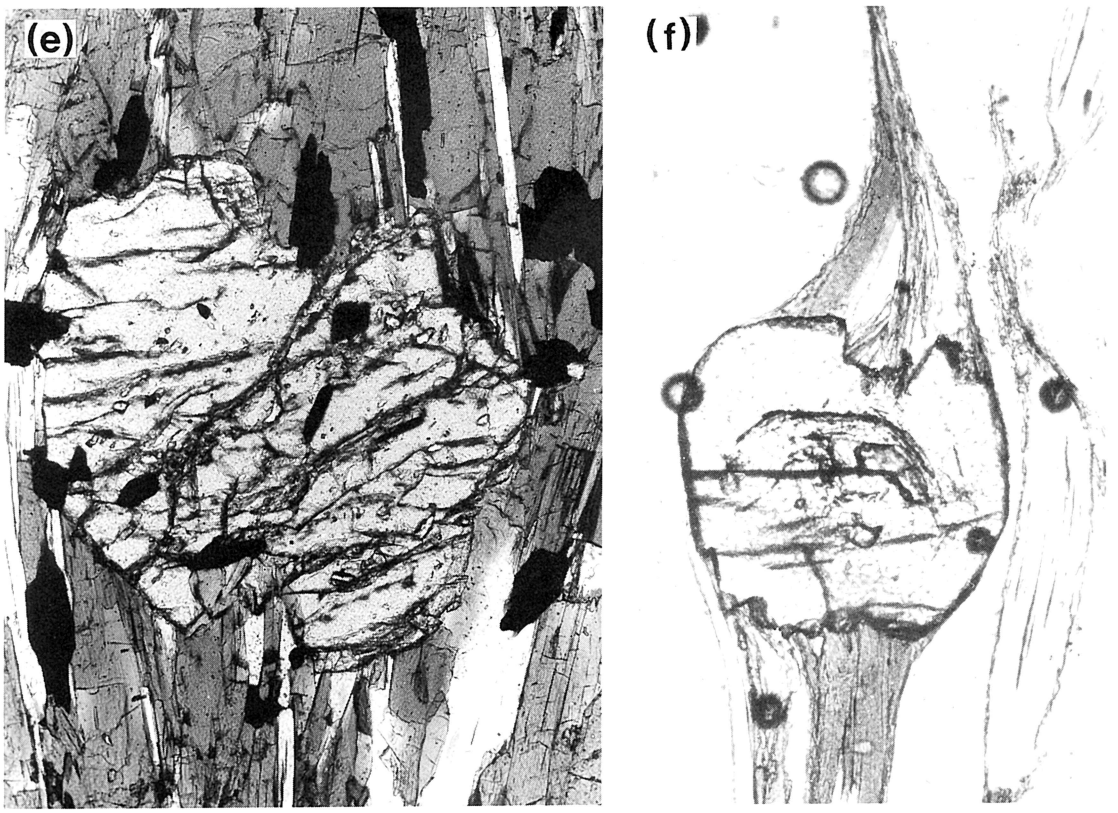

Fig. 31 a) Microphotograph of garnet in a specimen from pelitic schists of the Saruta nappe II of the River Asemi district, in which mantle is divided into three subzones with reference to Si fabric, b) microphotograph showing the relationship between Si fabrics of garnet and plagioclase porphyroblast in a specimen from pelitic schists of the Saruta nappe II of the River Asemi district (Hara *et al.*, 1984a). The Si fabric of garnet inner mantle and that of garnet outer mantle are harmonic with that of plagioclase porphyroblast core and that of plagioclase porphyroblast inner mantle respectively (see a sketch of Fig. 38). c) microphotograph of garnet in a specimen from pelitic schists of the Saruta nappe I of the Hodono district, showing a straight Si schistosity in the whole part from core to outer mantle. d) garnet of retrograde phase (Sb1 garnet) in a specimen from pelitic schists of the Saruta nappe II of the River Asemi district. Bt: biotite crystallized together with Sb1 garnet. e) replacement of the low Mn part of garnet by Sb1-forming amphibole in pressure shadow (data from the Shirataki V amphibole schist of the River Asemi), f) replacement of garnet by Sb1-forming biotite and chlorite in pressure shadow (data from siliceous schist of the oligoclase-biotite zone of the Saruta nappe II of the River Asemi). The Sb1-forming biotite replaces only the lowest Mn part of garnet but it is in paragenetic relation with the Sb1 garnet with higher Mn content and Mg content (d).

metamorphic history, i.e. prograde phase and retrograde phase, though retrograde phase porphyroblasts are rarely found in minor shear zones highly strained during the retrograde phase (Fig. 34-d). In this figure is found plagioclase porphyroblast including a median segment of conjugate kink bands.

Plagioclase porphyroblasts of prograde phase have so far been studied clarifying following points: They (PPP) are divided into two zones, cores and mantles (Fig. 35-a and c), or three zones, cores, inner mantles and outer mantles (Fig. 35-b and e), with reference to discontinuity of Si fabrics (Takagi and Hara, 1979; Hara *et al.*, 1980a, 1983, 1984a). Hara *et al.* (1983, 1990a) clarified that there are distinct variations in chemical composition and shape among amphibole in cores, that in inner mantles and that in outer mantles of PPP (Fig. 36-A and B). As shown in Fig. 35-b and c, amphibole in PPP inner mantles is coarse-grained with other kinds of metamorphic minerals as inclusions, while, as shown in Fig. 35-a and b, that in PPP outer mantles is clearly finer-grained than the former and shows slender shapes, which are preferably oriented along the bedding schistosity. The former is also found as relict mineral in matrix (Fig. 35-c and d). In most of basic schists of the Saruta unit, but, matrix amphibole grains are mostly of the same generation as PPP outer mantles as is obvious in Fig. 35, though equivalents of amphibole in PPP inner mantles are quite rarely found in greater volume in matrix (Hara *et al.*, 1983, 1990a). The chemical data of these three types amphibole are reproduced in Fig. 36, showing that amphibole in PPP inner mantles has the highest Al content and the crystallization of amphibole of PPP outer mantles corresponds to the beginning of retrograde metamorphism. Hara *et al.* (1984a) have analyzed the variation in chemical composition among biotite in cores, that in inner mantles and that in outer mantles of PPP, showing that biotite in PPP inner mantles has the highest Mg content and the crystallization of biotite in PPP outer mantles, as well as the bedding schistosity-forming biotite, corresponds to the beginning of retrograde metamorphism (Fig. 37). In the oligoclase-biotite zone is found plagioclase with

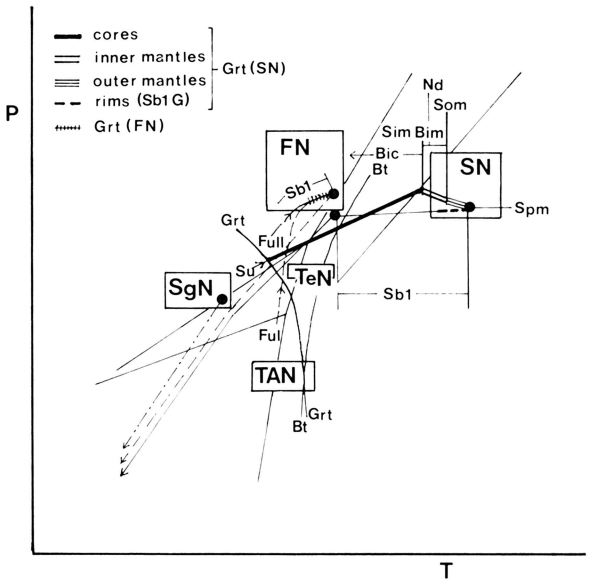

Fig. 32 Diagram showing the growth history of garnet on the P-T-D path of the Saruta nappe (I + II) schists and Fuyunose nappe schists and the field of appearance of garnet and biotite in pelitic schists of the Sambagawa megaunit and its surroundings. SN: Saruta nappes, (SU: Saruta unit), FN: Fuyunose nappe (FuI: Fuyunose subunit I, FuII: Fuyunose subunit II), SgN: Sogauchi nappe, TeN: Tenryu nappe, TAN: Tatsuyama nappe, Bt: biotite, Grt: garnet.

Fig. 33 Mn-Fe-Mg diagrams showing three types of chemical zonation for garnet in pelitic schists of the Saruta nappes [data from Hara *et al.* (1990a)]. a) abnormal garnet showing a reverse zoning in inner mantle just along the boundary (B1) between core and inner mantle. b) abnormal garnet showing a reverse zoning in outer mantle just along the boundary (B2) between inner mantle and outer mantle. c) normal garnet showing a normal zoning. d) diagram showing the distribution of pelitic schists with normal garnet (solid circles) and these with abnormal garnet (open circles) in the Saruta nappe (SNI) along the River Dozan. SNII: Saruta nappe II, FN: Fuyunose nappe, Js: Joshi, BB: Besshibashi, Tg: Togu, Nk: Nikubuchi, Hd: Hodono, Tk: Tokonabe, Sb: Seba.

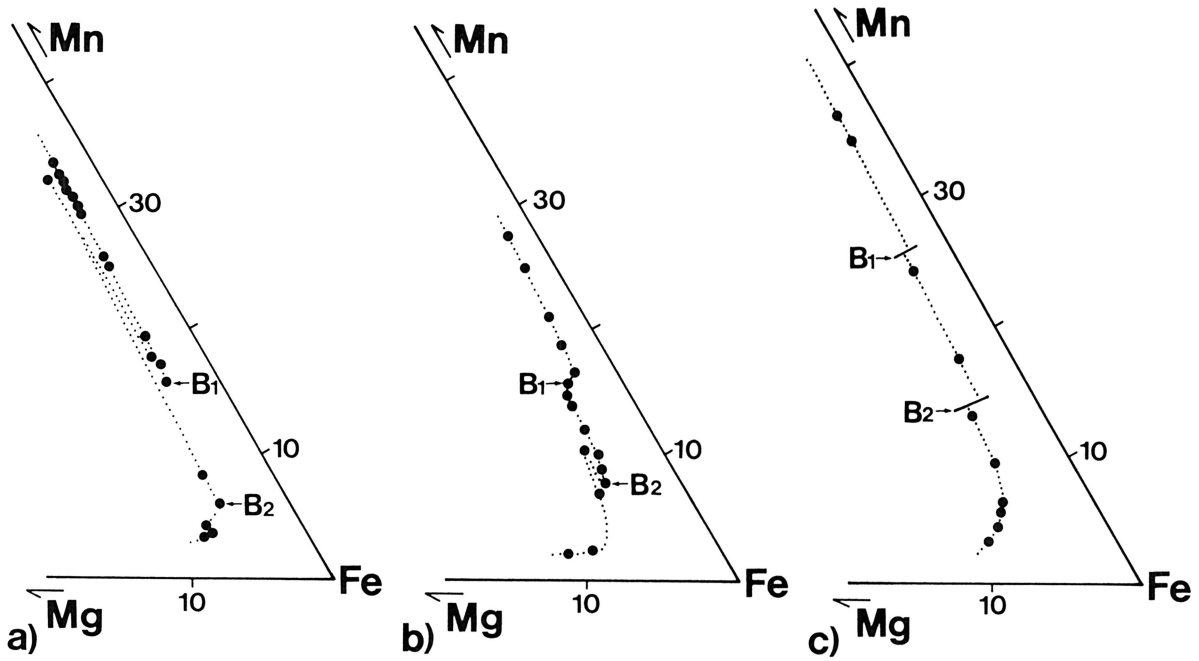

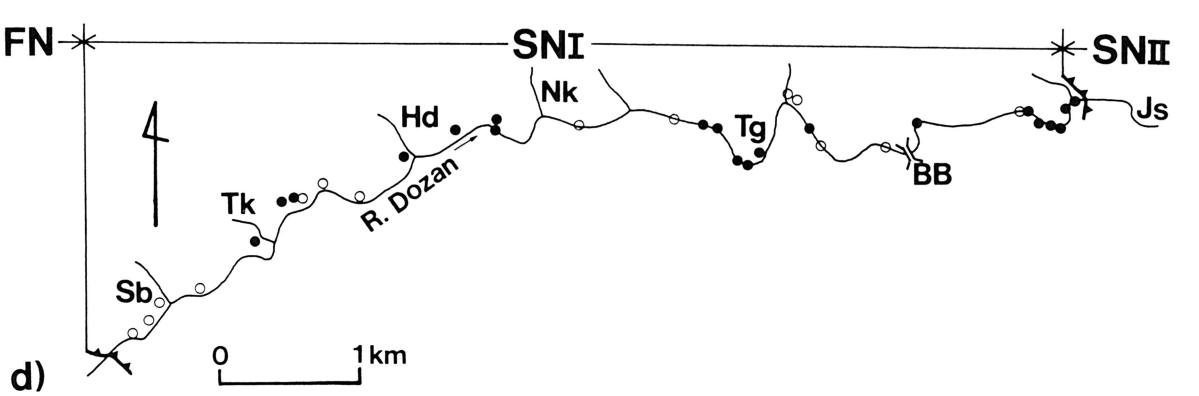

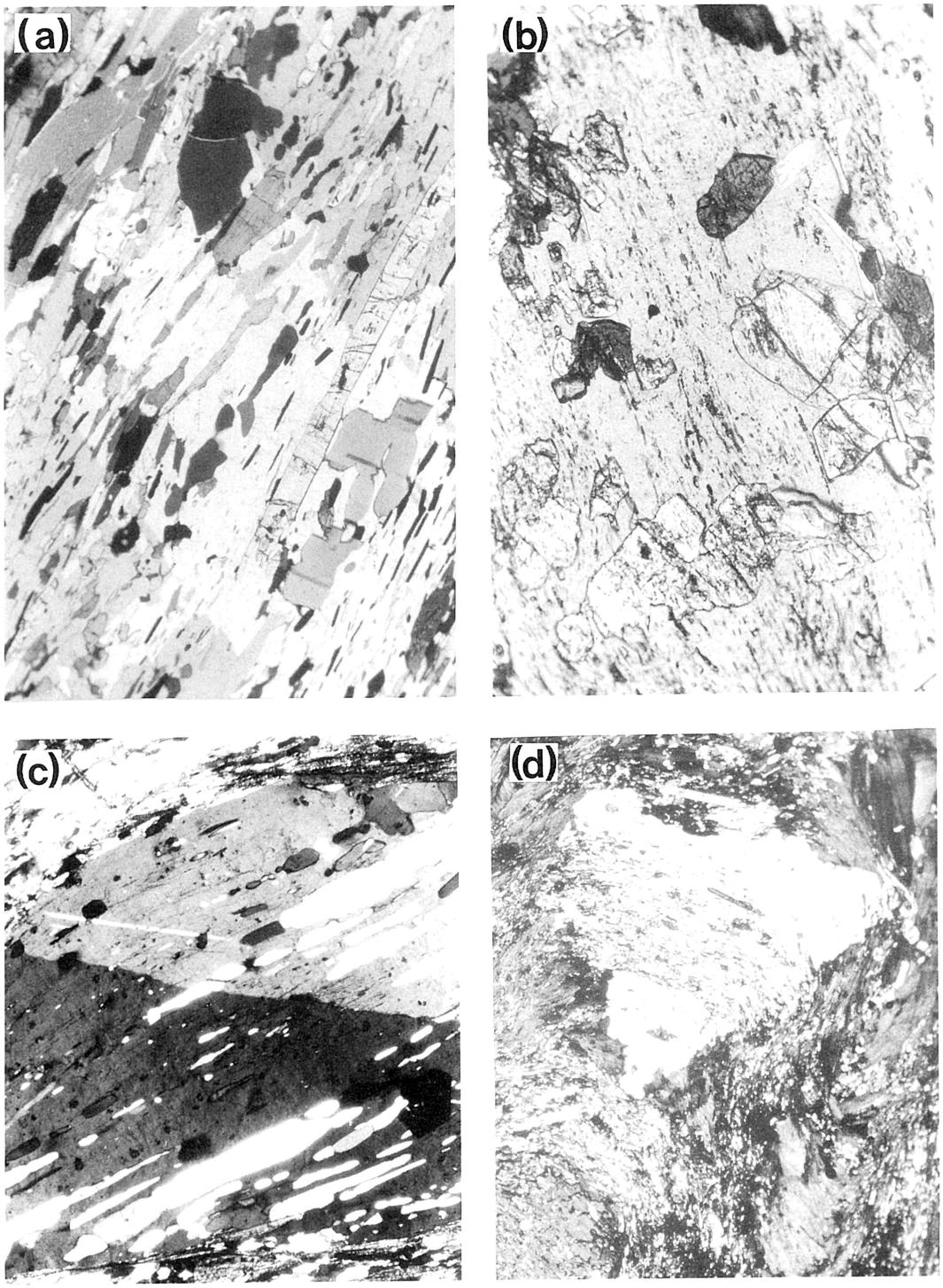

Fig. 34 Microphotographs of plagioclase porphyroblasts in the Saruta nappe (I + II) schists. a) plagioclase porphyroblast with inclusion amphibole and epidote showing preferred shape and lattice orientation (Tokuda and Hara, 1983). b) plagioclase porphyroblast with inclusion epidote showing random shape and lattice orientation. c) plagioclase porphyroblast with inclusion quartz showing preferred shape and lattice orientation (Fig. 24) (Hara *et al.*, 1989). d) plagioclase porphyroblast crystallized in a median segment of conjugate kink bands, which were developed in a narrow shear zone of basic schists of the Saruta nappe I under crystallization condition of actinolitic amphibole.

the highest An content in PPP inner mantles (Enami, 1983; Hara *et al.*, 1984a). Thus, it has been concluded by Hara *et al.* (1983, 1984a, 1990a) that PPP inner mantles grew, together with garnet outer mantles with the lowest Mn content during the peak metamorphism, while PPP outer mantles began to grow during the beginning phase (Sbl in Fig. 24) of retrograde metamorphism, and that now-observed fundamental characteristics of the bedding schistosity of the Saruta unit schists was printed during the Sbl phase.

Maeda and Hara (1984) and Hara *et al.* (1984a) clarified

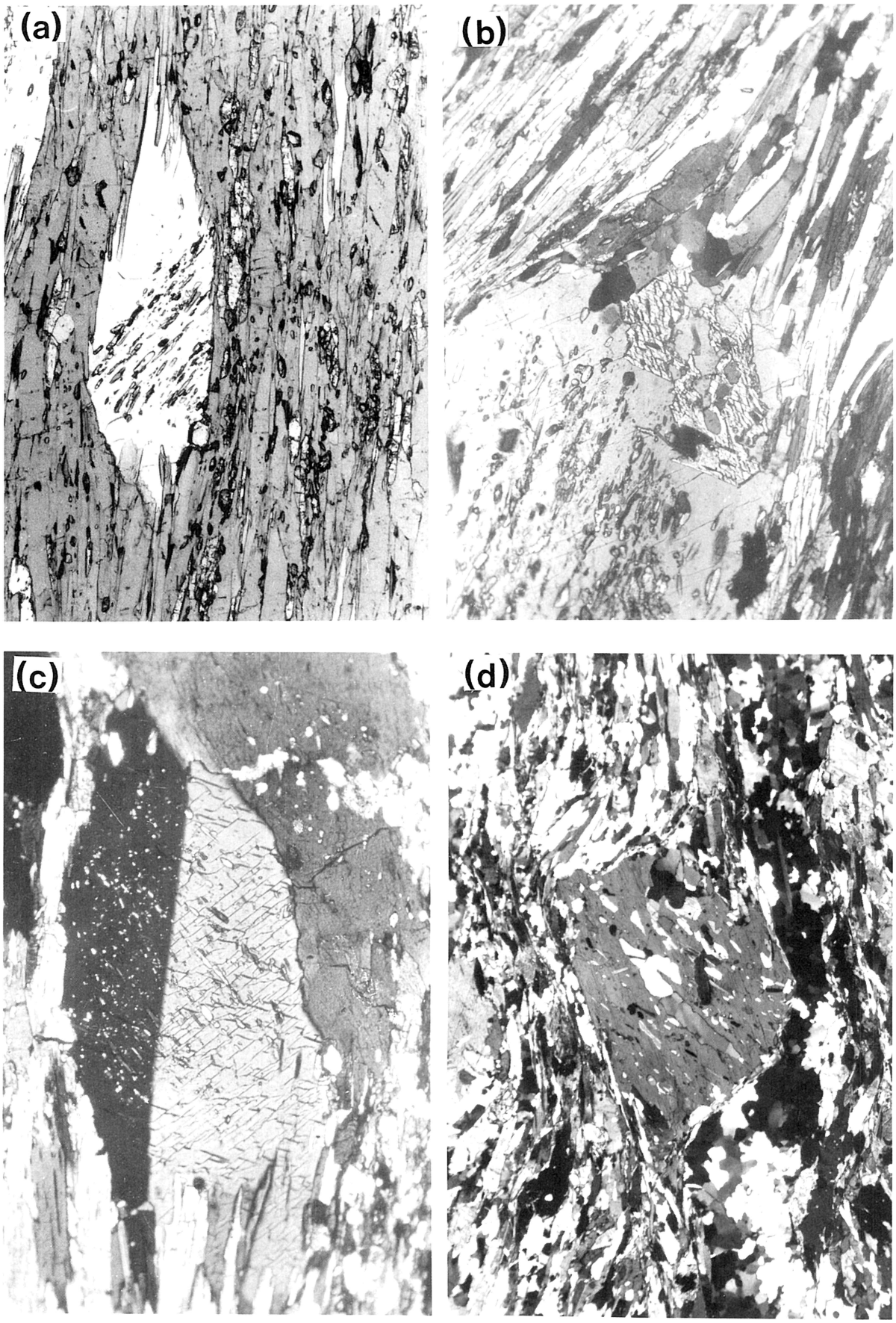
(a)
(b)
(c)
(d)

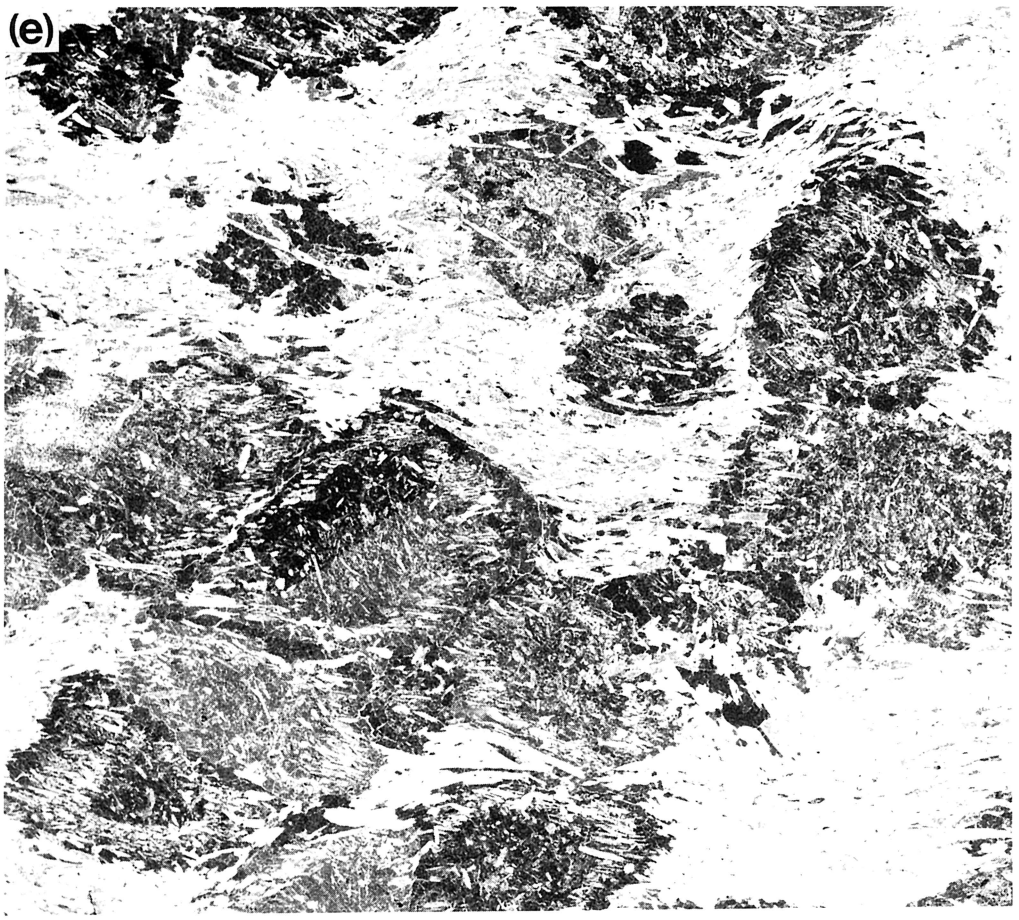

Fig. 35 a) Microphotograph showing the discontinuous relationship between Sim schistosity in plagioclase porphyroblast core and matrix Sb1 schistosity in a specimen from basic schists of the Saruta nappe II of the River Saruta district. b) microphotograph showing three zones, core, inner mantle and outer mantle, of plagioclase porphyroblast and associated three types of amphibole in a specimen from basic schists of the Saruta nappe I of the Shirataki district [data from Hara *et al.* (1983)]. Coarse-grained amphibole with other kind minerals as inclusions is found in inner mantle. c) microphotograph showing three types of amphibole, which are comparable with these of Fig. 35-b, though coarse-grained amphibole with inclusion minerals is not included in plagioclase porphyroblast inner mantle [data from Hara *et al.* (1983)]. The coarse-grained amphibole is clearly distinguishable from matrix amphibole. d) microphotograph showing coarse-grained amphibole with other kind minerals as inclusions and matrix amphibole in a specimen from the Shirataki V amphibole schists of the River Asemi district. Their chemical data are reproduced in Fig. 36 [data from Hara *et al.* (1990)]. e) microphotograph (reversal) showing three zones, cores, inner mantles and outer mantles, of plagioclase porphyroblast in a specimen from basic schists of the Saruta nappe II of the River Asemi district, which are clearly defined by orientation pattern of amphibole. The Sim schistosity in cores is oblique at high angles to the Som schistosity in inner mantles. The Som schistosity is oblique at small angles to and discontinuous with matrix Sb1 schistosity.

that PPP cores, as well as garnet inner mantles, grew under non-deformational condition of the Nd phase just after the Sim-Bim deformation. This is clear in Fig. 30-a [data of Maeda and Hara (1984)], where a Bim fold is included in both garnet mantle and plagioclase porphyroblast core, showing that the form of the Bim fold did not change during their growth. This point is also assumed from the data of Fig. 30-c and d: Garnet in this figure is included in PPP. It is divided into core and mantle with reference to Si fabric. The Si fabric of garnet mantle is continuous and harmonic with it of host PPP core, showing that its pattern did not change during the growth of garnet mantle and PPP core. The garnet is found in the same specimen as that of Fig. 29-a. It can be said with reference to Si fabric and chemical composition that the outer mantle of the latter is absent in the former. Fig. 38 is a sketch of garnet and PPP in Fig. 31-b, which have been described by Hara *et al.* (1984a). From their Si fabrics it has been assumed that garnet inner mantles grew together with PPP cores and garnet outer mantles grew with PPP inner mantles.

As is obvious in Fig. 39, fold and discrete cleavage (Bim fold) of Sim in PPP of the Saruta unit generally do not show any shape change during the growth of PPP cores. From Figs. 39-a, b and d it is clear that PPP cores grew along the form surfaces of Bim folds (= along Sim) under non-deformational condition during the Nd phase. The growth of PPP cores on the tectono-metamorphic history of the Saruta unit is now illustrated in Fig. 40.

Bim folds of minor to mesoscopic scales, which were scarcely destroyed by the later phases deformations, have

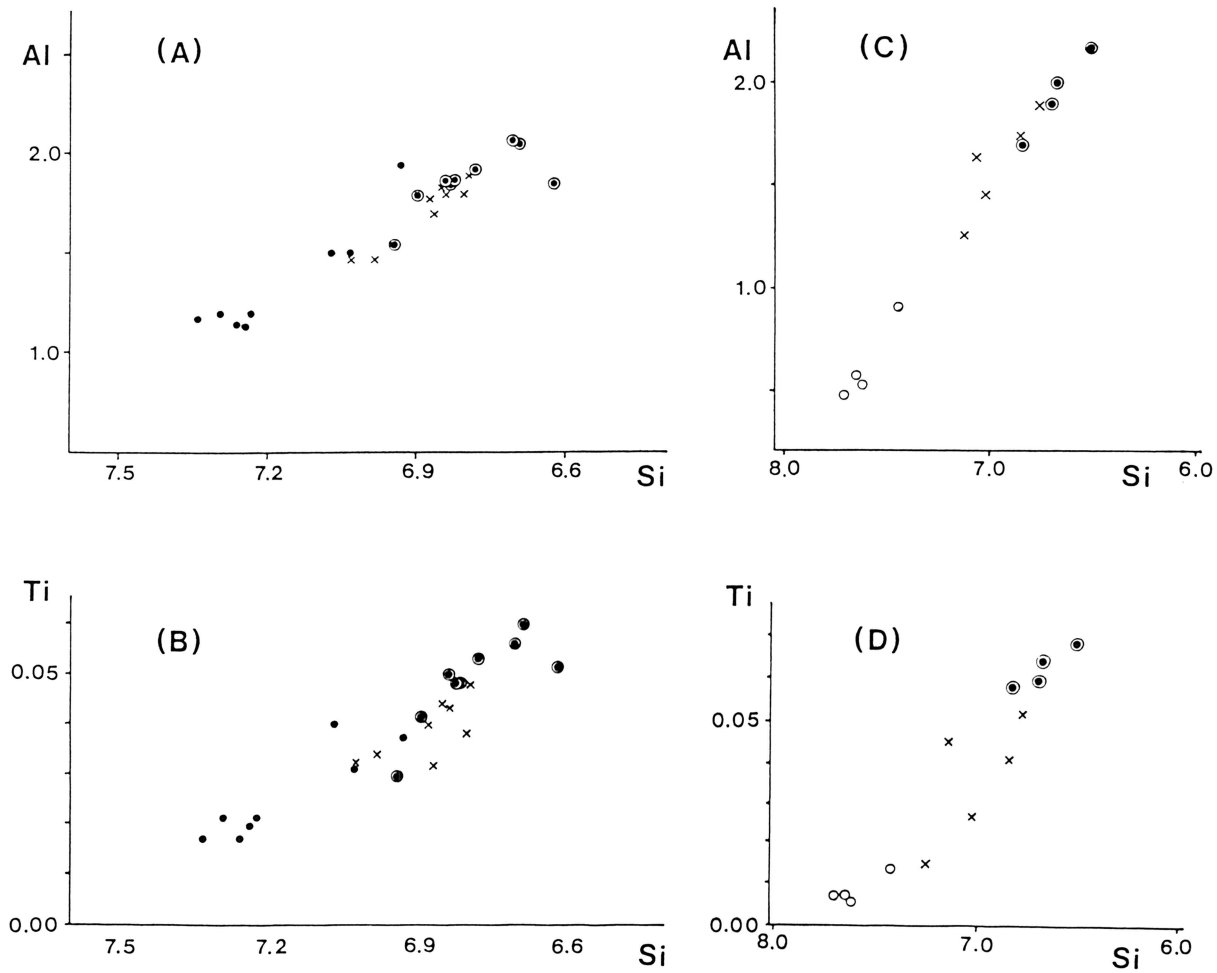

Fig. 36 Chemical composition of amphiboles of four types in basic schists of the Saruta nappes shown in Fig. 35. A) and B) data from the Shirataki I amphibole schists of the Saruta nappe I (Fig. 35-b and c). C) and D) data from the Shirataki V amphibole schists of the Saruta nappe II (Fig. 35-d). solid circles: Sim-forming amphibole, circled dots: Som-forming amphibole, crosses: Sb1 amphibole, circles: amphibole (probably of the Sb2 phase) crystallized in separations of boudins of Som-forming amphibole and Sb1-forming amphibole [data form Hara *et al.* (1990a)].

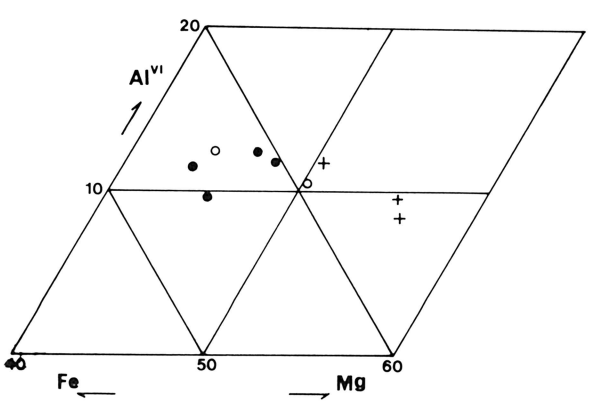

Fig. 37 Chemical composition of biotites of three types in a specimen from pelitic schists of the oligoclase-biotite zone of the Saruta nappe II of the River Asemi district. circles: biotite in plagioclase porphyroblast cores, crosses: biotite in plagioclase porphyroblast inner mantles, solid circles: biotite forming matrix Sb1 schistosity. [data from Hara *et al.* (1984a)].

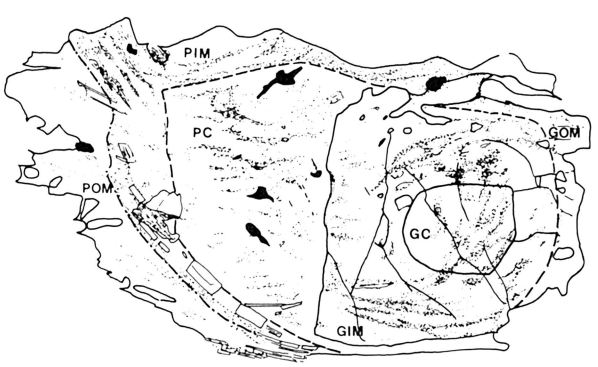

Fig. 38 Sketch of garnet and plagioclase porphyroblast in Fig. 31-b, showing correlation between Si fabrics of garnet and plagioclase porphyroblast. The Si fabric of plagioclase porphyroblast core (PC) is harmonic with that of garnet inner mantle (GIM). PIM: plagioclase porphyroblast inner mantle, POM: plagioclase porphyroblast outer mantle, GC: garnet core, GOM: garnet outer mantle.

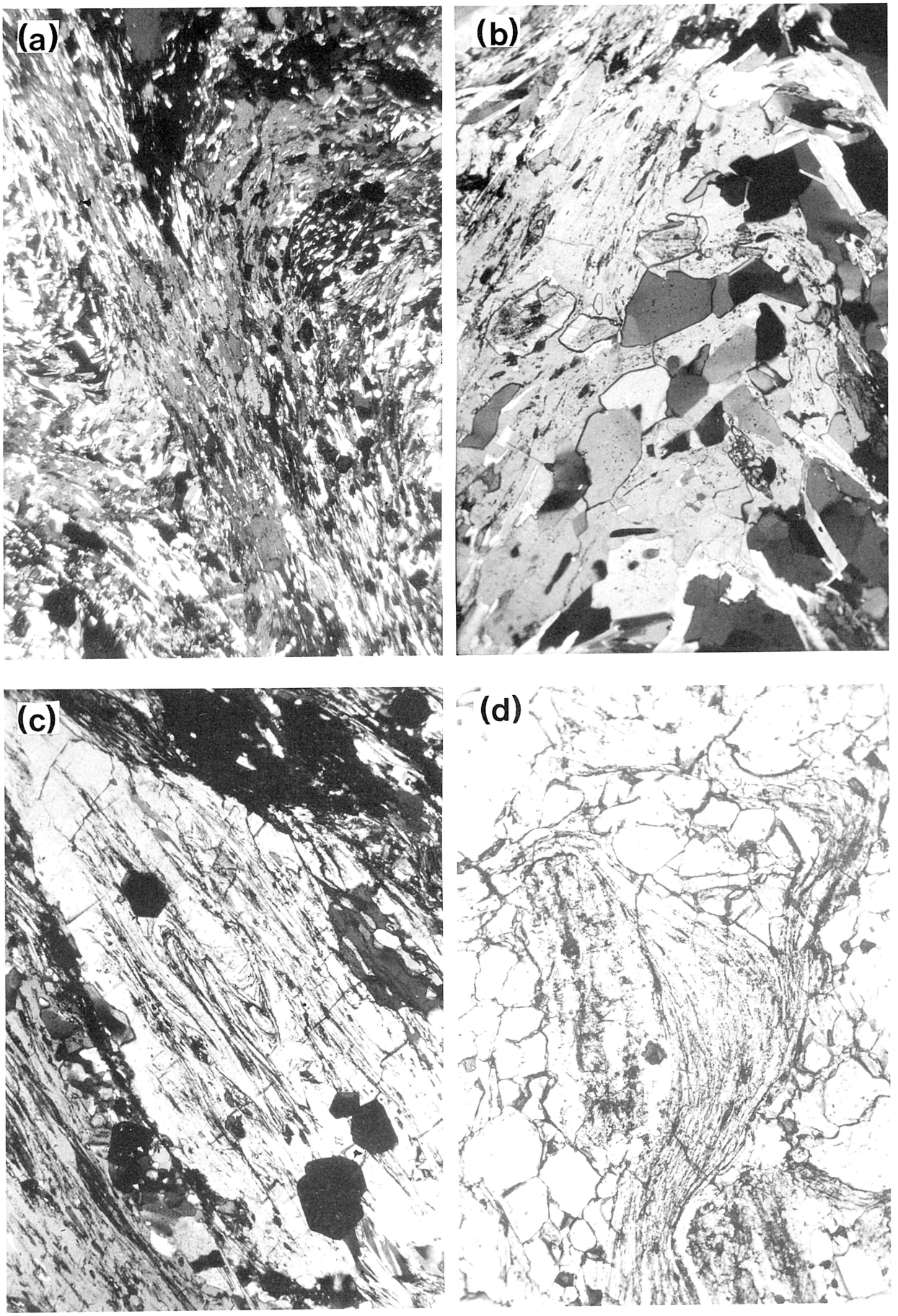

Fig. 39 Microphotographs of plagioclase porphyroblasts in the Saruta nappe (I + II) schists, which all mask microfolds and cleavages. All Si fabrics indicate that these were not changed their shapes during the crystallization of plagioclase porphyroblasts.

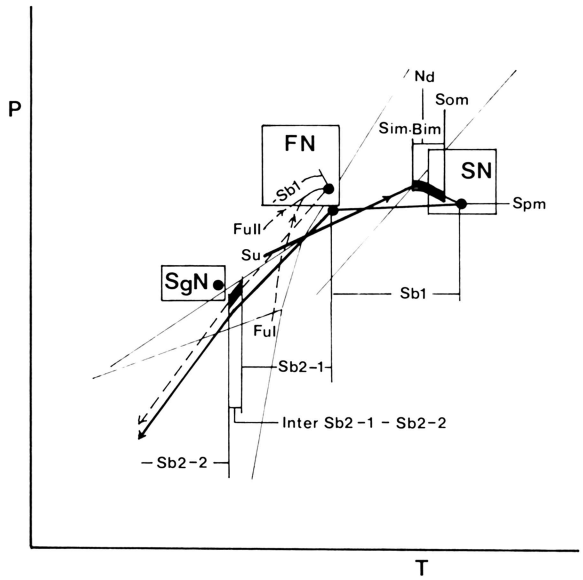

Fig. 40 Diagram showing the phases (Nd phase and Inter Sb2-1 - Sb2-2 phase) of crystallization of plagioclase porphyroblast cores in the Saruta nappe (I + II) schists (solid line) and the Fuyunose nappe schists (dashed line).

been also discovered by Maeda and Hara (1983, 1984). Bim folds in PPP cores show an orientation pattern corresponding to the axial-plane cleavage of crenulation type in large-scale ones, as reproduced in Fig. 41. Amphibole involved in Bim folds of basic schists shows commonly preferred orientation of c-axes parallel to their fold axes (*e.g.* Figs. 42 and 44), showing that the fold axes are in a direction of maximum extension. In the sample of Fig. 42, which has been collected from the Sebadani district, amphibole grains crystallized during the folding of the Bim phase, which are fine-grained and hornblende in chemical composition as a whole, are dominantly found in the axial zone and most of them on the limbs are coarse-grained and barroisite with hornblende rims (Fig. 42-e). The formation of fine-grained hornblende is ascribed to dynamic recrystallization of coarse-grained barroisite during the prograde phase. Fig. 42 indicates that the principal axis X of strain of the Sic phase, where $X > Y > Z$, was oriented normal to that of the Bim phase. While in the specimen of Fig. 43, which has been collected from the River Saruta district, lattice fabric of amphibole in PPP cores is externally rotated around the axis of Bim fold (Fig. 44): The orientation pattern of the principal vibration axis Z in the axial zone of Bim fold is essentially the same as that in the limb, but the fabric pattern of other principal vibration axes is externally rotated with rotation of Sim from the axial zone to the limb, though there appears to be a little change between the axial zone and the limb. This would mean the parallelism of X of strain of the Bim phase with that of the Sim phase.

Amphibole, epidote and quartz in PPP cores, which form straight Sim (*e.g.* Fig. 34-a and c), commonly show preferred lattice orientation (Takagi and Hara, 1979; Hara *et al.*, 1980a; Tokuda and Hara, 1983; Kaikiri *et al.*, 1991) (Figs. 45, 46 and 47), defining mean strain of flattened type and orientation of X of strain in the Sim-Bim (or Bim) deformation. Axial (= X) trends of Bim folds and X orientation in the Sim-Bim (or Bim) deformation have been determined in some parts of the Saruta nappes as shown in Fig. 48. It would be said on the basis of this figure that, in spite of a little observation number, X is in general oriented in NNE-SSW and oblique to the general trend of the distribution of the Sambagawa megaunit.

In hematite-bearing basic schist of the Saruta unit (albite-biotite zone of Saruta nappe I) of the Sebadani district has been found garnet with amphibole as inclusions, and the chemical composition of inclusion amphibole has been analyzed by Hara *et al.* (1988, 1990c) as illustrated in Fig. 49. In the high Mn part of garnet occurs crossite, in the middle Mn part barroisite and winchite and in the low Mn part magnesio-kathopholite, magnesio-hornblende, magnesian hastingsitic hornblende and ferroan pargasitic hornblende as inclusions, showing that the growth history of amphibole in the Saruta unit during the prograde phase of metamorphism is crossite - (winchite - barroisite) - magnesio-hornblende - ferroan pargasitic hornblende. Such the data for the growth history of amphibole (Fig. 49), as well as the chemical data for that of garnet (Fig. 33), are decisive to understand the P-T path of the Saruta unit during the prograde metamorphism as shown by Hara *et al.* (1990a).

The Sim-forming amphibole in PPP cores in hematite-bearing basic schists of the Sebadani district is magnesio-hornblende and edenitic hornblende, probably showing that they began to grow under P-T condition for crystallization of magnesio-hornblende and edenitic hornblende (Fig. 50). Thus, the P-T condition of the Sim-Bim phase and that of the Nd phase for the Saruta nappe I schists in the Sebadani district, which is for that of the crystallization of PPP cores, have been illustrated by Hara *et al.* (1990a) as shown in Fig. 40.

Fig. 51 illustrates the chemical composition (Si content) of the Sim-forming amphibole in hematite-bearing basic schists (albite-biotite zone of Saruta nappe II) of the River Saruta district, which shows scarcely overprint of retrograde metamorphism. From this figure it can be said that it, as well as bedding schistosity-forming amphibole, shows some variation in Si content from place to place probably with its lowest values near the central horizon of the biotite zone. The data of the Sim-forming amphibole in the Shirataki V amphibole schist (oligoclase-biotite zone) and these in the Shirataki I-II amphibole schist (albite-biotite zone) (Fig. 13) are illustrated in Fig. 52, showing that there is a distinct difference in minimum Si content between the former and the latter. Fig. 52 illustrates also relationship between the minimum Si content of the Sim-forming amphibole and that of the bedding schistosity-forming amphibole: The former is larger than the latter. It can be now said that the difference between the former and the latter is not constant throughout basic schists of the Saruta unit. As mentioned in the preceding page, the bedding schistosity-forming amphibole consists of Spm phase amphibole (amphibole crystallized during peak metamorphism) and Sb1-forming amphibole, which is in paragenetic relation with PPP outer mantles and crystallized during the beginning phase of retrograde metamorphism, though their rims show, in various degrees, overprint of retrograde metamorphism of the further later phases (Hara *et al.*, 1983). In most of basic schists, but, the former appear to be negligible in volume. As is obvious in Fig. 36, the minimum Si content of the

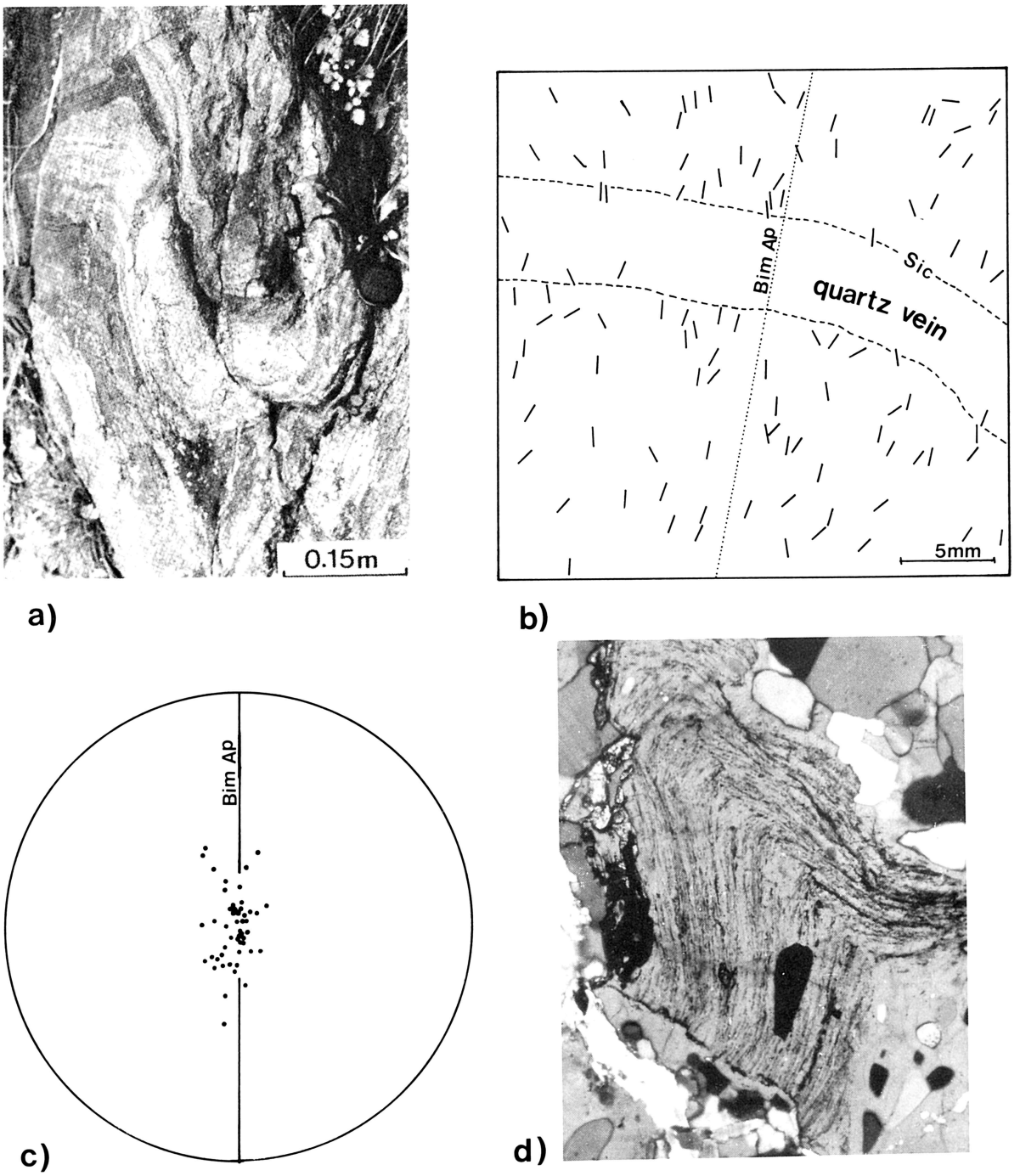

Fig. 41 Diagram showing the orientation of the axes (c) and axial planes (b) of Bim folds (d) in plagioclase porphyroblasts and the development of pre-Bim quartz vein in a Bim fold (a) of psammitic schists of the Saruta nappe II of the River Saruta district [data from Maeda and Hara (1984)].

Sb1-forming amphibole is larger only by a little value than that of the Spm-phase amphibole. It has been therefore assumed that the main part of Sb1-forming amphibole crystallized under temperature condition only a little lower than the Spm phase amphibole. It would be pointed out that plagioclase in the Saruta unit crystallized as porphyroblasts at an expense of pre-existing plagioclase under various temperature condition and non-deformational condition during the Nd phase immediately after the Sim-Bim deformation and that the difference in temperature between the Nd phase and the Spm phase is not constant throughout the Saruta unit, quite roughly speaking, for example, large in the Shirataki I-II amphibole schist and small in the Shirataki V amphibole schist (Hara *et al.*, 1980a). As plotted on the diagram for stability field of amphibole in hematite-bearing basic schists after Banno and Sakai (1989), the P-T condition of the Saruta unit during the Sim-Bim phase, which has been quite roughly estimated from the

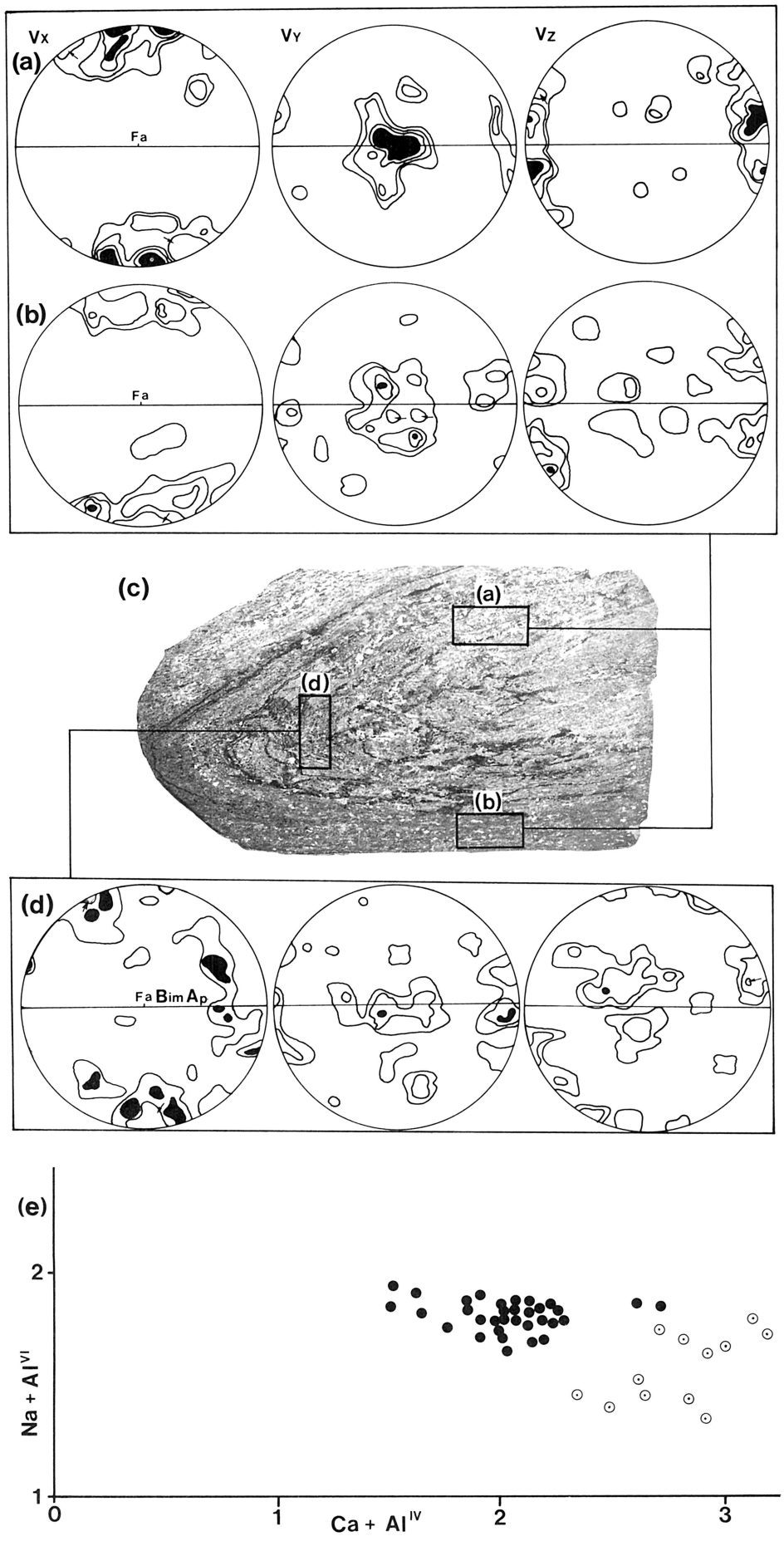
Vx
Vy
Vz
(a)
Fa
(b)
Fa
(c)
(a)
(d)
(b)
(d)
Fa Bim Ap
(e)
2
1
Na + AlVI
0
1
Ca + AlIV
2
3

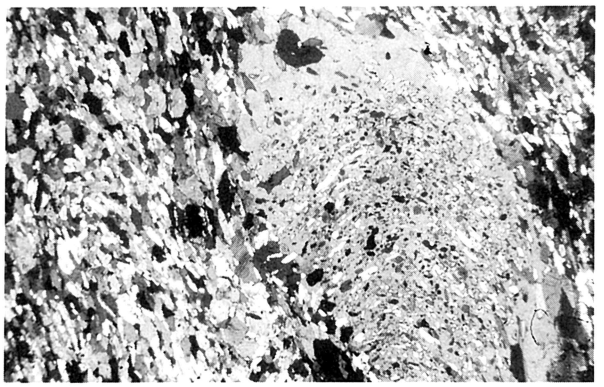

Fig. 43 Microphotograph of Bim fold in plagioclase porphyroblast in a specimen from basic schists of the Saruta nappe II of the River Saruta district.

minimum Si content of Sim-forming amphibole in hematite-bearing basic schists, would be assumed to change within a fairly widerange between barroisite field and hornblende field. The pressure and temperature of the oligoclase-biotite zone during the Spm phase have been estimated to be respectively ca. 10-11 kb and 560-600 C (Enami, 1983; Hara *et al.*, 1984a; Banno and Sakai, 1989). From the above-mentioned evidence and consideration, thus, the P-T-D path of the Saruta unit (biotite zone) and the growth condition of its PPP cores during the prograde phase of metamorphism would be roughly explained by Fig. 40.

B. Tectono-Metamorphic History of Prograde Phase of the Fuyunose Unit

From the chemical composition of amphibole included in plagioclase porphyroblasts of hematite-bearing basic schists, the Fuyunose unit has been divided into three subunits, subunit I, subunit II and subunit III (Hara *et al.*, 1990a, c). The subunit II is the main constituent of the Fuyunose unit, while the subunit I and subunit III are tectonic blocks derived from the Saruta unit, as mentioned in the later pages.

In the Fuyunose subunit II garnet shows commonly chemical zoning of normal type for prograde metamorphism (Fig. 28-d, e and f), while plagioclase porphyroblasts (Fig. 53-a) crystallized during retrograde metamorphism after the growth of garnet ceased (Hara *et al.*, 1988). Fig. 54 illustrates the representative growth history of amphibole in hematite-bearing basic schists of the Fuyunose subunit II, showing that amphibole in garnet cores crystallized during the high-temperature phase of prograde metamorphism is fine-grained crossite, while that in plagioclase porphyroblasts is coarse-grained, having glaucophane as cores, cros-

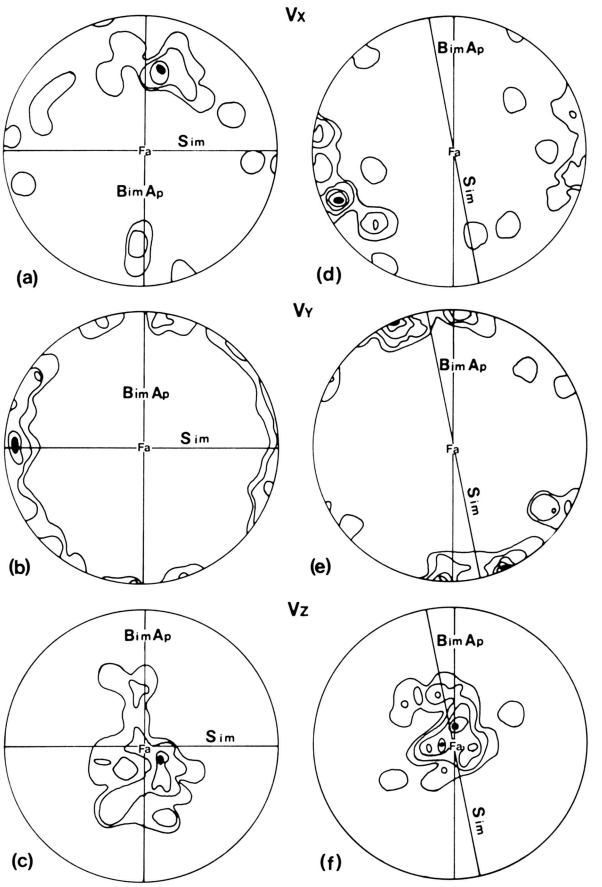

Fig. 44 Lattice fabrics of amphibole grains forming the Bim fold in plagioclase porphyroblast of Fig. 43. a), b) and c) data from the axial zone. d), e) and f) data from the limb of right side. BimAp: axial plane of Bim fold, Fa: fold axis. Vx: principal vibration axis X, Vy: principal vibration axis Y, Vz: principal vibration axis Z.

site and barroisite as mantles and winchite as rims. Crossite in garnet cores has higher (Na + Al^{VI}) content than crossite mantles of amphibole in plagioclase porphyroblasts as measured in a fixed value of (Ca + Al^{IV}) content. In the rims of matrix amphibole, which are widely developed in a direction parallel to the bedding schistosity, is found actinolite together with winchite. The growth history of amphibole in the Fuyunose subunit II of the River Asemi district, which corresponds to the southern part of the Fuyunose nappe, is, thus, assumed to be crossite with high (Na + Al^{VI}) content - glaucophane for the prograde phase and glaucophane - crossite with low (Na + Al^{VI}) content - barroisite - winchite - actinolite for the retrograde phase.

Fig. 42 Amphibole lattice fabrics in a Bim fold (c) of basic schists of the Saruta nappe I of the Sebadani district.
a) and b) data for coarse-grained amphibole from both limbs, d) data from axial zone, e) diagram showing the variation in chemical composition between amphibole in limbs (solid circles) and that in axial zone, Fa: fold axis, BimAp: axial plane, Vx: principal vibration axis X, Vy: principal vibration axis Y, Vz: principal vibration axis Z.

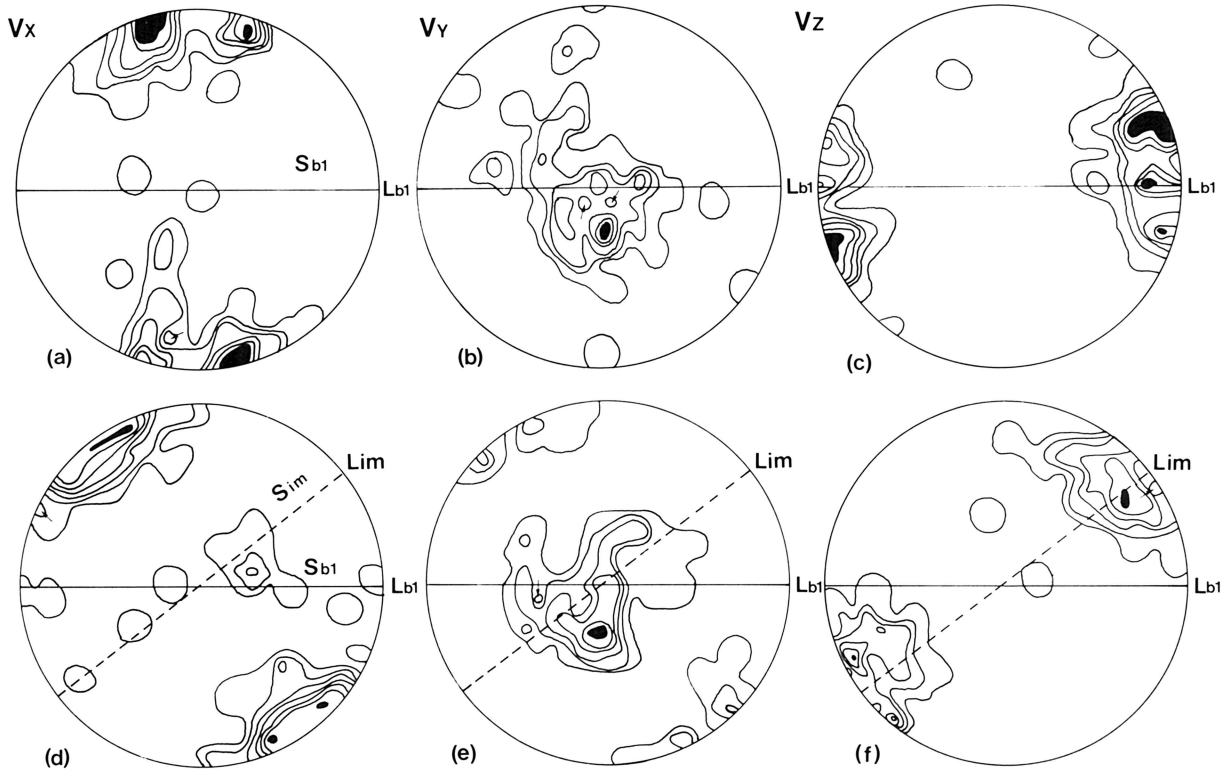

Fig. 45 Amphibole lattice fabrics in a specimen from the Shirataki V amphibole schists of the Saruta nappe II of the River Asemi district. a), b) and c) matrix Sb1-forming amphibole, d), e) and f) Sim-forming amphibole in plagioclase porphyroblast core. Lim: mineral lineation on Sim, Sb1: matrix bedding schistosity, Lb1: mineral lineation on Sb1, Vx: principal vibration axis X, Vy: principal vibration axis Y, Vz: principal vibration axis Z.

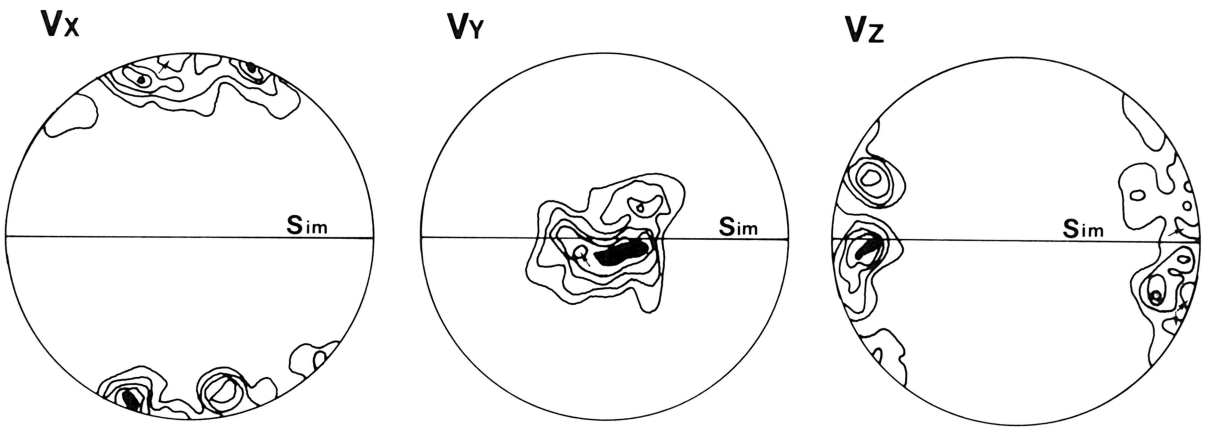

Fig. 46 Lattice fabric of epidote grains forming Sim in plagioclase porphyroblast in a specimen from the Shirataki I amphibole schists of the Shirataki district. Vx: principal vibration axis X, Vy: principal vibration axis Y, Vz: principal vibration axis Z.

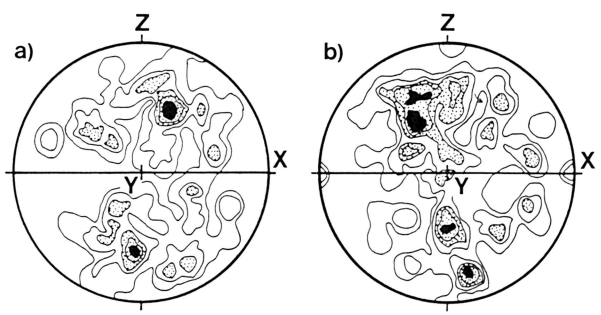

Fig. 47 c-axis fabrics of quartz grains forming Sim in plagioclase porphyroblasts in two specimens from pelitic schists of the Saruta nappe I. a) data form the Togu district, b) data from the Nikubuchi district, X, Y and Z: principal axes of strain (X > Y > Z) assumed from the quartz fabric pattern.

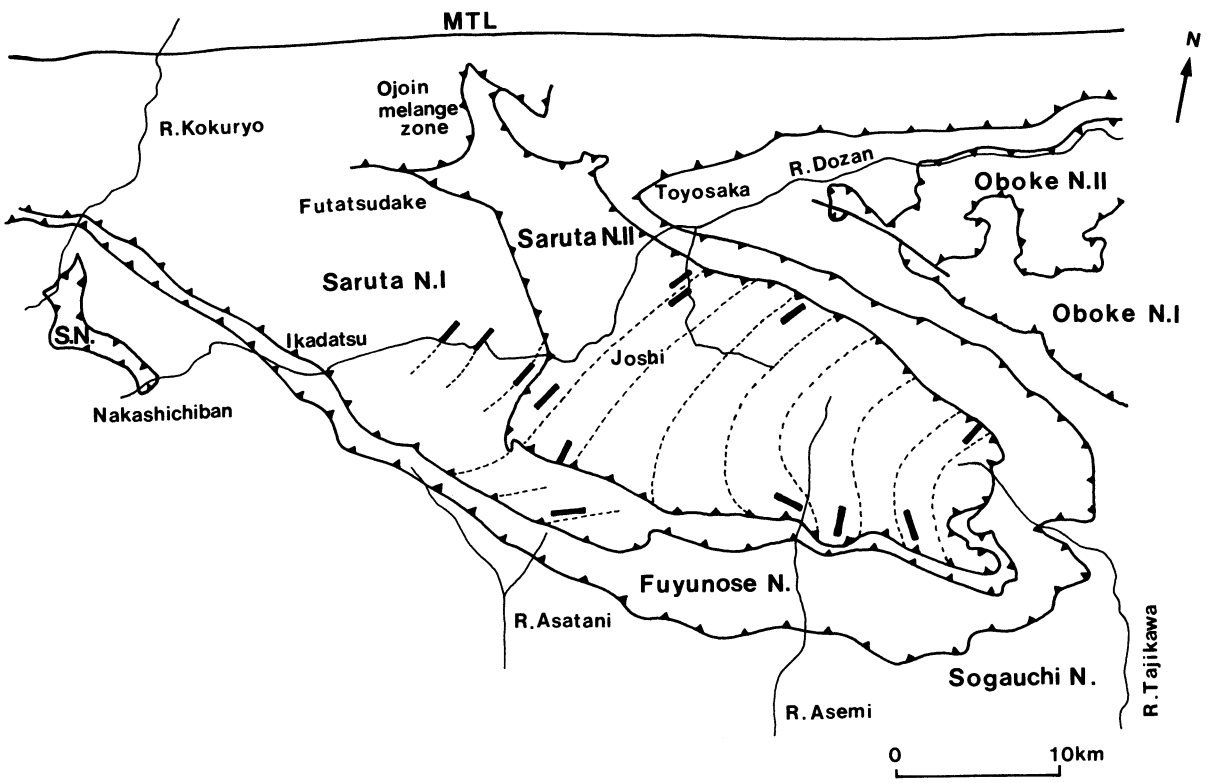

Fig. 48 Diagram showing the orientation of X of strain of the Sim-Bim phase in the Saruta nappes (Saruta N. II and Saruta N. I) as assumed from fabric patterns of quartz, amphibole and epidote grains forming Sim and Bim folds in plagioclase porphyroblasts. heavy short straight lines and dashed lines: measured data of orientation of X and assumed trends of X.

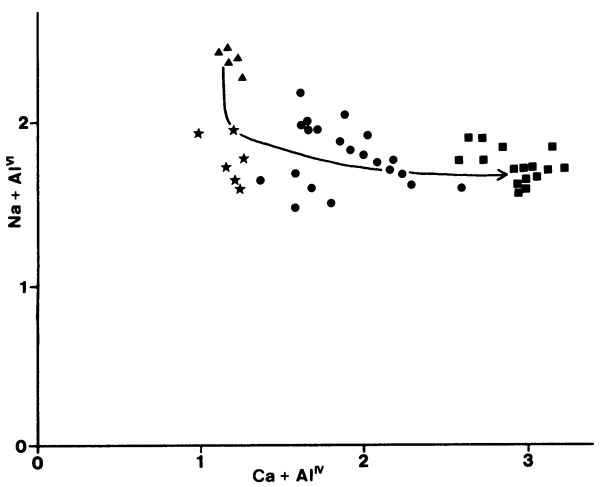

Fig. 49 Diagram showing the variation in chemical composition between amphibole grains included in garnet of a specimen from hematite-bearing basic schists of the Saruta nappe I of the Sebadani district. solid triangles: crossite, stars: winchite, solid circles: barroisite, solid squares: magnesio-hornblende, magnesian hastingsitic hornblende, ferroan-pargasitic hornblende.

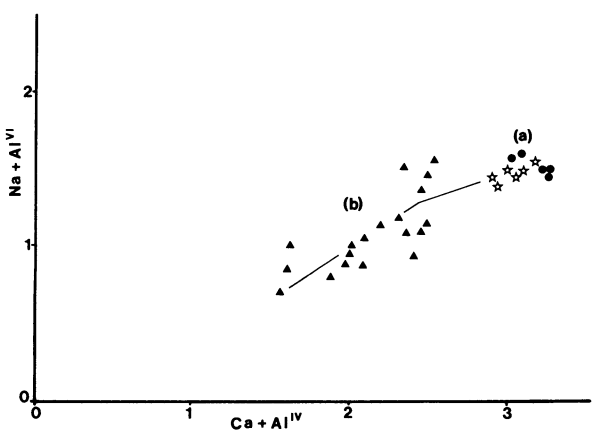

Fig. 50 Chemical data of amphibole in two specimens of hematite-bearing basic schists of the Saruta nappe I of the Sebadani district.
a) data for Sim-forming amphibole (stars) in plagioclase porphyroblasts and matrix Sb1-forming amphibole (solid circles), b) data for amphibole of a shear zone in basic schists showing the retrograde growth history of hornblende - barroisite - winchite path.

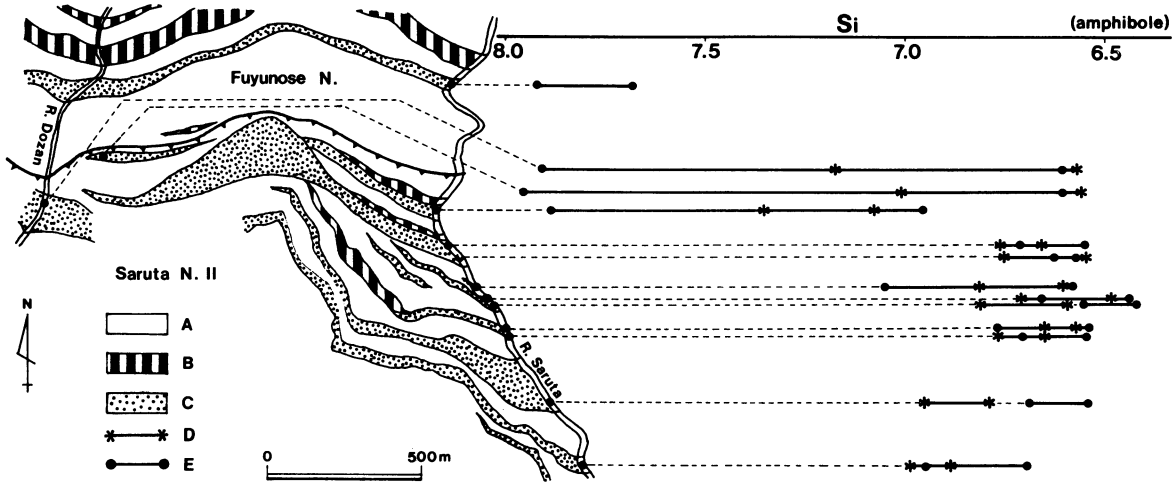

Fig. 51 Spatial variation in chemical composition of amphibole in hematite-bearing basic schists in the River Saruta district. A: pelitic schists, B: siliceous schists, C: basic schists, D: Sim-forming amphibole in plagioclase porphyroblasts, E: matrix bedding schistosity-forming amphibole. Sim-forming amphibole in the Saruta nappe II schists placed near the nappe boundary has commonly retrograde rims.

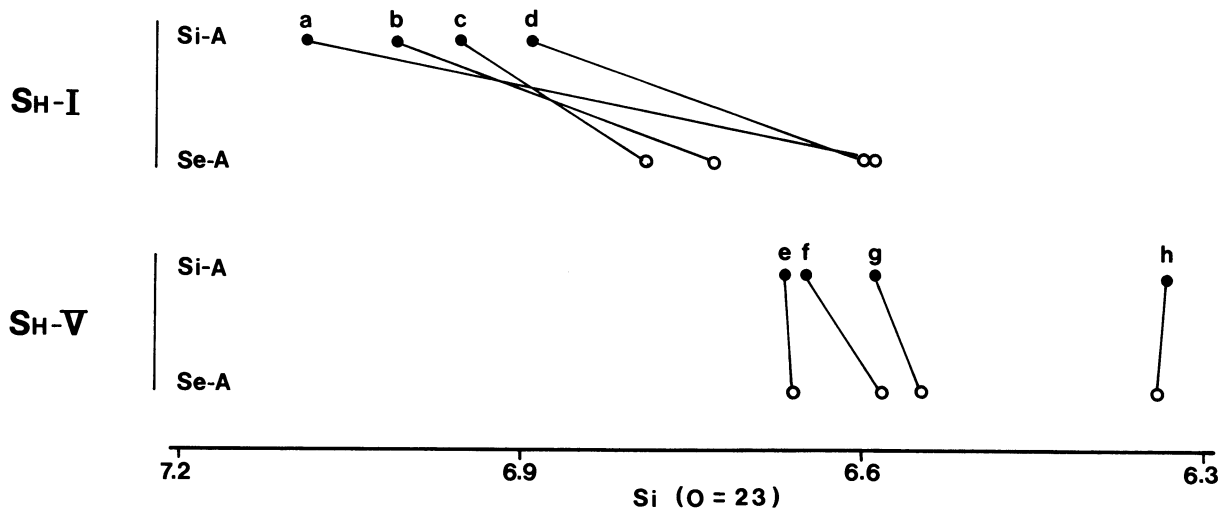

Fig. 52 Diagram showing the variation in chemical composition (minimum Si content) between the Sim-forming amphibole (Si-A: solid circles) in plagioclase porphyroblasts and the matrix Sb1-forming amphibole (Se-A: open circles). Sh-I: data from four specimens (a - d) of the Shirataki I amphibole schists, Sh-V: data from four specimens (e - h) of the Shirataki V amphibole schists.

Fromt (Na + Al^{VI}) content of crossite, it may be roughly assumed that the P-T path of the Fuyunose subunit II runs through the higher pressure route during the prograde phase than during the retrograde phase.

Fig. 55 is the data for amphibole in hematite-bearing basic schist from the Besshi district, which corresponds to the northern part of the Fuyunose nappe, showing the growth history of the prograde phase from tremolite in cores, through winchite in inner mantles, to crossite in outer mantles, though in rims is found the retrograde growth history. The retrograde growth history of amphibole in hematite-bearing basic schist of the Besshi-Sazare district, which is placed in the northern part of the Fuyunose subunit II, has been explained in term of glaucophane - crossite - winchite - actinolite (Fig. 56) by Hara *et al.* (1988, 1990a, b), showing that plagioclase porphyroblasts appeared during the crystallization of winchite of retrograde phase. Thus, the P-T path of the Fuyunose subunit II has roughly been assumed as schematically shown in Fig. 57. The northern part of the Fuyunose subunit II was placed in the higher pressure condition during the retrograde tectonometamorphic history than the southern part (Fig. 57) (Hara *et al.*, 1988, 1990a, b).

As observed on the Mn-Fe-Mg diagrams for garnet in pelitic schists the Fuyunose subunit II appears to be divided into two parts with reference to its minimum Mn content, high-temperature part containing garnet with minimum Mn content of less than 5 per cent and low-

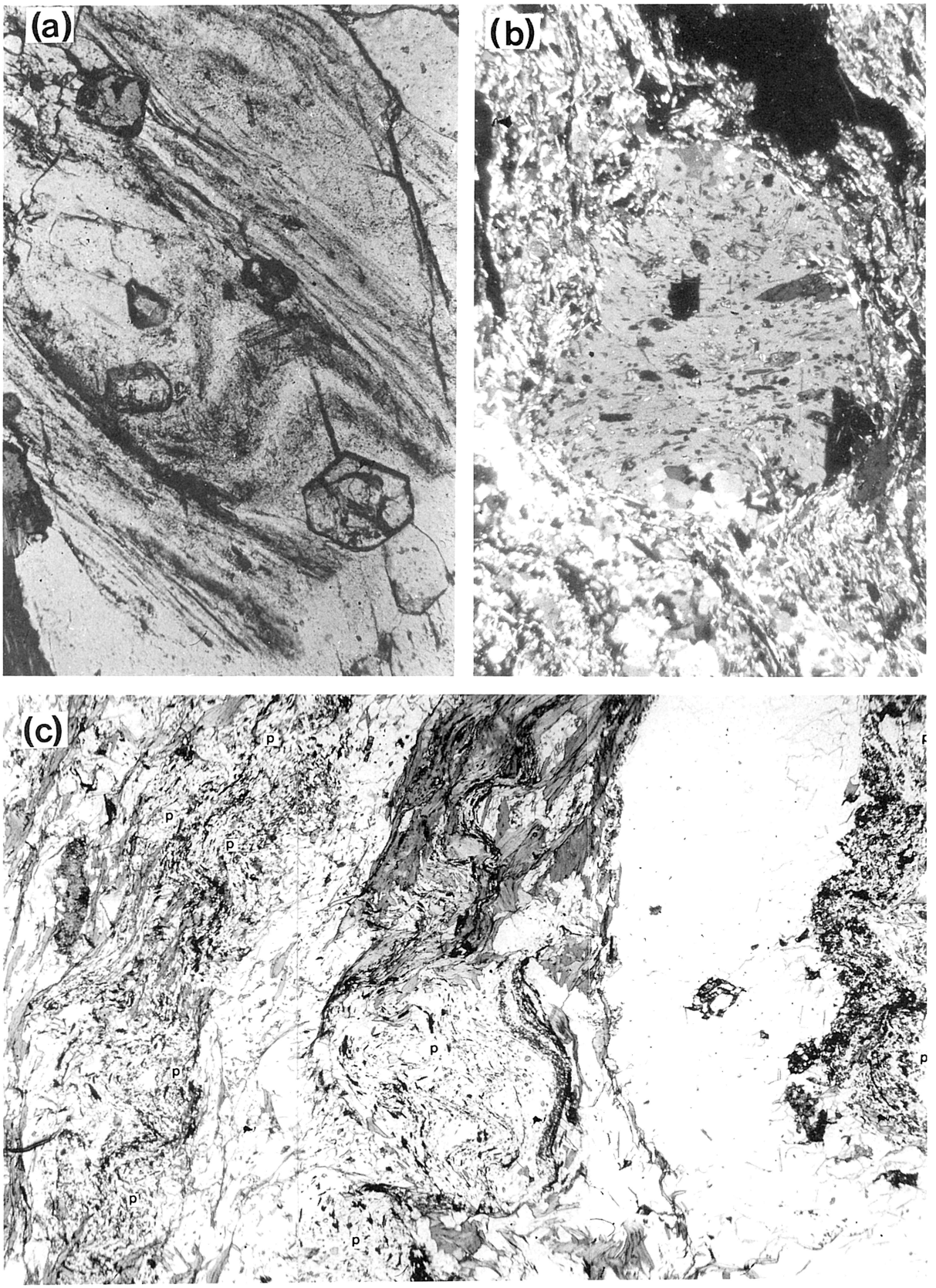

Fig. 53 Microphotographs of plagioclase porphyroblasts in the Fuyunose nappe schists.
a) plagioclase porphyroblast in a specimen from pelitic schists of the River Asemi district, which includes differentiated crenulation cleavage and garnet, b) plagioclase porphyroblast in a specimen from basic schists of the Shirataki district. c) plagioclase porphyroblasts (p) in the axial zone of a minor parasitic fold of the Kuwanokawabashi fold of the River Asemi district. Microfolds of Si schistosity in plagioclase porphyroblasts are comparable with the axial-plane cleavage of the Kuwanokawabashi fold.

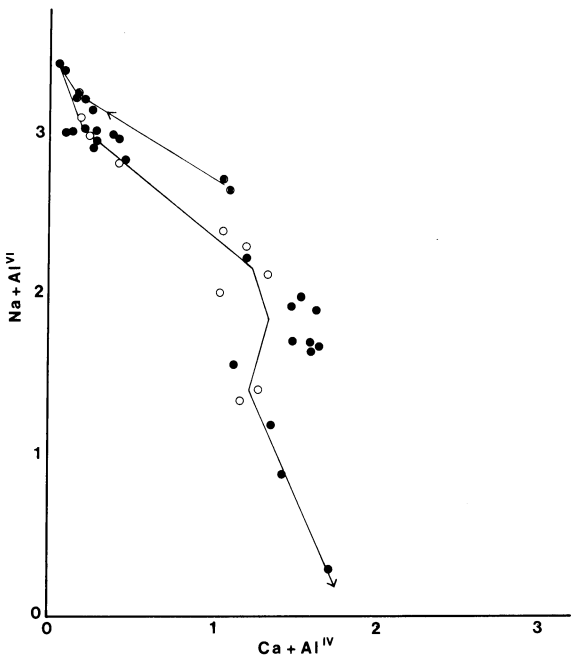

Fig. 54 Diagram showing the growth history of amphibole in hematite-bearing basic schists involved in the Kuwanokawabashi fold of the Fuyunose nappe of the River Asemi district. circled dots: data for amphibole grains included in garnet cores, open circles: data for amphibole grains included in plagioclase porphyroblast cores, solid circles: matrix bedding schistosity-forming amphibole.

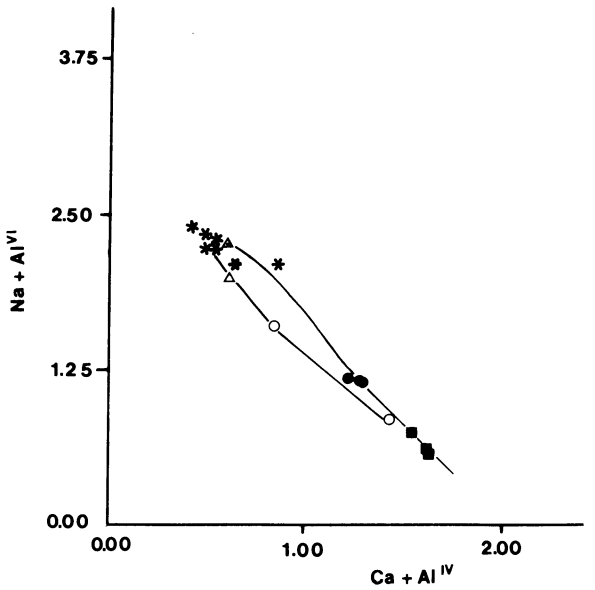

Fig. 55 Diagram showing the growth history of amphibole in a specimen from hematite-bearing basic schists (Fuyunose nappe schists) of the Besshi mine, 15L, E1-0 (Kazuki).
Solid squares: data from innermost part of amphibole cores—tremolite, solid circles: data from middle part of cores—winchite, stars and triangled dot: data from outer part (= main part) of cores—magnesio-riebeckite (triangled dot) and crossite (stars), open triangle: data from innermost part of mantle—magnesio-riebeckite, open circle: data from main part of mantle and rim—winchite. These data suggest that the prograde growth history is tremolite - winchite - magnesio-riebeckite - crossite and the retrograde growth history is crossite - magnesio-riebeckite with low (Na + Al^{VI}) content - winchite.

temperature part containing garnet with minimum Mn content of larger than 5 per cent, for convenience' sake. Fig. 58 illustrates the distribution of the former part and the latter part in the Fuyunose nappe, which has been drawn on the basis of the data of specimens from field outcrops and boreholes, showing that the former part is developed in the upper horizon and thesoutheastern part of the nappe (Hara *et al.*, 1990c). Thus, the orientation of the Fuyunose nappe and so the overliying Saruta nappes in the subduction zone may roughly be explained by Fig. 59.

C. Subduction, Underplating and Exhumation

The retrograde growth history of amphibole in hematite-bearing basic schists of the Fuyunose nappe (subunit II) and its overlying and underlying nappes (Saruta unit and Sogauchi unit) in central Shikoku has been analyzed by Hara *et al.* (1988, 1989, 1990b) as follows (Fig. 56): Type I = hornblende - actinolitic hornblende - actinolite, Type II = hornblende - barroisite - actinolite, Type III = X - barroisite - winchite - actinolite and Type IV = X - crossite (magnesio-riebeckite) - winchite - actinolite. X of Type III is hornblende in the biotite zone (Saruta nappe) and glaucophane (ferro-glaucophane) - crossite (Magnesio-riebeckite) in the garnet zone (Fuyunose nappe). X of Type IV is hornblende - barroisite in the biotite zone (Saruta nappe) and glaucophane (ferro-glaucophane) or barroisite in the garnet zone (Fuyunose nappe). The boundaries between these four types of retrograde metamorphism cut across the nappe boundaries, showing a series of successive change in the mineralogical zoning developed both during and after the coupling of the Saruta nappe II, Saruta nappe I, Fuyunose nappe and Sogauchi nappe (Hara *et al.*, 1988, 1990b) (Fig. 60).

In the cores of plagioclase porphyroblasts of hematite-bearing basic schist of the Fuyunose subunit I, which have been collected from the Tachikawa (Tajikawa) district (Hara *et al.*, 1990a, c), are found actinolite, winchite and actinolitic hornblende (Fig. 61). The chemical composition of actinolitic hornblende is near that of barroisite. All inclusion amphibole is fine-grained. While matrix amphibole is coarse-grained, showing that its cores consist of glaucophane and crossite, its mantles of crossite and winchite and its rims of winchite and actinolite (Fig. 61), and is deflected around plagioclase porphyroblasts, being partly incorporated into their mantles. Matrix amphibole crystallized during the growth of plagioclase porphyroblast outer mantles, showing that the growth history of amphibole is actinolite - actinolitic hornblende - winchite - glaucophane for the prograde phase and glaucophane - crossite - winchite - actinolite for the retrograde phase. The retrograde growth history of amphibole of the Fuyunose subunit I is quite harmonic with that of its surrounding Fuyunose subunit II, which was mentioned in the preceding paragraph, but plagioclase porphyroblasts of the Fuyunose

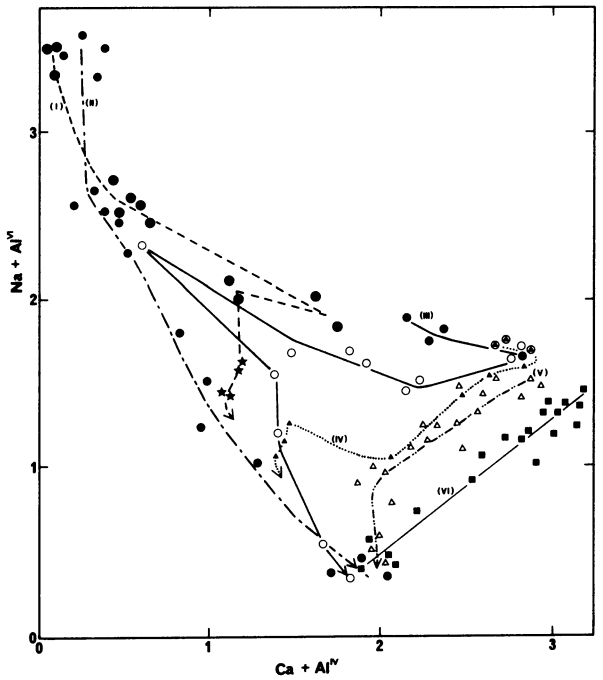

Fig. 56 Diagram showing six types of retrograde phase chemical zoning of amphibole in hematite-bearing basic schists [data from Hara *et al.* (1988)]. Arrows indicate the retrograde direction of chemical zoning. I: data from the Fuyunose nappe of the Shirataki district, II: data from the Fuyunose nappe of the Tomisato district, III: data from the Saruta nappe II of the Tomisato district, IV: data from the Saruta nappe II of the Sazare district, V: data from the Saruta nappe I of the Shirataki district, VI: data form the Saruta nappe II of the River Asemi district. circled stars, circled dots and circled solid triangles: data for amphibole grains included in plagioclase porphyroblasts.

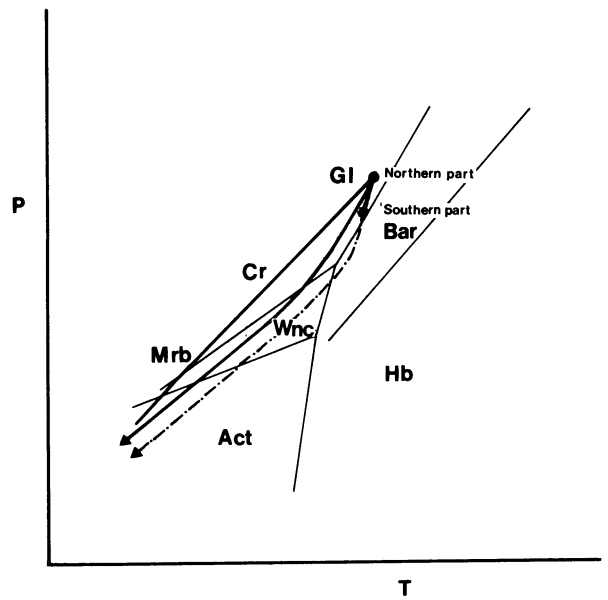

Fig. 57 P-T path of the Fuyunose subunit II as assumed from the growth history of amphibole in hematite-bearing basic schists.

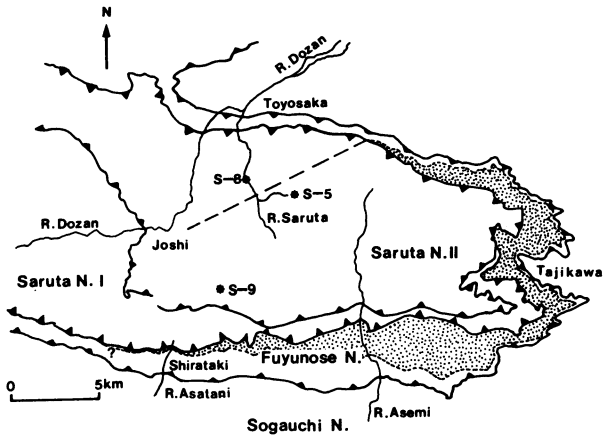

Fig. 58 Diagram showing the division of the Fuyunose nappe based on minimum Mn content of garnet in specimens from pelitic schists collected from field and boreholes (S-8, S-5 and S-9). stipled part: distribution area of garnet with minimum Mn content of less than 5% and remaining part: distribution area of garnet with minimum Mn content of larger than 5%.

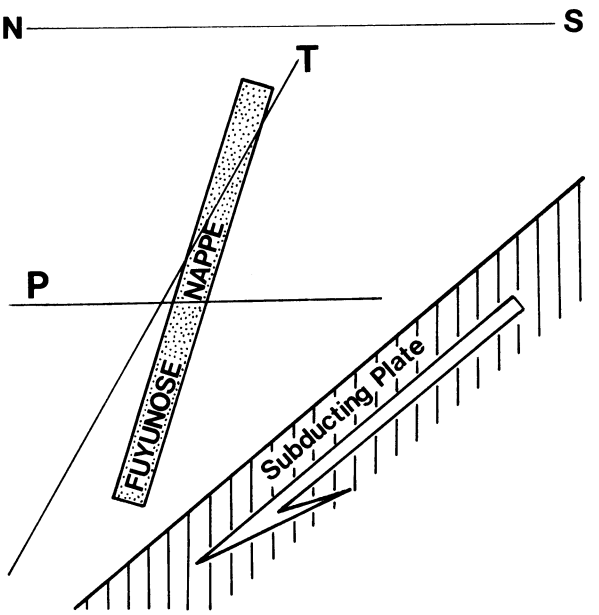

Fig. 59 Schematic diagram showing the orientation of the Fuyunose nappe in subduction zone as assumed from garnet and amphibole data. T: isothermal surface, P: isobaric surface.

subunit I crystallized during the prograde phase of metamorphism, unlike the case of the Fuyunose subunit II. It has been, thus, said by Hara *et al.* (1990a, c) that the P-T path of the Fuyunose subunit I can be roughly drawn on the diagram for the stability field of amphibole in hematite-bearing basic schists as shown in Fig. 21 and is different for the prograde phase from but identical for the retrograde phase to that of the Fuyunose subunit II (Fig. 21). It is clear that the retrograde metamorphism of the

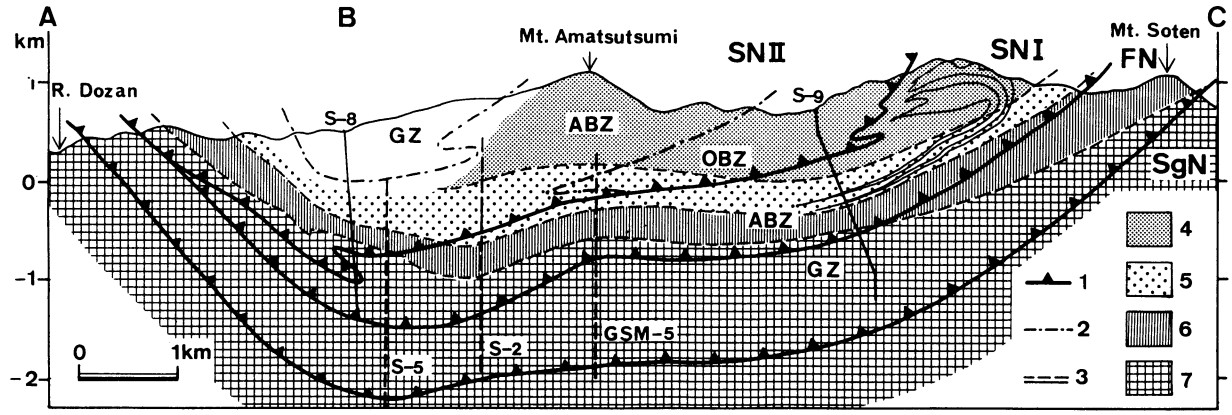

Fig. 60 Diagram showing the distribution of four types of retrograde chemical zoning of amphibole in hematite-bearing basic schists on the profile along the A-B-C line in Fig. 13 [data from Hara *et al.* (1988)]. 1: nappe boundary, 2: mineral zone boundary, 3: boreholes (S-8, S-5, S-2, GSM-5, S-9), 4: type I, 5: type II, 6: type III, 7: type IV, GZ: garnet zone, ABZ: albite-biotite zone, OBZ: oligoclase-biotite zone, SNII: Saruta nappe II, SNI: Saruta nappe I, FN: Fuyunose nappe, SgN: Sogauchi nappe.

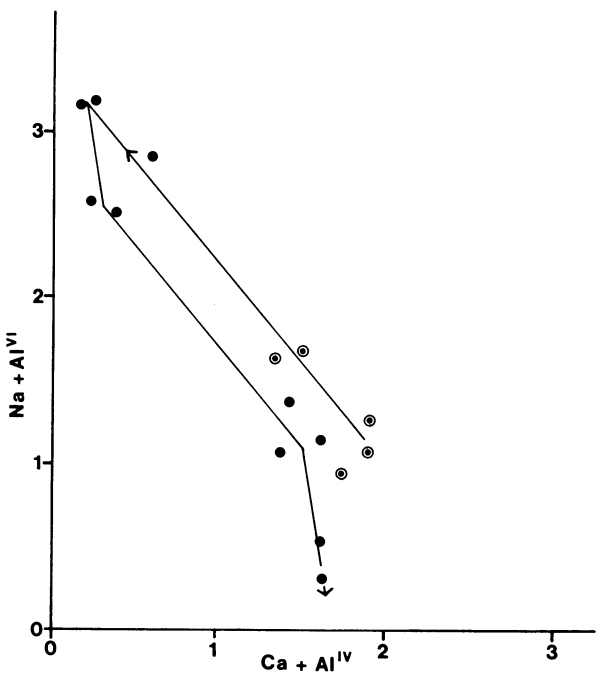

Fig. 61 Diagram showing the growth history of amphibole in hematite-bearing basic schists of the Fuyunose subunit I which has been collected from the Tajikawa district. circled dots: data for amphibole grains included in plagioclase porphyroblast cores, solid circles: data from amphibole grain included in plagioclase porphyroblast outer mantle and bedding schistosity-forming amphibole grain which show distinct chemical zonation.

Fuyunose subunit I simultaneously occurred with that of the Fuyunose subunit II, and so that the growth of crossite - glaucophane in the Fuyunose subunit I, which occurred just after the appearance of plagioclase porphyroblasts, is of the same phase as that (prograde metamorphism) in the Fuyunose subunit II. The Fuyunose subunit I must be a low-pressure equivalent of the Saruta unit, though mentioned again in the later page. It would be assumed that the mixing of the Fuyunose subunit II and the Fuyunose subunit I occurred during the subduction of the former.

On the basis of the data showing a systematic variation of Mg values of garnet in pelitic schists (Fig. 13-b), Hara *et al.* (1988, 1990b) have said that the Saruta nappe II and Saruta nappe I were overturned and mechanically coupled with the Fuyunose unit during the Sb1 phase, forming their now-observed piling relation (Fig. 62), though it was partly modified during the later phase deformation. While the

Fig. 62 Schematic diagrams illustrating the Sb1 phase tectonics of the Sambagawa metamorphic field.
a) nearly isobaric cooling of the Saruta nappe (I + II) schists (SN) and nearly isothermal heating of the Fuyunose subunit I (FuI). Spm phase TG line: thermal gradient along the plate boundary during the peak metamorphism of the Saruta unit, SgN: Sogauchi nappe. Fpm phase TG line: thermal gradient along the plate boundary during the peak metamorphism of the Fuyunose unit. b) and c) diagrams illustrating the subduction of the Fuyunose unit [Subunit II (FuII) and subunit I (FuI)], which gave rise to separation of the Saruta unit into the Saruta nappe I(SNI) and the Saruta nappe II(SNII) in the depth zone accompanying their overthrusting. KC: Kurosegawa-Koryoke continent, ChM Chichibu supermegaunit, SP: subducting plate. For fuller explanation see the text.

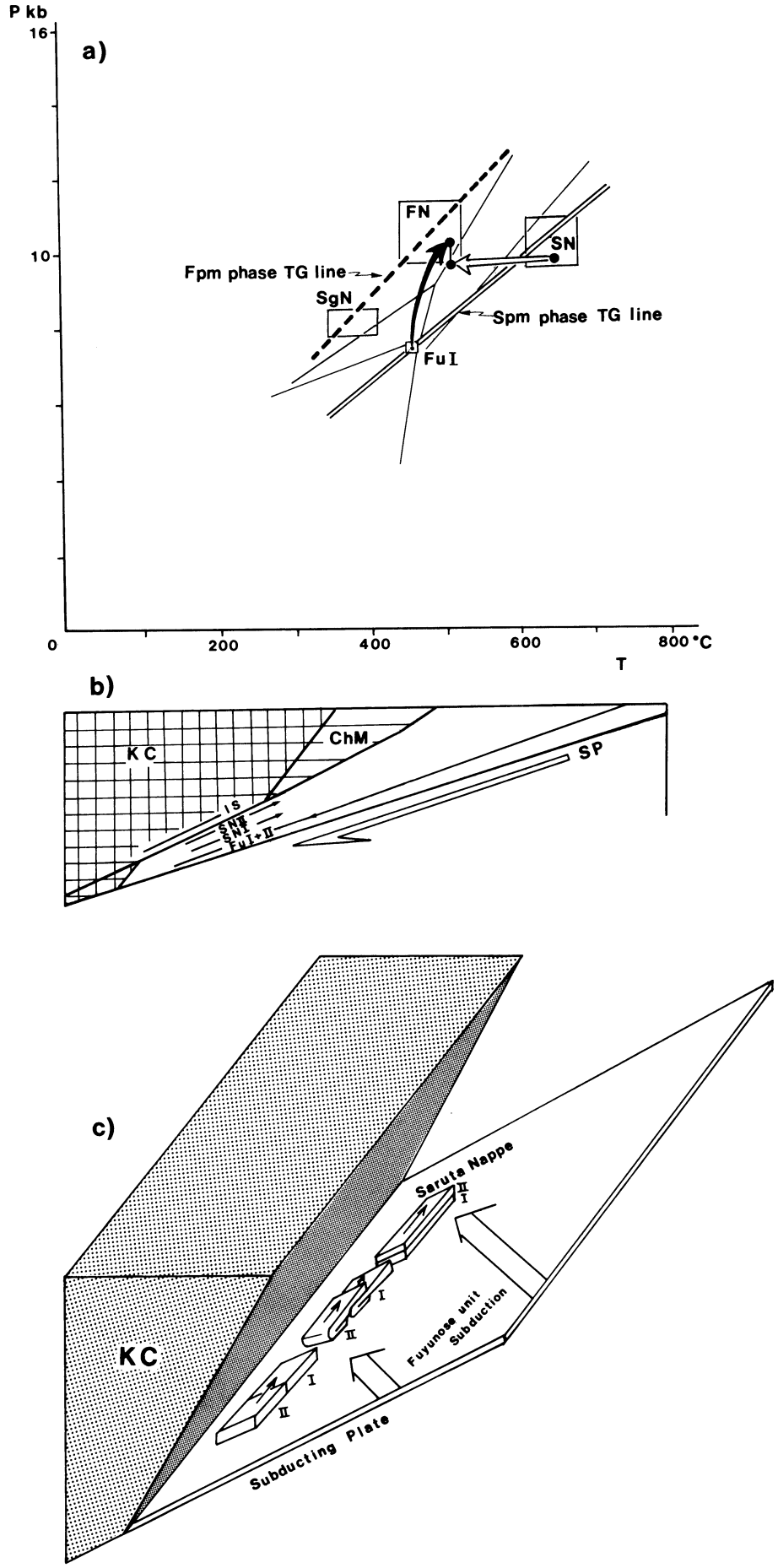
P kb
16
10
a)
FN
SN
Fpm phase TG line
SgN
Spm phase TG line
FuI
0
200
400
600
800 °C
T
b)
KC
ChM
SP
IS
SN I
SN II
FuI+II
c)
Seruta Nappe
II
I
I
II
Fuyunose unit
Subduction
KC
I
II
Subducting Plate

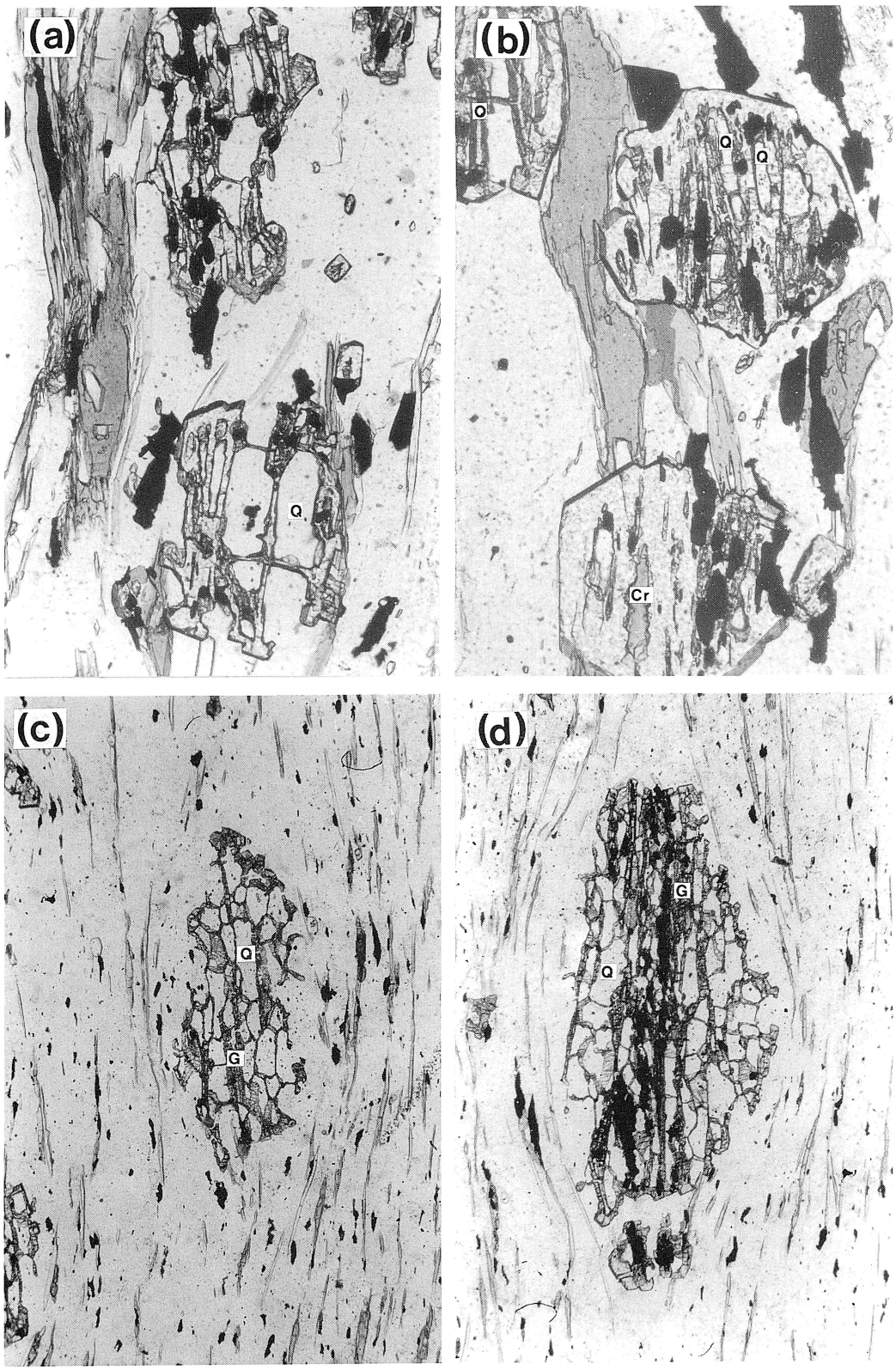

Fig. 63 Microphotographs of garnet in siliceous schists. a) and b) data from the Fuyunose nappe of the River Asemi district (Kuwanokawabashi). Garnet (G) contains crossite (Cr) and quartz (Q) as inclusions. c) and d) data from the Tsuji nappe (Fuyunose unit) of the Tsuji district. Garnet occurs in network fashion coating grain boundaries of quartz.

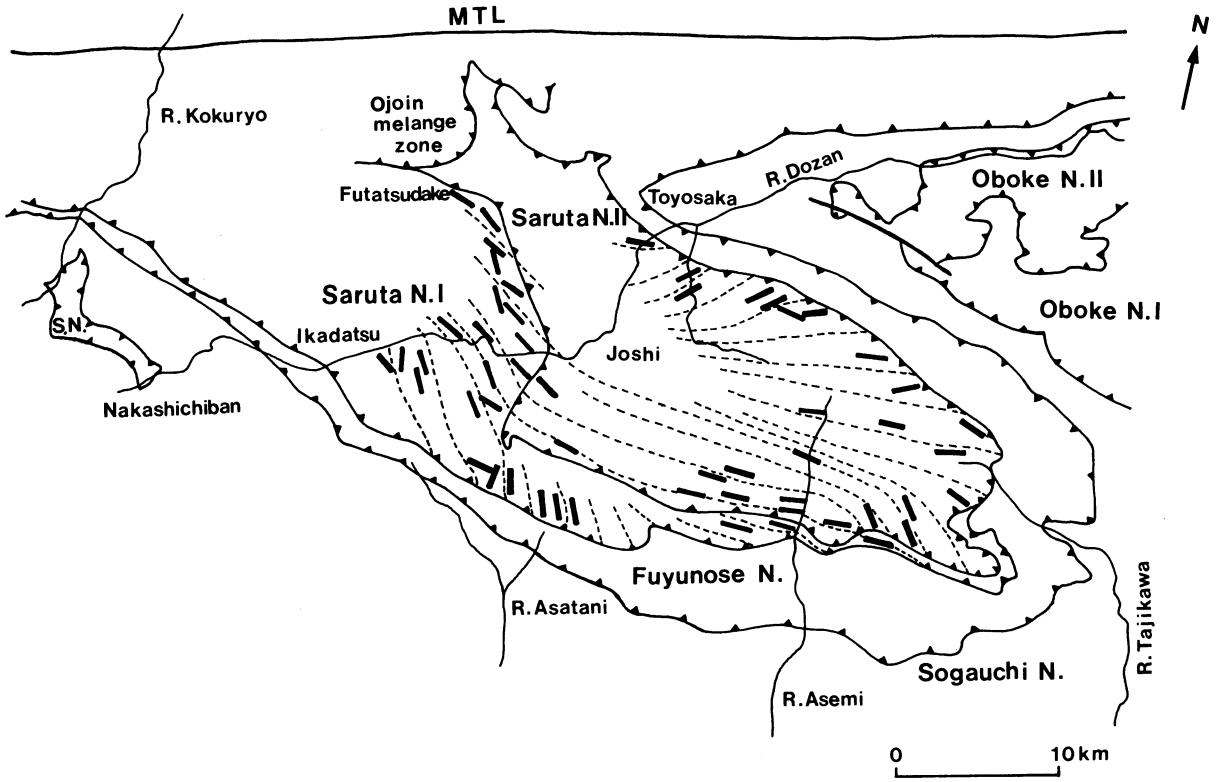

Fig. 64 Diagram showing the orientation of X of strain of the Sb1 phase in the Saruta nappe (I + II) schists as assumed from direction of preferred orientation of minerals crystallized together with plagioclase porphyroblast outer mantles. heavy short straight lines and dashed lines: measures data of orientation of X and assumed trends of X.

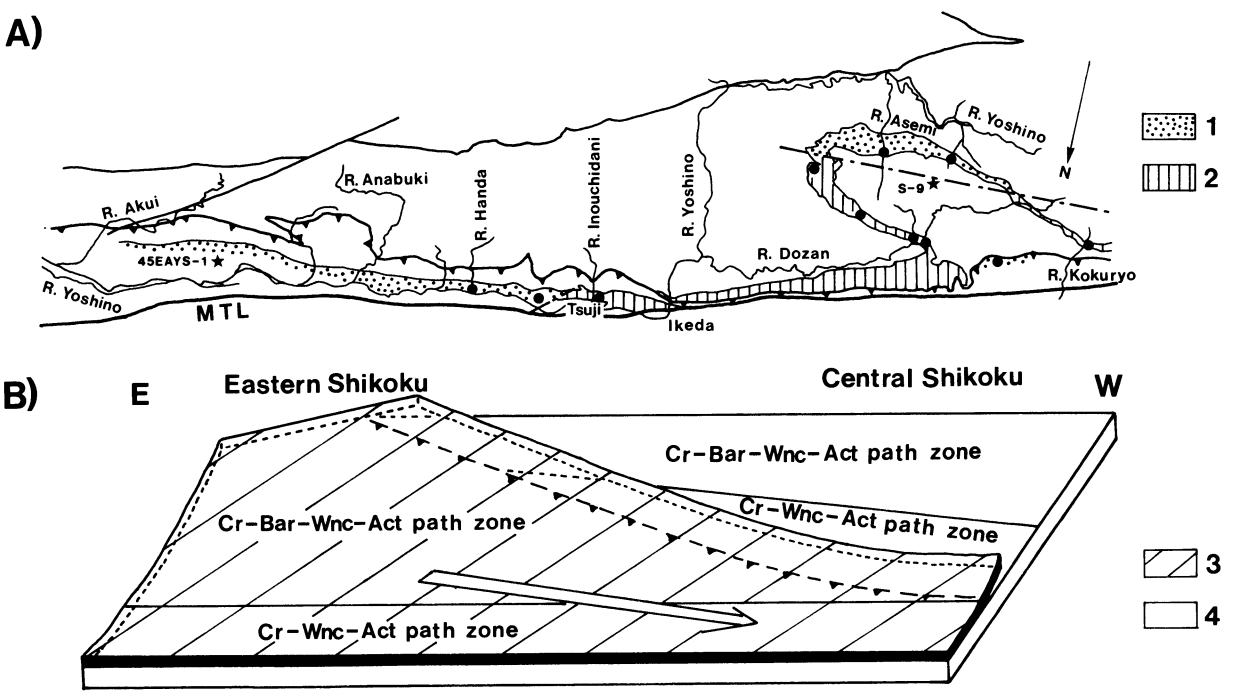

Fig. 65 A) Diagram showing the distribution of the boundary between the crossite-barroisite-winchite path zone and the crossite-winchite path zone in the Fuyunose nappe and the Tsuji nappe, which are of the retrograde growth history of amphibole in hematite-bearing basic schists. The data are from the specimens collected in the field (areas shown by solid circles) and boreholes (S-9, S-2, S-5, S-8 and 45EAYS-1).

B) schematic diagram showing the relationship between the Fuyunose nappe in central shikoku and the Tsuji nappe in eastern shikoku.

1: crossite-barroisite-winchite path zone, 2: crossite-winchite path zone, 3: Tsuji nappe, 4: Fuyunose nappe, Arrow: assumed displacement direction of the Tsuji nappe

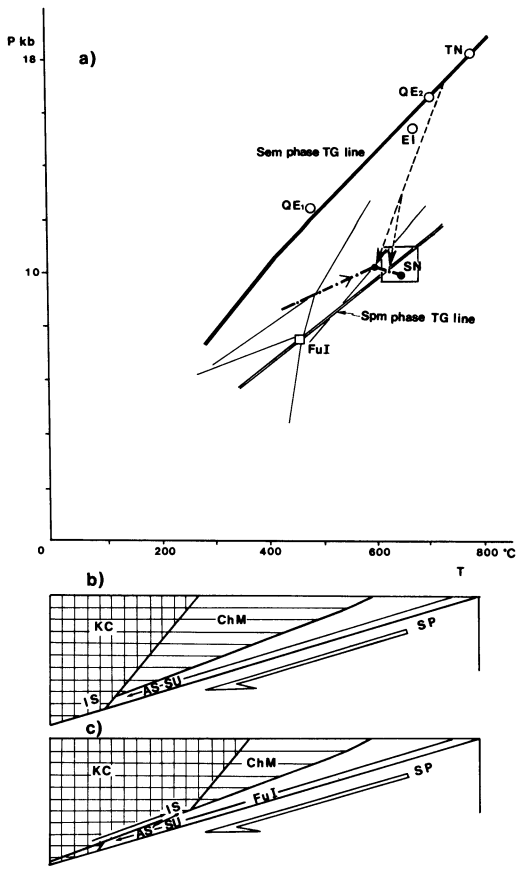

Fig. 66 Schematic diagrams illustrating the Bic-Spm phase tectonics in the Sambagawa metamorphic field.
a) exhumation of the Kurosegawa-koryoke continent giving rise to heating of the Saruta unit and to mixing of its blocks [Iratsu metagabbro, Tonaru metagabbro (TN), Quartz eclogite (QE1 and QE2), Higashiakaishiyama peridotite and Sebadani metagabbro] with the Saruta unit schists. Sem phase TG line: thermal gradient along the plate boundary during the earlier phase of metamorphism of the Saruta unit, Spm phase TG line: thermal gradient along the plate boundary during the peak metamorphism of the Saruta unit. The change from the Sem phase TG line to the Spm phase TG line occurred owing to thrusting of the Kurosegawa-koryoke continent onto the Saruta unit. FuI: P-T condition of the Fuyunose subunit I (= lower-pressure part of the Saruta unit) during the Spm phase, b) tectonics during the earlier phase of metamorphism of the Saruta unit, c) tectonics during the Sim-Spm phase. AS: initial position of Saruta unit schists with abnormal garnet, SU: Saruta unit schists with normal garnet, FuI: initial position of the Fuyunose subunit I, IS: initial position of tectonic blocks such as Iratsu metagabbro and Tonaru metagabbro, KC: Kurosegawa-koryoke continent, ChM: Chichibu supermegaunit, Sp: subducting plate.

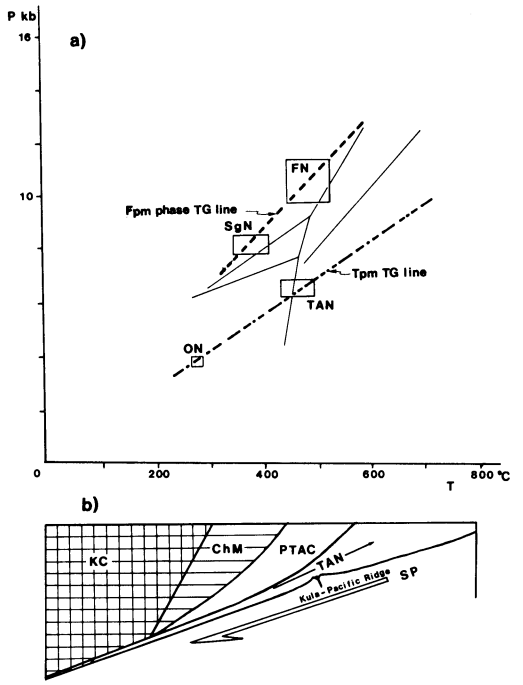

Fig. 67 Schematic diagrams illustrating the tectonics of the Tatsuyama phase.
a) diagram illustrating the change of thermal gradient along the plate boundary from the phase (Fpm phase) of peak metamorphism of the Fuyunose unit to the phase (Tpm phase) of peak metamorphism of the Tatsuyama unit. FN: Fuyunose nappe, SgN: Sogauchi nappe, TAN: Tatsuyama nappe, ON: Oboke nappe.
b) diagram illustrating the relationship between the peak metamorphism of the Tatsuyama unit and the subduction of the Kula-Pacific ridge. SP: subducting plate, KC: Kurosegawa-Koryoke continent, ChM: Chichibu megaunit, PTAC: pre-Tatsuyama accretionary complexes.

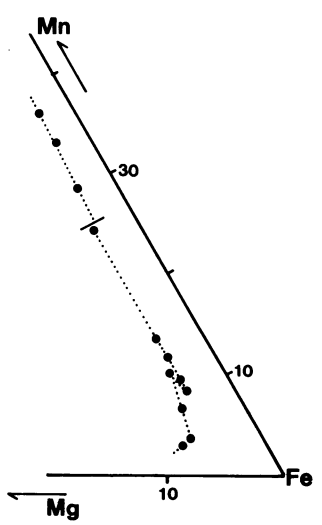

Fig. 68 Mn-Fe-Mg diagram of garnet of Fig. 31-c, in which only a straight Si schistosity is developed from core to outer mantle. In the middle part of mantle is found a reverse zoning.

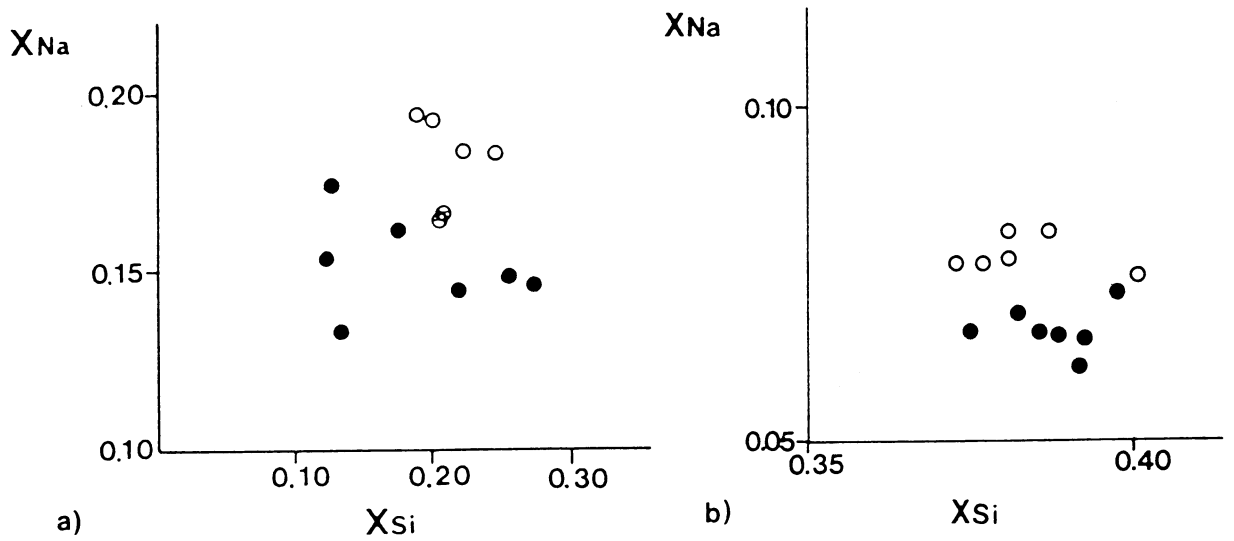

Fig. 69 Diagrams showing the variation in chemical composition between muscovites of different crystallization phases.
a) data from pelitic schists of the oligoclase-biotite zone of the Saruta nappe II of the River Asemi district (Hara *et al.*, 1984). open circles: muscovite in plagioclase porphyroblast cores and inner mantles, circled bars: muscovite in plagioclase porphyroblast outer mantles, solid circles: matrix bedding schistosity-forming muscovite.
b) data from pelitic schists of the garnet zone of the Fuyunose nappe of the Shirataki district (Hara *et al.*, 1990a). open circles: muscovite in plagioclase porphyroblast cores, solid circles: matrix bedding schistosity-forming muscovite. XNa: Na/(Na + K), XSi: (Si/2-3).

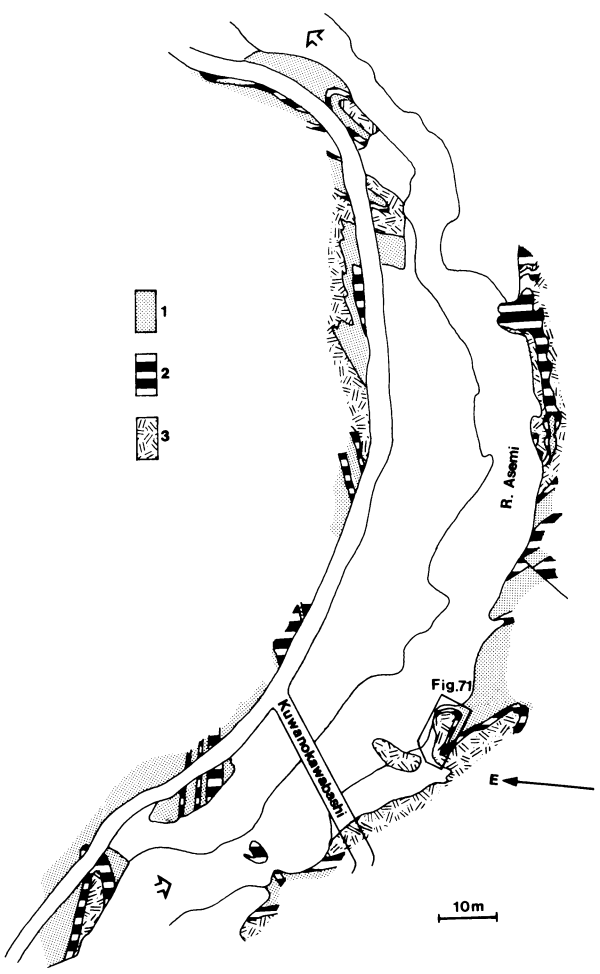

data (Fig. 60) for the growth history of amphibole in hematite-bearing basic schists in the Saruta unit, Fuyunose unit and Sogauchi unit suggest the phases when the coupling of these units occurred (Hara *et al.*, 1988, 1990a , b, c): The underplating of the Fuyunose unit (subunit II and subunit I) beneath the Saruta nappe II and Saruta nappe I is considered to have occurred during the Sb1 phase, because the metamorphic grade (glaucophane zone) of the highest temperature phase of the Fuyunose nappe schists appears to be continuous with that (barroisite zone - hornblende zone) of the retrograde phase of the overlying Saruta nappe (I + II) schists, and the underplating of the Sogauchi unit beneath the Saruta nappe II, Saruta nappe I and Fuyunose nappe is considered to coincide with the beginning of the retrograde metamorphism of the Fuyunose nappe schists, because the metamorphic grade (crossite zone) of the highest temperature phase of the Sogauchi nappe schists appears to coincide and to be continuous with that of the retrograde phase of the overlying Fuyunose nappe and Saruta nappe (I + II) schists. The deformation related to the formation of the Si schistosity in garnet of the Fuyunose subunit I and subunit II (Fig. 63) is of the Sb1 phase. The deformation related to the formation of the Si schistosity in plagioclase porphyroblasts of the

Fig. 70 Route map along the River Asemi around Kuwanokawabashi, showing the location of Fig. 71 [data from Shiota and Hara (1972)]. The diagram illustrating the development of the Kuwanokawabashi fold. 1: pelitic schists, 2: siliceous schists, 3: basic schists.

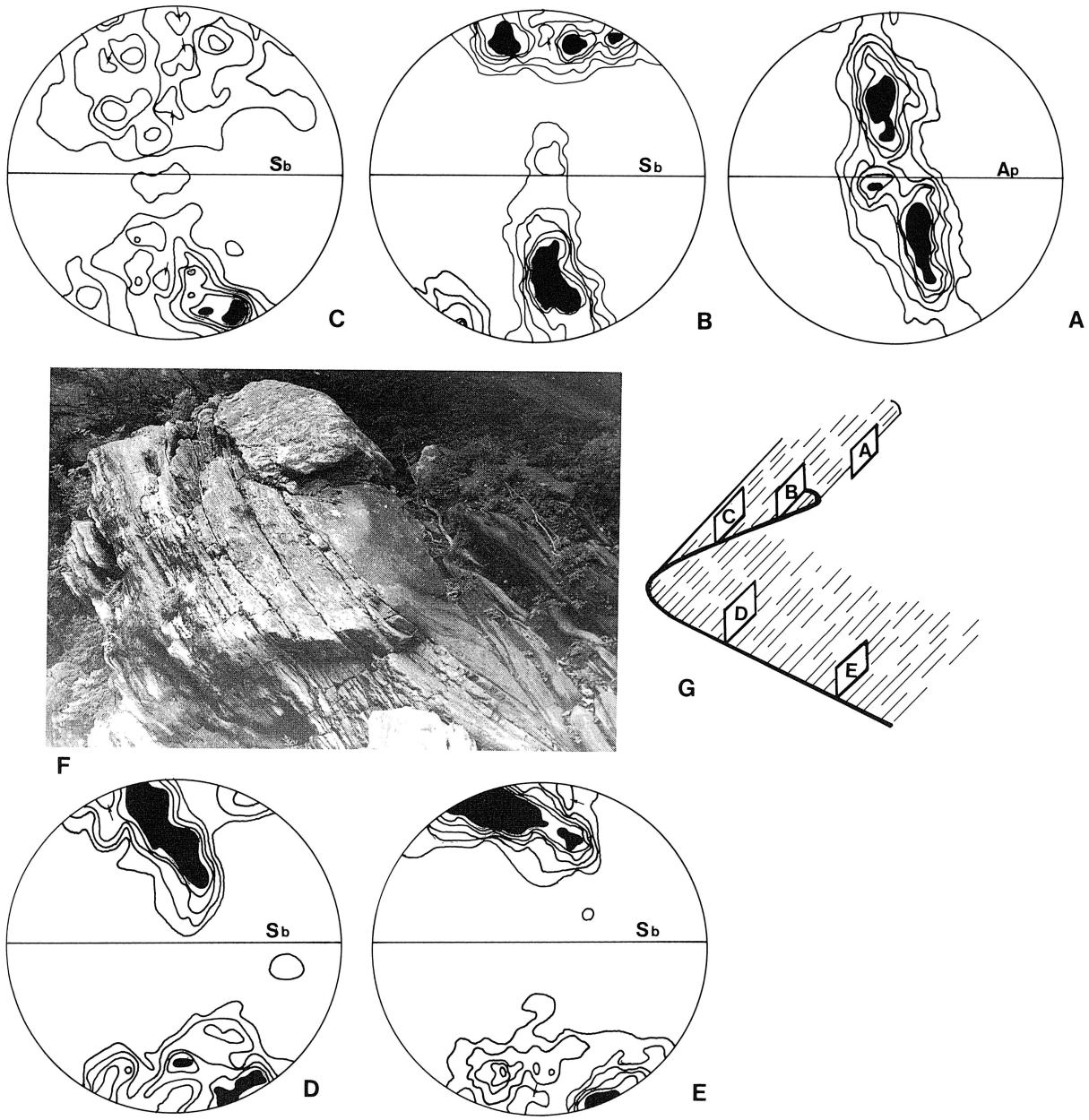

Fig. 71 Quartz c-axis fabrics of siliceous schists involved in the Kuwanokawabashi fold (F). The orientation of thin section of five analyzed specimens (A, B, C, D and E), which are parallel to the fold axis, are shown in G of this figure. Ap: axial plane, Sb: bedding schistosity.

Fuyunose subunit II, which is of the beginning phase of its retrograde metamorphism, has been called Sb2-1 deformation (Hara *et al.*, 1990a) (Fig. 40). As shown in the later page, the orientation of X of strain in the Fuyunose nappe schists is quite different between the Sb1 phase and the Sb2-1 phase and oblique at high angles to each other. However, that of the Sb2-1 phase is as a whole approximately parallel to that in the Sogauchi nappe schist, though displacement occurred along the nappe boundary between the Fuyunose nappe and the Sogauchi nappe during the Sb2-2 phase after their coupling. Thus, it may be said that the tectonics of the Sb1 phase and that of the Sb2-1 phase is quite harmonic with two-way street model for sediment subduction, underplating and exhumation in subduction zone (*e.g.* Suppe, 1972).

The movement picture of the Saruta nappes during the Sb1 phase may be partly explained by Fig. 64. This figure illustrates the orientation pattern of X of strain of the Sb1 phase in the Saruta nappes. The orientation direction of X is highly oblique to that of the Sim-Bim phase (Fig. 48) in many places. The Saruta nappe (I + II) schists show nearly isobaric cooling during the Sb1 phase as mentioned in the preceding page (Fig. 62). However, the Sb1 phase deformation of the Saruta nappe (I + II) schists was of high magnitude of strain forming the now-observed fundamental characteristics of their bedding schistosity. The shear sense of the Sb1 phase ductile flow of the Saruta nappe (I + II) schists was to roughly determine by the Si (Si in PPP outer

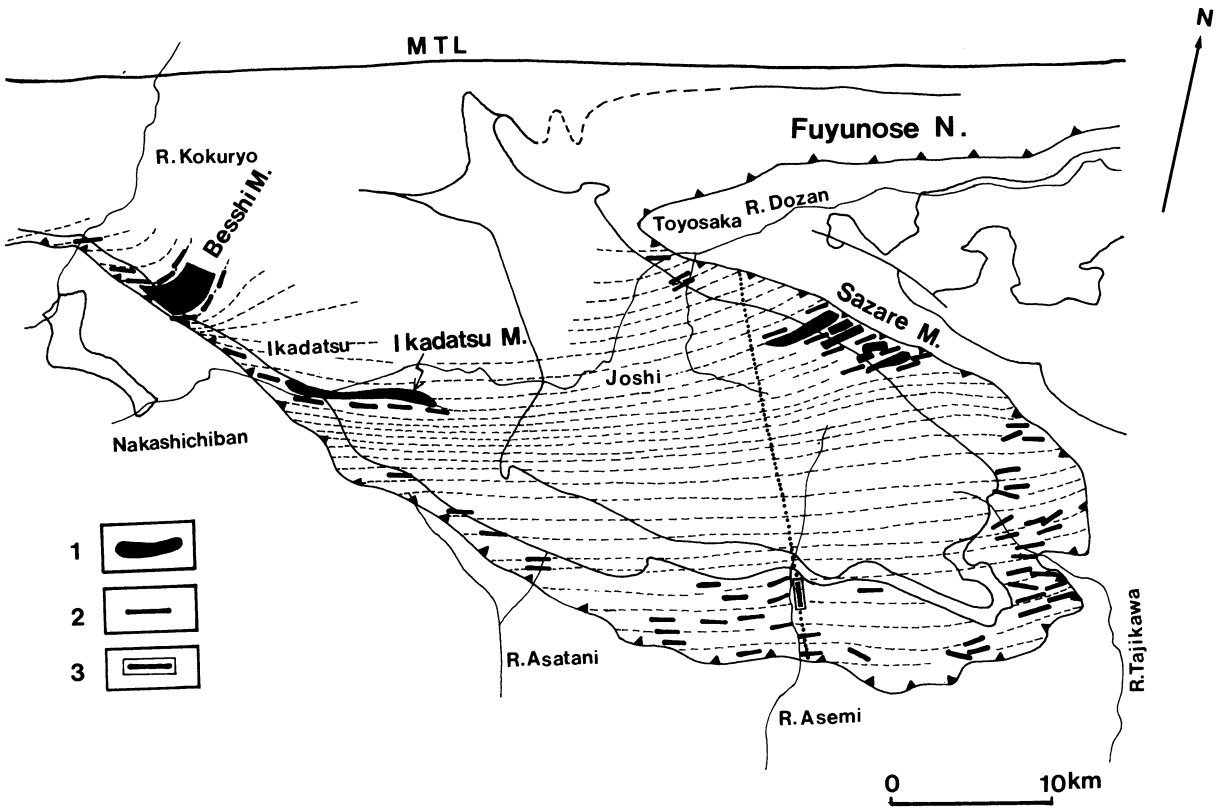

Fig. 72 Diagram showing the orientation of X of strain of the Sb2-1 phase in the Fuyunose nappe as assumed from preferred orientation of amphibole on the bedding schistosity. 1: orientation of bonanza of Besshi-type ore deposit (Besshi mine, Ikadatsu mine and Sazare mine) (Sumitomo Metal Mining Co. Ltd., 1981), 2 heavy short straight lines and dashed lines: measured data of orientation of X and assumed trends of X, 3: orientation of X of the Sb1 phase assumed from c-axis fabric of quartz grains included in garnet.

mantles) - Se relation in basic schists of only some places. Such the data suggest eastward shear for the Sb1 phase deformation of the Saruta nappe (I + II) schists (Hara *et al.*, 1990c). The exhumation of the Sambagawa schists, Saruta nappe (I + II) and Fuyunose nappe schists, in great volume had not occurred until the Sb2-1 phase when the subduction of the Kula-Pacific ridge began in Kyushu and Shikoku. The ductile flow of the Sambagawa schists during the Sb2-1 - Sb2-2 phase appears to be of westward sense, unlike the case of the Sb1 phase, as mentioned in the later pages (Hara *et al.*, 1988, 1990a; Wallis, 1990). The orientation direction of X in the Saruta nappes (Fig. 64) appears to be only slightly oblique to the isobaric line (Fig. 65) of the Fuyunose nappe during the exhumation phase (Sb2-1 phase).

Plagioclase porphyroblasts in the Fuyunose subunit I crystallized during the prograde phase of metamorphism before the Sb1 deformation. It has been therefore assumed by Hara *et al.* (1990a, c) that the Fuyunose subunit I belongs to the Saruta unit and was derived from its low-pressure part when the subduction of the Fuyunose subunit II occurred (Fig. 62). If so, the chemical composition of inclusion amphibole in plagioclase porphyroblasts of the Fuyunose subunit I should indicate the physical condition of the low-pressure part of the Saruta unit during the Spm phase just before the Sb1 phase and along the plate boundary. Namely, the thermal gradient along the plate boundary during the Spm phase must be to be roughly estimated from such the data for the Fuyunose subunit I as a line (Spm phase TG line) in Fig. 66. The P-T field of the Spm phase for the oligoclase-biotite zone schists of the Saruta unit is placed near the Spm phase TG line.

The P-T field of the Fuyunose subunit I greatly changed during the Sb1 phase, showing nearly isothermal subduction (Fig. 62). This fact suggests that the thermal gradient greatly changed during the period from the Spm phase to the Sb1 phase. The Fpm phase TG line in Fig. 67 is the thermal gradient along the plate boundary as roughly estimated from the P-T field of the peak metamorphism of the Fuyunose nappe schists. The change of thermal gradient from the Spm phase TG line to the Fpm phase TG line would be ascribed to the high-speed subduction of low-temperature plate during the Sb1 phase (Hara *et al.*, 1990a).

In the Saruta unit are mixed tectonic blocks such as the Higashi- akaishiyama peridotite, Iratsu metagabbro, Tonaru metagabbro and Sebadani metagabbro, which were directly tectonically introduced from the hanging wall of the lower crust - upper mantle possibly of an island arc (K-continent) (*e.g.* Kunugiza, 1980; Takasu, 1984, 1989; Kunugiza *et al.*, 1986). The metamorphic histories of these tectonic blocks have been analyzed by Takasu (1984, 1989) as shown in Fig. 66. The mixing has been assumed by Hara *et al.* (1990a) to have occurred during the period from the Sim-Bim phase to the Wd phase (Fig. 32), owing to the over-

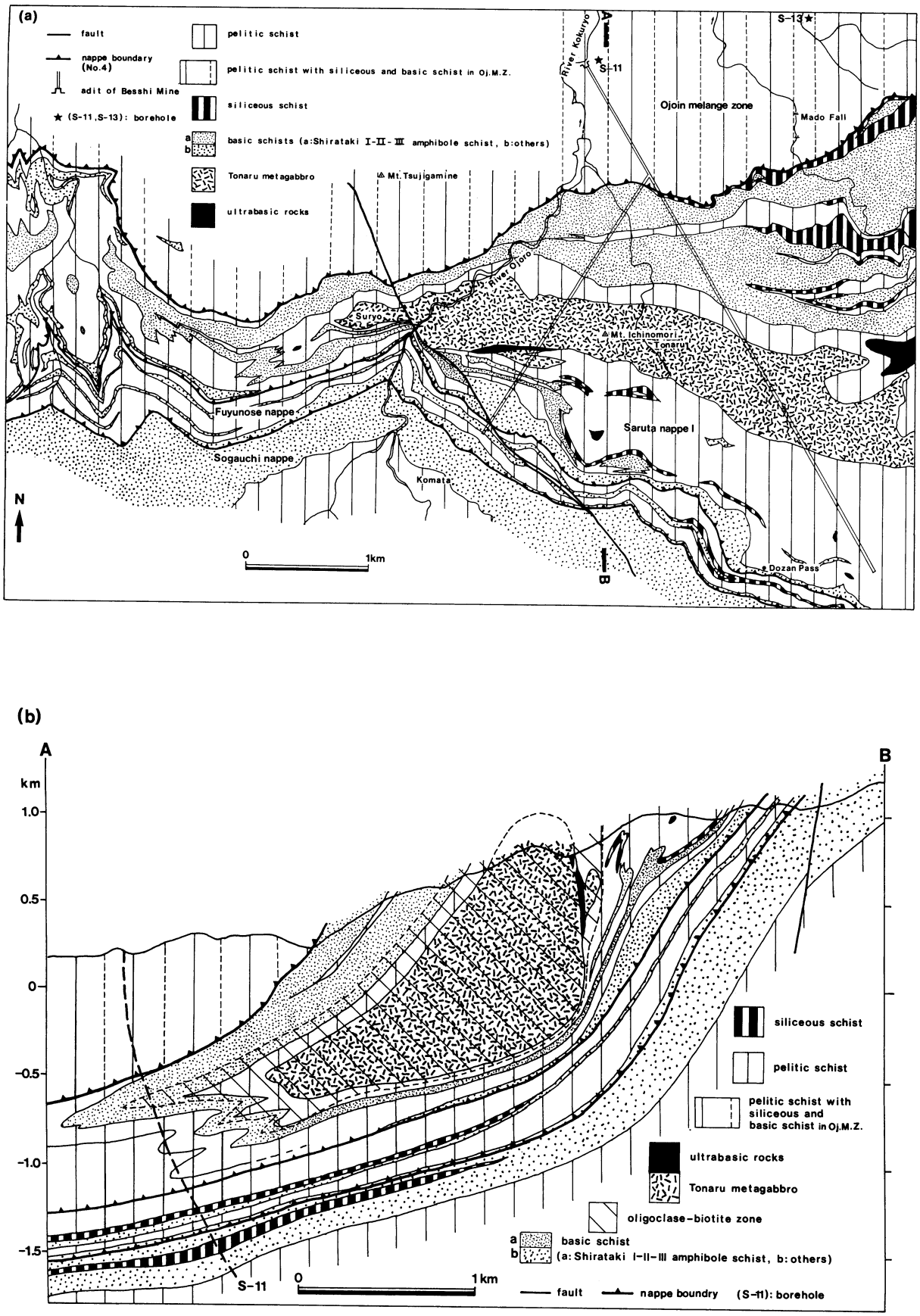

Fig. 73 Geological map (a) and profile (b) of the Besshi mine district [partly modified from Hara *et al.* (1990b)].

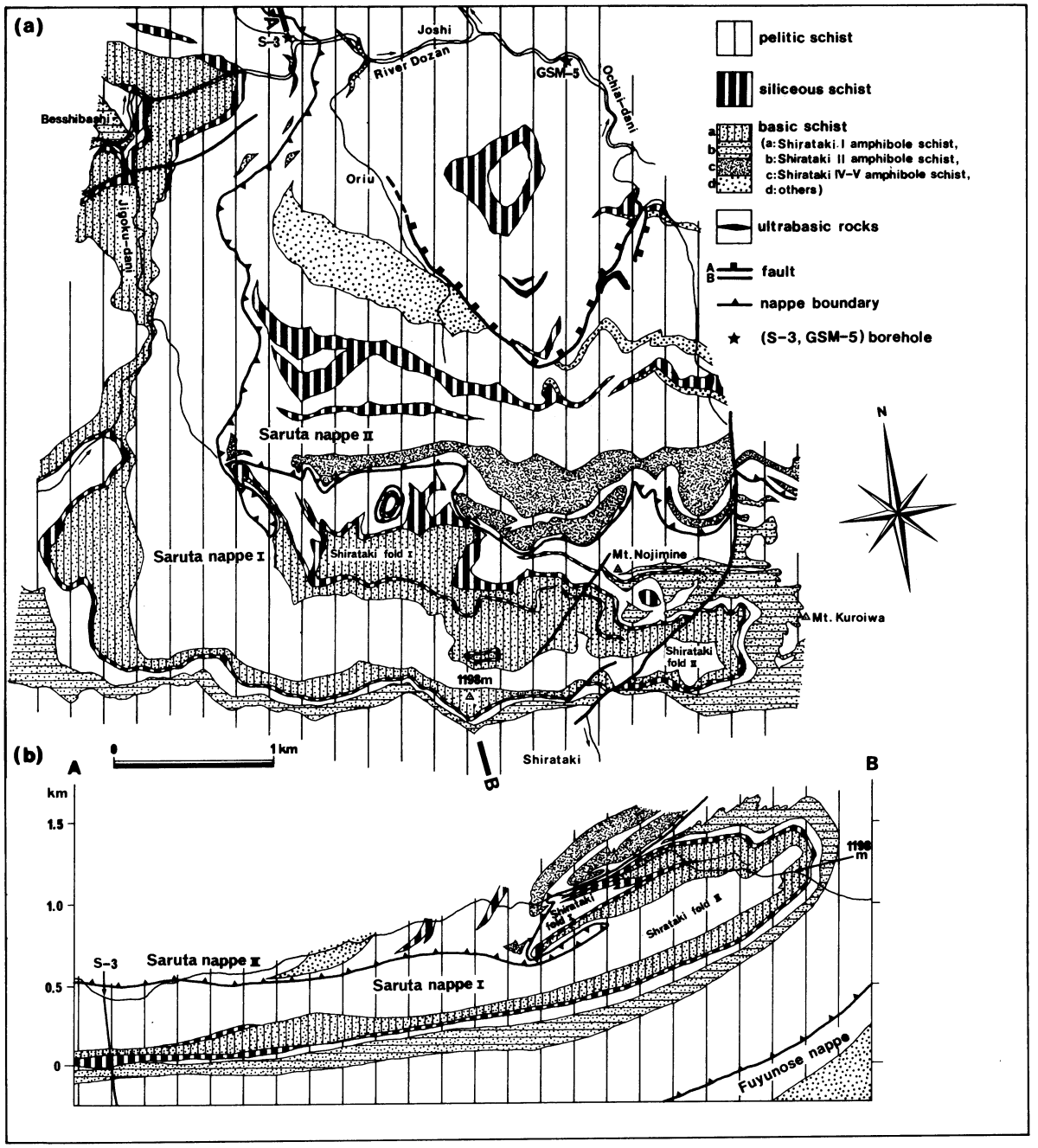

Fig. 74 Geological map (a) and profile (b) of the Shirataki-Joshi district [partly modified from Hara *et al.* (1990b)]. fault-A: thrust with cataclasite, fault-B: steeply dipping fault.

thrusting of the K-continent onto the Saruta unit (Fig. 66). The P-T field of the K-continent blocks just before the beginning of their cooling should be related to the thermal gradient along the plate boundary in the subduction zone, which was responsible for the formation of the Saruta nappe (I + II) schists. From Fig. 66 (Sem TG line), the thermal gradient of this phase appears to have been near the Fpm phase TG line. The cooling path of the K-continent related to its overthrusting-mixing should correspond to the heating path of the Saruta unit. The overthrusting-mixing of the K-continent gave rise to the great increase of thermal gradient along the plate boundary which corresponds to the Spm phase TG line (Fig. 66). The nearly isobaric heating path of the Saruta unit from the Bic phase to the Spm phase must correspond to the phase of the overthrusting of the K-continent. Garnet in pelitic schists of the Saruta nappe I is divided into two types with reference to chemical zonation, normal garnet with simple bell-shaped chemical zonation (except for its rims), and abnormal garnet showing partly reverse zonation within mantles which is developed in the boundary between the cores and the inner mantles and between the inner mantles and the outer mantles (Fig. 33-a and b). Such a reverse zonation in mantles is also found in garnet where the Si fabric is homogeneous throughout

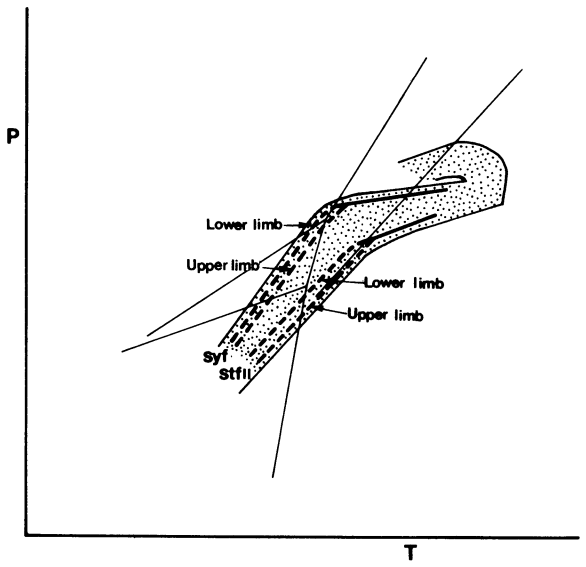

Fig. 75 Diagram showing the retrograde growth history of amphibole in hematite-bearing basic schists involved in the Suryo fold (Syf) and the Shirataki fold II (StfII) of the Saruta nappe I [data from Hara *et al.* (1988, 1990b)]. It is clearly different between the upper limb and the lower limb of both folds.

its whole part as shown in Fig. 31. That is illustrated in Fig. 68. In such garnet had not occurred its resorption during the Sim-Bim phase and Som phase. The reverse zonation in mantles must be a chemical zonation which corresponds to decrease of temperature. Fig. 33-d illustrates distribution of pelitic schists with normal garnet and these with abnormal garnet in the Saruta nappe I of the River Dozan district, showing that the former and the latter occur as blocks. Such a structure has been explained by Hara *et al.* (1990a) as follows: The pelitic schists of higher temperature were intermingled with these of lower temperature during the Sim-Bim deformation and the Som deformation, giving rise to abnormal garnet in the former and normal garnet in the latter. The temperature of the metamorphic field increased still, throughout the Wd phase, until the Spm phase after such the deformations. This is ascribed to the thermal metamorphism by the overthrusting K-continent. During this overthrusting occurred the tectonic mixing of geological bodies placed in various positions of between ca. 10 kb depth and ca. 17 kb depth in the subduction zone. Hara *et al.* (1991a) have pointed out a possibility that the overthrusting (collapse) of the K-continent in its southern-frontal subduction zone is ascribed to its collision with the IA supermegaunit and Hida continent.

D. Tectonics of Retrograde Phase of the Fuyunose Nappe

Fig. 53-b illustrates Si-Se relations for plagioclase porphyroblasts of the Fuyunose subunit II, showing that the

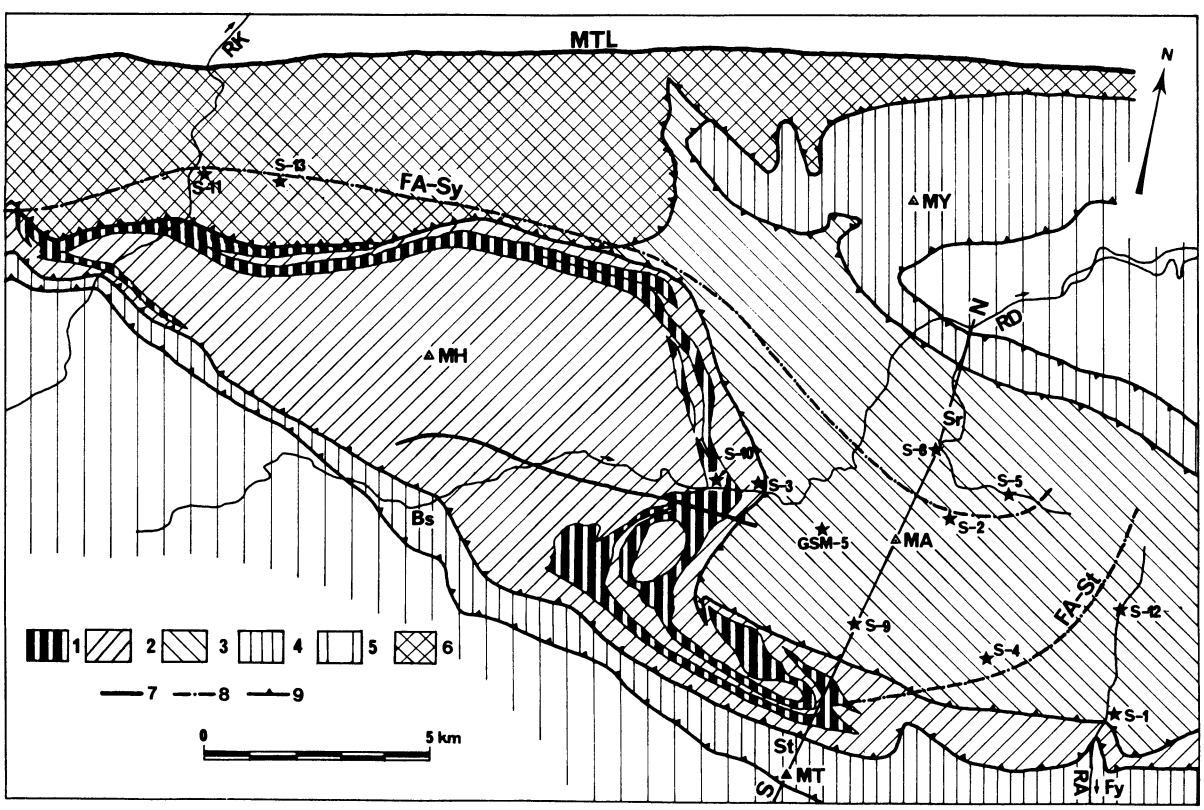

Fig. 76 Diagram showing the position of the axis of the Suryo fold (FA-Sy) and that of the Shirataki fold II as assumed from the data of field and boreholes (S-11, S-13, S-8, S-5, S-2, S-4, S-1 and S-12 by MMEAJ).
1: Shirataki I-II amphibole schists, 2: Saruta nappe I, 3: Saruta nappe II, 4: Fuyunose nappe, 5: Sogauchi nappe, 6: Ojoin melange zone, 7: fault, 8: fold axis, 9: nappe boundary.

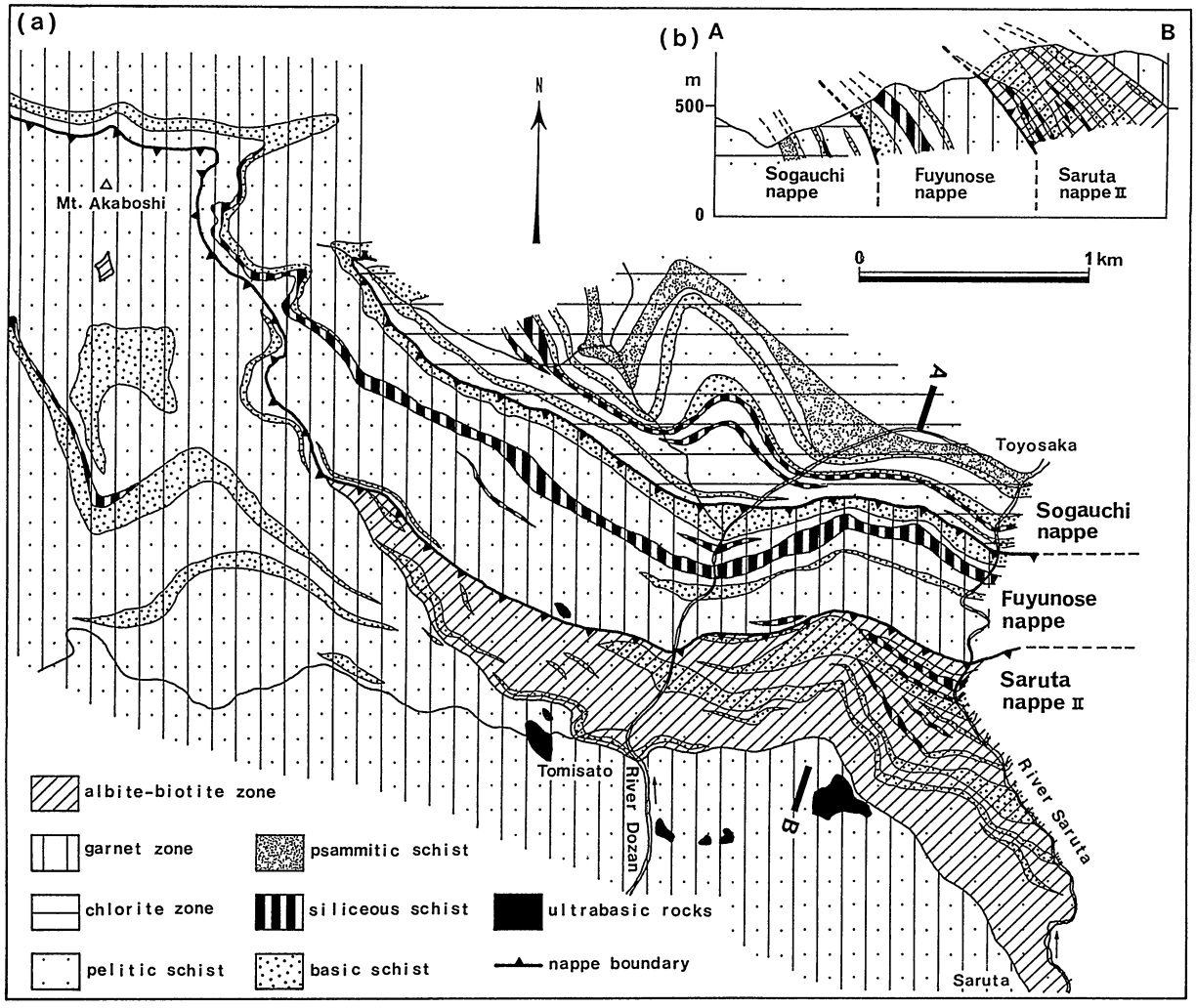

Fig. 77 Geological map (a) and profile (b) of the Tomisato district [partly modified from Hara *et al.* (1990b)].

bedding schistosity Se (Sb2-2) around them is oblique to and discontinuous with the Si schistosity (Sb2-1) in them. The deformation related to the formation of the Sb2-2 schistosity has been called Sb2-2 deformation (Hara *et al.*, 1990a,c). Fig. 69 illustrates the variation in chemical composition between the Sb2-1-forming muscovite and the Sb2-2-forming muscovite, showing further retrograde metamorphism of the Fuyunose nappe schists during the Sb2-2 phase.

The geological structure of the Fuyunose nappe, which was produced by the Sb2-1 deformation, is clearly observed in the River Asemi district. That is illustrated in Fig. 70, being characterized by isoclinal folds of mesoscopic scales (Kuwanokawabashi fold) which have E-W trending axes and northward dipping axial surfaces. The Si fabrics (B2-1 fold) of plagioclase porphyroblasts in these folds (Fig. 53-c) indicate that the Kuwanokawabashi folding had already occurred before the crystallization of the porphyroblasts: The B2-1 folds correspond to the axial plane cleavage (crenulation type folds) of the Kuwanokawabashi fold. They do not show disharmonic variation in fold form between cores and mantles of plagioclase porphyroblasts. It is clear that the Kuwanokawabashi folding stopped when their crystallization occurred.

Fig. 71 illustrates quartz c-axis fabrics in a Kuwanokawabashi fold of siliceous schists found just in south of the bridge Kuwanokawabashi. The c-axis fabric of quartz grains included in garnet (Fig. 63-a and b) shows a type I crossed girdle, though c-axis concentration is of low magnitude, (Fig. 24) and X of strain, as assumed from its pattern, is oriented in a direction subnormal to the fold axis and to mineral lineation defined by preferred dimensional orientation of amphibole. Matrix quartz grains show elongate shape, forming a schistosity oblique at low angles to the bedding schistosity, i.e. Type II S-C mylonite (cf. Lister and Snoke, 1984), and to Sb2-1 in plagioclase porphyroblasts (Fig. 89-c), as observed on sections parallel to mineral lineation (= fold axis) and normal to the bedding schistosity. Their c-axis fabrics, which have been measured on both limbs and axial zone, show type I crossed girdle and a single girdle of shear strain type (Fig. 71), whose shear sense is westward. The deformation related to the formation of the matrix quartz microtextures mentioned above is of the Sb2-2 phase. Thus, it can be said that the Kuwanokawabashi fold appeared during the Sb2-1 phase but was modified under non-deformational condition of

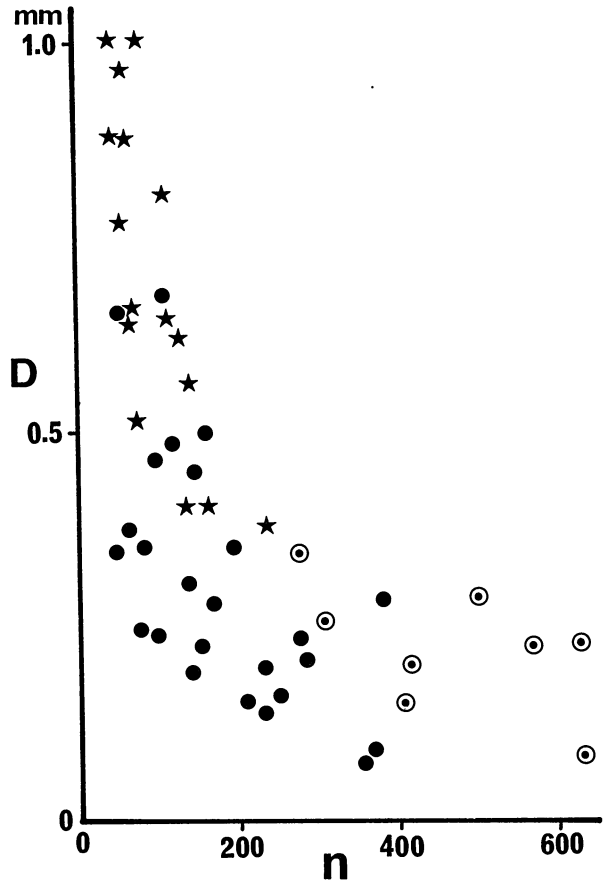

Fig. 78 Diagram showing the relationship between size (D) and grain number (n) of plagioclase porphyroblasts in pelitic schists as measured within 1cm^2 on thin sections parallel to mineral lineation and normal to the bedding schistosity.
stars: data from the Saruta nappes, solid circles and circled dots: data from the Fuyunose nappe, though these shown by circled dots are derived from pelitic schists placed near the nappe boundaries in the Shirataki district and Ikadatsu district.

the inter Sb2-1 - Sb2-2 phase and by the Sb2-2 deformation.

The axes of the Kuwanokawabashi fold are commonly parallel to mineral lineation defined by preferred shape orientation of amphibole. Mineral lineation (= X of strain) in the Fuyunose nappe may be explained to be preferably oriented as shown in Fig. 72. The elongation directions of the bonanzas of Besshi-type ore deposit in the Fuyunose nappe are in general oriented along and in the axial zones of folds with their axes parallel to such mineral lineation (cf. Hide, 1961). These, as well as orientation of mineral lineation, are shown in Fig. 72. This figure illustrates also the movement picture of the Fuyunose nappe, direction of ductile flow of the Fuyunose nappe schists, during the Sb2-1 deformation.

The geological structures of the Sb2-1 phase in the Saruta nappes are Suryo fold (Fig. 73), Shirataki fold II (Fig. 74) and other isoclinal folds. Mineral lineation (Lb1) defined by preferred shape orientation of hornblende grains, which crystallized during the Sb1 phase, is externally rotated around their axes, showing that their formation began just after the Sb1 deformation (Fig. 75). From the growth history of amphibole in hematite-bearing basic schists (Fig. 60), it is clear that the folding for these folds began during the Sb2-1 phase (Hara *et al.*, 1990a, b). Fig. 76 illustrates the axial trends of the Suryo fold and Shirataki fold II which have been drawn on the basis of the field data and borehole data.

The contact relationship between the Saruta nappe II and the Saruta nappe I and that between the Saruta nappes and the Fuyunose nappe were modified by the Sb2-1 and Sb2-2 deformations as is obvious from the development of the Suryo fold and Shirataki fold II (Figs. 73 and 74). Analogous modification of the nappe boundary is also slightly found in the Saruta district (Fig. 77). The block of biotite zone schists in the Fuyunose nappe of the River Asemi district, which is the Fuyunose subunit III (Fig. 13), has been considered by Shiota (1987, 1991) and Hara *et al.* (1990b) to have been tectonically derived from the Saruta nappe I during the Sb2-1 deformation. These facts clearly indicate the structural discontinuity between the Saruta nappe (I + II) schists and the Fuyunose nappe schists (Hara *et al.*, 1988, 1990b), in spite of Banno and Sakai's (1989) interpretation that the former is structurally continuous with the latter. Banno and Sakai (1989) have said that the facies series of the Sambagawa metamorphism can be explained in terms of mineralogical zoning such as crosite zone - barroiste zone - hornblende zone in hematite-bearing basic schists and these zones are continuously developed throughout the Saruta nappe (I + II) schists and Fuyunose nappe schists in such a fashion that their boundary is placed within the barroisite zone. As compared with each other with reference to metamorphic minerals crystallized during the highest-temperature phase, however, the biotite zone of the Saruta nappes belongs to the hornblende zone and the garnet zone of the Fuyunose nappe just adjacent with the Saruta nappes belongs to the glaucophane zone, being absent from the barroisite zone, (Hara *et al.*, 1988, 1990b). The metamorphic grade of the Fuyunose nappe is of a glaucophane zone in contact with both the biotite zone and the garnet zone of the Saruta nappes. In the Saruta district (Fig. 77), namely, the Fuyunose nappe schists are in discontinuous contact with the biotite zone schists and garnet zone schists of the Saruta nappe II with respect to geological structure and metamorphic grade (Hara *et al.*,1988, 1990a, b). Thus it is at present impossible to introduce a large-scale recumbent fold to illustrate the inverted metamorphic zonation of the Sambagawa schists containing the Saruta nappe (I + II), Fuyunose nappe and Sogauchi nappe schists, though Banno and Sakai (1989) have tried that based on their impression. In the Sambagawa schists are found large-scale transposition structures of various kinds as defined in terms of geological structure, thermal structure of the highest-temperature phase, radiometric age and P-T-t-D path etc. In order to synthesize a comprehensive and initial geological-structure such as Banno and Sakai's recumbent fold, first, the above-mentioned large-scale transposition structures all found in the Sambagawa schists must be unrolled. Higashino (1990) has also shown that in the Sambagawa schists there are large-scale transpositions with respect to thermal structure. When complete unrolling of transposition structures defined in terms of P-T-t-D path is impossible, it can be said that the Sambagawa schists contain different subcretion units as discontinuous units. The Saruta unit, Fuyunose unit and Sogauchi unit are de-


(a)
(b)
(c)

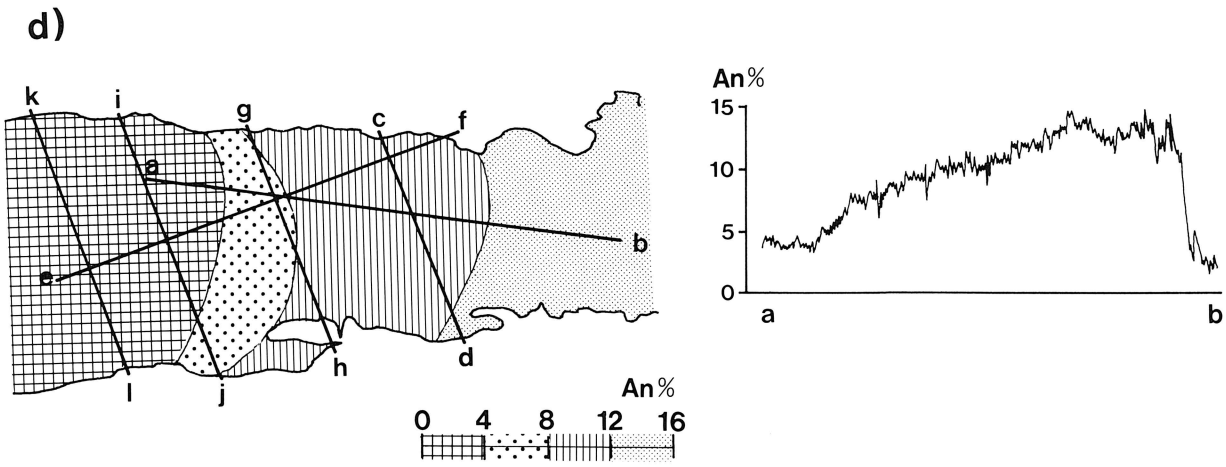

Fig. 79 Microphotographs of ellipsoidal plagioclase porphyroblasts in pelitic schists of the Saruta nappes and a representative example of their chemical zonations.
a) data from the albite-biotite zone of the Saruta nappe I of the Besshibashi district. Sim and Bim folds are not found in matrix, being cut across by the Sb1 schistosity. b) data from the oligoclase-biotite zone of the Saruta nappe II of the River Asemi district (Hara *et al.*, 1984a). The discontinuous relationship between shape and zonal structure of An content is shown in Fig. 79-d. c) data from the albite-biotite zone of the Saruta nappe I of the Shirataki district (Hara *et al.*, 1984b). In microlithon are found granular plagioclase porphyroblasts, while in zone of continuous cleavage are found ellipsoidal ones. d) chemical zonation (An content) in a plagioclase porphyroblast of Fig. 79-b. a-b, c-d,··· and k-l: profile lines of chemical analysis, though only the data of the a-b line is shown. An content increases gradually from the point a (core of PPP: albite) to the point b (inner mantle of PPP: oligoclase), but near the point b appear peristerites.

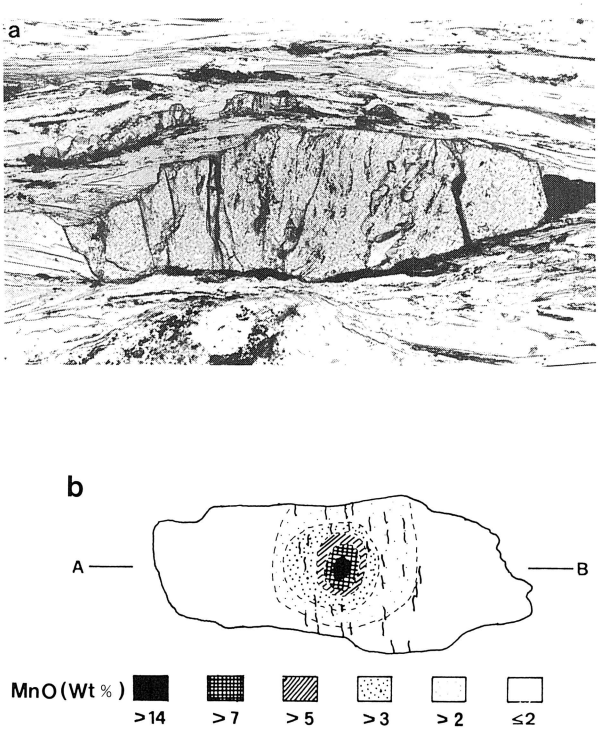

Fig. 80 Microphotograph of one ellipsoidal garnet (a) and chemical zonation (MnO content) of other one (b) in a specimen from pelitic schists of the albite-biotite zone of the Saruta nappe I of the Shirataki district (Hara *et al.*, 1984b). In the diagram (b) A-B shows the general trend of matrix bedding schistosity and dashed lines show Si schistosity.

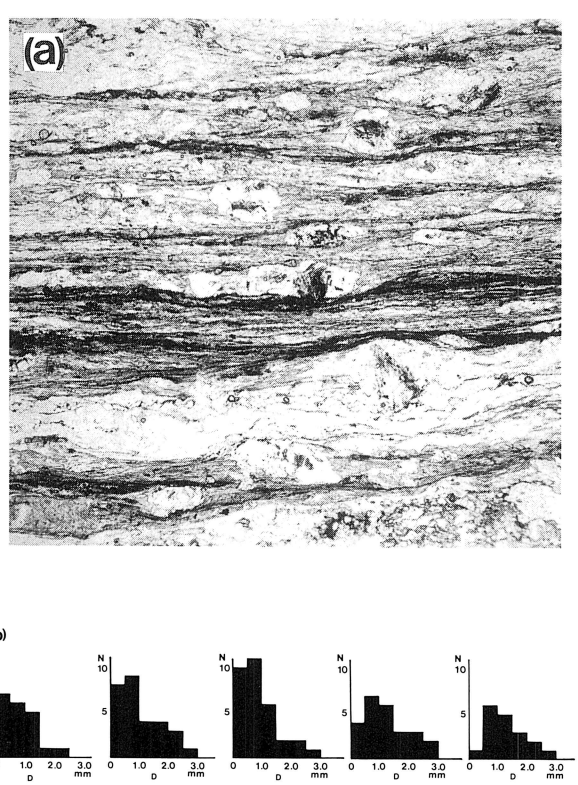

Fig. 81 Microphotograph of cleavage lamellae as dark lamellae (a) and histograms showing the spacing of cleavage lamellae (b) in pelitic schists of the Saruta nappe II of the River Saruta district. N: observation number, D: lamellar spacing.

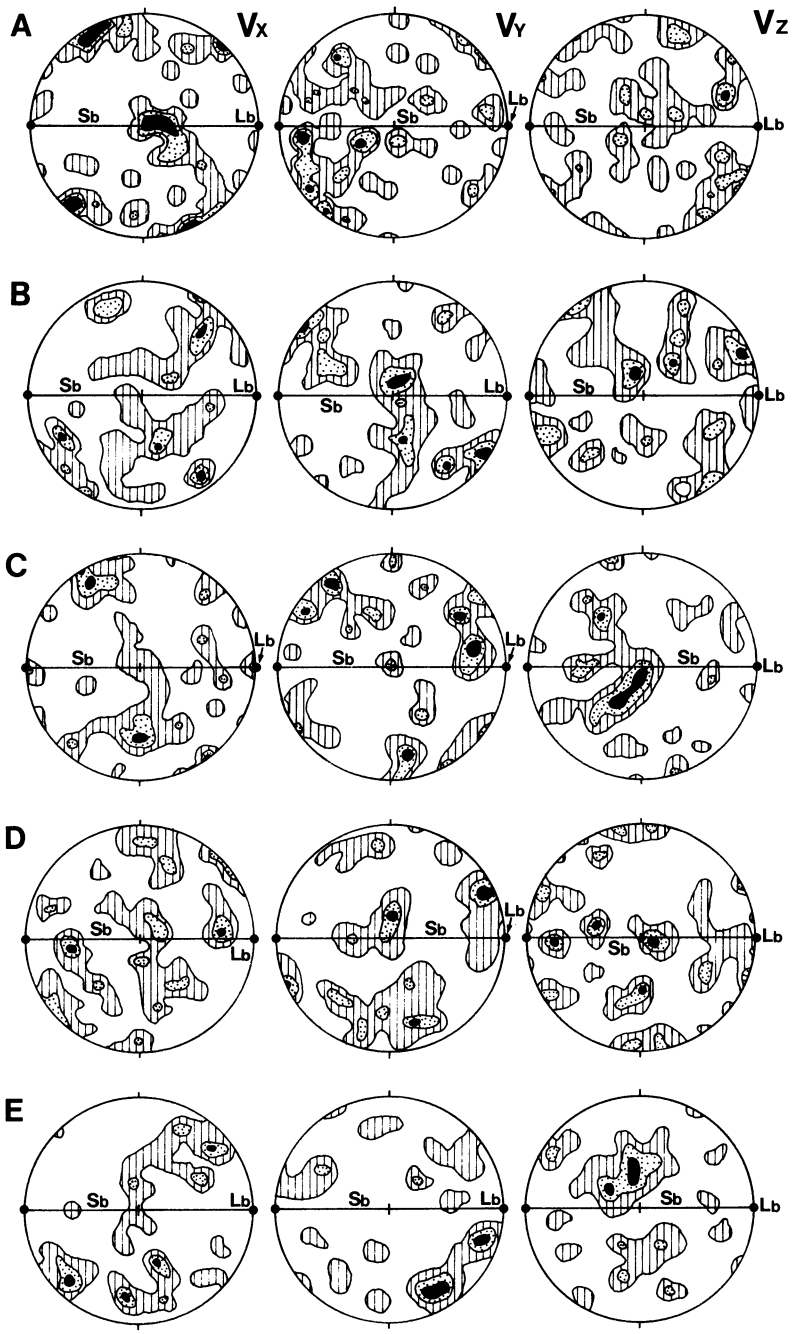

Fig. 82 Diagrams showing the lattice fabrics of ellipsoidal plagioclase porphyroblasts in pelitic schists (five specimens), which show preferred shape orientation along the bedding schistosity (Sb). The data are from the Saruta nappe II of the River Saruta district. Lb: mineral lineation on Sb. Vx: principal vibration axis X, Vy: principal vibration axis Y, Vz: principal vibration axis Z.

veloped as structurally discontinuous nappes different from each other and have different P-T-t-D path from each other, showing that these are different subcretion units from each other.

From the growth history of amphibole in hematite-bearing basic schists, it has been assumed by Hara *et al.* (1988, 1990a) that the Sogauchi unit was coupled with the Fuyunose nappe during the Sb2-1 phase, when the highest-temperature metamorphism (crossite zone) of the former occurred with the retrograde metamorphism (crossite-winchite zone) of the latter. Immediately after this coupling, plagioclase porphyroblasts crystallized in the schists of both Fuyunose nappe and high temperature part of the Sogauchi unit (Hara *et al.*, 1988, 1990a).

E: Crystallization of Plagioclase Porphyroblasts

Plagioclase porphyroblasts in the Fuyunose subunit II appeared under retrograde metamorphism and non-deformational condition during the inter Sb2-1 - Sb2-2

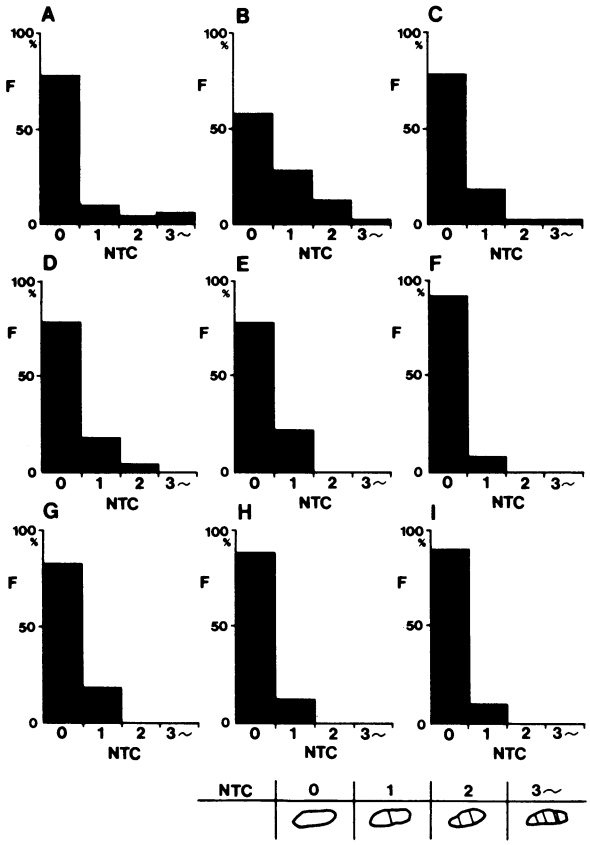

Fig. 83 Diagram showing the degree (NTC) of development of twin in plagioclase porphroblasts in pelitic shists of the Saruta nappe II (specimen A - specimen F) and Fuyunose nappe (specimen G - specimen I) of the River Saruta district.
NTC: number of composition plane of twin observed in each grain.

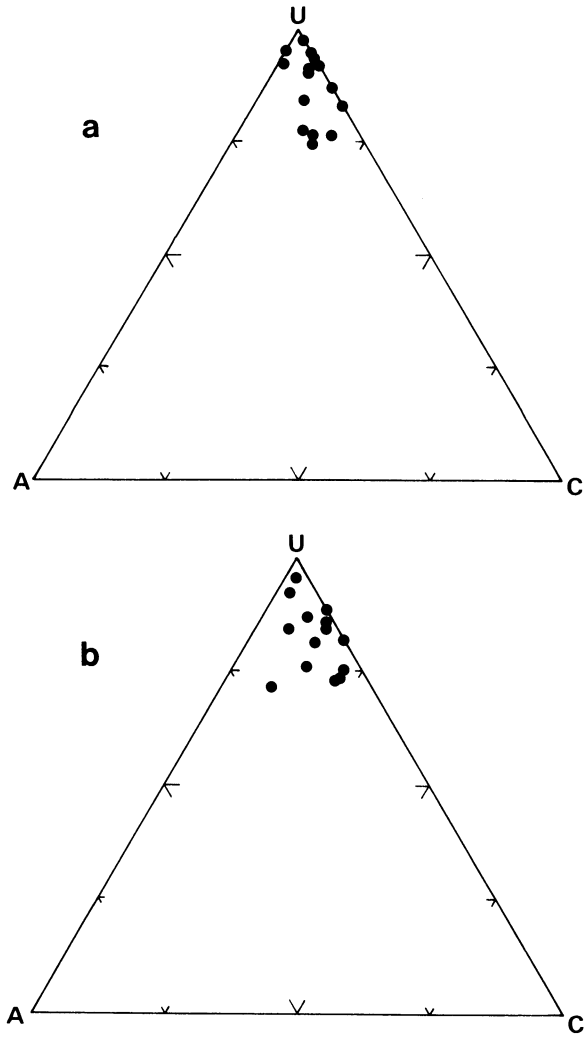

Fig. 84 U-A-C diagrams of plagioclase porphyroblasts in pelitic shists.
a: data from the Saruta nappes, b: data from the Fuyunose nappe.
U (untwining), A (A-twin) and C (C-twin) are based on Gorai's (1951) definition.

phase just after the Sb2-1 deformation, while these in the Saruta unit appeared under prograde metamorphism during the Nd non-deformational phase just after the Sim-Bim deformation (Hara *et al.*, 1988, 1990a). Hara *et al.* (1989), Sakakibara *et al.* (1991, 1992) and Kaikiri *et al.* (1991) clarified that the Sim-forming quartz grains and Sb2-1-forming quartz grains in plagioclase porphyroblasts both show type I crossed girdle (Figs. 24 and 47). Takagi and Hara (1979), Hara *et al.* (1980a, 1983) and Tokuda and Hara (1983) showed that the Sim-forming epidote and amphibole in plagioclase porphyroblasts have also commonly preferred lattice orientation, whose pattern is quite comparable with that of their deformational fabrics (Figs. 43, 45 and 46). It is clear that epidote, amphibole and quartz fabrics produced by the Sim-Bim deformation and quartz fabrics produced by the Sb2-1 deformation were included without their pattern change into plagioclase porphyroblats.

In the Saruta unit, Fuyunose unit and uppermost part of the Sogauchi unit, plagioclase quite newly crystallized as porphyroblasts under non-deformational condition just after the intense deformation in complete expense of pre-existing plagioclase grains (Hara *et al.*, 1980a, 1983; Maeda and Hara, 1984). Fig. 78 illustrates the relationship between size and number for plagioclase porphyroblasts in pelitic schists of the Fuyunose subunit II and the Saruta unit of the Shirataki-Ikadatsu district as measured in an unique domain on sections parallel to lineation observed on the bedding schistosity and normal to the bedding schistosity. From this figure it can be pointed out that their size decreases with increase of their number and that for these in the Fuyunose subunit II their size (number) decreases (increases) within narrow zones along the nappe boundary (Fuyunose - Sogauchi boundary), though fine-grained porphyroblasts are also found in some restricted small domains within the central part of the Fuyunose nappe as mentioned by Hara *et al.* (1990d).

According to Hara *et al.* (1984b, 1989), plagioclase porphyroblasts and their host pelitic schists, as well as garnet, are frequently deformed by pressure solution, giving rise to ellipsoidal shapes of plagioclase porphyroblasts (Fig. 79) and garnet (Fig. 80) and to cleavage lamellae (Fig. 81). Such the phenomena might have modified the initial size - num-

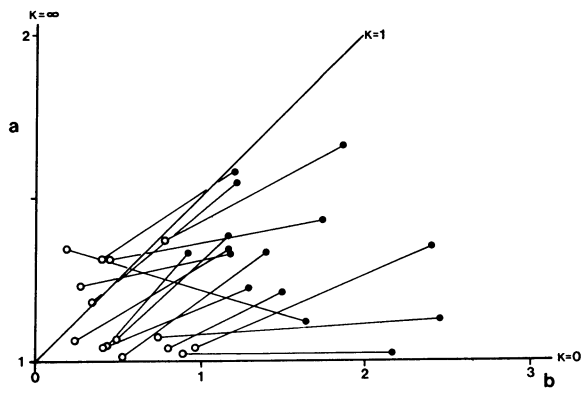

Fig. 85 Flinn's plot of shapes of plagioclase porphyroblasts in basic schists of the Saruta nappe II of the River Saruta district as assumed from the shape data on thin sections normal to mineral lineation (Lb1) and thin sections parallel to mineral lineation and normal to bedding schistosity (Sb1). open circles: data for plagioclase porphyroblast cores, solid circles: data for plagioclase porphyroblasts (core + mantle).

ber relationship for plagioclase porphyroblasts. As pointed out by Hara *et al.* (1990d), however, the data of Fig. 78 must be interpretted in such terms that nucleation of plagioclase porphyroblasts occurred in high magnitude within the domains of high strain concentration of the Sb2-1 phase, because the strain of the Sb2-1 phase must have been concentrated in narrow domains along the Fuyunose - Sogauchi boundary and activation energy of nucleation commonly depends upon stored strain energy in mineral grains. (Hara *et al.*, 1990d). As is obvious in Fig. 78, size of plagioclase porphyroblasts is generally much greater in the Saruta nappe (I + II) schists than in the Fuyunose nappe schists. From the data it would be said that their size is also greatly depending upon temperature.

Ellipsoidal plagioclase porphyroblasts in pelitic schists, whose long axes show preferred orientation along the bedding schistosity, commonly do not show preferred lattice orientation in unique pattern (Fig. 82), even though they are strongly elongated (Hara *et al.*, 1984b). They do not show polysynthetic twinning. Many of them are of untwinning type, and many of twinned grains have only one composition plane, which is frequently of Carlsbad twin type, (Figs. 83 and 84). The Si fabrics are never deformed by twinning (Figs. 34-c and 79-b). Those characteristics of plagioclase porphyroblasts must support also the abovementioned assumption (Hara *et al.*, 1984b) for their crystallization under non-deformational condition just after strong deformation.

Fig. 85 (Flinn diagram) illustrates average shape of ellipsoidal plagioclase porphyroblasts in each of many speci-

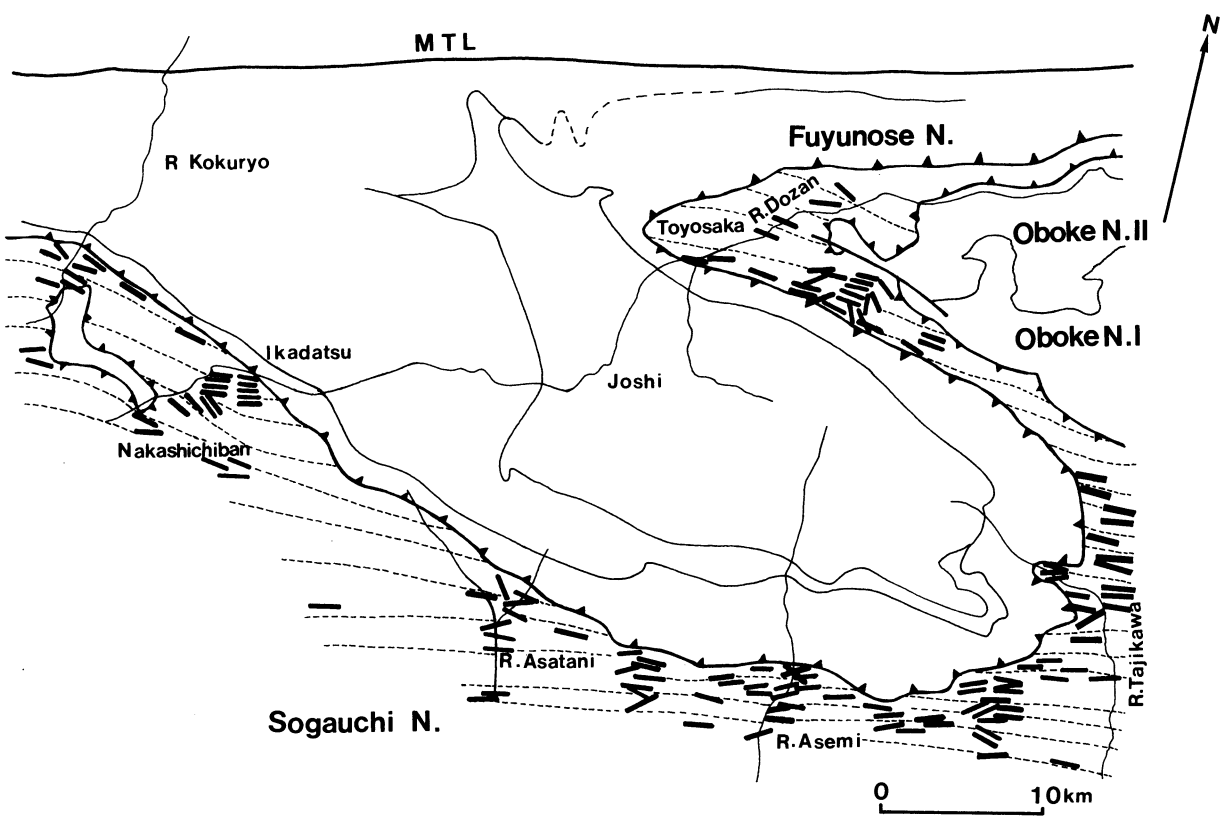

Fig. 86 Diagram showing the orientation of X of strain of the Sb2-1 phase in the Sogauchi nappe of central Shikoku as assumed from preferred shape orientation of amphibole.
heavy straight lines and dashed lines: measured data of orientation of X and assumed trends of X respectively.

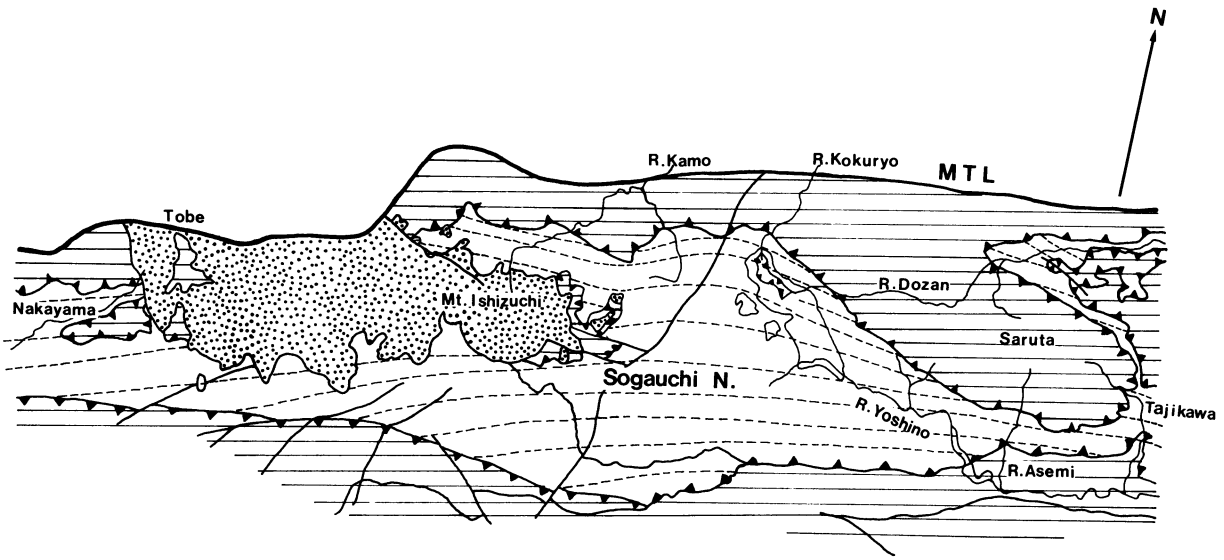

Fig. 87 Diagram showing the trend of X of strain of the Sb2-1 phase throughout the Sogauchi nappe of central - western Shikoku as assumed from preferred orientation of amphibole.

mens from basic schists of the Saruta nappe of the River Saruta district. The examined basic schists, in which amphibole has scarcely retrograde growth rims, have a planer bedding schistosity (probably Sb1) and a mineral lineation (probably Lb1). The shape data of Fig. 85 have been obtained from observation on sections normal to Lb1 and these normal to Sb1 and parallel to Lb1. The longest axes of plagioclase porphyroblasts are preferably oriented parallel to Lb1, but these of PPP cores are not always oriented parallel to Lb1. k-values of PPP cores are in wide range from flattened type to constricted type, while overall shapes of PPP all are plotted within the whole range of flattened types, probably owing to great overgrowth of mantles in a direction parallel to Lb1 during the Sb1-deformation, as shown by Takagi and Hara (1979) and Hara *et al.* (1984b). This fact must mean that the strain picture of the Saruta nappe schists related to the Sb1 deformation, as well as that for the Sim-Bim deformation, generaly was of flattened type in mean strain.

F: Tectonics Related to the Further Exhumation of the Sambagawa Megaunit

The compositional difference between the Sb2-1-forming and the Sb2-2- forming muscovite in the Fuyunose nappe schists (Fig. 69) shows retrograde metamorphism during the Sb2-2 deformation. This retrograde metamorphism is related to the further exhumation of the Sambagawa megaunit. It has been shown by Hara *et al.* (1990a, 1991a) that the Sambagawa megaunit was mechanically coupled with the Chichibu megaunit I (Sakamoto nappe) during the Sb2-2 deformation (Fig. 21). This fact means that the change of the exhumation route of the Sambagawa megaunit occurred during the Sb 2-2 deformation, giving rise to the separation of the Chichibu supermegaunit into the Chichibu megaunit II and the Chichibu megaunit I (Fig. 20). The Chichibu megaunit I was metamorphosed in the grade of prehnite-pumpellyite facies in southern part (Niyodo nappe) and in the grade of pumpellyite-actinolite facies characterized by the appearance of quartz-lawsonite-albite assemblage in the northern part (Sakamoto nappe) (cf. Banno and Sakai, 1989). Such the metamorphism of the Chichibu megaunit I has been assumed by Hara *et al.* (1990a, 1991a) to have simultaneously occurred with its coupling with the Sambagawa megaunit. This assumption illustrates the movement picture of the Sambagawa megaunit during the Sb 2-2 deformation as shown in Fig. 21.

Fig. 65 illustrates the boundary between the crossite-winchite path zone and the crossite-barroisite path zone for the retrograde growth history of amphibole in the Fuyunose nappe, which has been determined by the field data and borehole data. The separation of these two path zones occurred during the Sb2-1 phase. The boundary of these zones, which is an isobaric line, trends in WNW-ESE and in a direction oblique to the general trend of mineral lineation (Lb2-1) in such a fashion as is obvious in comparison of Fig. 65 and Fig. 72. The NW-SE trending isobaric line of the Sb2-1 phase in the Sogauchi nappe, which is quite roughly assumed from Fig. 22, appears to be oblique to its mineral lineation (Figs. 86 and 87) and to the shear direction (Fig. 88) in the Sb 2-2 deformation as determined from quartz microtextures. The lower-pressure parts of the Fuyunose nappe and Sogauchi nappe are placed in the top of the shear direction and on the western side of the general trend of mineral lineation: The lower-pressure path zone of the Fuyunose nappe is placed in its southwestern part (Fig. 65). The lower-pressure part of the Sogauchi nappe corresponds to its western part (Fig. 22). Mineral lineation (Lb2-1) in the Sogauchi nappe, which is defined by preferred shape orientation of amphibole, is preferably oriented in E-W trend (Figs. 86 and 87). Lb2-1 in the Sogauchi nappe of western Shikoku is in trend of ENE-WSW (Hide, 1972; the present authors' data). It can be said that the lower-pressure part of the Sogauchi nappe is placed in the western side on the line parallel to the general trend of Lb2-1. That of the Chichibu megaunit I is the Niyodo nappe.

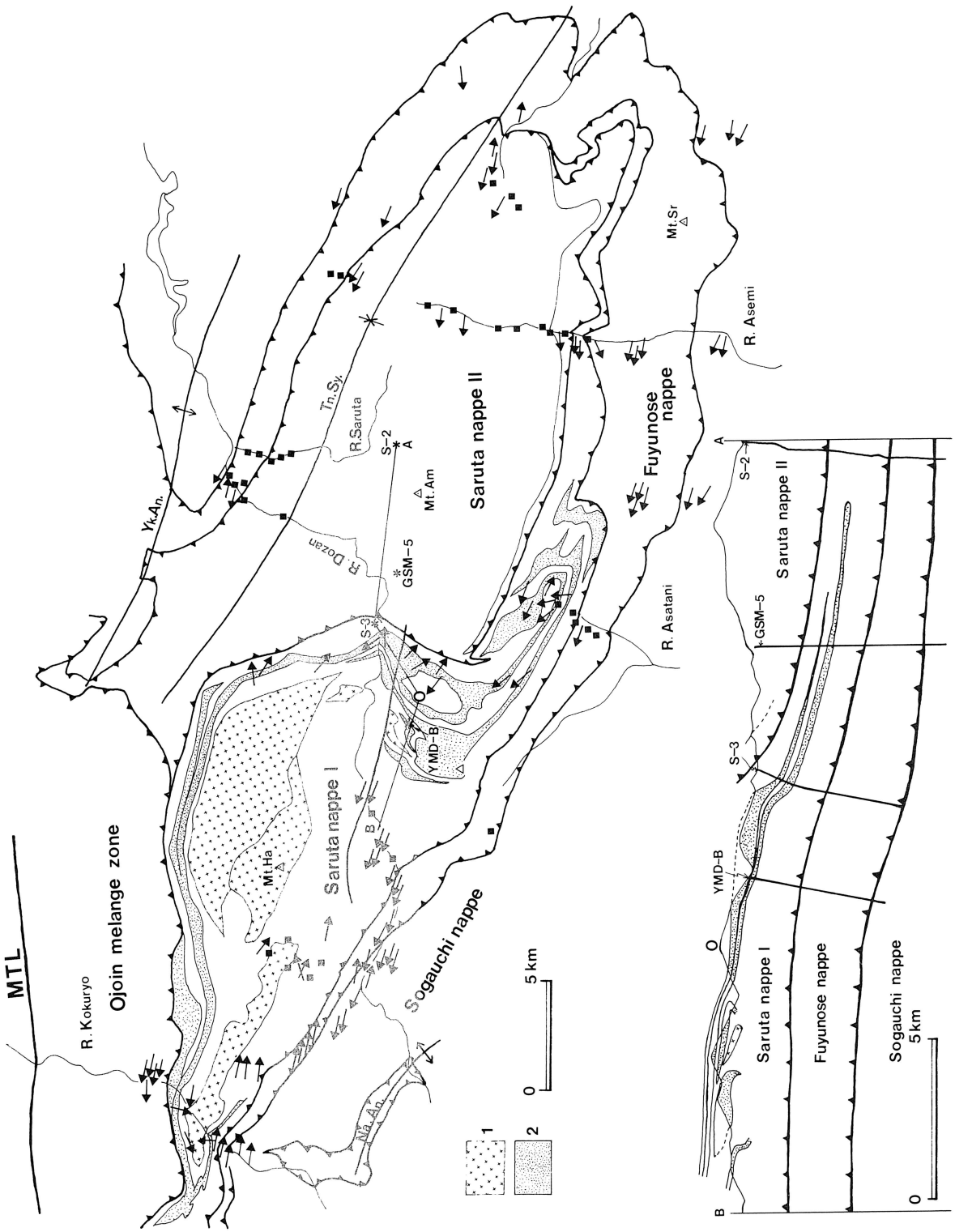

Fig. 88 Diagram showing the distribution of Type II (solid squares) and Type III (arrows) microtextures of quartz and the shear sense (arrows) determined from Type III microtextures in the Saruta nappes, Fuyunose nappe and Sogauchi nappe [data from Hara *et al.* (1986b, 1988, 1990c) and the present authors] and the geological profile along the line A-(S-3)-O-B. S-2, GSM-5, S-3 and YMD(Yokomichidani)-B: boreholes (MMEAJ, 1968; Sumitomo Metal Mining Co. Ltd, 1981), 1: tectinic blocks of metagabbros and peridotite such as Tonaru mass, Iratsu mass and Higashiakaishiyama mass, 2: Shirataki I-II amphibole schist and associated basic schist. YkAn: Yakushi antiform, TnSy: Tsuneyama synform, NaAn: Nakashichiban antiform, Mt.Ha: Mt.Higashiakaishiyama, Mt.Am: Mt.Amatsutsumi, Mt.Sr: Mt.Shiraga.

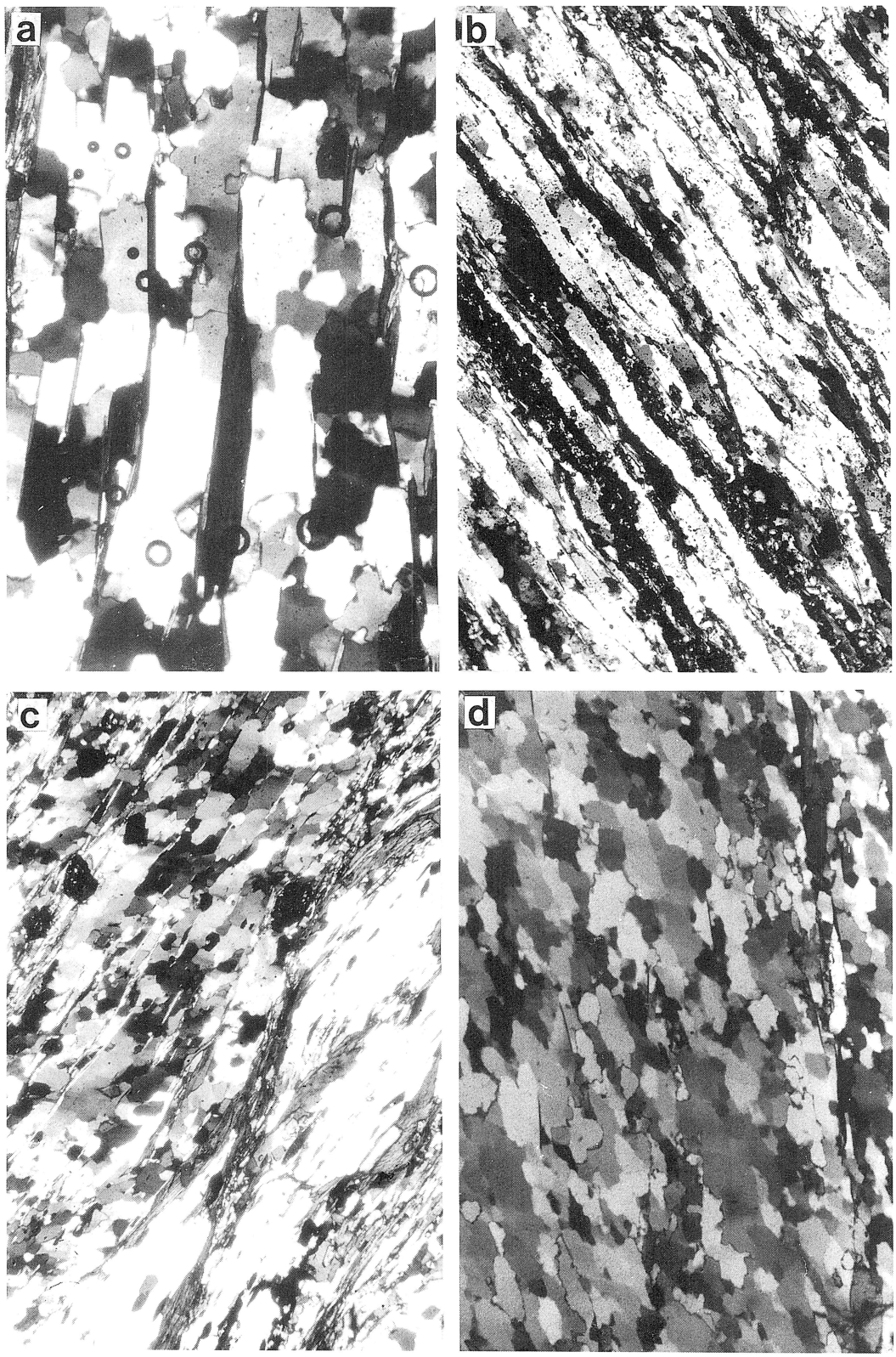

Fig. 89 Microphotographs of quartz microtextures of three types, Type I, Type II and Type III, in planar siliceous schists of the Saruta nappe, Fuyunose nappe and Tsuji nappe.
a) Type II (from the Saruta nappe II of the River Asemi district), b) Type I (from the Tsuji nappe of the Tsuji district), c) and d) Type III (from the Fuyunose nappe of the River Asemi district).

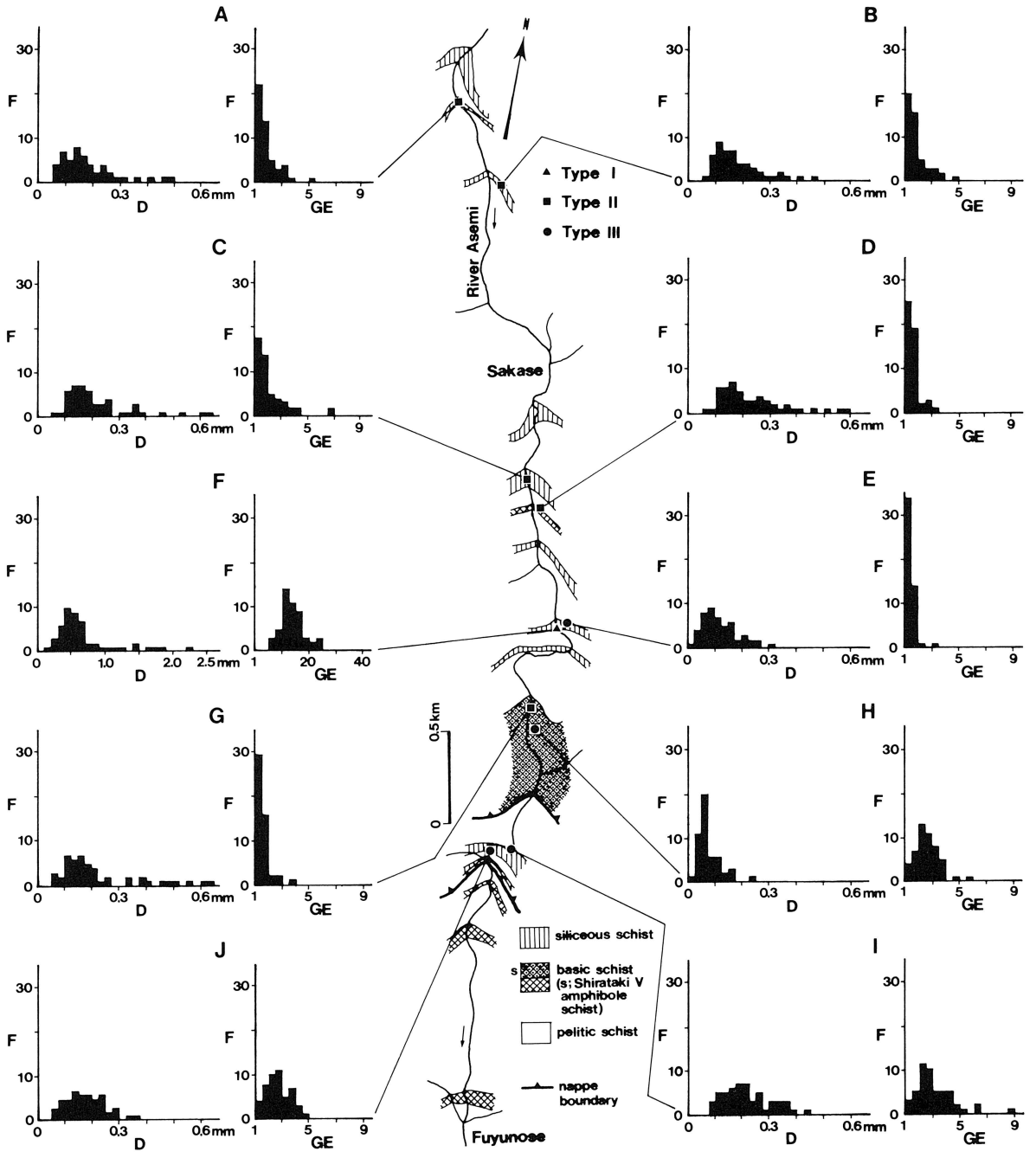

Fig. 90 Diagram illustrating the shape fabrics of Type I, Type II and Type III quarz in planer siliceous schists of the Saruta nappes and Fuyunose nappe along the River Asemi as measured on thin sections parallel to mineral lineation and normal to the bedding schistosity.
D: grain size, GE: aspect ratio, F: observation numbers.

As is obvious from the above-described data of quartz fabrics in the siliceous schists involved in the Kuwanokawabashi fold, information from quartz microtextures is quite important to understand the movement picture of the Sambagawa megaunit during the Sb2-2 deformation. As Hara *et al.* (1986b, 1988, 1990a) and Sakakibara *et al.* (1992) have clarified, quartz microtextures of planar siliceous schists of the Sambagawa megaunit are divided into three types , Type I (highly elongated grains: Fig. 91-b), Type II (polygonal grains showing dominant migration recrystallization: Fig. 91-a) and Type III (elongate mosaic quartz forming Type II S-C structure), (Figs. 89 and 90). The movement picture of the Sb2-2 phase is illustrated from Type III quartz microtextures [= Type II S-C mylonite after Lister and Snoke (1984)]. Two representative examples for Type III quartz microtextures, which have been so far described in two districts by Kojima and Hide (1958), Hide (1961), Hara *et al.* (1986b, 1988) and Sakakibara *et al.* (1992), are reproduced in Figs. 92 and 93. For Type III quartz microtextures the movement pic-

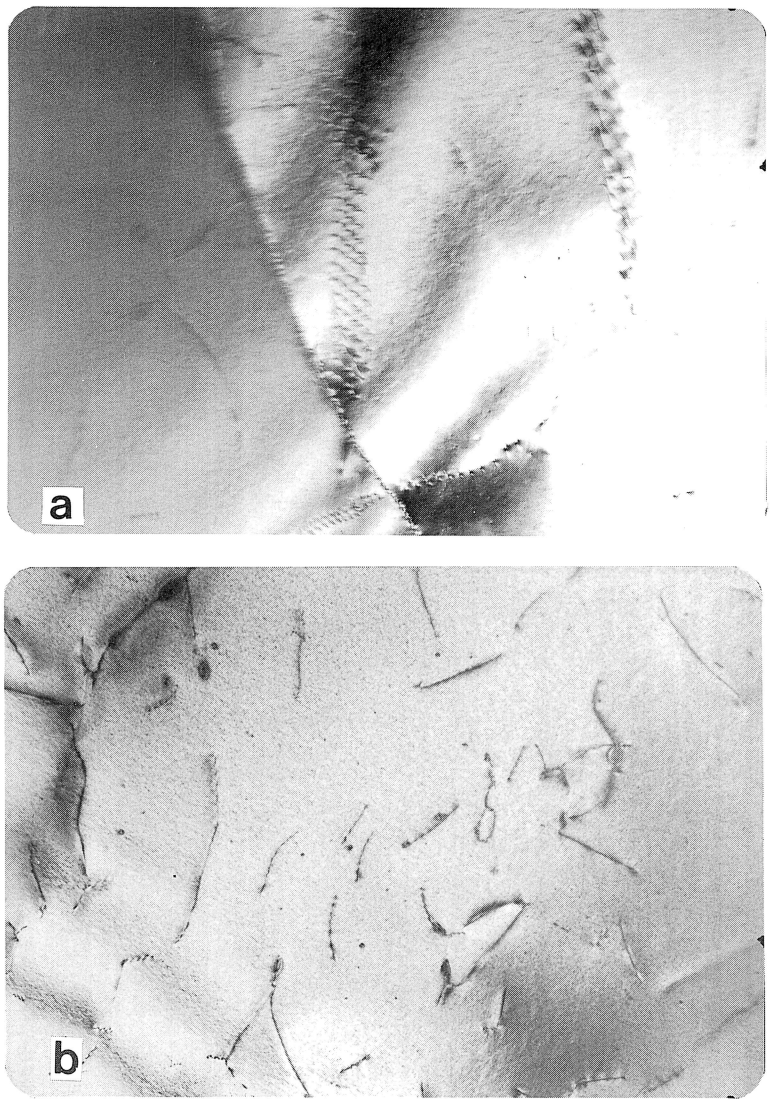

Fig. 91 Diagram showing dislocation microtextures of Type II quartz (a) and Type I quartz (b) observed under electron microscope.

ture deduced from the shape fabrics is quite harmonic with that deduced from the c-axis fabrics. Though the trend of mineral lineation is different between Lb1 of the Saruta nappes and Lb2-1 of the Fuyunose nappe and Sogauchi nappe, the shear direction assumed from Type III quartz microtextures is in harmonic orientation through these nappes (Fig. 88).

Regarding to shear sense, westward shear zones and eastward shear zones are found in the Saruta, Fuyunose and Sogauchi nappes cutting across their nappe boundaries. The quartz data from the Besshi mine (Fig. 92) show eastward shear, while these from the River Asemi district (Fig. 93) do westward shear sense. Hara *et al.'s* (1986b, 1988) and the present authors' observation result in the River Asemi district is quite harmonic with these of Wallis (1990). The eastward shear zone of the Besshi mine is traced to the east and south of the Iratsu metagabbro body, cutting across the nappe boundaries and forming a great shear zone

Fig. 92 Quartz c-axis fabrics of siliceous schists associated with the bonanza of the Besshi main ore deposit [data from Kojima and Hide (1958) and Hide (1961)].
a) projection of location of analyzed specimens onto vertical section, b) schematic profile of the Besshi main ore deposit along horizontal plane and projection of analyzed specimens. C1, C2 and C3: data from axial zone and both limbs of minor isoclinal fold, 1: bonanza, 2: t shows down side on mineral lineation, 3: basic schists, 4: bonanza, 5: siliceous schists. The schematic diagram of the Besshi main ore deposit are after Sumitomo Metal Mining Co. Ltd. (1981).

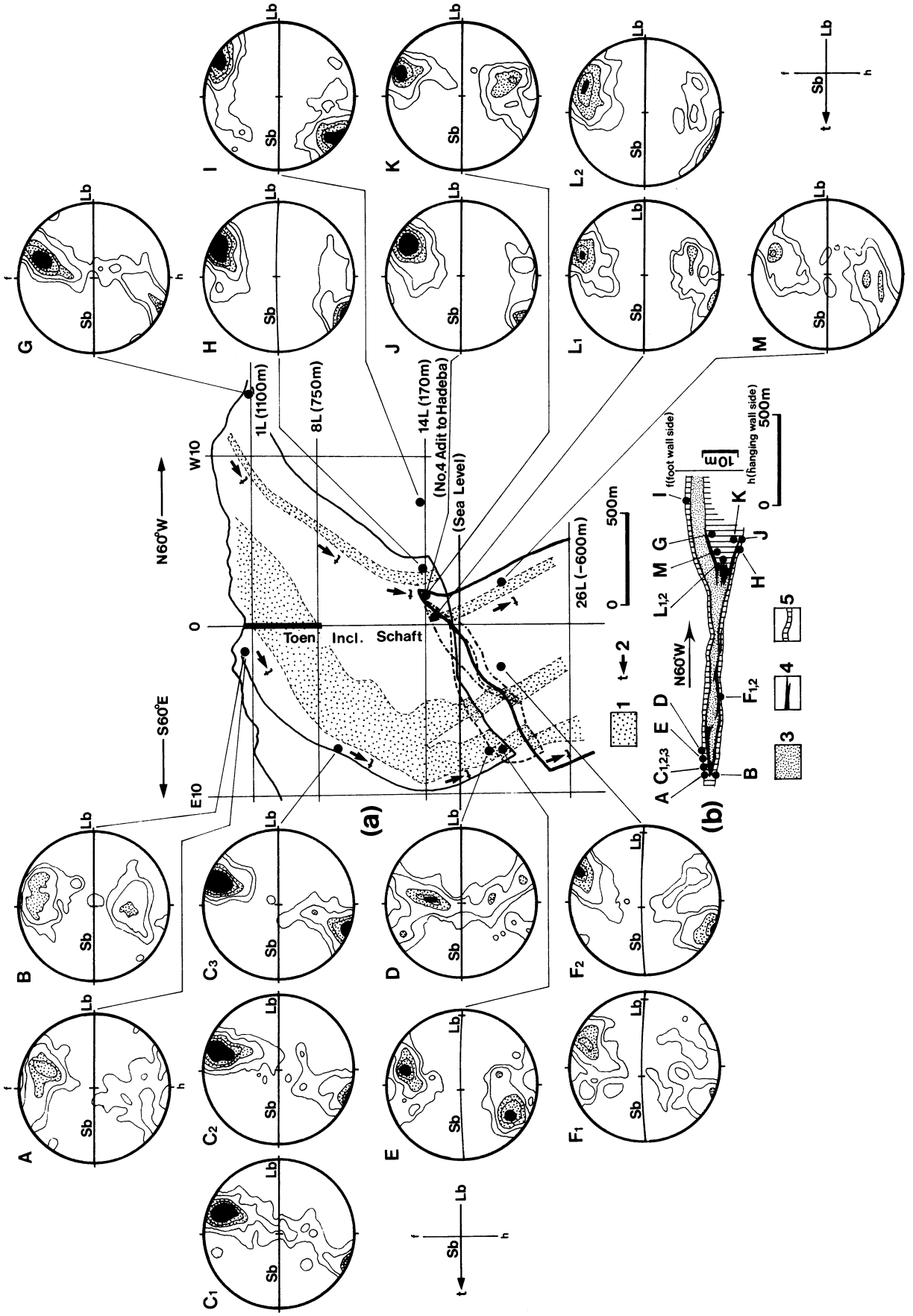
N60°W
S60°E
W10
E10
0
1L (1100m)
8L (750m)
14L (170m)
(No.4 Adit to Hadeba)
(Sea Level)
26L (-600m)
Toen
Incl.
Schaft
500m
0
1
2
3
4
5
(a)
(b)
f(foot wall side)
h(hanging wall side)
10m
500m
N60°W
A
B
C1,2,3
D
E
F1,2
G
H
I
J
K
L1,2
M
Lb
Sb
f
h
t

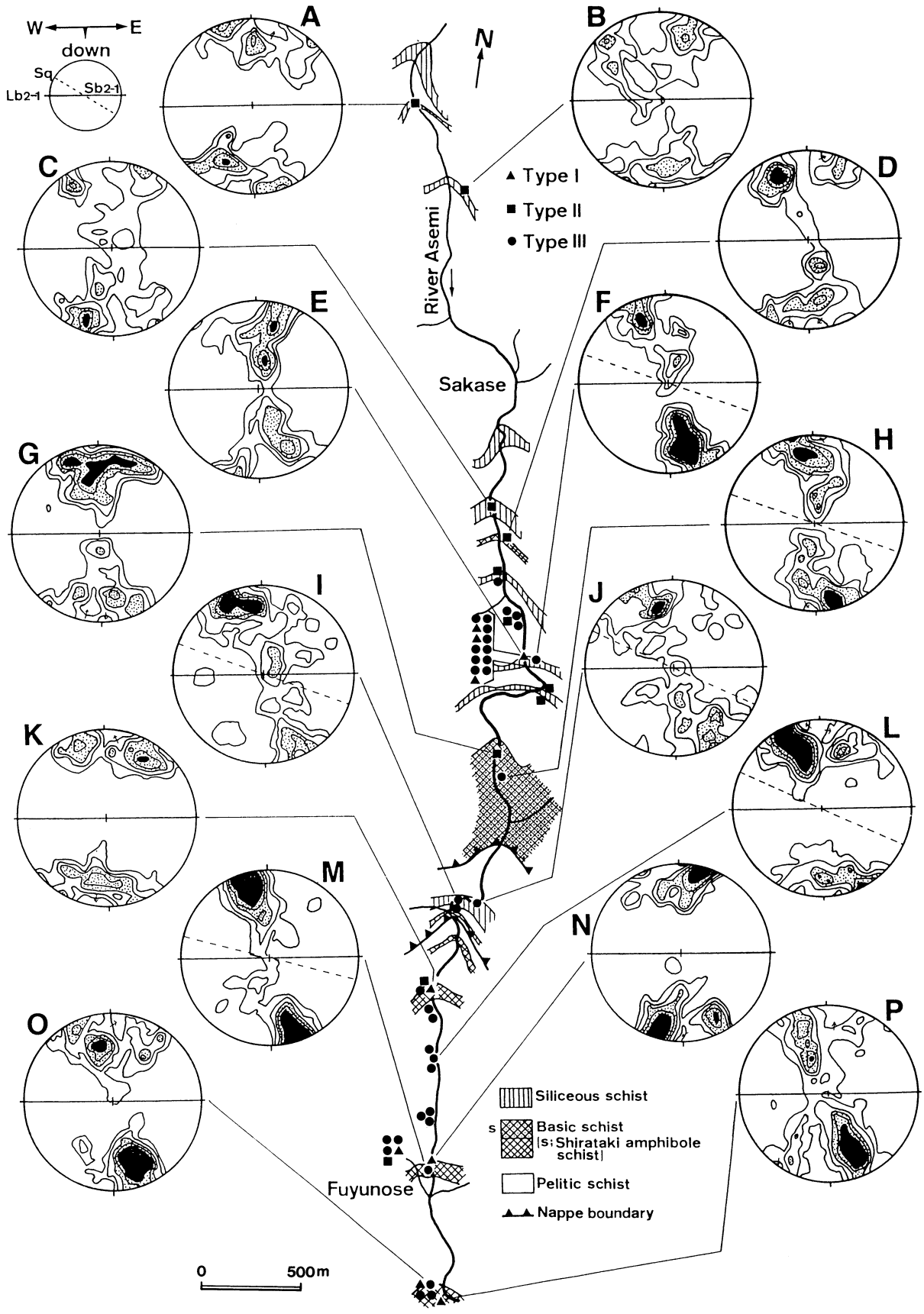

Fig. 93 Diagram showing the distribution of three types, Type I, Type II and ype III , of quartz microtexture and their c-axis fabrics of planer siliceous schists of the Saruta nappes and Fuyunose nappe along the River Asemi.

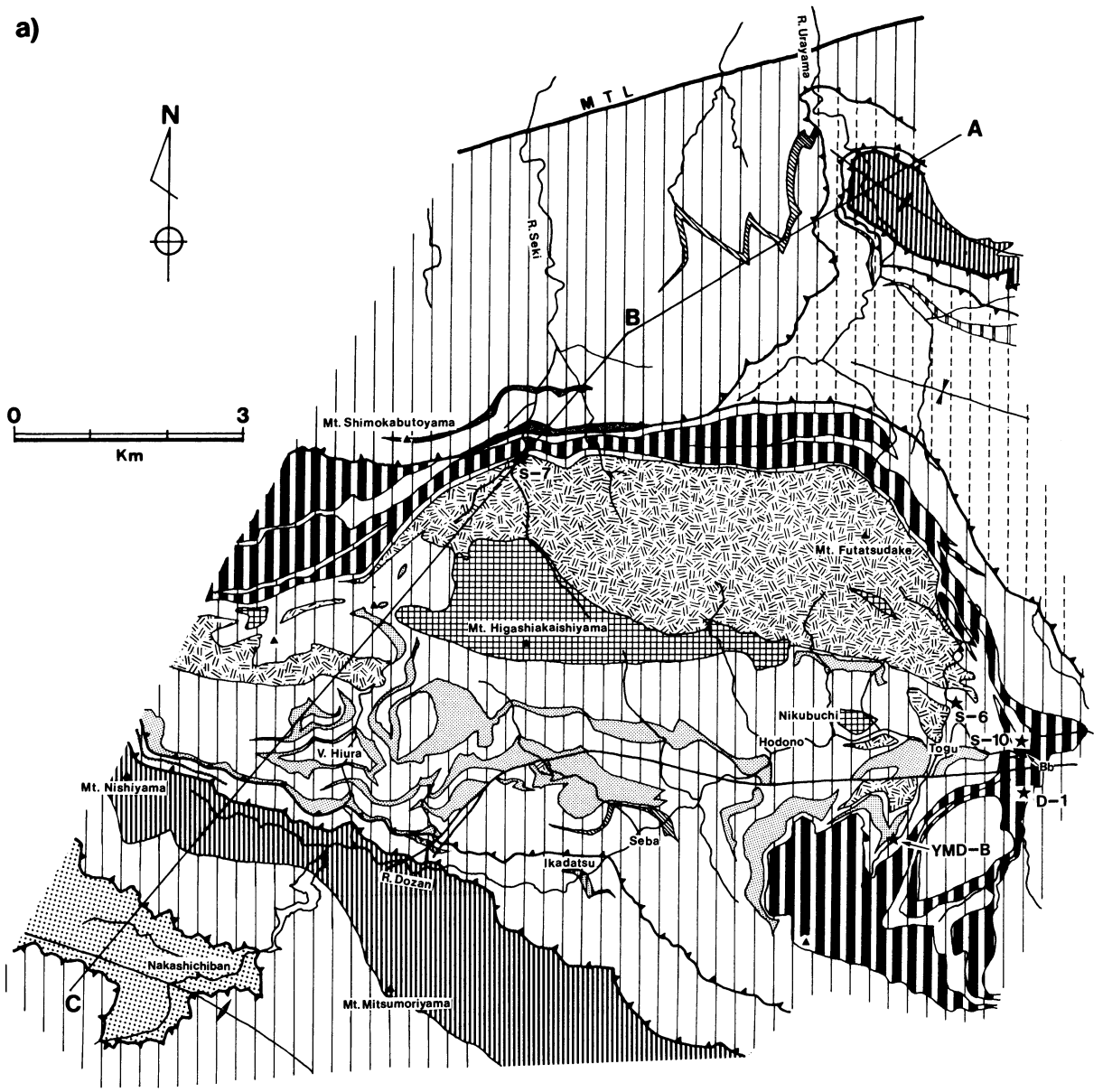

Fig. 94 Geological map (a) and profile (b) of the Besshiyamamura district [data from Hide, Hara, Takagi, Furuyama, Nakamura (T) and Joichi (1992)]. 1: pelitic schists, 2: psammitic schists, 3: basic schists in the Sogauchi nappe, 4: basic schists in the Saruta nappe II, 5: Besshi main ore deposit, 6: basic schists in the Fuyunose nappe, 7: basic schists in the Saruta nappe I, 8: Shirataki I-II-III amphibole schists, 9: pelitic schists in the Saruta nappe II, 10: basic schists in the Ojoin melange zone, 11: siliceous schists, 12: tectonic blocks such as Tonaru and Iratsu masses 13: ultrabasic rocks, a: fault, b: nappe boundary, c: antiform of upright fashion, d: synform of upright fashion, e: boreholes (S-7, S-6, S-10, D-1 and YMD-B), MTL: Median Tectonic Line, 36L, 32L···1L: projection of adits of the Besshi main ore deposit (Sumitomo Metal Mining Co. Ltd, 1981). A little part of the profile, which is around the borehole S-7, is based on Sumitomo Metal Co. Ltd.(1981), MMEAJ (1967, 1969).

(Besshi-Iratsu eastward shear zone) (Fig. 88). Such the data indicate that the displacement along the nappe boundaries for the Saruta nappes, Fuyunose nappe and Sogauchi nappe in central Shikoku was not essentially significant during the Sb2-2 deformation and further later deformations.

The above-mentioned distribution pattern of the lower-pressure parts of the Fuyunose nappe, Sogauchi nappe and Chichibu megaunit I and the development of westward shear zones in many places (Fig. 88) suggest that the Sb2-2 deformation occurred under overall shear with westward sense along the general trend of Lb2-2. The Besshi-Iratsu eastward shear zone (Fig. 88) can be explained in this context as schematically shown in Fig. 94. Namely, its development would be ascribed to anticlockwise rotation of competent lenses (Iratsu body, Tonaru body, other small basic rock bodies and Nakashichiban psammitic schist body) with eastward shear along these lenses, which occurred under westward shear with N-S direction compression (Figs. 73 and 95). The formation of such fold forms of small basic rock bodies as shown in Figs. 95 and 88 would be related

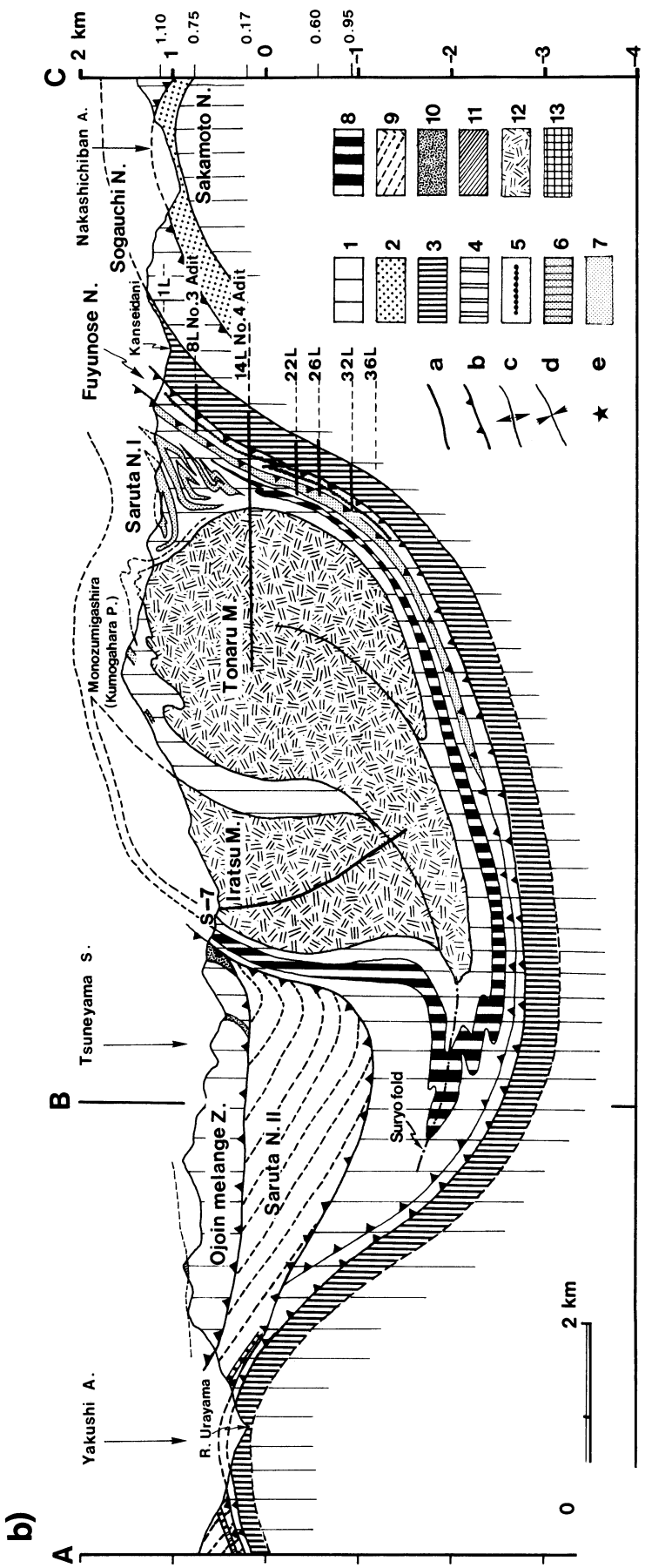
b)
A
B
C
2 km
1.10
0.75
0.17
0.60
0.95
1
0
-1
-2
-3
-4
Yakushi A.
R. Urayama
Tsuneyama S.
Nakashichiban A.
Fuyunose N.
Sogauchi N.
Sakamoto N.
Kanseidani
1L
8L No.3 Adit
14L No.4 Adit
22L
26L
32L
36L
Saruta N.I
Monozumigashira
(Kumogahara P.)
Tonaru M.
Iratsu M.
S-7
Ojoin melange Z.
Saruta N. II
Suryo fold
1
2
3
4
5
6
7
8
9
10
11
12
13
a
b
c
d
e
2 km
0

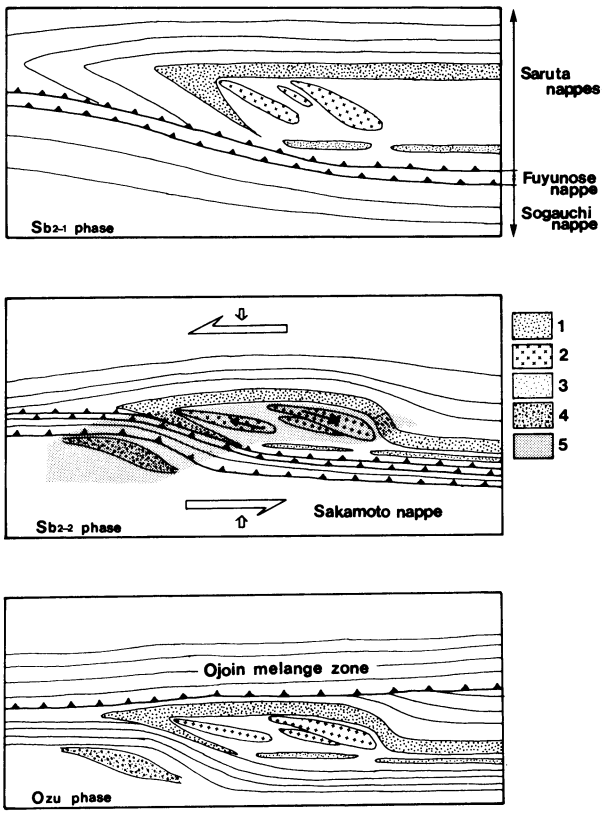

Fig. 95 Schematic diagram illustrating the structural development of the Sambagawa megaunit and the development of a local eastward shear zone (Besshi eastward shear zone) under overall shear with westward sense during the Sb2-2 phase in central Shikoku.
1: Shirataki I-II-III amphibole schists, 2: tectonic blocks such as Tonaru mass , Iratsu mass and so on, 3: basic schists, 4: psammitic schists of the Sakamoto nappe in the Nakashichiban district, 5: eastward shear zone.

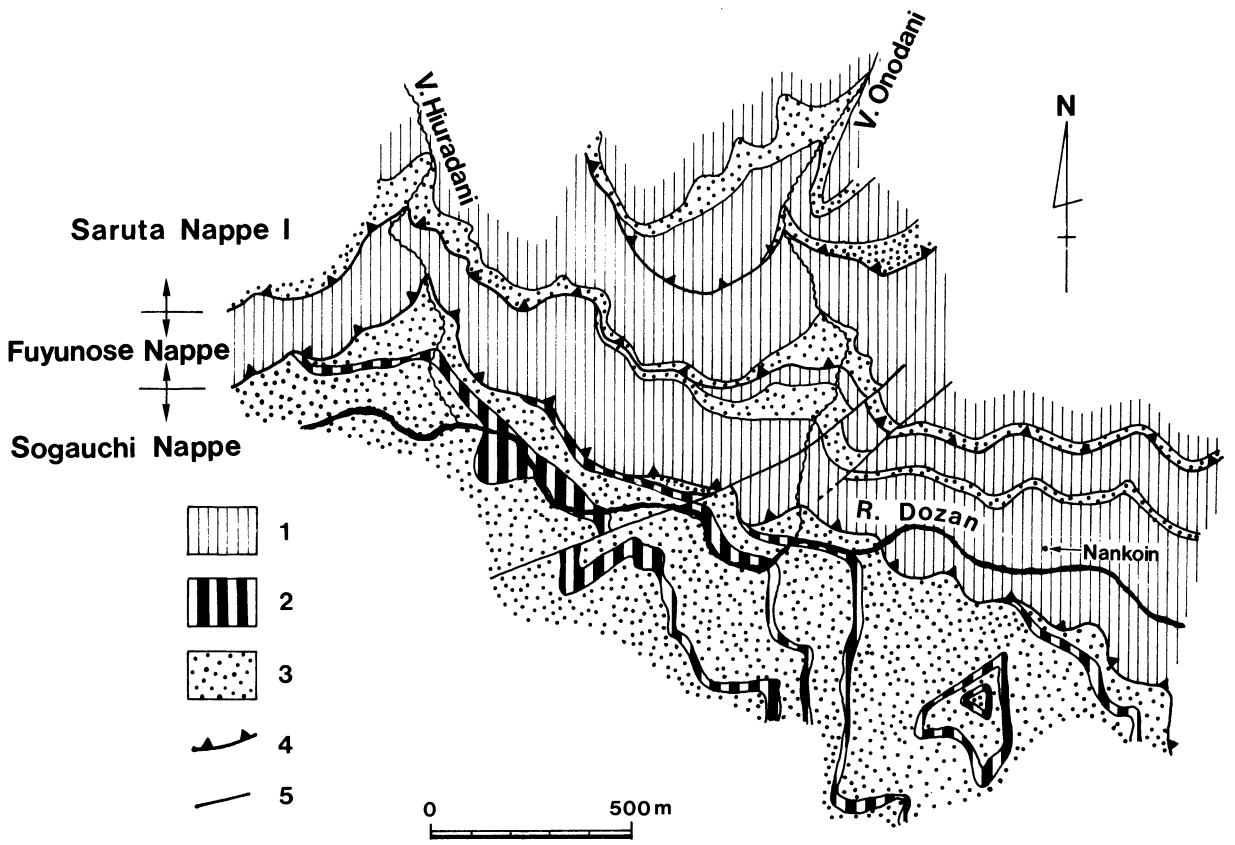

Fig. 96 Geological map of the Nankoin district [data from Hide, Hara, Shiota and Okamoto (1992)].
1: pelitic schists, 2: siliceous schists, 3: basic schists, 4: nappe boundary, 5: fault.

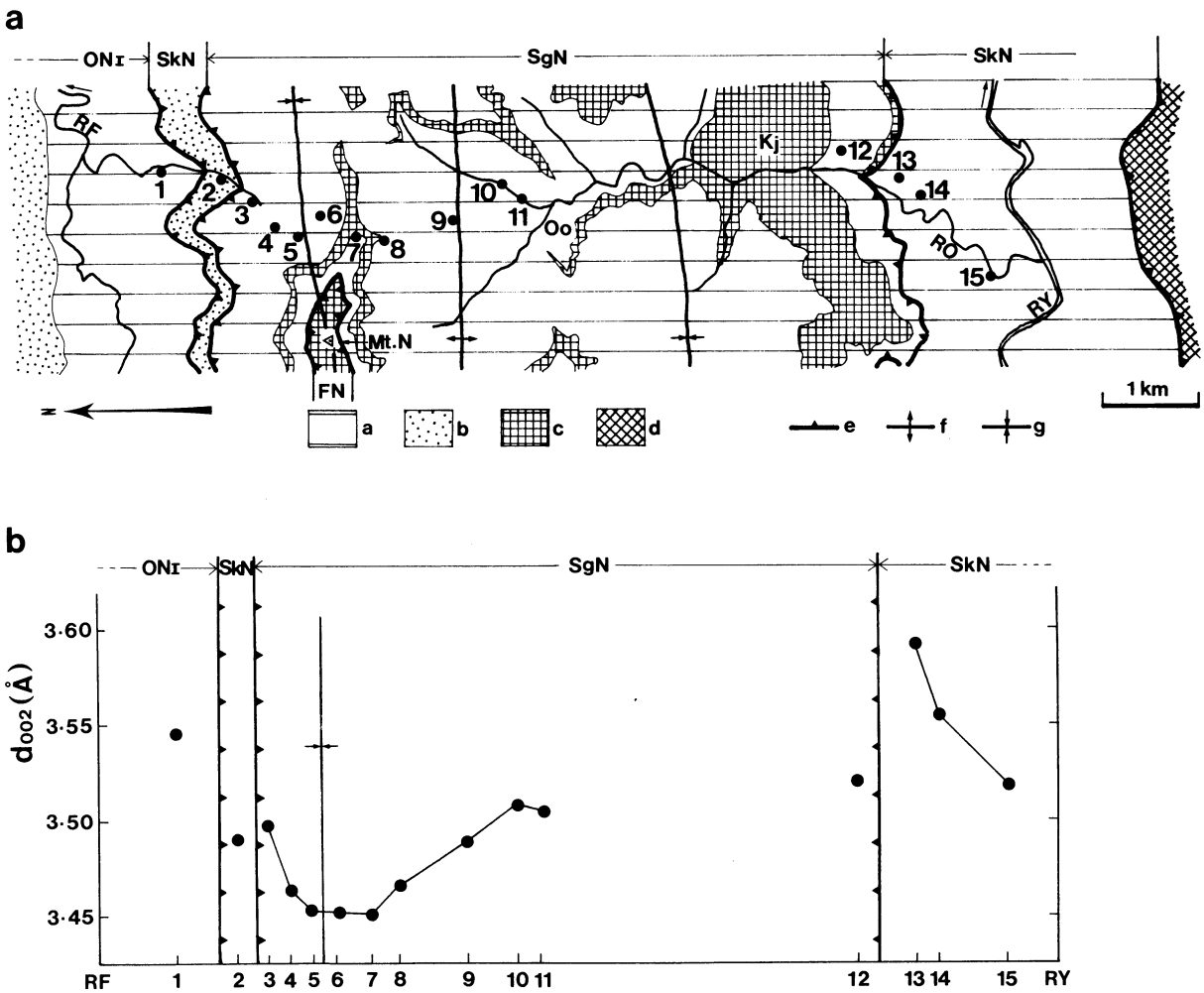

Fig. 97 Geological map (a) and degree of graphitization of carbonaceous materials in pelitic schists (b) of the Noganoike district (Hara *et al.*, 1990d).

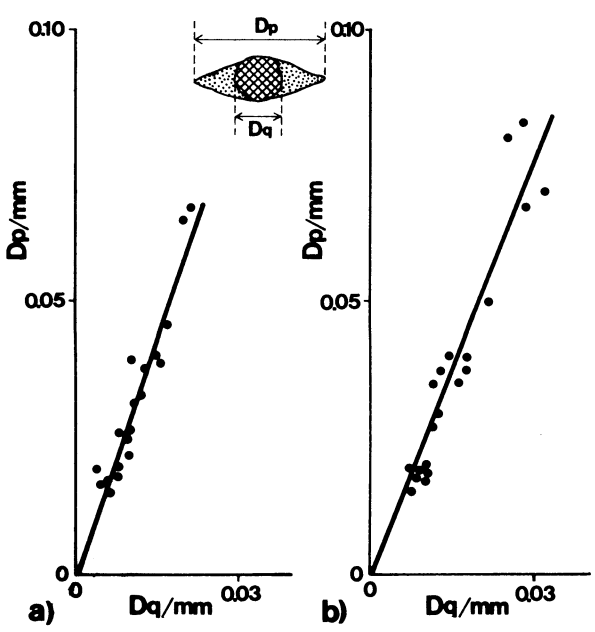

Fig. 98 Diagram showing the shape data of pressure shadows in a specimen from pelitic schists of the Niyodo nappe of the Ikegawa district.
a) data from thin section normal to bedding schistosity and parallel to lineation, b) data from thin section normal to lineation. Dq: diameter of spherical opaque grain, Dp: diameter of pressure shadows.

Fig. 99 Photographs of pebbles in conglomerate schists of the Oboke nappe I of the Oboke-Itchu district.
a) photograph of section subnormal to lineation (axis of crenulation on the bedding schistosity, b) photograph of section subparallel to lineation and normal to the bedding schistosity, though crenulation cleavage is only quite weakly developed.
a) and b) show preferred shape orientation of pebbles along the bedding schistosity.
c) and d) microphotographs of pressure shadow around coarse-grained quartz in deformed quartz-porphyry pebble and matrix psammitic schists, respectively, as observed on thin sections parallel to the bedding schistosity (Hara *et al.*, 1966).

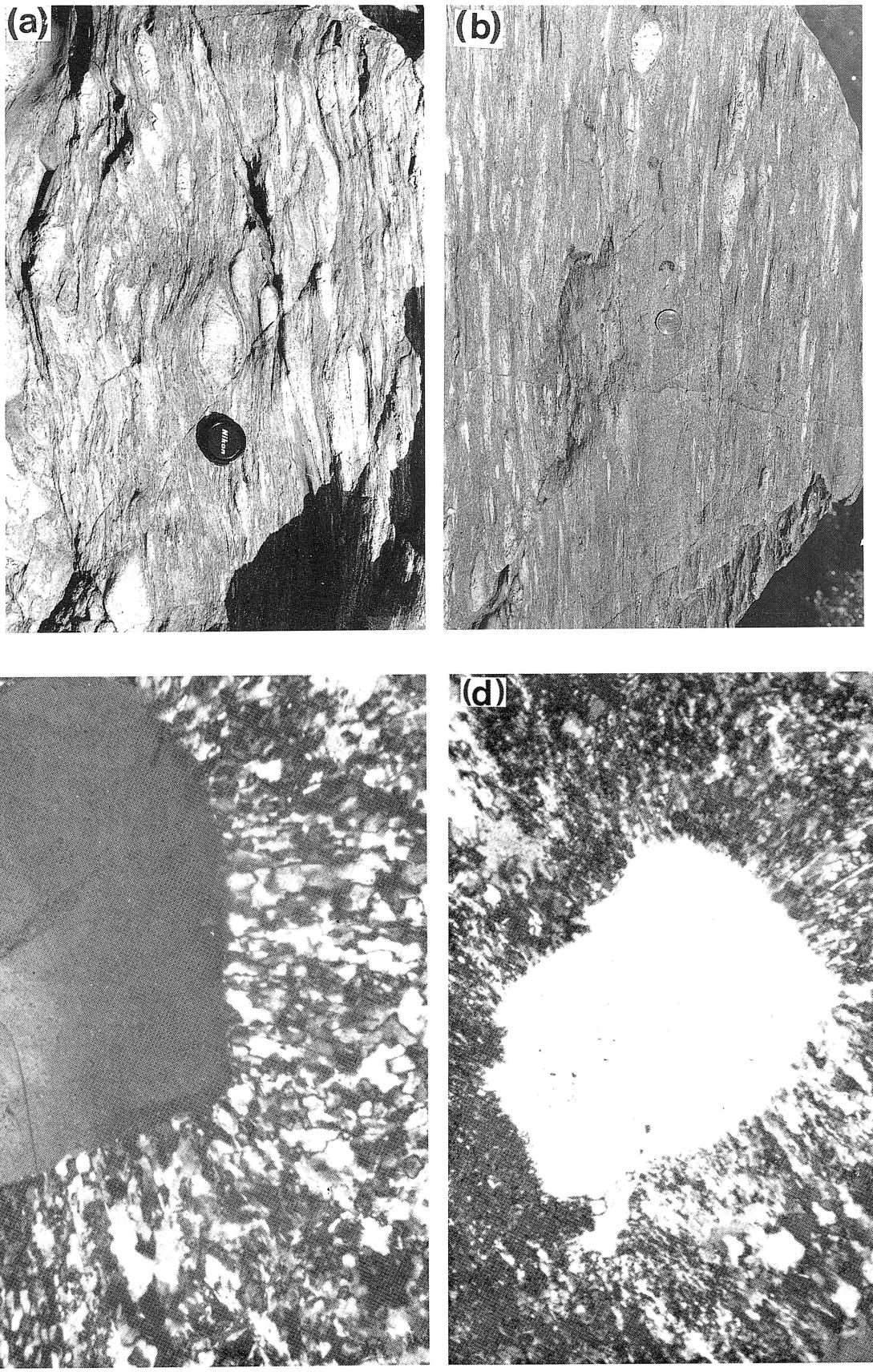
(a)
(b)
(c)
(d)

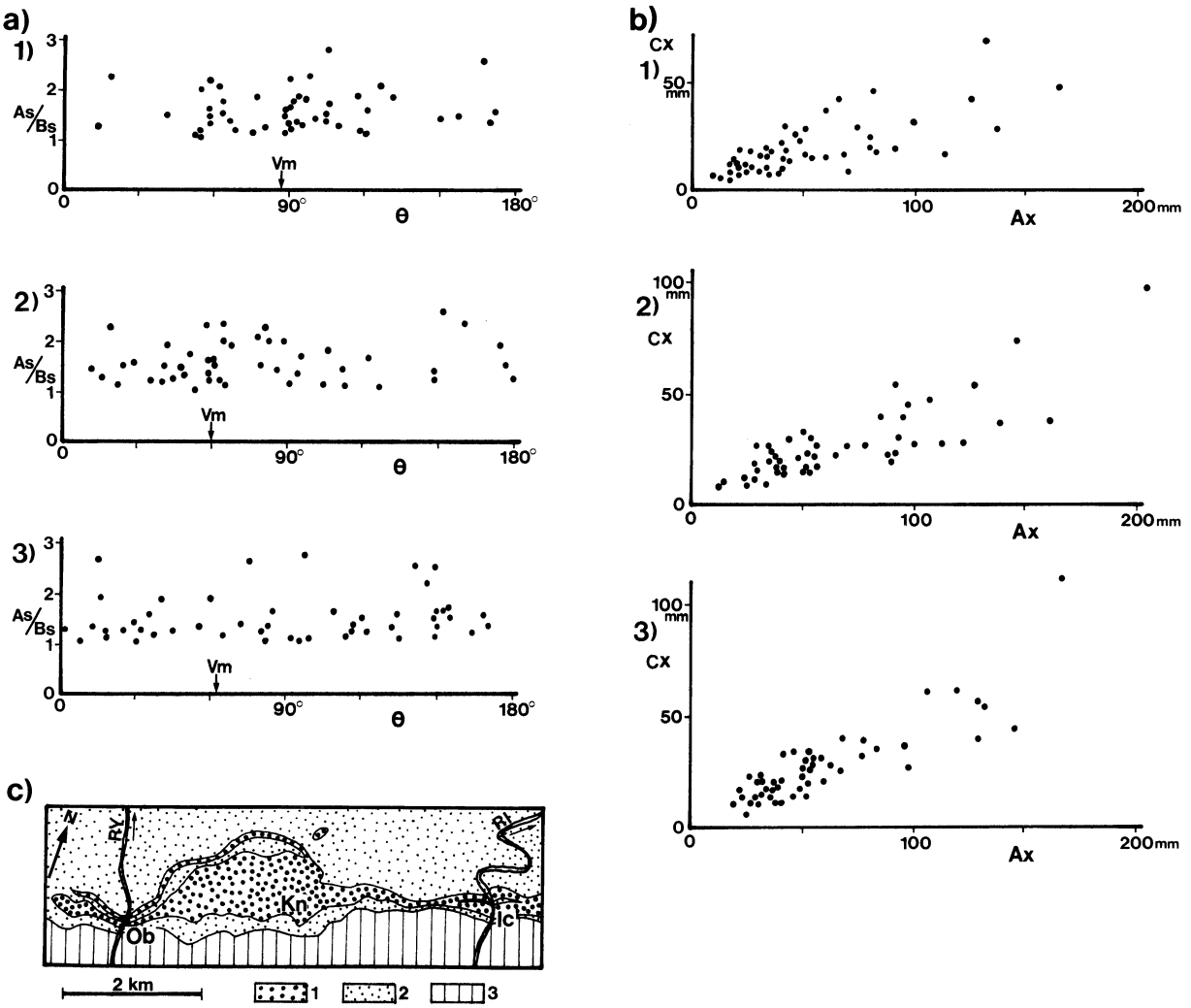

Fig. 100 Diagram showing the shape data of pebbles in conglomerate schists of the Oboke nappe I which were measured in three localities (Ic, Kn and Ob) of the Oboke district (c) [data from Hara *et al.* (1973)].
a-1), a-2) and a-3) relationship between the aspect ratio (As/Bs) and the orientation of the longest axis (As) for pebbles as observed on the bedding schistosity. In (a-1) for locality (Ic) vector magnitude = 49.8 and average As/Bs = 1.58, in (a-2) for locality (kn) vector magnitude = 38.4 and average As/Bs = 1.52 and in (a-3) for locality (Ob) vector magnitude = 6.9 and average As/Bs = 1.51. b-1), b-2) and b-3) relation between the longest axis (Ax) and its normal (Cx) for rhyolite - quartz porphyry pebbles (greatly competent pebbles) as measured on sections, which are subparallel to the direction of vector mean for the longest axes of pebbles on the bedding schistosity and subnormal to the bedding schistosity. The average aspect ratio measured on a section subnormal to the bedding schistosity in each locality is nearly constant as compared with each other for the data from differently orientation sections. Vm in the diagrams is vector mean showing the direction of preferred shape orientation of pebbles. Vector magnitude for pebbles oriented preferably along the bedding schistosity, as measured on both sections parallel to vector mean and normal to the bedding schistosity and section normal to vector mean, is 93 and 85 in locality (Ic), 93 and 87 in locality (Kn) and 95 and 90 in locality (Ob) respectively. 1: conglomerate schists, 2: psammitic schists, 3: pelitic schists, RY: River Yoshino, RI: River Iya.

to their eastward shear.

The discontinuous geological structure produced during the Sb2-1 deformation is found along the boundary between the Fuyunose nappe and the Sogauchi nappe of the Nankoin district as shown in Fig. 96. The lithologic layering (= bedding schistosity) of siliceous schists and basic schists of the Sogauchi nappe is cut across by the pelitic schists of the Fuyunose nappe. The Besshi-Iratsu eastward shear zone cuts across the nappe boundary, accompanying formation of shear lenses (S-C structure) and Type III quartz microtextures, which are clearly observed in the schists developed along the River Dozan.

The major geological structure of the Chichibu megaunit I in central Shikoku is, as a whole, characterized by a nearly flat-lying structure of lithologic layering, though locally folded in overturned fashion [for example, Sakaidani antiform after Kojima and Suzuki (1958)] and, as a whole, gently folded in upright fashion. Following Nakajima *et al.'s* (1977), Aiba's (1982) and Banno and Sakai's (1989) data for metamorphic facies analysis and Takeda *et al.'s* (1977) and Tsukuda *et al.'s* (1981) data (Figs. 3 and 7) of geological structure analysis, the middle pumpellyite-

actinolite zone and the lower pumpellyite-actinolite zone - prehnite-pumpellyite zone are, respectively, developed on the northern limb and the southern limb of the Kamiyagawa-Ikegawa antiform, showing that the facies boundaries appear to cut across the lithologic layering. The horizontal distance between the quartz-lawsonite-albite assemblage part of middle pumpellyite-actinolite zone (northern part of Sakamoto nappe) and the prehnite-pumpellyite zone (southern part of Niyodo nappe) is roughly estimated to be ca. 10 km, as measured in a direction normal to the general trend of the Sambagawa megaunit (Fig. 2). While pressure difference between the former and the latter appears to be less than 2kb (Fig. 21). If these estimations were correct and the piling style of lithologic layering produced during the peak metamorphism was scarcely modified by the later phases deformations, the Chichibu megaunit I should have formed a high-angle dipping structure of lithologic layering during the peak metamorphism. On the basis of analysis of graphitization degree of carbonaceous material in pelitic schists, Hara *et al.* (1990d) have clarified that the metamorphic grade of the Sakamoto nappe schists shows a downward increase (Fig. 97). The orientation of the Chichibu megaunit I in the subduction zone may be, therefore, explained in terms of a downward increase of temperature. This is different from the cases of the Saruta nappes and Fuyunose nappe (Fig. 59), which have been shown by Hara *et al.* (1990a, b, c). Now, it may be said that, though the Saruta, Fuyunose and Sogauchi units were placed in parts of inverted thermal structure of the subduction zone during the period from the Spm phase to the Sb2-1 phase, their nappes were emplaced into a part of normal thermal structure, thrusting onto the Chichibu megaunit I, during the Sb2-2 phase.

In pelitic schists of the Niyodo nappe are found pressure shadows developed around opaque mineral grains, which are fine-grained. The shapes of such pressure shadows in pelitic schists with single planar schistosity should give an important information to understand the strain picture related to the formation of the schistosity (= bedding schistosity), which would be regarded as to be of the Sb2-2 phase. Fig. 98 is a representative example of such data. From this figure it would be said that the strain picture of the Niyodo nappe schists during the Sb2-2 deformation is of flattened type in mean strain.

The Shimanto megaunit, which is underlain by the Sambagawa megaunit and contains the Oboke unit, shows the metamorphic grade of the highest- temperature phase which is comparable with a pumpellyite-actinolite facies (without quartz-lawsonite-albite assemblage) and a prehnite-pumpellyite facies (cf. Banno and Sakai, 1989; Kanai *et al.*, 1990) (Fig. 21). The deformation related to the coupling of the Shimanto megaunit with both Sambagawa megaunit and Chichibu megaunit I is the Sb3 deformation and was responsible for the exhumation path of the Sambagawa megaunit as shown in the P-T diagram of Fig. 21 (Hara *et al.*, 1990a).

The strain picture of the Shimanto megaunit rocks developed during the Sb3 deformation has been analyzed in pebbles of conglomerate schist of the Oboke nappe I (Fig. 99) by Hara *et al.* (1966, 1973). Strongly elongated pebbles are preferably oriented parallel to the bedding schistosity. Their longest axes on the bedding schistosity are random in some places and preferably oriented in some other places (Fig. 100). Regardless of the magnitude of orientation of the longest axes, the aspect ratios as measured on the bedding schistosity, are constant in an average value of ca. 1.5 (Fig. 100). Fig. 99-c and d shows pressure shadows developed around coarse-grained quartz in quartz-porphyry pebble and matrix psmmitic schist. These appear to be developed almost uniformly around coarse-grained quartz. From pebble shapes and such pressure shadows it would be said that the strain picture of the conglomerate schist during the Sb3 deformation was of flattened type.

G: Tectonics Related to the Collapse of the Kurosegawa-Koryoke Continent and the Sambagawa Megaunit—Ozu Phase Deformation

The pile nappe structures of the Sambagawa megaunit, which had been produced by the deformations during the period from the Sb1 phase to the Sb3 phase (Table 2), are greatly destroyed in its upper parts and its northern parts as shown in Fig. 12. The deformation related to the collapse of such the initial pile nappe structures of the Sambagawa megaunit is of the Ozu phase and was responsible for the formation of new (Ozu-phase) pile nappe structures. The Ozu phase pile nappe structures in eastern Shikoku are Inouchi melange zone and Tsuji nappe after Shiota (1981) (Figs. 12 and 101). The Sambagawa megaunit involved in the Tsuji nappe is Saruta unit (biotite zone) in lower part and Fuyunose unit in upper part. In Fig. 102 are shown the geological profiles of the Tsuji nappe and the pattern of growth history of amphibole in the Tsuji district and the Kamojima district. In the Tsuji district the retrograde growth history of amphibole in the Saruta unit is hornblende - barroisite - actinolite and that in the just overlying Fuyunose unit is glaucophane - crossite - winchite - actinolite, showing missing of barroisite - winchite - actinolite path zone and so that the coupling of the former and the latter occurred under the pressure-temperature condition of actinolite stability field (or much lower temperature condition) as is shown in Fig. 102. Therefore it can be said that

Fig. 101 Geological map and profiles of the Tsuji district [partly modified from (Shiota, 1981)].
1: pelitic schists, 2: pelitic-psammitic schists, 3: psammitic schists, 4: siliceous schists, 5: basic schists without plagioclase porphyroblasts, 6: basic schists with plagioclase porphyroblasts, 7: metagabbro, 8: ultrabasic rock, 9: Izumi Group, 10: boundary between basic schists with and without plagioclase porphyroblasts, 11: fault (post-Tsuji phase), 12: nappe boundaries (a: subcretion unit boundary, b: boundary between nappes in a subcretion unit, c: nappe boundary of the Tsuji phase), SU: Saruta unit, TN: Tsuji nappe, IMZ: Inouchi melange zone, FN Fuyunose nappe, SgN: Sogauchi nappe (Syosanji nappe), ONII: Oboke nappe II, ONI: Oboke nappe I, Gn: Mt. Gonomaru, Tn: Mt. Tsunatsuki, Kn: Mt. Kaina, Hn: Mt. Hinomaru, Fr: Mt. Furodo, Mz: Mizunokuchi Pass, Sj: Sajiki Pass.

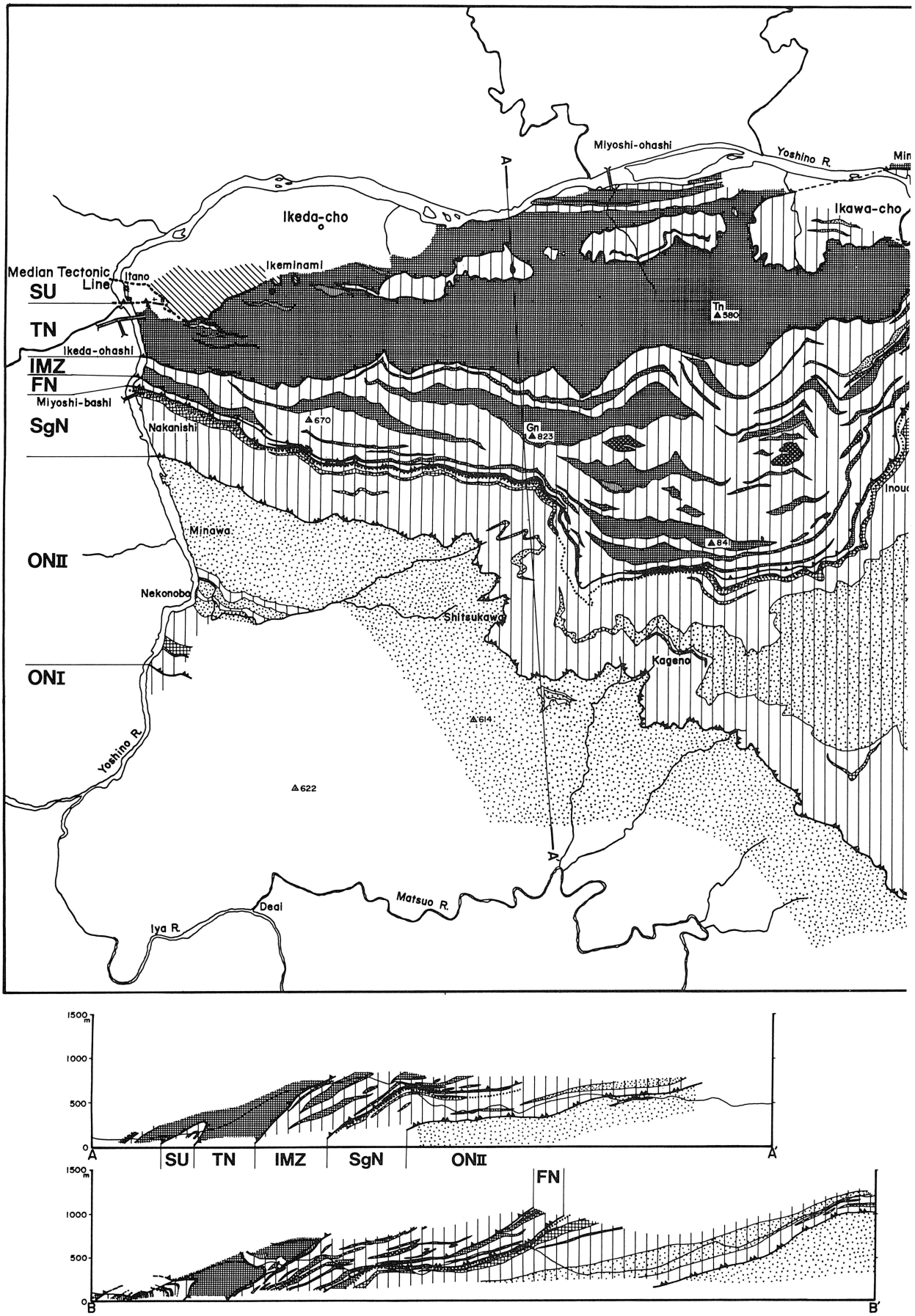
Miyoshi-ohashi
Yoshino R.
Ikeda-cho
Ikawa-cho
Median Tectonic Line
Itano
Ikeminami
SU
TN
Ikeda-ohashi
IMZ
FN
Miyoshi-bashi
SgN
Nakanishi
Th
△580
△670
Gn
△823
Minawa
ONII
Nekonoba
Shitsukawa
Kageno
ONI
△614
△622
Yoshino R.
Matsuo R.
Deai
Iya R.
A
A'
B
B'
1500m
1000
500
0
SU
TN
IMZ
SgN
ONII
FN

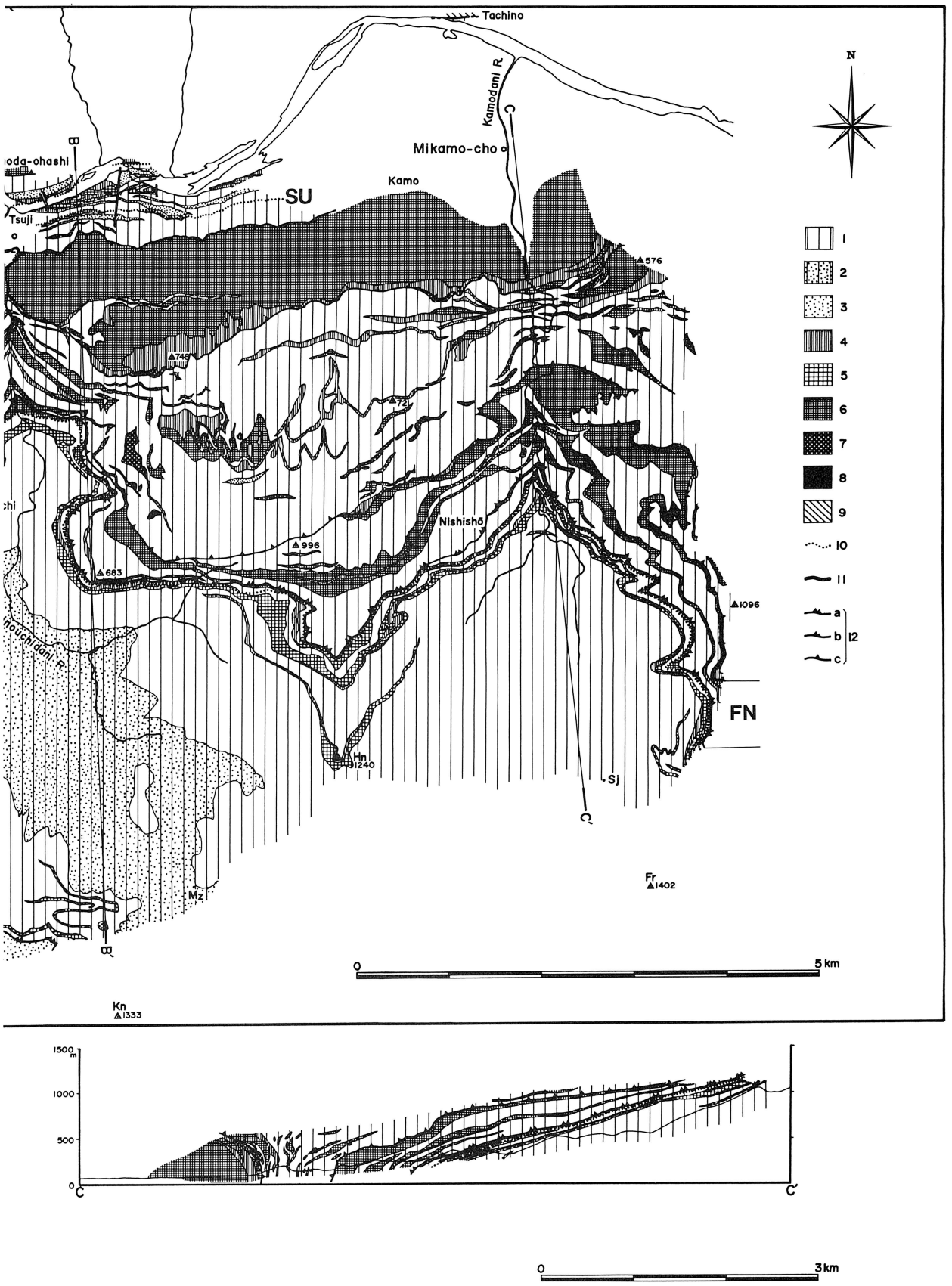
Tachino
Kamodani R.
Mikamo-cho
Kamo
SU
Tsuji
B
C
N
1
2
3
4
5
6
7
8
9
10
11
a
b
c
12
576
745
721
996
683
Nishishō
1096
FN
Hn
1240
SJ
Fr
1402
Mz
Kn
1333
0
5 km
1500 m
1000
500
0
C
C'
0
3km

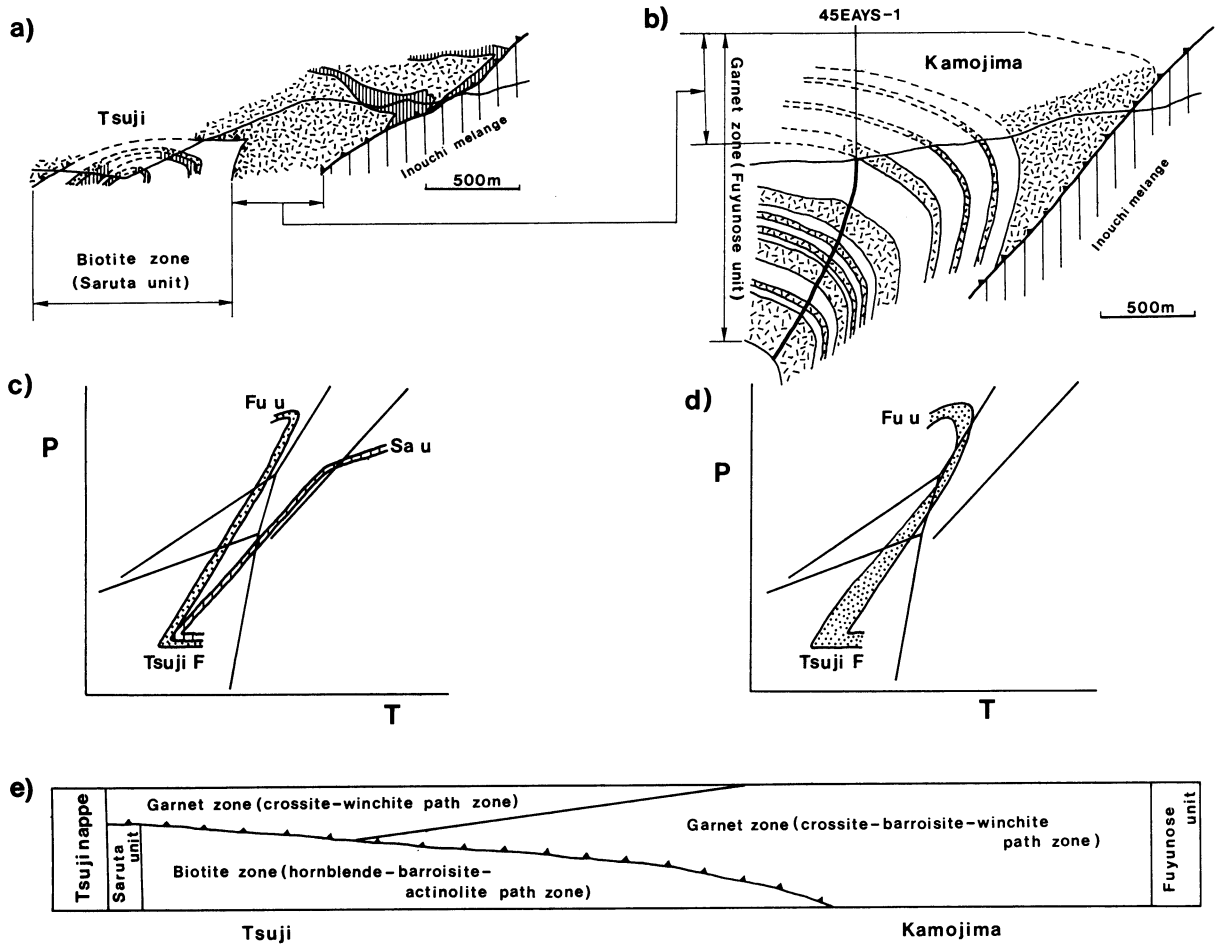

Fig. 102 Diagram showing the spatial variation in retrograde growth path of amphibole in hematite-bearing basic schists throughout the Tsuji nappe.
a) unit-division (garnet zone = Fuyunose unit and biotite zone = Saruta unite) of the Tsuji nappe of the Tsuji district, b) profile (garnet zone = Fuyunose unite) of the Tsuji nappe of the Kamojima district based on the data of the field and borehole (MMEAJ, 1971b), c) relation in amphibole growth history between the Fuyunose unit (Fu u) and the Saruta unit (Sa u) in the Tsuji district, d) amphibole growth history of the Fuyunose unit (Fu u) in the Kamojima district, e) spatial variation in amphibole growth history throughout the Tsuji nappe, Tsuji F: Tsuji overturned fold.

Table 2 The phases (main phase: heavy lines and subordinate phase: heavy dashed lines) when displacement along the nappe boundaries in the Sambagawa megaunit and its surroundings in Shikoku occured.

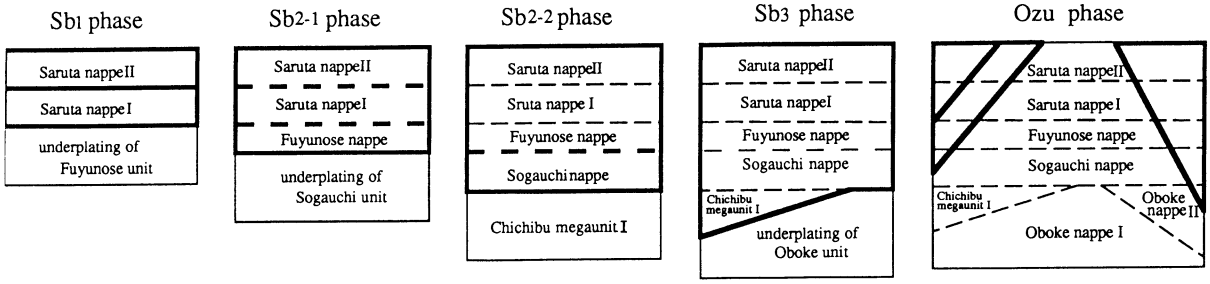

the pile nappe structure of the Saruta unit and the Fuyunose unit of the Tsuji district is not equivalent to the initial (pre-Ozu phase) pile nappe structures which are developed in central Shikoku (Fig. 60). In the Kamojima district to east of the Tsuji district the retrograde growth history of amphibole in the Fuyunose unit is, as a whole, crossite - barroisite - winchite - actinolite. Thus the Fuyunose unit of the Tsuji nappe is divided into two zones with reference to the retrograde growth history of amphibole in hematite-bearing basic schists, crossite - winchite path zone and crossite - barroisite path zone (Fig. 65). From this figure it can be said that the boundary between the crossite - winchite

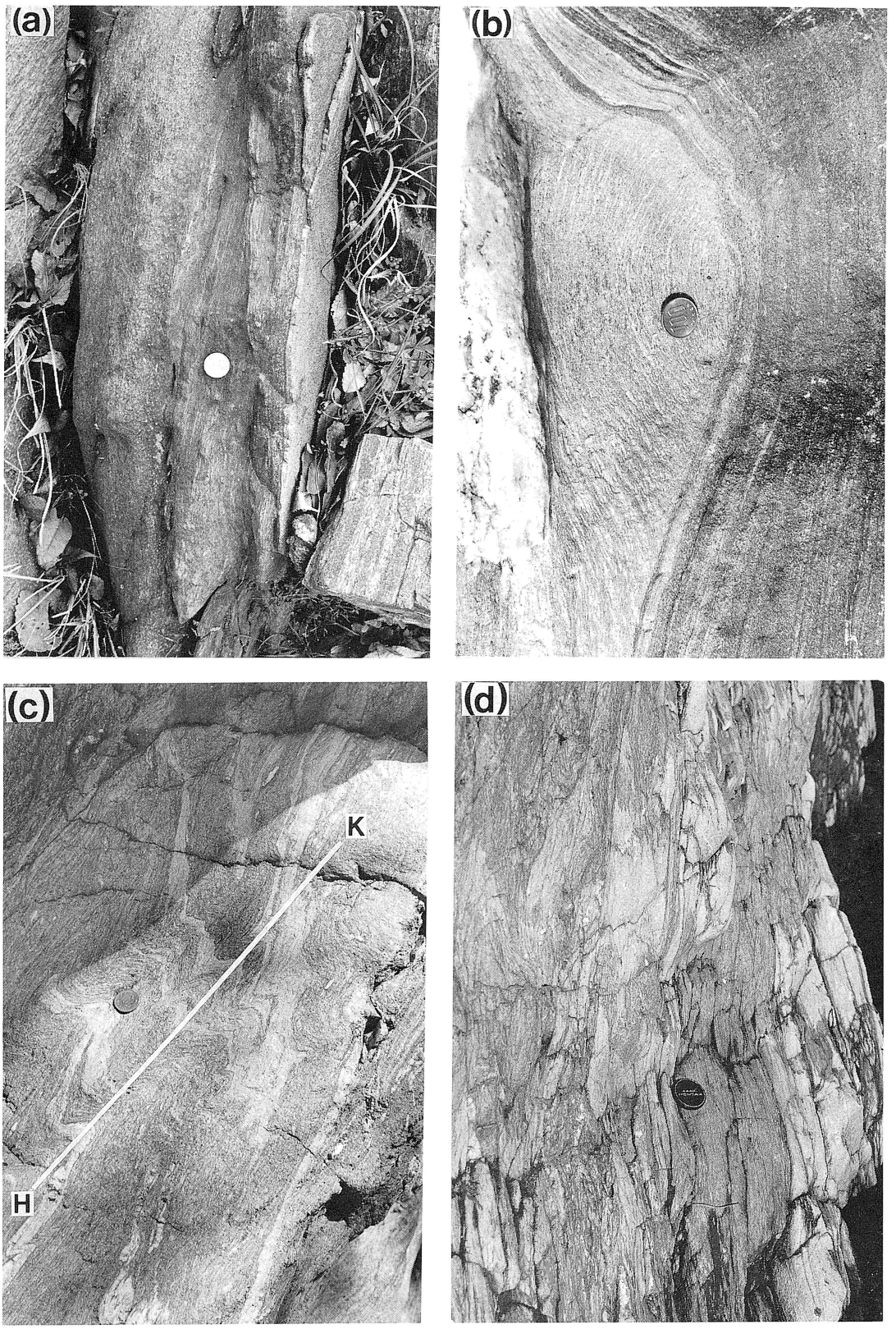

Fig. 103 Photographs of rock structures developed in the Inouchi melange zone.
a) transposition structure oblique to the bedding schistosity in the Sadamitsu district, b) transposition structure oblique to the bedding schistosity of the Anabuki district, c) mesoscopic fold of the Tsuji stage with superposition of minor-micro folds of the Hijikawa-Oboke phase (H-K) in the Mikamo district, d) mesoscopic fold of the Tsuji stage in the Mikamo district.

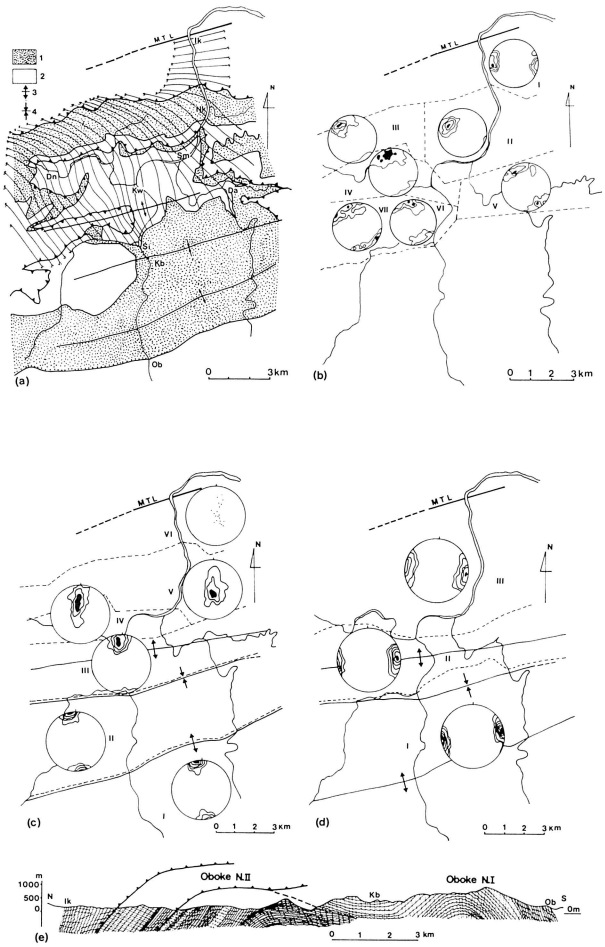

Fig. 104 Structural data of the Sambagawa megaunit-Shimanto megaunit in the Oboke - Ikeda district [data from Yokota (1969) and Hara *et al.* (1977)]. a) axial traces (solid lines) of minor folds of the Tsuji stage. 1: psammitic schists, 2: pelitic schists, 3: antiform of the Hijikawa- Oboke phase, 4: synform of the Hijikawa-Oboke phase, b) diagrams showing orientation of axes of minor folds of Tsuji phase in seven domains, c) π-diagrams for axial planes of minor folds of the Hijikawa-Oboke phase, d) diagrams showing orientation of axes of minor folds of the Hijikawa-Oboke phase, e) geological profile along the line Ikeda-Oboke showing orientation of axial planes of minor folds of the Hijikawa-Oboke phase. Ik: Awaikeda, Nk: Nekonbo, Sm: Shimokawa, Kw: Kawaguchi, Da: Deai, Dn: Daino, Si: Sirakawaguchi, Kb: Koboke, Ob: Oboke.

path zone and the crossite - barroisite path zone in the Fuyunose unit of the Tsuji nappe is greatly displaced toward the north from that in the Fuyunose nappe of the pre-Ozu phase pile nappe structures, which is now found in central Shikoku. In the Inouchi melange zone are commonly found transposition structures and shear lenses produced by the Ozu phase deformation (Fig. 103). The eclogitic rocks (Takasu and Kaji, 1985), biotite zone schists and garnet zone schists are intermingled with each other in the zone, owing to the collapse of the initial supeposition of the Saruta nappes and Fuyunose nappe during the Ozu phase deformation.

The Ozu phase rock structures of various scales, cleavages and folds, are commonly found in the Tsuji nappe, Inouchi melange zone and their underlying Sogauchi nappe (= Syosanji nappe) and Oboke nappe (I + II) schists, which have been described by Yokota (1969), Shiota (1976, 1981) and Hara *et al.* (1977). The Tsuji overturned fold (Figs. 101 and 102), whose lower limb is transposed, is one of them. The Ozu phase folds show commonly asymmetric style and their axial surfaces traverse the pre-Ozu phase nappe boundaries, as shown in Fig. 104. They had first been described by Kojima and Suzuki (1958), showing that they are deformed by the last phase folding [Hizikawa (Hijikawa)-Oboke phase deformation] of the Sambagawa megaunit (Fig. 105), which will be described in the next section.

The western extension of the Inouchi melange zone is called Ojoin melange zone, which is widely developed in the region between the River Urayama district and the Omogiyama district (Fig. 14). The base of the Ojoin melange zone on the north of Mt. Higashiakaishiyama (Fig. 94) and in the Besshi mine district (Fig. 73) is placed just near the top of Shirataki I + II + III amphibole schist of the Saruta nappe I. In the area just to the west of the River Urayama is clearly found the structural discontinuity between the Saruta nappe II and the Ojoin melange zone, as shown in the geological map and profile of Fig. 94. The northward - northwestward dipping structure of siliceous schist layers and basic schist layers of the Ojoin melange zone is quite disharmonic with the upright fold (Tsuneyama synform) of the Saruta nappe II, owing to structural discontinuity between them produced before the formation of the synform. Analogous structural discontinuity between the Ojoin melange zone and its underlying geological unit is also clearly observed in the Omogiyama district as mentioned in the later page.

In the Ojoin melange zone are intermingled eclogitic rocks, ultrabasic rocks, biotite zone schists and garnet zone schists, like in the case of the Inouchi melange zone. An outline of the mode of occurrence of various grades rocks in the Ojoin melange zone just on the north of the Urayamagawa - Besshi mine district has been, though roughly, given by Higashino (1990). The retrograde growth history of amphibole in hematite-bearing basic schist of the garnet zone, which is developed in the basal part of the Ojoin melange zone just on the north of Mt. Higashiakaishiyama (Fig. 94), is crossite - barroisite - winchite - actinolite, though that in the just underlying Shirataki amphibole schist is assumed to be of Type I, hornblende - actinolitic hornblende - actinolite, (Fig. 106). The boundary between the Saruta nappe I and the Ojoin melange zone is, thus, not of the pre-Ozu phase pile nappe structures.

Fig. 107 illustrates the pile nappe structure of the Omogiyama district. It is characterized by three nappes, Omogiyama nappe, Ojoin melange zone and Futami nappe in ascending order of structural level, which overlie the Sogauchi nappe. The Omogiyama nappe has a large scale recumbent fold with southward closure (Omogiyama fold), which consists of garnet zone schists in its core and chlorite zone schists in its mantle. The fold is partly cut across by the Ojoin melange zone and further by the Futami nappe, forming nearly flat-lying structure, (Fig. 107). Such pile nappe structure is refolded in upright fashion by the Hijikawa-Oboke phase deformation, showing superposition

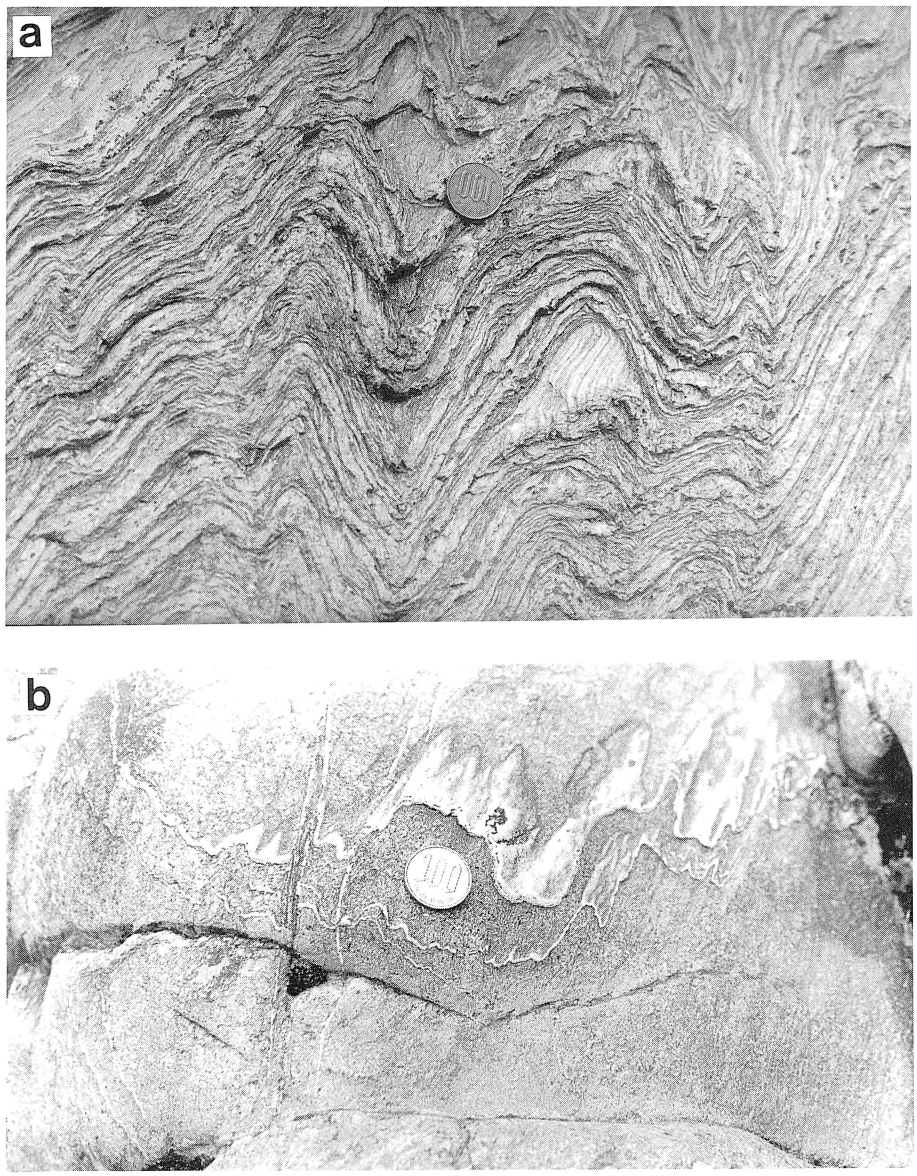

Fig. 105 a) Photograph showing the superposition of the Ozu-phase minor folds (microlithons) and the Hijikawa-Oboke phase minor folds of pelitic schists in the Sakamoto nappe of the River Asemi (Waseda).
b) Photograph of the Hijikawa-Oboke phase minor folds in psammitic schists with quartz veins of the Oboke nappe I of the River Yoshino (Koboke).

of rock structures of the Ozu phase and these of the Hijikawa-Oboke phase which is comparable with that of Fig. 105-a.

The Ozu phase pile nappe structure in western Shikoku (Fig. 6), which overlies the Sogauchi nappe and Chichibu megaunit I (Hataki nappe), is characterized by the development of three nappes, Futami nappe with Karasaki mylonites, Terano-Isozu nappe and Kabayama-Saredani-Izushi nappe in descending order of structural level. The pile nappe structure is refolded in upright fashion by the Hijikawa-Oboke phase deformation. Thus, the pile nappe structures of the Sambagawa megaunit and its surrounding megaunits will be summarized as shown in Table 3.

The Futami nappe cuts across the pile nappe structure which is formed by the Terano-Isozu nappe, Kabayama-Saredani-Izushi nappe, Sogauchi nappe and Hataki nappe, (Fig. 6). The coupling of the Sambagawa megaunit and the Mikabu unit of Chichibu megaunit II (= Futami nappe) and that of the Futami nappe and the Karasaki mylonites are also ascribed to the Ozu phase deformation (Hara *et al.*, 1977, 1990a; Takeda *et al.*, 1977). As shown in Figs. 108 and 16, the Mikabu nappe cuts across the structures of the underlying Sogauchi nappe (Syosanji nappe) and Chichibu megaunit I. The above-mentioned displacement of the Chichibu megaunit II contains a component of southward displacement. That is quite disharmonic with the movement picture of the Tsuji nappe, which has been assumed to contain a component of northward displacement. The deformation related to the formation of the Tsuji nappe must have been responsible for the formation of the Inouchi

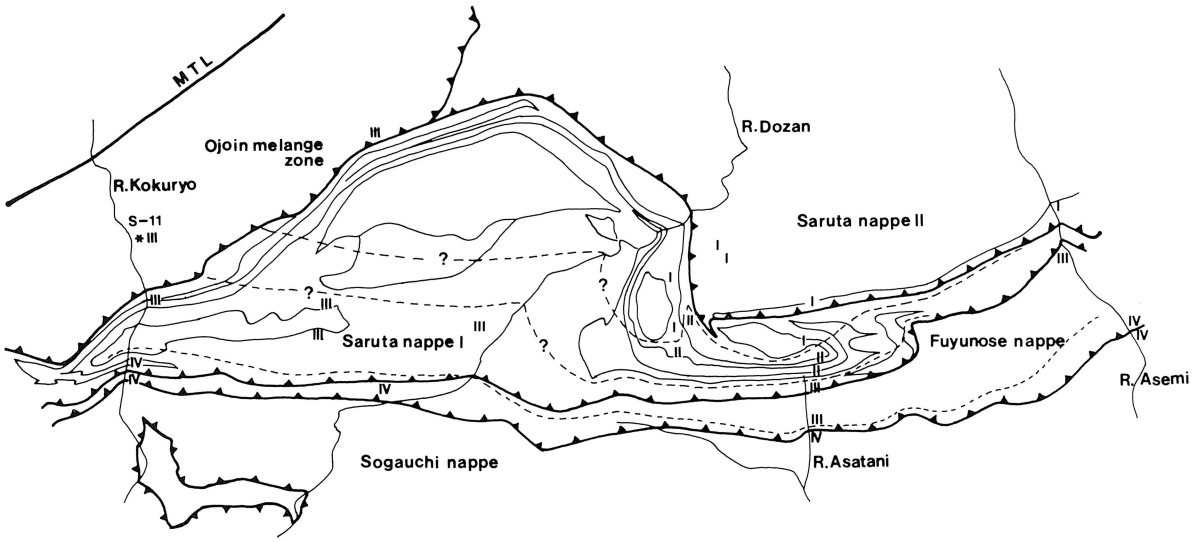

Fig. 106 Diagram showing the spatial variation of the retrograde growth history of amphibole in hematite-bearing basic schists of the Sambagawa megaunit in central Shikoku.
I, II, III and IV: four types of retrograde growth history, dashed lines: assumed boundaries of zones of four types.

melange zone and also Ojoin melange zone, as assumed from the mode of their structural relation. The displacement of the Chichibu megaunit II appears to postdate that of the Tsuji nappe-Inouchi melange zone-Ojoin melange zone, judging from cross-cutting relation between the former (displacement of Futami nappe-Mikabu nappe) and the latter (Figs. 6 and 107). The displacement of the Tsuji nappe and Ojoin-Inouchi melange zone is therefore called here the deformation during the earlier stage of Ozu phase (Tsuji-stage) and the displacement of the Chichibu megaunit II that during the later stage of Ozu phase (Futami stage).

H: Hijikawa (Hizikawa)-Oboke Phase Folding

As shown in Figs. 7, 10 and 14, the nappes of the Chichibu megaunit II, Sambagawa megaunit, Chichibu megaunit I and Shimanto megaunit and their constituent schist layers form a series of sinistral en echelon upright folds with a half wavelength of less than 20km, which belongs to the last phase of the folding history in the Sambagawa megaunit. This phase of deformation has been called the Hizikawa (Hijikawa) phase (Hara *et al.*, 1977) and F3 phase by Faure (1983, 1985). The most excellent example of the Hijikawa phase folds is observed in the Oboke district (Fig. 104). These in the Oboke district have been so far studied in the most details (*e.g.* Hara *et al.*, 1968; Yokota, 1969; Hara and Paulitsch, 1971). Therefore, the Hijikawa phase, when these folds were produced, has been called Hijikawa-Oboke phase in this paper. Before the sedimentation of the Kuma Group of Middle Eocene (Nagai, 1972) occurred the folding of the Hijikawa-Oboke phase.

Antiforms and synforms of the Hijikawa-Oboke phase have been mentioned as the major structure of the Sambagawa megaunit and its surrounding megaunits by many authors for long time. Fig. 94 indicates that the trough trace of the Tsuneyama synform is clearly different between the Saruta nappe II and the Fuyunose-Sogauchi nappes reflecting the mode of occurrence of the Saruta nappe I which contains the Suryo fold with large-scale tectonic blocks in its core. Namely, the synform is not traced on the main part of Saruta nappe I in the area of Fig. 94. However, the Saruta nappe I schists of this area are also deformed during the Hijikawa-Oboke phase forming folds with axial planes in various attitudes. The Hijikawa-Oboke phase folds with low-angle dipping axial planes are found in many outcrops. Thus, the deformation of the Saruta nappe (I + II), Fuyunose nappe, Sogauchi nappe, Sakamoto nappe and Oboke nappe (I + II) schists during the Hijikawa-Oboke phase can be also understood only by rock and micro-structure analysis.

The first description of the Hijikawa-Oboke phase structure based on rock and micro-structure analysis had been performed by Kojima and Suzuki (1958) in the Iwahara district (Fig. 14), distingushing between the Ozu phase structure as a large-scale antiform (Sakaidani antiform) with associated axial plane cleavage and the Hijikawa-Oboke phase mesoscopic folds of upright fashion with axial plane cleavage. The second clear description of the Ozu phase (Tsuji stage) and the Hijikawa-Oboke phase structures based on microstructures had been done by Yokota (1969) in the Oboke district as reproduced in Fig. 104. The third clear description of these structures is of Hide (1972) in the Hijikawa district, distinguishing between the large-scale Ozu overturned fold with axial plane cleavage and the upright Hijikawa fold with axial plane cleavage (Fig.6) on the basis of analysis of superposition of these cleavages. Analogous type work had been done by Ikeda (1972) and Hara *et al.* (1977) in the Nakashichiban district just on the south of the Besshi district as shown in Fig. 109. The Hijikawa-Oboke phase structure had been also described all over the Sambagawa megaunit [*e.g.* Iwahashi (1960, 1962) and Kamiyama *et al.* (1964) in Kii Peninsula; Nakano (1966) in the River Tenryu district, Central Japan; Tokuda (1976, 1986) in the Kanto Mountains, as synthesized by Hara *et al.* (1977)]. It has been then pointed out by Hara *et al.* (1977)

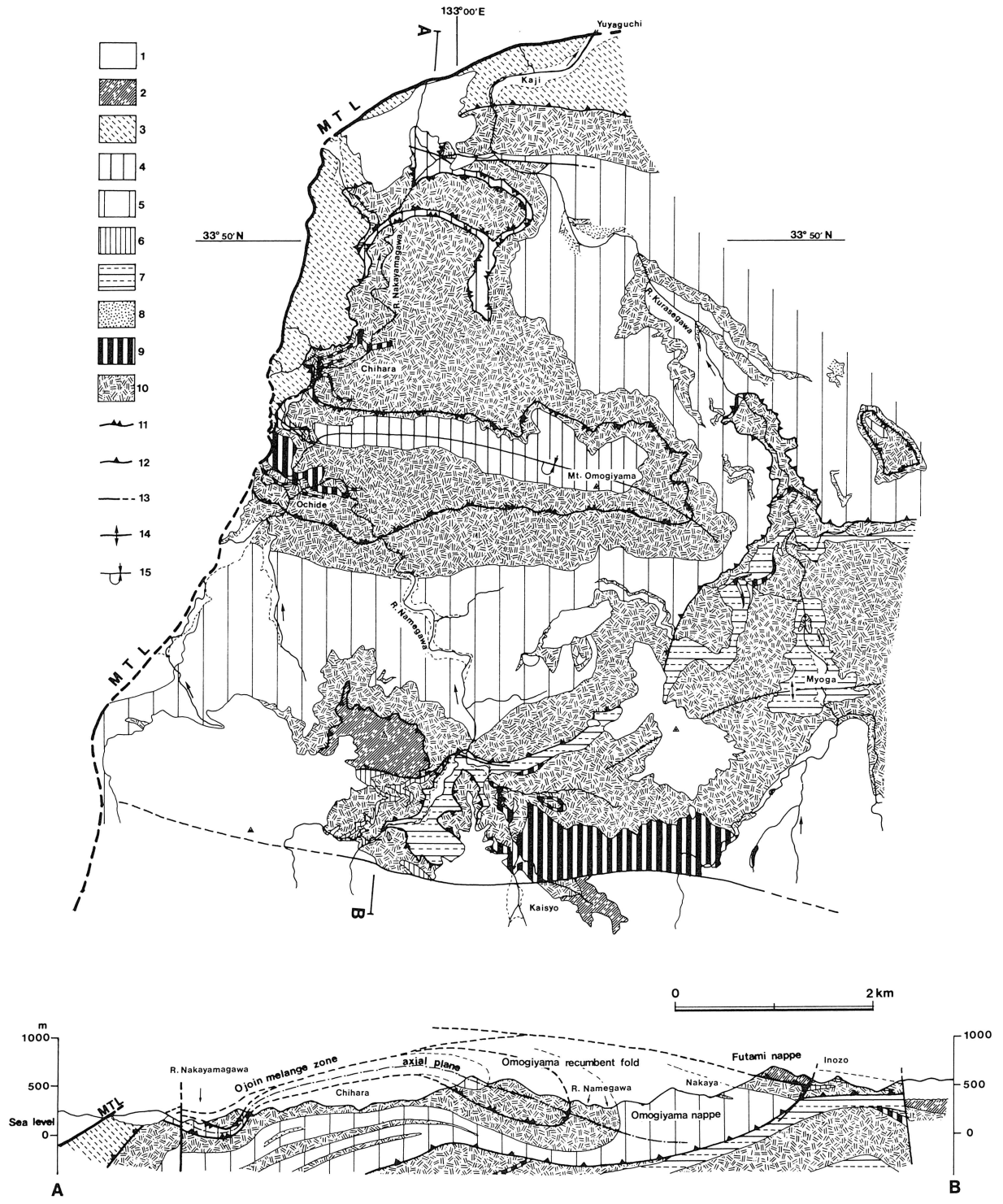

Fig. 107 Geological map and profile of the Omogiyama district (Hide, Hara, Shiota and kajitani 1985, 1992).
1: Cenozoic rocks, 2: pelitic schists with basic and siliceous schists in the Futami nappe, 3: pelitic-psammitic schists in the Ojoin melange zone, 4: pelitic schists in garnet zone (Fuyunose unit) of the Omogiyama nappe, 5 and 6: pelitic schists in chlorite zone (Sogauchi unit) of the Omogiyama nappe, 7: pelitic schists of the Sogauchi nappe, 8: psammitic schists, 9: siliceous schists, 10: basic schists, 11 and 12: nappe boundaries (11: subcretion unit boundary, 12: nappe boundary of the Ozu phase), 13: fault, 14: antiform of the Hijikawa-Oboke phase, 15: Omogiyama recumbent fold. MTL: Median Tectonic Line.

Table 3 Summary of pile nappe structures of the Sambagawa megaunit and its underlying and overlying structural units in central-western Shikoku.

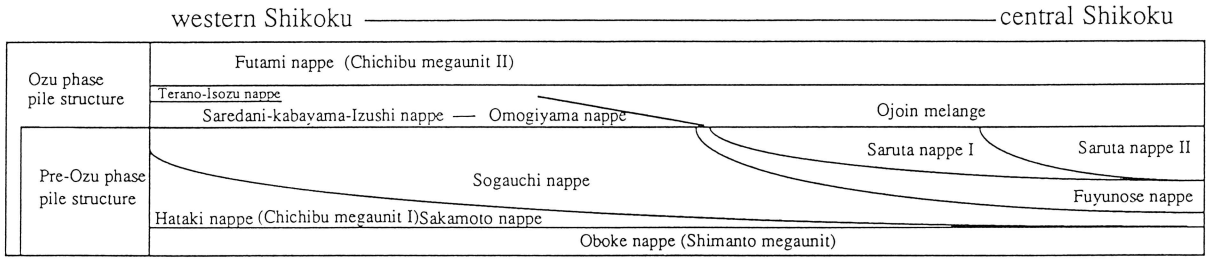

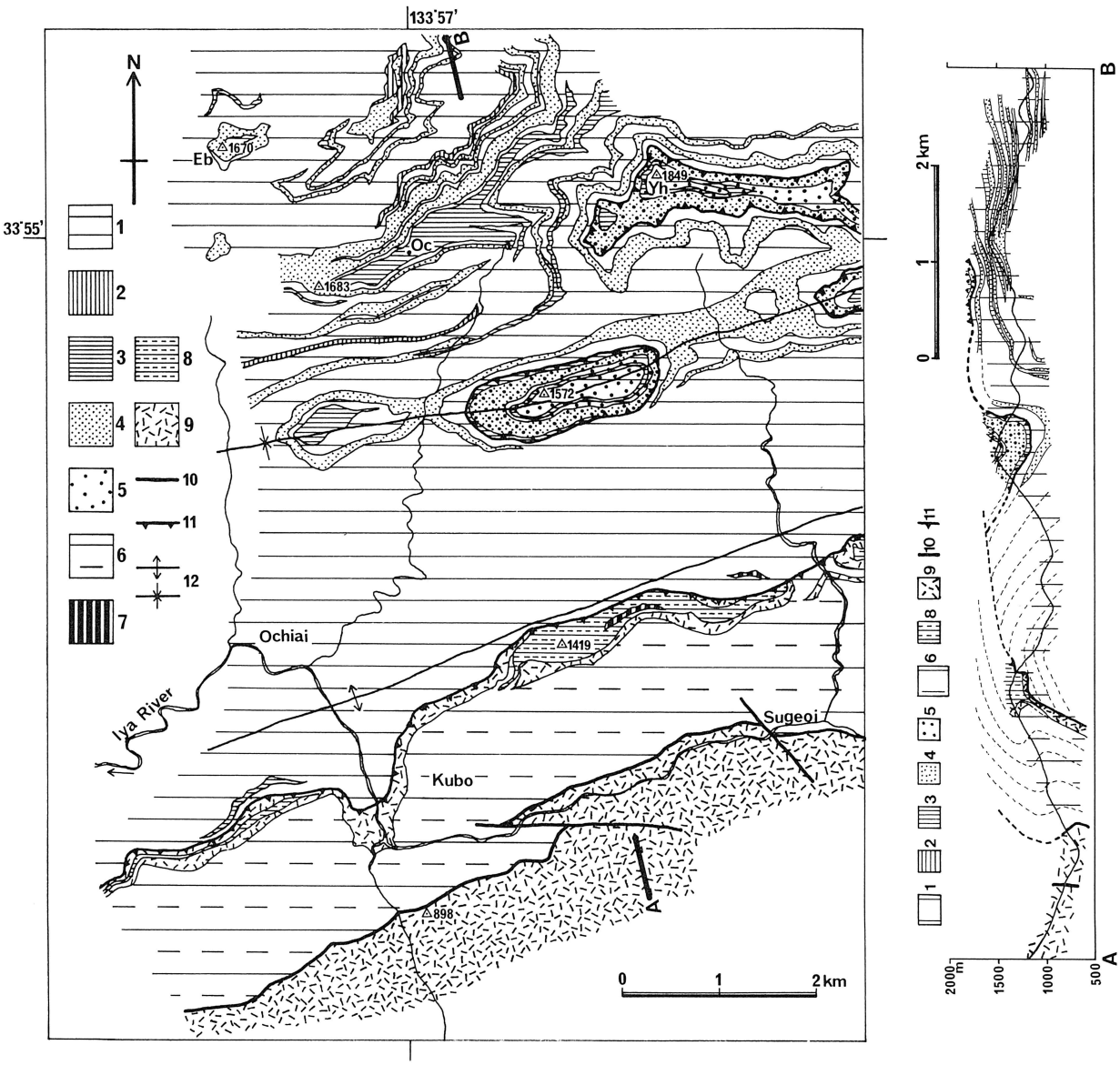

Fig. 108 Geological map and profile of the Iya district [partly modified from Takeda (1976, 1984) and Hara *et al.* (1977)] 1: pelitic schists in the Sogauchi (Syosanji) nappe, 2: psammitic schists, 3: siliceous schists, 4: basic schists, 5: Fuyunose nappe, 6, 7, 8, and 9: Mikabu nappe (6: pelitic schists, 7: calcareous schists, 8: siliceous schists, 9: Mikabu greenstones), 10: fault, 11: nappe boundary, 12: antiform of the Hijikawa-Oboke phase, dashed lines: trend of the bedding schistosity, Yh: Mt. Yahazu, Oc: Ochiai Pass, Eb: Mt. Eboshi.

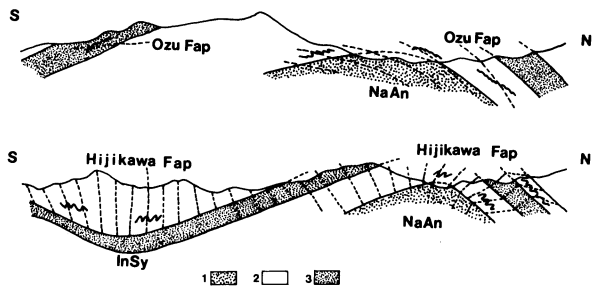

Fig. 109 Schematic diagram showing the orientation of the axial planes of minor folds in the Nakashichiban antiform (NaAn) and the Inamurasan synform (InSy) [data from Ikeda (1974) and Hara *et al.* (1977)]. Ozu Fap: axial planes of minor folds of the Ozu phase, Hijikawa Fap: axial planes of minor folds of the Hijikawa-Oboke phase.

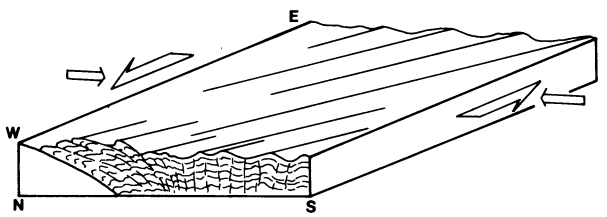

Fig. 110 Diagram illustrating the tectonics related to the formation of a series of sinistral en echelon upright folds of the Hijikawa-Oboke phase.

that the general characteristics of the Hijikawa-Oboke phase folds is sinistral en echelon arrangement and northward vergence.

Hara *et al.* (1968) analyzed structural characteristics of quartz veins (Fig. 105-b) randomly oriented in psammitic schist of an outcrop in the axial zone of the Koboke synform of the Oboke district (Figs. 18 and 104) and clarified strain mode of the Hijikawa-Oboke phase deformation, showing that X and Y are normal to and parallel to the fold axis respectively. Quartz c-axis fabrics in the axial zones of buckle folds of these quartz veins (Fig. 105-b), whose axes (= axis of the Koboke synform) are oriented parallel to Y of bulk strain, had been analyzed by Hara and Paulitsch (1971), clarifying that in the axial zones X is in general oriented normal to their fold axes. The folds of the Hijikawa-Oboke phase are developed as a series of sinistral en echelon arrangement all over the Sambagawa megaunit and overlying and underlying megaunits as, for example, shown in Fig. 14. It would be therefore said that the Hijikawa-Oboke phase folding occurred by sinistral shear under non-uniform compression in a direction normal to the general trend of the Sambagawa megaunit (Fig. 110). In such the context would be explained the northward vergence structures of the Hijikawa-Oboke phase (Figs. 104 and 109), which had been described by Yokota (1969), and Hara *et al.* (1977). Because the attitude of the axis and axial plane of a fold of a layer depends upon the initial attitude of the layer and bulk strain magnitude, of course, the spatial variation in attitude of axes and axial planes of the Hijikawa-Oboke phase folds should be in details analyzed in such a point of view. However, the detailed analysis of the movement and strain pictures of the Hijikawa-Oboke phase folds is not the scope of this paper but given in other paper.

IV. Radiometric Ages of Tectonic Events

Radiometric ages of constituent rocks of the Chichibu megaunit II, Chichibu megaunit I and Sambagawa megaunit, which were developed as accretionary complexes in the southern front of the K-continent during the period from early Jurassic to late Cretaceous age, have recently been measured by many authors. Because the constituent rocks all were metamorphosed during their accretionary

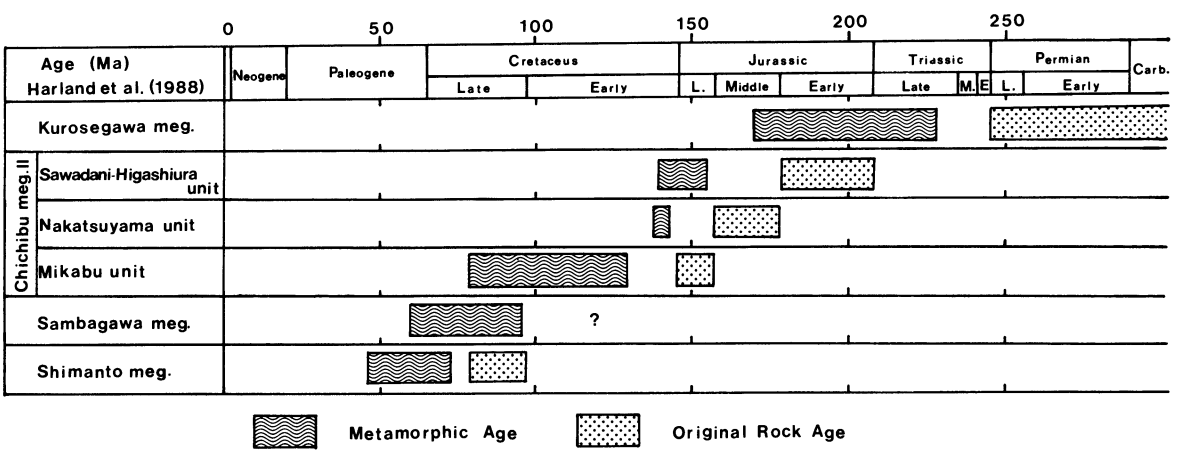

Fig. 111 Age relationship between the original rocks (fossil age) and the metamorphism (radiometric ages) for the Kurosegawa megaunit, Chichibu megaunit, Sambagawa megaunit and Shimanto megaunit in Shikoku based on the data from Maruyama *et al.* (1984), Iwasaki *et al.* (1984), Isozaki (1988), Itaya and Takasugi (1988), Monie *et al.* (1988), Fukui and Itaya (1989), Takasu and Dallemeyr (1989a, b), Takasu (1990), Isozaki and Itaya (1990a, b), Isozaki *et al.* (1990), Suzuki *et al.* (1990a, b), Kawato *et al.* (1990), Tominaga (1990), Kanai *et al.* (1990) and the present authors.

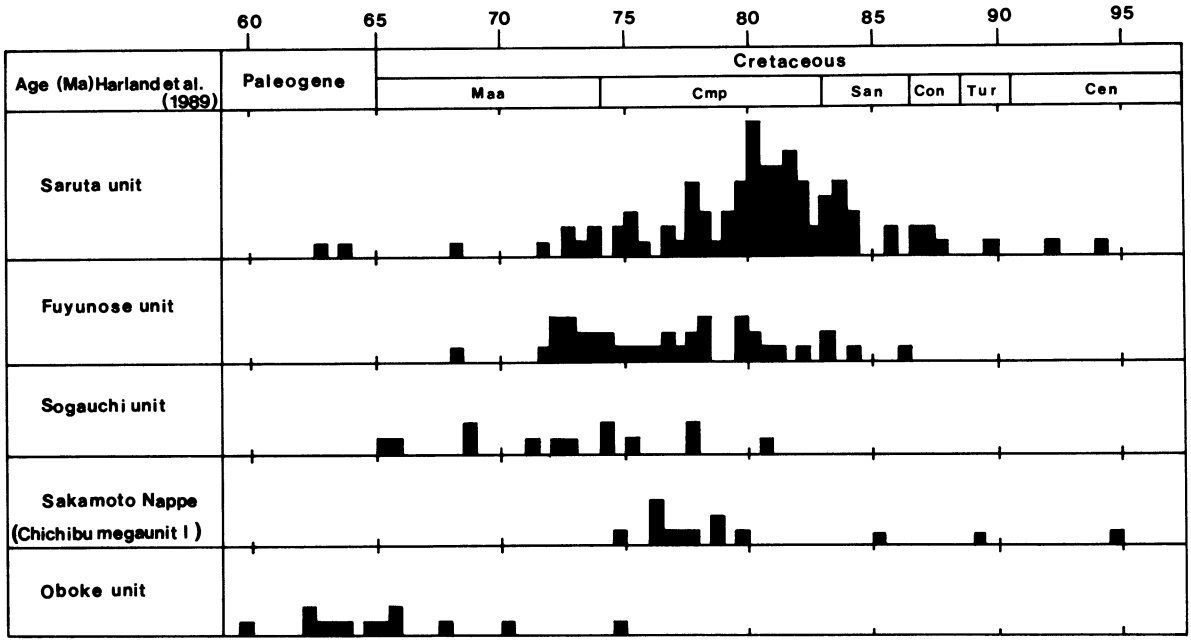

Fig. 112 Frequency distribution of radiometric ages of the Sambagawa megaunit and its underlying schists in central Shikoku based on the data from Monie *et al.* (1988), Itaya and Tkasugi (1988), Tkasu and Dallmeyer (1989a, b), Takasu (1990) and the present authors.

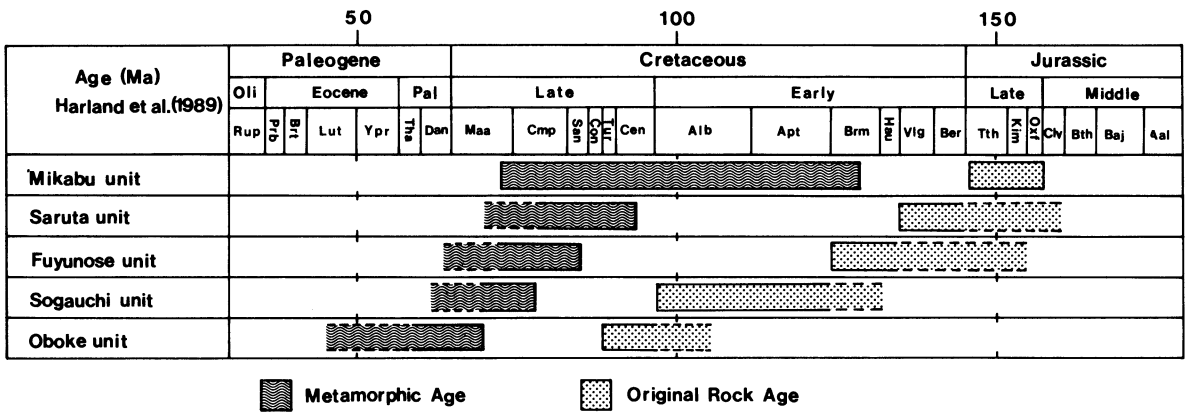

Fig. 113 Assumed age relationship between the original rocks and the metamorphism for the Chichibu megaunit II (Mikabu unit), Sambagawa megaunit and Shimanto megaunit (Oboke unit). For fuller explanation see the text.

processes, their radiometric age data are considered to show ages of the metamorphism. On the basis of their recently reported radiometric age data, therefore, the time relationships of the above-mentioned tectono-metamorphic processes of the Sambagawa megaunit will be examined in this section, following Hara *et al.*'s (1990a, 1991a) preliminary study.

K-Ar ages of muscovite in the late Permian accretionary unit of the Kurosegawa-Koryoke Terrane, which have been given by Isozaki and Itaya (1990a), Suzuki *et al.* (1990a, b) and the present authors (Table 1), range from 233 Ma to 174 Ma. According to Suzuki *et al.*'s (1990b), Kawato *et al.*'s (1990) and Isozaki *et al.*'s (1990) data, K-Ar ages of muscovite in the Sawadani-Higashiura unit as late early Jurassic accretionary unit and in the Nakatsuyama unit as late middle Jurassic accretionary unit range from 165 Ma to 139 Ma and from 143 Ma to 112 Ma respectively. The radiometric ages of muscovite in the Mikabu unit as latest Jurassic accretionary unit, which have been given by Fukui and Itaya (1989), Suzuki *et al.* (1990a), Kawato *et al.* (1990) and the present authors, range 128 Ma to 78 Ma. These of the constituent minerals and rocks of the Sambagawa megaunit in central Shikoku and western Kii Peninsula, which have recently been reported by Itaya and Takasugi (1988), Monie *et al.* (1988), Shibata *et al.* (1988), Takasu and Dallmeyer (1989a, b), Takagi *et al.* (1989), Takasu (1990), Kanai *et al.* (1990), Kurimoto and Shibata (1991) and the present authors (Table 1), range from 94 Ma to 65

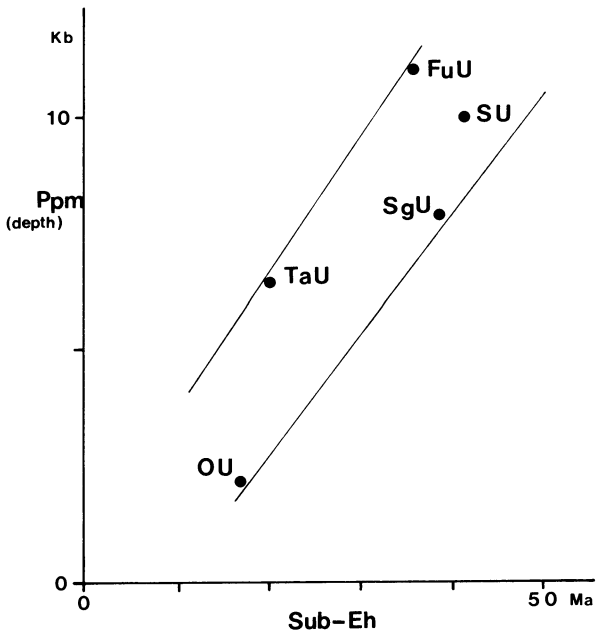

Fig. 114 Diagram illustrating the average subduction velocity of the Sambagawa megaunit and Shimanto megaunit.
Ppm: pressure of peak metamorphism, Sub: Beginning age of subduction (fossil age of original rocks), Eh: beginning age of exhumation (oldest one of radiometric ages), SU: Saruta unit, FU: Fuyunose unit, SgU: Sogauchi unit, OU: Oboke unit, TaU: Tatsuyama unit.

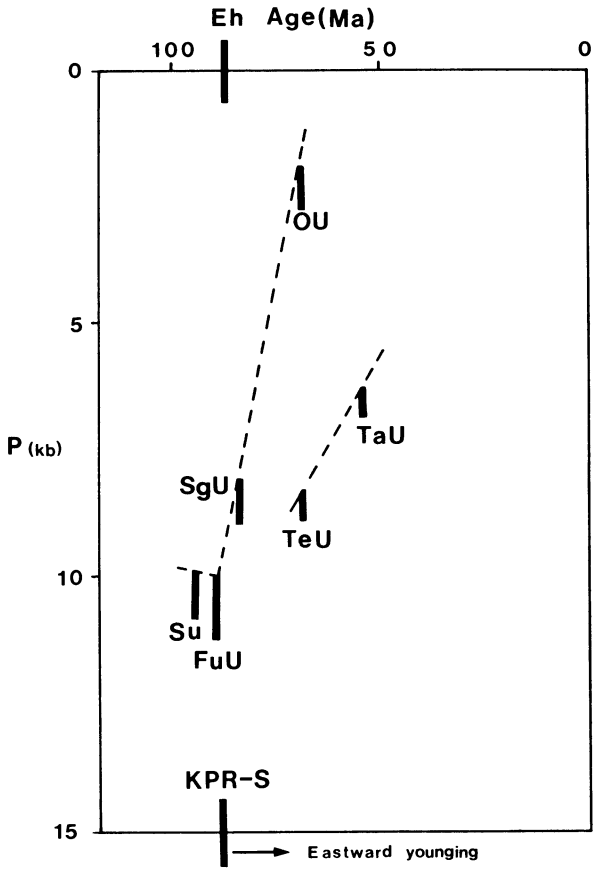

Fig. 115 Diagram illustrating the beginning ages of the exhumation and the pressures of peak metamorphism of the Sambagawa megaunit and Shimanto megaunit, roughly showing the average exhumation velocities of them. Eh Age: beginning age of exhumation (oldest one of radiometric ages), KPR-S: beginning age of the subduction of the Kula-Pacific ridge, SU: Saruta unit, FuU: Fuyunose unit, SgU: Sogauchi unit, OU: Oboke unit, TeU: Tenryu unit, TaU: Tatsuyama unit.

Ma. And in the Shimanto megaunit in central Shikoku and central Kii Peninsula, which is covered by the Sambagawa megaunit and contains the Oboke unit, radiometric ages of its constituent minerals and rocks have been measured by Itaya and Takasugi (1988), Takasu (1990) and Kanai *et al.* (1990, in preparation), showing that these range from 74 Ma to 62 Ma. The above-described data are summarized in Fig. 111, clearly showing a downward younging age polarity as compared for the oldest radiometric age of each unit (or megaunit). It can be said that such the radiometric age data is quite harmonic with the assumed accretionary history for the Chichibu megaunit II, Sambagawa megaunit, Chichibu megaunit I and Shimanto megaunit (Fig. 111).

Radiometric ages of the constituent minerals such as muscovite and hornblende of the Saruta unit, Fuyunose unit and Sogauchi unit of the Sambagawa megaunit in central Shikoku have been recently measured by Itaya and Takasugi (1988), Takasu and Dallmeyer (1989a, b), Takasu (1990) and the present authors (Table 1), giving the result of Fig. 112. Though these show greatly wide range, it is clear that, as compared for the oldest radiometric age of each unit, there is a downward younging age polarity in the Sambagawa megaunit. The variation range shows a downward decreasing. It is the smallest in the Oboke unit as the oldest accretionary unit of the Shimanto megaunit. The wide variation of radiometric age must be ascribed to that metamorphic minerals in individual units recrystallized during the deformations of the phases mentioned in the preceding section, changing their chemical composition as clarified by Hara *et al.* (1984a, 1990a): The chemical composition of muscovite included in the cores and mantles of plagioclase porphyroblasts and that of matrix muscovite in both Saruta unit and Fuyunose unit are different from each other as is obvious in Fig. 69-a and b. These figures indicate that the bedding schistosity- forming muscovite must have recrystallized during the Sb2-1 phase (and further later phase) in many part of the Saruta unit and during the Sb2-2 phase in many part of the Fuyunose unit. The age data for muscovite in many part of the Saruta unit and these in many part of the Fuyunose unit have been therefore assumed by Hara *et al.* (1990a) to be of the Sb2-1 phase and of the Sb2-2 phase respectively. The difference in chemical composition between the Sb2-1 phase muscovite in the Saruta nappes and that (muscovite in plagioclase porphyroblast cores) in the Fuyunose nappe (Fig. 69) would indicate that the former was still under higher-temperature condition than the latter. From Itaya and Takasugi's (1988), Kanai *et al.*'s (1990), Kurimoto and Shibata's (1991) and the present authors data, K-Ar ages of muscovite in the Sogauchi unit, which is just in contact with the uppermost

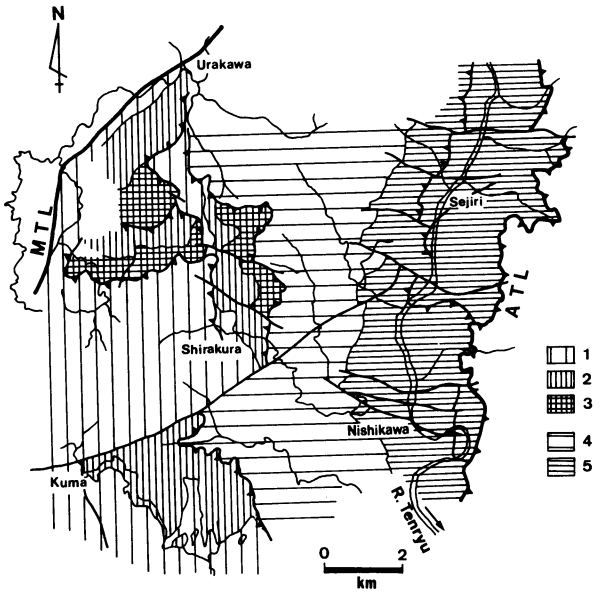

Fig. 116 Geological map of the River Tenryu district, showing the Tenryu nappe comprising four subnappes and the Tatsuyama nappe comprising two subnappes, (Goto, 1987).
1, 2 and 3: chlorite zone, garnet zone and biotite zone in the Tenryu nappe respectively. 4 and 5: chlorite zone and garnet zone in the Tatsuyama nappe. MTL: Median Tectonic Line.

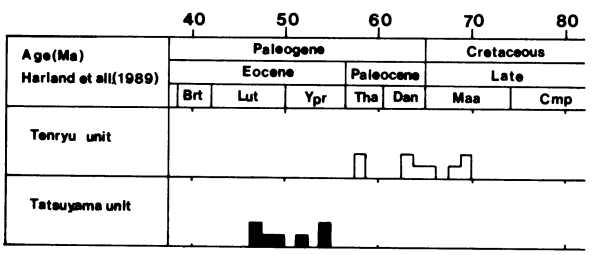

Fig. 117 Frequency distribution of radiometric ages of the Tenryu nappe schists and Tatsuyama nappe schists based on the data of Ueda *et al.* (1977), Watanabe *et al.* (1982), Shibata and Takagi (1988) and Kanai *et al.* (in preparation). Age data for the Tatsuyama nappe schists all are after Kanai et al.

unit of the Shimanto megaunit, are ca. 75-65 Ma, being comparable with these in the latter unit. These data for the Sogauchi unit are for muscovite, which recrystallized during the coupling of this unit with the Oboke unit. Muscovite flakes recrystallized in the axial zones of intrafolial folds of the Oboke nappe (I + II) schists, which are comparable with the Tsuji stage folds in Fig. 101, show radiometric ages of ca. 63 Ma (Fig. 18, Table 1). From the radiometric age data by Itaya and Takasugi (1988), Takasu and Dallmeyer (1989a, b), Takasu (1990) and the present authors, thus, Hara *et al.* (1990a) and the present authors have assumed the radiometric ages of the Spm phase, Sb1 phase, Sb2-1 Phase, Sb2-2 phase, Sb3 phase and Tsuji stage of Ozu phase

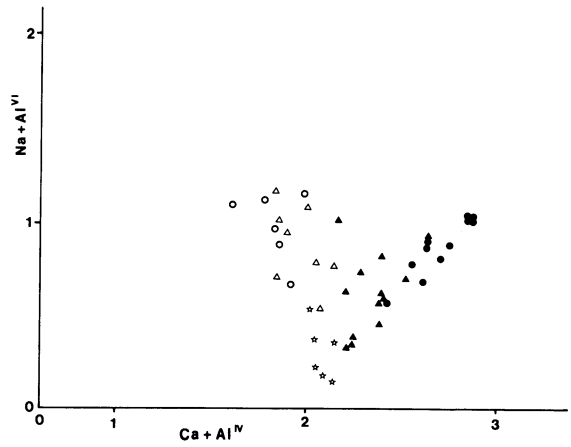

Fig. 118 Diagram showing the composition of amphiboles which crystallized in hematite-bearing basic schists of Tenryu nappe and Tatsuyama nappe [data from Goto (1987)]. open stars, open triangles and open circles : data from the Tenryu nappe [open stars : amphibole crystallized with plagioclase porphyroblast outer mantles, open triangles : amphibole crystallized with plagioclase porphyroblast cores, open circles : amphibole crystallized with plagioclase porphyroblast inner mantles (= highest temperature phase)]. solid triangles and solid circles : data from the Tatsuyama nappe [solid triangles : amphibole crystallized with plagioclase porphyroblast mantles, solid circles : amphibole crystallized with plagioclase porphyroblast cores (= higher temperature phase)].

as shown in Fig. 21.

From Fig. 21 the age of the ending of the highest temperature metamorphism of any unit of the Sambagawa megaunit, except for the Saruta unit, is considered to correspond to the beginning age (Eh age) of the exhumation of the unit. It would be now said that the Eh age of the Fuyunose subunit II is ca. 88 Ma as the beginning age of the Sb2-1 deformation, that of the Sogauchi unit is ca. 85 Ma as the beginning age of the Sb2-2 deformation and that of the Sakamoto unit is ca. 80 Ma as the beginning age of the Sb3 deformation. The oldest one of radiometric ages of the uppermost unit of the Shimanto megaunit would be also regarded as to be comparable with the age of the ending of its highest temperature metamorphism, which must correspond to its Eh age. Following such an assumption, the Eh age for the Oboke unit is ca. 74 Ma. However, the beginning age ("Eh age") of exhumation of the Saruta unit, which was associated with decreasing temperature, is ca. 94 Ma as the beginning age of the Sb1 deformation, which is also just near to the age of the Spm stage (Fig. 21).

The beginning ages (Sub age) of the subduction of constituent units of the Sambagawa megaunit have been assumed in the previous section as follows: The Sub age of the Saruta unit is Valanginian, that of the Fuyunose subunit II is Barremian and that of the Sogauchi unit is Albian. The Sub age of the Oboke unit is Cenomanian-Turonian. From the time interval (Sub-Eh) between the Sub age and the Eh age of any unit (Fig. 113) may be roughly estimated an average subduction velocity of the unit (Fig. 114), as the pressure (Ptm) of its highest temperature phase is de-

termined (Fig. 21). The time path and average velocity of the exhumation for the Saruta unit, Fuyunose unit, Sogauchi unit, Sakamoto unit and Oboke unit may be also roughly assumed on the basis of Fig. 21, as shown in Fig. 115. The average subduction velocity and average exhumation velocity of the Sambagawa megaunit, as roughly estimated on the above-mentioned basis and as 10 kb = 35 km, are 0.9 mm/year and 2.0 mm/year respectively.

Figs. 114 and 115 must be great important data to understand the tectonic conditions such as strain rate of the Sambagawa megaunit. Quartz fabrics may also give important information for such understanding. The pattern variation of quartz c-axis fabrics on the tectono-metamorphic history of the Sambagawa megaunit has been so far analyzed by Hara *et al.* (1989) and Sakakibara *et al.* (1992), clarifying slip systems dominantly acting and further tectonic condition (*e.g.* strain rate) during each deformation phase. The results are reproduced in Fig. 24. As pointed out by some authors (*e.g.* Lister & Price, 1978; Lister & Hobbs, 1980; Price, 1985), quartz appears to be quite easily deformed, missing its c-axis fabrics of the earlier phases of the tectono-metamorphic history. Therefore, the quartz c-axis fabrics of the high-temperature phases of the prograde and retrograde metamorphism have been attempted to understand from quartz grains included in garnet and plagioclase porphyroblasts: The c-axis fabrics of the Sim-Bim phase, Sb1 phase and Sb2-1 phase have been obtained from Sim-forming quartz grains in plagioclase porphyroblasts of pelitic schists, Sb1-forming quartz grains in garnet of basic schist of the Fuyunose subunit II and Sb2-1-forming quartz grains in plagioclase porphyroblasts in pelitic schists of the Fuyunose subunit II, respectively. These of the Sb2-2 phase have been obtained from quartz grains around plagioclase porphyroblasts in siliceous schist of the Fuyunose subunit II. Quartz fabrics of the Hijikawa phase have been analyzed in buckled quartz veins of the axial zone of uplight fold by Hara and Paulitsch (1971). Most of these quartz c-axis fabrics appear to be described in terms of type I crossed girdle and single girdle without high concentration in Y. Quartz grains included in cores of relict garnet of Tonaru metagabbro and of that of quartz eclogite have been assumed to give an available data for understanding tectonic condition of the K-continent along the plate boundary. The data indicate that quartz deformation in the depth part of 15-17 kb in the subduction zone occurred in dominant prism slip. Further details of fabric data mentioned above are given by Sakakibara *et al.* (1992).

The data of quartz c-axis fabrics produced under other tectonic conditions can be also referred from the Ryoke metamorphic belt of Japan (Hara, 1962; Hara *et al.*, 1973; Sakakibara *et al.*, 1989; Okudaira, 1992), the Variscan shear zone of Southwest Iberian Peninsula (Burg *et al.*, 1981) and the shear zones of Central Massif (Mainprice & Bouchez, 1987). As compared with these data, it can be pointed out that rhomb [a] and basal [a] were active as dominant slip systems under higher temperature in the Sambagawa megaunit (= high P/T type metamorphic belt = subduction zone) than in the low P/T type and intermediate P/T type metamorphic belts (= magma arc). Following Hobbs (1985), thus, Sakakibara *et al.* (1992) said that strain rate [and/or (OH) content] of quartz was higher (and/or lower) in the subduction zone related to the formation of the Sambagawa megaunit than in the low P/T type and intermediate P/T type metamorphic belts such as magma arcs.

Radiometric ages of the Sambagawa megaunit schists in central Japan, which just underlie the Mikabu unit of the Chichibu megaunit II, appear to indicate that these are divided into two units, Tenryu unit (West unit) and Tatsuyama unit (East unit) in descending order (Kanai *et al.* in preparation), though the Tenryu unit consists of four nappes and the Tatsuyama unit of two nappes as shown by Hara *et al.* (1977), Goto and Hara (1985) and Goto (1986) (Fig. 116). The radiometric age data for the Tenryu unit and Tatsuyama unit are reproduced in Fig. 117 from Kanai *et al.* (in preparation), indicating a downward younging age polarity. These for the Tenryu unit, which range from 70.0 Ma to 57.8 Ma, appear to be comparable with these for the Oboke unit and its equivalent in Kii Peninsula (= uppermost unit of the Shimanto megaunit), though the oldest one is younger by ca. 5 Ma for the former than for the latter. The radiometric ages of the Tatsuyama unit schists range from 54.6 Ma to 41.5 Ma. The Tatsuyama unit is therefore considered to be the second subduction unit of the Shimanto megaunit. According to Kurimoto and Shibata's (1991) and Kanai *et al.'s* (1990) data, accretionary complex in Kii Peninsula, which follows Cenomanian-Turonian one, is considered to be the Hanazono Formation which is of Coniacian - Campanian age. Thus, it may be here roughly assumed that the Sub age of the Tatsuyama unit is Coniacian - Campanian.

Radiometric ages of the schists (garnet zone and biotite zone) in the Kanto Mountains, which just underlie the Mikabu unit (chlorite zone ocks), appear to be comparable with these of the Oboke unit and Tenryu unit, according to Hirajima *et al.'s* (1992) data. It may be therefore said that in central Japan and the Kanto Mountains are not found exhumation units which are correlated with the Saruta unit, Fuyunose unit and Sogauchi unit developed in Kyushu, Shikoku and Kii Peninsula, showing an eastward younging age polarity of them.

According to Goto's (1986) data for the growth history of amphibole in hematite-bearing basic schists, the prograde growth history and the retrograde growth history of amphibole in the Tenryu unit are actinolite - winchite - barroisite and barroisite - actinolite respectively, while in the Tatsuyama unit the prograde growth history of amphibole is actinolite - magnesio-hornblende (Fig. 118). Thus, the P-T condition of the metamorphism of the Tenryu unit and that of the Tatsuyama unit would be illustrated as drawn in Fig. 30. Because the Tenryu unit schists were produced under higher pressure condition than the Oboke unit schists (Fig. 62), the oldest one of radiometric ages may be a little younger in the former than in the latter.

From the data of the metamorphism of the Tatsuyama unit schists it may be said that the thermal gradient along the plate boundary was greater during the highest-temperature phase for the Coniacian-Campanian accretionary complexes (Tpm TG line in Fig. 62) than for the Fuyunose unit (Barremian accretionary complex) (Fpm TG line in Fig. 58). Goto (1986) described that in increase of metamorphic grade garnet and biotite simultaneously appear in the Tatsuyama unit schists, though the appearance of biotite is rarely, unlike the cases of the Sambagawa schists of Shikoku and Kii Peninsula and the Tenryu unit schists (Fig. 30). The Tpm TG line gives a thermal gradient of 30 C/km. It would be therefore said that the metamorphic condition of the Tatsuyama unit schists is clearly different from but near that of medium P/T type metamorphism (cf.

Miyashiro, 1973).

Kiminami *et al.* (1990) have said that the intrusion of MORB type basalt in the Shimanto megaunit which occurred together with sedimentation of its constituents, corresponds in time to the beginning of subduction of the Kula-Pacific ridge and the subduction began at ca. 85 Ma in Kyushu, showing eastward younging age polarity. This age is comparable with that of the beginning of the Sb2-1 deformation (Fig. 115). In the subduction zone which was responsible for the formation of the Sambagawa megaunit, the great exhumation of subducted sediments in Shikoku had not occurred until ca. 88 Ma (Fig. 115). The assumed difference in thermal gradient along the plate boundary between the highest-temperature phase of the Fuyunose unit (Fpm TG line in Fig. 67) and that of the Tatsuyama unit (Tpm TG line in Fig. 67) would be ascribed to the subduction of the Kula-Pacific ridge. As mentioned in the preceding page radiometric ages of the exhumation units, which postdate the Mikabu unit, clearly show a eastward younging polarity. Namely, the exhumation of the Saruta unit, Fuyunose unit and Sogauchi unit did not occur in central Japan and the Kanto Mountains. Such a phenomenon may be also ascribed to the eastward younging of the subduction age of the Kula-Pacific Ridge. The exhumation of the Tatsuyama nappe may be a component of the deformation of the Ozu phase, when the Kula-Pacific ridge reached the greater depth of the subduction zone.

In pelitic schists of the Tenryu unit are found garnet in the winchite zone and barroisite zone and brown biotite in the barroisite zone, while in these of the Tatsuyama unit are garnet and green biotite in the hornblende zone (Goto, 1986). The growth history of amphibole, which was in paragenetic relation with garnet in hematite-bearing basic schist of the Saruta unit, is crossite - (winchite-barroisite) - hornblende (Fig. 45). While garnet is generally absent in crossite zone of the Sogauchi unit. On the basis of the above-mentioned data, the occurrence field of garnet and biotite in the Sambagawa schists and associated schists may be roughly explained by Fig. 30.

V. Tectonic Framework and Tectonics

The Sambagawa schists as early Cretaceous accretionary complexes, as well as Jurassic accretionary complexes, were produced in the subduction zone developed in the southern front of the Kurosegawa-Koryoke Terrane. The thermal gradient along the plate boundary of this subduction zone was of high P/T type during the period of the subduction of the original rocks of Saruta nappe schists, Fuyunose nappe schists and Sogauchi nappe schists, except for during the period when the overthrusting of the K-continent occurred along that (Figs. 61 and 62). Relict fragments of the Kurosegawa-Koryoke Terrane (Takeda *et al.*, 1987, 1992; Ohtomo and Kagami, 1990; Hayama, 1991) indicate that Jurassic - early Cretaceous magmatism and high-temperature type metamorphism occurred on this terrane. The juxtaposition of the IA supermegaunit and the K-continent occurred during early Cretaceous age, giving rise to early Cretaceous magmatism and further later ages magmatism on the latter and also the former, which correspond to the formation of the Ryoke belt,(Hara *et al.*, 1991a). The juxtaposition event induced the overthrusting of the K-continent onto the Saruta nappe schists, just at this moment giving rise to thermal gradient of intermediate high P/T type along the plate boundary.

The granite intrusion in the Ryoke belt, which occurred after the juxtaposition of the IA supermegaunit and the K-continent, is mainly divided into two phases, older phase and younger phase. The older phase intrusion is of sheet type of large-scale, while the younger phase intrusion appears to be mainly of stock type (Hara *et al.*, 1980b, 1991a). After the intrusion of older granite sheets, many flat-lying thrust sheets consisting of granites and associated high-temperature metamorphic rocks , which show westward-southwestward displacement, were produced in the Ryoke belt [in the Asaji district after Hayasaka *et al.* (1989), in the Iwakuni-Yanai district after Okudaira (1992), in the Kayumi district after Sakakibara *et al.* (1989, 1990) and in the Wada - Sakuma district after Ohtomo (1991)]. The southern part of these thrust sheets appears to have been emplaced on lower-grade metamorphic and non-metamorphic rocks of the southern margin of the Ryoke belt (Ohtomo, 1989; Sakakibara *et al.*, 1989, 1990). The younger phase granites intruded after the formation of the thrust sheets (Sakakibara *et al.*, 1989; Hara *et al.*, 1991a). In the northern part of Shikoku and the western part (Sennan) of Kii Peninsula are found the younger phase granite bodies intruding non-metamorphic rocks. This fact may mean that the southern front of granite intrusion in the Ryoke belt migrated toward the south during the younger phase. Most of younger phase granites appear to be younger than 85 Ma, showing an eastward younging age polarity (cf. Ohtomo, 1992). Kiminami *et al.* (1990) have clarified that the subduction of the Kula-Pacific ridge in Kyushu and Shikoku began at ca. 85-80 Ma, showing an eastward younging polarity of its subduction age. Thus, it may be assumed that the tectonics related to the formation of many thrust sheets in the Ryoke belt and the intrusion of younger phase granites with eastward migration of their intrusion front are ascribed to the subduction of the Kula-Pacific ridge. This assumption is quite harmonic with the metamorphic condition of the Tatsuyama unit schists (Fig. 62), which shows that the thermal gradient along the plate boundary became nearly of medium P/T type owing to the subduction of the Kula-Pacific ridge.

As schematically shown in Fig. 62, the thermal structure in the arc-trench system (IA supermegaunit - Kurosegawa-Koryoke Terrane - OA supermegaunit) must have been quite different between the period before and that during the subduction of the Kula-Pacific ridge. During the latter period occurred nearly medium P/T type metamorphism in subducted sediments (Tatsuyama unit schists). This fact suggests also such a possibility that during the period of the subduction of the Kula-Pacific ridge magmatism occurred even in the OA supermegaunit as accretionary wedge. High temperature type metamorphic rocks of ca. 50 Ma in the Kanto Mountains (Tokuda and Seo, 1985) may be evidence of such type magmatism.

After the intrusion of the younger phase granites the Ryoke rocks, together with the Kurosegawa-Koryoke Terrane rocks, were transported as many nappes onto the OA supermegaunit, forming their cataclastic rocks (Ohtomo, 1989, 1990; Hara *et al.*, 1990a; Takeda *et al.*, 1992). According to Ohtomo and Kagami's (1990) data, the deformation related to the formation of the cataclastic rocks appears to have occurred at ca. 62 Ma. As correlated with the deformation history of the OA supermegaunit, this tec-

tonics is of the later stage of Ozu phase, when the Chichibu megaunit II were emplaced onto the Sambagawa schists. It may be therefore said that the later stage of Ozu phase is ca. 62 Ma.

Movement pictures and deformation styles of the Sambagawa schists and surrounding rocks during the late Mesozoic tectonics mentioned above will be in details described and discussed in the other paper.

References

Aiba, K., 1982: Sanbagawa metamorphism of the Nakatsu-Nanokawa district, the northern subbelt of the Chichibu belt in western central Shikoku. *Jour. Geol. Soc. Japan*, **88**, 875–885.*

Assoc. of Earth Scientist of Toyo, 1980: Geological map of the Saijo-Niihama district; 1:50,000. Tomoeya (Matsuyama).**

Banno, S. and Chii, S., 1976: Origin of zonal structure in garnets. *Jour. Japan. Assoc. Min. Petrol. Econ. Geol., Spec. Issue*, no. 1, 283–299.**

Banno, S. and Sakai, C., 1989: Geology and metamorphic evolution of the Sambagawa metamorphic belt, Japan. *In* Daly, J.S., Cliff, R.A. and Yardley, B.W.D. eds., *Evolution of Metamorphic Belts, Geol. Soc. Spec. Pub.*, no. 43, 519–532.

Burg, J. P., Igresias, M., Laurent, Ph., Matte, Ph. and Riberio, A., 1981: Variscan intracontinental deformation: The Coimbra-Cordoba shear zone (SW Iberian Peninsula). *Tectonophysics*, **78**, 161–177.

Cloos, M. and Sherve, R. L., 1988: Subduction-Channel model of prism accretion, melange formation, sediment subduction, and subduction erosion at convergent plate margins: 2. Implications and discussion. PAGEOPH, *In* Ruff, L.J. and Kanamori, H. eds., *Subduction zones*, **128**, 501–546.

Enami, M., 1983: Petrology of pelitic schists in the oligoclase-biotite zone of the Sanbagawa metamorphic terrain, Japan: phase equilibria in the highest grade zone of a high-pressure intermediate type of metamorphic belt. *Jour. Metamorphic Geol.*, **1**, 141–161.

Faure, M., 1983: Eastward ductile shear during the early tectonic phase in the Sanbagawa belt. *Jour. Geol. Soc. Japan*, **89**, 319–329.

Faure, M., 1985: Microtectonic evidence for eastward ductile shear in the Jurassic orogen of SW Japan. *Jour. Struc. Geol.*, **7**, 175–186.

Fukui, S. and Itaya, T., 1989: Muscovite K-Ar ages of the pelitic schists from the Sambagawa Southern Marginal belt. Japan. *Assoc. Min. Pet. Econ. Geol.*, **84**, 132.**

Gorai, M., 1951: Petrological studies on plagioclase twins. *Am. Mineralogist*, **36**, 884–901.

Goto, M., 1987: Metamorphism and tectonism of the Sambagawa metamorphic belt, Central Japan. *Abst. 41st Ann. Meet. Assoc. Geol. Collab. Japan*. 225–230.**

Goto, M. and Hara, I., 1985: Metamorphism of the Sambagawa belt in the Tenryu district, Shizuoka Prefecture. *Abst. 92nd Ann. Meet. Geol. Soc. Japan*, 392.**

Hada, S. and Suzuki, T., 1983: Tectonic environments and crustal section of the Outer Zone of Southwest Japan. *In* Hashimoto, M. and Uyeda, S. eds., *Accretion Tectonics in the Circum-Pacific Regions*, 207–218. TERRAPUB, Tokyo.

Hada, S. and Kurimoto, C., 1990: Northern Chichibu Terrane. *In* Ichikawa, K. *et al.* eds., *Pre-Cretaceous Terranes of Japan, Publication of IGCP Project, 224*, 165–184.

Hara, I., 1962: Studies on the structure of the Ryoke metamorphic rocks of the Kasagi district, Southwest Japan. *Jour. Sci. Hiroshima Univ., Ser. C.* **4**, 163–224.

Hara, I. and Goto, M., 1986: Analysis of uplifting processes of Sambagawa metamorphic rocks. *In Prof. N. Kitamura Mem. Vol.*, Tohoku Univ., pp. 81–89.*

Hara, I., and Paulitsch, P. 1971: c-axis fabrics of quartz in buckled quartz veins. *N. Jb. Miner. Abh.*, **115**, 31–53.

Hara, I., Nishiyama, Y. and Isai(Shiota), T., 1966: On the difference in deformation behaviour between phenocryst and ground-mass quartz of deformed rhyolite pebbles in the Oboke conglomerate schist. *Jour. Sci. Hiroshima Univ., Ser. C*, **5**, 179–216.

Hara, I., Uchibayashi, S., Yokota, Y., Umemura, H. and Oda, M., 1968: Geometry and internal structures of flexural folds (1). Folding of a single competent layer enclosed in thick incompetent layer. *Jour. Sci. Hiroshima Univ., Ser. C*, **6**, 51–113.

Hara , I., Fujii, S., Nishimura, Y., Shiota, T. and Moriyama, K., 1973: Preferred shape orientation of pebbles in the Oboke conglomerate schists. *In Prof. Y. Umegaki, Mem. Vol., Hiroshima Univ.*, 103–111.**

Hara, I., Hide, K., Takeda, K., Tsukuda, E. Tokuda, M. and Shiota, T., 1977: Tectonic movement in the Sambagawa belt. *In* Hide, K. *ed., The Sambagawa Belt*, pp. 309–390. Hiroshima Univ. Press, Hiroshima.*

Hara, I., Hide, K., Tokuda, M., Takagi, K. and Shiota, T., 1980a: The relationship between tectonism and metamorphism in the Sambagawa belt in central Shikoku (preliminary report). *Studies on Late Mesozoic Tectonism in Japan*, no. 2, 1–14.**

Hara, I., Syoji, K., Sakurai, Y., Yokoyama, S. and Hide, K., 1980b: Origin of the Median Tectonic Line and its initial shape. *Mem. Geol. Soc. Japan*, no. 18, 27–49.

Hara, I., Shiota, T., Maeda, M. and Miyaoka, H., 1983: Deformation and recrystallization of amphiboles in Sambagawa schist with special reference to history of Sambagawa metamorphism. *Jour. Sci. Hiroshima Univ., Ser. C*, **8**, 135–147.

Hara, I., Miyaoka, H., Seo, T., Maeda, M., Shiota, T. and Hide, K., 1984a: Microtexture analysis for metamorphic facies analysis. *Journal of the Tectonic Research Group in Japan*, no. 30, 41–54.*

Hara, I., Shiota, T. and Hide, K., 1984b: Pressure solution of plagioclase and garnet during Nagahama folding in the Sambagawa belt of central Shikoku. *Jour. Geol. Soc. Japan*, **90**, 33–42.

Hara, I., Hayasaka, Y. and Miyamoto, T., 1985: Pile nappe structure and tectonics of the Sangun-Chugoku belt. *Abst. 92nd Ann. Meet. Geol. Soc. Japan*, 20–21.**

Hara, I., Suzuki, M. and Kakuda, K., 1986a: Structural relationship between the Hida and Sangun belt. *High pressure metamorphic belt of Inner zone of Southwest Japan*, no. 3, 41–43.**

Hara, I., Shiota, T., Nakamura, T. and Saito, T., 1986b: Analysis of uplifting of Sambagawa belt based on quartz microtextures. *News of Osaka Micropaleontology, Special Volume*, **7**, 197–201.*

Hara, I., Takeda, K., Shiota, T., Tominaga, R., Goto, M. and Hide, K., 1987: Tectonics of the Sambagawa Terrane. *Abst. 94th Ann. Meet. Geol. Soc. Japan*, 70–71.**

Hara, I., Shiota, T., Takeda, K. and Hide, K., 1988: Tectonics of the Sambagawa Terrane. *Earth, Monthly*, **10**, 372–378.**

Hara, I., Shiota, T., Takeda, K., Okamoto, K., Kanai, K. and Hide, K., 1989: Subduction zone tectonics inferred from tectono-metamorphic processes of the Sambagawa schists. *DELP Publication* no. 28, 73-82.

Hara, I., Shiota, T., Takeda, K. Okamoto, K. and Hide, K., 1990a: The Sambagawa Terrane. *In* Ichikawa, K. *et al.* eds.,

Pre-Cretaceous Terranes of Japan, Publication of IGCP, 224, 137–163.

Hara, I., Shiota, T., Hide, K., Okamoto, K., Takeda, K., Hayasaka, Y. and Sakurai, Y., 1990b: Nappe structure of the Sambagawa belt. *Jour. Metamorphic Geol.*, **8**, 441–456.

Hara, I., Shiota, T., Hide, K., Okamoto, K., Takeda, K., Hayasaka, Y. and Sakurai, Y., 1990c: P-T-t-D path of Sambagawa metamorphic rocks in central Shikoku. *Earth, Monthly*, **12**, 419–424.**

Hara, I., Sakurai, Y., Okudaira, T., Hayasaka, Y., Ohtomo, Y. and Sakakibara, N., 1991a: Tectonics of the Ryoke belt. *Excursion Guidebook, 98th Ann. Meet. Geol. Soc. Japan*, 1–20.**

Hara, I., Shiota, T., Takeda, K., Kanai, K., Okamoto, K., Sakurai, Y., Ohtomo, Y., Sakakibara, N., Okudaira, T., Hayasaka, Y. and Hide, K., 1991b: Tectonics of Southwest Japan as inferred from structural development of the Ryoke and Sambagawa belts. *Abst. 98th Ann. Meet. Geol. Soc. Japan*, 22–23.**

Hayama, Y., 1991: The restoration of the Paleo-Ryoke land. *Jour. Geol. Soc. Japan*, **97**, 475–491.*

Hayama, Y., Shibata, K. and Utsumi, S., 1990: K-Ar age of the rocks from the northern margin of the Kanto Mountains. *Jour. Geol. Soc. Japan*, **96**, 319–322.**

Hayasaka, Y., Hara, I. and Yoshigai, T., 1989: Nappe structure of the Asaji metamorphic rocks, with special reference to geological structure of the basement complexes in Kyushu. *Mem. Geol. Soc. Japan*, no. 33, 177–186.*

Hayase, I. and Ishizaka, K., 1967: Rb-Sr dating on the rocks in Japan; (I) South Western Japan, *Jour. Min. Pet. Econ. Geol.*, **58**, 201–212.

Hide, K., 1961: Geologic structure and metamorphism of the Sambagawa crystalline schists of the Besshi-Shirataki mining district in Shikoku, Southwest Japan. *Geol. Rept. Hiroshima Univ.* no. 9, 1–87.*

Hide, K., 1972: Significance of the finding of two recumbent folds in the Sambagawa metamorphic belt of the Nagahama-Ozu district, west Shikoku - Re-examination of the Besshi recumbent fold (1) -. *Mem. Fac. General Educ., Hiroshima Univ.*, III, **5**, 35–51.*

Hide, K., Hara, I., Shiota, T. and Kajitani, H., 1985: On the spotted schists of the Sambagawa belt near Sakuragi bending, Shikoku, with special reference to their continuity and correlation. *Abst. 92nd Ann. Meet. Geol. Soc. Japan*, 378.**

Higashino, T., 1975. Biotite zone of Sanbagawa metamorphic terrain in the Siragayama area, central Shikoku, Japan. *Jour. Geol. Soc. Japan*, **81**, 653–670.*

Higashino, T., 1990. Metamorphic zones of the Sambagawa metamorphic belt in central Shikoku Japan. *Jour. Geol. Soc. Japan*, **96**, 703–718.

Hirajima, T., 1984: The greenrock melange in the Yorii area, in the northeastern part of the Kanto Mountains. *Jour. Geol. Soc. Japan*, **90**, 629–642.

Hirajima, T., Isono. T. and Itaya, T., 1992: K-Ar age and chemistry of white mica in the Sanbagawa metamorphic rocks in the Kanto Mountains, central Japan. *Jour. Geol. Soc. Japan*, **98**, 445–455.*

Hobbs, B. E. 1985: The geological significance of microfabric analysis. *In* Wenk, H.-R. ed., *Preferred orientation in deformed materials and rocks.* Academic press Inc., 463–479.

Ichikawa, K., 1990: Pre-Cretaceous Terranes of Japan. *In* Ichikawa *et al.* eds. *Pre-Cretaceous Terranes of Japan*, 1–11.

Ikeda, Y., 1972: Study of large-scale folding. *Master Th. (MS), Hiroshima Univ.*

Ishida, K., 1985: Pre-Cretaceous sediments in the southern North Zone of the Chichibu belt in Tokushima Prefecture, Shikoku. *Jour. Geol. Soc. Japan*, **91**, 553–567.

Isozaki, Y., 1986: The Shingai Formation in the northern Chichibu belt, Southwest Japan, and the end-Permian convergent zone along the northern margin of the Kurosegawa landmass. *Jour. Geol. Soc. Japan*, **92**, 497–516.*

Isozaki, Y., 1988: Sanbagawa metamorphism and its relation with the development of Sanbosan-Shimanto belt. *Earth, Monthly*, **10**, 367–371.**

Isozaki, Y. and Itaya, T., 1990a: K-Ar ages of weakly metamorphosed rocks at the northern margin of Kurosegawa Terrane in central Shikoku and western Kii Peninsula - extent of the Kurosegawa Terrane in Southwest Japan -. *Jour. Geol. Soc. Japan*, **96**, 623–639.*

Isozaki, Y. and Itaya, T., 1990b: Chronology of Sambagawa metamorphism. *Jour. Metamorphic Geol.*, **8**, 401–411.

Isozaki, Y., Itaya, T. and Kawato, K., 1990: Metamorphic age of Jurassic accretionary complex in the northern Chichibu belt, Southwest Japan. *Jour. geol. Soc. Japan*, **96**, 557–560.**

Isozaki, Y., Maruyama, S. and Itaya, T., 1991: Structure of the Southwest Japan Cordillera. *Abst. 98th Ann. Meet. Geol. Soc. Japan*, 14.**

Itaya, T. and Takasugi, H., 1988: Muscovite K-Ar ages of the Sanbagawa schists, Japan and argon depletion during cooling and deformation. *Contri. Min. Pet.*, **100**, 281–290.

Iwahashi, T., 1960: Anticlinal structure in the central part of Sambagawa matamprphic zone in Wakayama Prefecture. *Bull., Liberal Arts College, Wakayama Univ.*, no. 10, 151–157.*

Iwahashi, T., 1962: Geological structure of the spotted crystalline schist zone on the southern side of the Kinokawa (a preliminary report). *Bull., Liberal Arts College, Wakayama Univ.*, no. 12, 53–60.*

Iwasaki, M., Ichikawa, K., Yao, A. and Faure, M., 1984: Age of greenstone conglomerate in the Mikabu greenstones of eastern Shikoku. *Abst. Joint Meet. Kansai Division* (no. 97) and *Nishinihon Division* (no. 81), *Geol. Soc. Japan*, 21.**

Kagami, H., Tainosyo, Y., Iizumi, S. and Hayama, Y., 1987: Rb/Sr and Sm/Nd ages of Ryoke gabbroic rocks from Kajishima. *Abst. 94th Ann. Meet. Geol. Soc. Japan*, 458.**

Kaikiri, K., Hara, I., Shiota, T., Okamoto, K. and Hide, K., 1991: Strain picture variation in folding history of the Sambagawa belt, central Shikoku. *Abst. 98th Ann. Meet. Geol. Soc. Japan*, 442.**

Kamiyama, T., Kojima, G., Iwahashi, T., Hide, K., Yoshida, H., Nakamura, T., Fukumoto, H., Yonebayashi, S., Hamajima, I., Kamura, Y., Okubo, Y., Yui, S., Kanehira, K., Nureki, T., Kanda, S., Miura, F., Nakagawa, M. and Oyagi, N., 1964: Geology and situation of ore deposits in the region of the Iimori mine. Collaborative studies on geology and ore deposits of the region of the Iimori mine, no. 1. *Mining Geology*, **14**, 336-349.*

Kanai, K., Hara, I., Tanino, K., Shiota, T., Hide, K., Hayasaka, Y. and Okamoto, K., 1990: Age problem of the Sambagawa metamorphic rocks. *Abst. 97th Ann. Meet. Geol. Soc. Japan*, 468.**

Karakida, Y., Yamamoto, H., Miyachi, S., Oshima, T. and Inoue, T., 1969: Characteristics and geological situations of metamorphic rocks in Kyushu. *Mem. Geol. Soc. Japan*, no. 4, 3–20.*

Kawato, K., Isozaki, Y. and Itaya, T., 1990: Tectonic boundary between the Sanbagawa metamorphic rocks and the Jurassic complex of Northern Chichibu belt in central Shikoku, Southwest Japan. *Abst. 97th Ann. Meet. Geol. Soc. Japan*, 159.**

Kiminami, K., Miyashita, S. and Kawabata, K., 1990: Migration of the Kula-Pacific Ridge along the Japan margin: its ge-

ologic significance. *Earth, Monthly*, **12**, 507–515.**

Kojima, G., 1958: Formation of the Sambagawa belt. *Geol. Rep. Hokkaido*, **36**, 24–34.

Kojima, G. and Suzuki, T., 1958: Rock structure and quartz fabric in a thrusting shear zone: the Kiyomizu Tectonic Zone. *Jour. Sci. Hiroshima Univ., Ser. C*, **2**, 173–193.

Kojima, G. and Hide. K. 1958a : Kinematic interpretation of the quartz fabric of triclinic tectonites from Besshi, central Shikoku, Japan. *Jour. Sci. Hiroshima Univ. Ser. C.* **2**, 195–226.

Komatsu, M., Ujihara, M. and Chihara, K., 1985: Pre-Tertiary basement structure in the Inner zone of Honshu and the North Fossa Magna region. *Contri. Dept. Geol. Miner. Niigata Univ.*, **5**, 133–148.

Kunugiza, K., 1980: Dunite and serpentinite in the Sanbagawa metamorphic belt, central Shikoku and Kii Peninsula, Japan. *Jour. Japan Assoc. Min., Petr. Econ. Geol.*, **75**, 14–20.

Kunugiza, K., Takasu, A. and Banno, S., 1986: The origin and metamorphic history of the ultramafic and metagabbro bodies in the Sambagawa metamorphic belt. *Geol. Soc. Amer. Mem.*, **164**, 375–385.

Kurata, H. and Banno, S., 1974: Low-grade progressive metamorphism of pelitic schists of the Sazare area, Sanbagawa metamorphic terrain in central Shikoku. *Jour. Petrology*. **15**, 361–382.

Kurimoto, C., 1991: K-Ar ages of pelitic rocks of Sambagawa, Chichibu and Shimanto terranes in the western Kii Peninsula, Southwest Japan. *Abst. 98th Ann. Meet. Geol. Soc. Japan*, 153.**

Lister, G. S. and Hobbs, B. E. 1980: The simulation of fabric development during plastic deformation and its application to quartzite: the influence of deformation history. *Jour. Struc. Geol.*, **2**, 355–370.

Lister, G. S. and Price, G. P. 1978: Fabric development in quartz-feldspar mylonite. *Tectonophysics*, **49**, 37–78.

Lister, G. S. and Snoke, A. W., 1984: S-C mylonite. *Jour. Struc. Geol.*, **6**, 617–638.

Maeda, M. and Hara, I., 1983: Growth condition of plagioclase porphyroblasts in Sambagawa schists from central Shikoku, Japan. *Jour. Sci. Hiroshima Univ., Ser. C*, **8**, 131–134.

Maeda, M. and Hara, I., 1984: Pre-Nagahama fold in the Sambagawa belt of the Sarutagawa district, central Shikoku. *Jour. Geol. Soc. Japan*, **90**, 73–80.*

Mainprice, D. H. and Bouchez, J.-L. 1987: Characterization of slip systems in naturally deformed quartz by microstructural, goniometry and transmission electron microscopy studies: Application to simple fabric types as a function of temperature. *In Conference Report: Crystallographic fabrics and deformation histories (reported by R. D. Law), Jour. geol. soc. London*, **144**, 677 (abstract).

Makisaka, S., Takeda, K., Tokuda, M., Tominaga, R. and Hara, I., 1982: Geologic structure and metamorphic facies of the "Mikabu zone" in the Yawatahama City area, Shikoku. *Abst. 89th Ann. Meet. Geol. Soc. Japan*, 450.**

Maruyama, S., Banno, S., Matsuda, T. and Nakajima, T., 1984: Kurosegawa zone and its bearing on the development of the Japanese Islands. *Tectonophysics*, **110**, 47–60.

Matsuoka, A. and Yao, A., 1990: Southern Chichibu Terrane. *In* Ichikawa, K. *et al.*, eds., *Pre-Cretaceous Terranes of Japan, Publication of IGCP Project*, **224**, 203–216.

Miyamoto, T., 1990: Discovery of Early Jurassic radiolarians from the Shimodake Formation, Kumamoto Prefecture, and its significance. *In Prof. A. Soeda, Mem. vol., Hiroshima Univ.*, 169-174.**

Miyamoto, T., Kuwazuru, J., Nomoto, T., Yamada, H., Tominaga, R. and Hase, A., 1985: Discovery of Late Permian radiolarians from the Kakisako and Kuma Formations in the Futae district, Izumi-mura, Yatsushiro County, Kumamoto Prefecture, Kyushu. *Earth Science (Chikyu Kagaku)*, **39**, 78–84.**

Miyamoto, T., Futami, K., Yamada, H., Kuwazuru, J. and Tominaga, R., 1989: Terrigenous clastic sequence and olistostromal sequence in the middle subbelt of the Chichibu Belt, Western Kyushu, Japan. *Abst. 96th Ann. Meet. Geol. Soc. Japan*, 115.

Miyashiro, A., 1973: *Metamorphic Rocks and Metamorphic Belts*, Allen and Sons, London, 492pp.

MMEAJ (Metallic Minerals Exploration Agency of Japan), 1967: *Regional geological survey report 1966, Mt. Shiraga-yama district.* Ministry of International Trade and Industry. (MITI).

MMEAJ, 1968: *Detailed geological survey report 1966, Mt. Shiraga-yama district.* MMEAJ.**

MMEAJ, 1969: *Detailed geological survey report 1967, Mt. Shiraga-yama district.* MMEAJ.**

MMEAJ, 1970: *Detailed geological survey report 1968, Mt. Shiraga-yama district.* MMEAJ.**

MMEAJ, 1971a: *Detailed geological survey report 1969, Mt. Shiraga-yama district.* MMEAJ.**

MMEAJ, 1971b: *Regional geological survey report 1970, River Yoshino-gawa district.* MITI.**

MMAJ (Metal Mining Agency of Japan), 1975: *Regional geological survey report 1974, The area to south of Matsuyama.* MITI.**

Monie, P., Faure, M. and Maluski, H., 1988: First 40Ar/39Ar dating of the high-pressure Mesozoic metamorphism of Sambagawa (SW Japan). *C.R. Acad. Sci. Paris, Ser. 2*, **304**, 1221–1224.

Nagai, K., 1957: The Upper Eocene Flora of the Kuma Group, in the Ishizuchi Range, Shikoku, Japan. *Mem. Ehime Univ., Ser. 2*, **2**, 73–82.

Nagai, K., 1972: The Eocene Kuma Group, Shikoku. *Mem. Ehime Univ., Sci., Ser. D (Earth Sci.)*, **7**, 1–7.*

Nakajima, T., Banno, S. and Suzuki, T., 1977: Reactions leading to the disappearance of pumpellyite in low-grade metamorphic rocks of the Sanbagawa metamorphic belt in central Shikoku, Japan. *Jour. Petrology*, **18**, 263–284.

Nakano, N., 1966: Studies on the geology and rock structure of the Sambagawa metamorphic rocks in the district of Kuma-Yokoyama, Shizuoka Prefecture. *Master Th. (MS), Hiroshima Univ.*

Nakamura, F., 1991: Geological structure of the Sambagawa belt of the River Kamo district. *Grad. Th. (BS), Hiroshima Univ.*.**

Ohtomo, Y., 1989: Nappe structures along southern margin of the Ryoke belt around the Aichi-Shizuoka Prefecture border. *Abst. 96th Ann. Meet. Geol. Soc. Japan*, 394.**

Ohtomo, Y., 1990: Deformation mode and Tectonics of the Ryoke granites. *Earth Monthly*, **12**, 473–477.**

Ohtomo, Y., 1991: Tectonics of the Ryoke metamorphic belt for the formation of mylonite zone. *Abst. 98th Ann. Meet. Geol. Soc. Japan*, 314.**

Ohtomo, Y., 1992: Origin of the Median Tectonic Line. *Jour. Sci. Hiroshima Univ., Ser. C*, **9**, (in preparation).

Ohtomo, Y. and Kagami, H., 1990: Rb-Sr ages of granitic rocks from the Ryoke nappe complex. Abst. *97th Ann. Meet. Geol. Soc. Japan*, 355.**

Okudaira, T., 1992: Tectonic evolution of the Ryoke belt in the Iwakuni-Yanai district, Southwest Japan. *Master Th. (MS), Hiroshima Univ.*

Ono, A., 1983: Gatsuzoyama metamorphic belt and its significance. *Abst. 90th Ann. Meet. Geol. Soc. Japan*, 391.**

Osanai, Y., Masao, S., Kagami, H., Komatsu, M. and Owada, M., 1992: Isotopic study of Cretaceous granites from the Inner zone in Kyushu. *Abst. 92nd. Ann. Meet. Geol. Soc. Japan.* 434.**

Platt, J. P. and Wallis, S. 1991: How had high pressure metamorph-

ic rocks been exhumed uplifted ? *Science Journal KAGAKU,* **61**, 535-543.**

Price, G. P. 1985: Preferred orientation in quartzite. *In* Wenk, H.-R. ed., *Preferred Orientation in Deformed Metals and Rocks*, Academic Press, Inc, London, 385–406.

Sakai, C., Banno, S., Toriumi, M. and Higashino, T., 1985: Growth history of garnet in pelitic schists of the Sanbagawa metamorphic terrain in central Shikoku. *Lithos*, **18**, 18-19.

Sakakibara, N., Hara, I. and Ohtomo, Y., 1989: Deformation of granitic rocks in the Ryoke belt; (I) Deformation style of quartz. *DELP Publication*, no. 28, 47–51.

Sakakibara, N., Hara, I and Ohtomo, Y., 1990: Deformation style and tectonics of granitic rocks of the Ryoke belt; (III) Deformation style of quartz. *Earth, Monthly,* **12**, 466–469.**

Sakakibara, N., Hara. I., Kanai, K., Kaikiri, K., Okamoto, K., Shiota, T. and Hide, K., 1991: Quartz fabrics observed on P-T path of the Sambagawa metamorphic rocks of central Shikoku. *Abst. 98th Ann. Meet. Geol. Soc. Japan*, 414.**

Sakakibara, N., Hara, I., Kanai, K., Kaikiri, K., Shiota, T., Okamoto, K., Hide, K. and Paulitsch, P., 1992: Quartz microtextures of the Sambagawa schists and their implication in convergent margin processes. (in press).

Shibata, K. Sugiyama, Y., Takagi, H. and Uchiumi, S., 1988: Isotopic ages of rocks along the Median Tectonic Line in the Yoshino area, Nara Prefecture. *Bull. Geol. Surv. Japan*, **39**, 759–781.*

Shiota, T., 1976: Geological structure of the Sambagawa crystalline schists in the Tsuji area, Ikawa town, Tokushima Prefecture. *In Prof. G. Kojima, Mem. Vol., Hiroshima Univ.*, 154–159.**

Shiota, T., 1981: Structural, geological and petrological study of the Sambagawa crystalline schists of the Ikeda-Mikamo district, East Shikoku. *Jour. Gakugei, Tokushima Univ., (Nat. Sci.)*, **32**, 29–65.*

Shiota, T., 1985: Tsuji nappe in the Sambagawa metamorphic belt of the Mikamo-Yamakawa district, eastern Shikoku. *Jour. Gakugei, Tokushima Univ., (Nat. Sci.)*, **36**, 13–20.*

Shiota, T., 1991: Nappe structure of the Sambagawa belt in the Mt. Shiraga district, central Shikoku. *Natural Sci. Resarch, Tokushima Univ.*, **4**, 29–44.*

Sonoda, K., 1985: The geology of the Sambagawa belt of the Saganoseki Peninsula, Kyushu. *In Prof. H. Yoshida, Mem. Vol., Hiroshima Univ.*, 371–385.**

Sonoda, K. and Hara, I., 1984: Geological structure of the Chichibu belt of the Mikuni toge district, Oita Prefecture. *Abst. 91st Ann. Meet. Geol. Soc. Japan*, 555.**

Sumitomo Metal Mining Co. Ltd., 1981: Recent progress of exploration for the Kieslager in the Besshi and Sazare mines district and the gold-bearing quartz vein deposits in the Konomai mine district. *In Exploration of Ore Deposits in Japan: Jublee Publ. Commem. 30 Anniv. Soc. Mining Geologists, Japan*, **1**, 219–293.

Suppe, J., 1972: Interrelationships of high-pressure metamorphism, deformation and sedimentation in Franciscan tectonics, USA. *24th IGC, Section 3*, 552–559.

Suzuki, H., Isozaki, Y. and Itaya, T., 1990a: Relationship among the Sanbagawa belt, the northern Chichibu belt and the Kurosegawa belt in the Kamikatsu Town, Tokushima Prefecture. *Abst. 97th Ann. Meet. Geol. Soc. Japan*, 158.**

Suzuki, H., Isozaki, Y. and Itaya, T., 1990b: Tectonic superposition of the Kurosegawa Terrane upon the Sanbagawa metamorphic belt in eastern Shikoku, Southwest Japan - K-Ar ages of weakly metamorphosed rocks in northeastern Kamikatsu Town, Tokushima Prefecture -. *Jour. Geol. Soc. Japan*, **96**, 143–153.*

Tainosho, Y., Iizumi, S., Kagami, H. and Hayama, Y., 1989: Petrogenesis of basic rocks in the Ryoke belt of the Kinki and Setouchi districts, Southwest Japan. *Earth Science (Chikyu Kagaku)*, **43**, 16–27.*

Takagi, K. and Hara, I., 1979: Relationship between growth of albite porphyroblasts and deformation in a Sambagawa schist, central Shikoku, Japan. *Tectonophysics*, **58**, 113–125.

Takagi, H., Shibata, K., Uchiumi, S. and Fujimori, H., 1989: K- Ar ages of granitic rocks in the northern marginal area of the Kanto Mountains. *Jour. Geol. Soc. Japan,* **95**, 369–380.*

Takasu, A., 1984: Prograde and retrograde eclogites in the Sanbagawa metamorphic belt, Besshi district, Japan. *Jour. Petrology*, **25**, 619–643.

Takasu, A., 1989: P-T histories of peridotite and amphibolite tectonic blocks in the Sanbagawa metamorphic belt, Japan. *In* Daly *et al. eds., Evolution of Metamorphic Belt, Geol. Soc. Spec. Pub.*, no. 43, 533–538.

Takasu, A., 1990: Study on the evolutional process of the Sambagawa accretionary prisms using 40Ar/39Ar age determination. *Earth Monthly*, **12**, 591–596.**

Takasu, A., 1991: Uplifting of the Sanbagawa metamorphic rocks from deeper part of accretionary prism - an examination using 40Ar/39Ar age determination -. *Earth Crust Flow*, 85–59.

Takasu, A. and Kaji, A., 1985: Existence of the eclogite facies in the Sambagawa metamorphic belt - eclogitic rock from Kotsu-Besshi area, Shikoku -. *Abst. 92nd Ann. Meet. Geol. Soc. Japan*, 374.**

Takasu, A. and Dallmeyer, R. D., 1989a: Age determination using 40Ar/39Ar method. *Earth Monthly*, **11**, 661–666.**

Takasu, A. and Dallmeyer, 1989b: 40Ar/39Ar mineral ages of the Sambagawa metamorphic rocks in Shikoku, Japan. *Abst. 96th Ann. Meet. Geol. Soc. Japan*, 582.**

Takeda, K., 1984: Geological and petrological studies of the Mikabu greenstones in eastern Shikoku, Southwest Japan. *Jour. Sci. Hiroshima Univ., Ser. C*, **8**, 221–280.

Takeda, K. and Makisaka, S.,1991: Geology and tectonic process of the Kurosegawa belt in the Mikame area, Ehime Prefecture. *Abst. 98th Ann. Meet. Geol. Soc. Japan*, 335.**

Takeda, K., Tsukuda, E., Tokuda, M. and Hara, I., 1977: Structural relationship between the Sambagawa and Chichibu belt. *In* Hide, K. ed., *The Sambagawa Belt,* Hiroshima Univ. Press, Hiroshima, 107–151.*

Takeda, K., Hide, K. and Hara, I., 1987: Mylonitic rocks of the Karasaki Formation in the Sambagawa belt, western Shikoku. *Abst. 94th Ann. Meet. Geol. Soc. Japan,* 495.**

Takeda, K. and Hide, K., 1991: Sambagawa Belt (western Shikoku). In Suyari, K., Iwasaki, M. and Suzuki, T. eds: *Regional Geology of Japan 8 (Shikoku)*, Kyoritsu Shuppan Co.Ltd., 47–50.**

Takeda, K., Makisaka, S., Itaya, T. and Nishimura, Y., 1992: The Kurosegawa belt in the Mikame area, western Shikoku - especially on petrology and K-Ar ages of metamorphic rocks. *Jour. Geol. Soc. Japan*, **98** (in press).*

Teraoka, Y., 1970: Cretaceous Formations in the Onogawa basin and its vicinity, Kyushu, Southwest Japan. *Rept. Geol. Surv. Japan*, no. 237, 87p.*

Tokuda, M., 1986: Study on the geological structure of the Sambagawa-Chichibu belts in the Kanto Mountains. *Geol. Rept. Hiroshima Univ.*, no. 26, 195–260.*

Tokuda, M. and Hara, I., 1983: Epidote porphyroblasts in Sambagawa schists of central Shikoku, Japan. *Jour. Sci. Hiroshima Univ., Ser. C*, **8**, 123–129.

Tokuda, M. and Seo, T., 1985: K-Ar ages of the metamorphic rocks in the Yoshimi hill. *In Prof. H. Yoshida, Mem. Vol., Hiroshima Univ.*, 289–295.**

Tominaga, R., 1990: Jurassic accretionary prism of the northern

part of the Chichibu belt, eastern Shikoku. *Jour. Geol. Soc. Japan*, **96**, 505–522.*

Tsukuda, E., Hara, I., Tominaga, R., Tokuda, M. and Miyamoto, T., 1981: Geological structure of the Chichibu Belt in the central and western parts of Shikoku. *Studies on Late Mesozoic tectonism in Japan*, **3**, 49–59.**

Ueda, Y. and Onuki, H., 1969: K-Ar dating on the metamorphic rocks in Japan (1)-Yatsushiro gneiss, Kiyama and Sonogi metamorphic rocks in Kyushu-. *Jour. Japan. Assoc. Min. Petr. Econ. Geol.*, **75**, 230–233.

Wallis, S. R., 1990: The timing of folding and stretching in the Sanbagawa belt, the Asemigawa region, central Shikoku. *Jour. Geol. Soc. Japan*, **96**, 345–352.

Watanabe, T. and Kobayashi, H., 1984: Occurrence of lawsonite in pelitic schists from the Sambagawa metamorphic belt, central Shikoku, Japan. *Jour. Metamorphic Geol.*, **2**, 365–369.

Yamaguchi, M. and Minamishin, M., 1986: Metamorphic process and its correlation to the isotopic age of metamorphic rocks - Example of the Higo metamorphic rocks -. *In Prof. M. Yamaguchi, Mem. Vol.*, 137–151.

Yanagida, J., 1958 : The Upper Permian Mizukoshi Formation. *Jour. Geol. Soc. Japan*, **64**, 222–231.*

Yokota, Y., 1969: Evolution of Oboke anticlinorium. *Master Th.(MS), Hiroshima Univ.*

Yokoyama, K. and Itaya, T., 1990: Clasts of high-grade Sanbagawa schist in middle Eocene conglomerates from the Kuma Group, central Shikoku, southwest Japan. *Jour. Metamorphic Geol.*, **8**, 467–474.

Yoshikawa, K., Shirai, K. and Ebina, K., 1980: Geological survey of Sea-bottom tunnel in the Strait of Hoyo. *App. Geol.*, **21**, 19–28.

Yoshikura, S., Hada, S. and Isozaki, Y., 1990: Kurosegawa Terrane. *In* Ichikawa, K. *et al.*, eds., *Pre-Cretaceous Terranes of Japan, Publication of IGCP Project, 224*, 185–201.

*: in Japanese with English abstract
**: in Japanese

Ikuo HARA, Kei HIDE, Sachiyo SEKI, Yasutaka HAYASAKA, Takami MIYAMOTO and Yasuhiro SAKURAI
Department of Earth and Planetary Systems Science, Faculty of Science, Hiroshima University, Higashi-hiroshima, 724, Japan.

Tsugio SHIOTA
Division of Natural Science, Faculty of Integrated Arts and Sciences, Tokushima University, Tokushima, 770, Japan.

Masumi GOTO
Yutaka Upper Secondary School, Yutaka Town, Hiroshima Prefecture, 734-03, Japan.

Kenji KANAI
Mobil Oil Co. Ltd., Osaka Branch Office, Osaka, 565, Japan.

Kenji KAIKIRI
Hiwa Lower Secondary School, Hiwa Town, Hiroshima Prefecture, 723-03, Japan.

Kenji TAKEDA
Institute of Earth Science, Faculty of Education, Yamaguchi University, Yamaguchi, 753, Japan.

Yukiko OHTOMO
Earthquake Research Institute, University of Tokyo, Tokyo, 113, Japan.